

**Microbial communities
and microbial nitrogen cycling
in soil depth profiles over
120,000 years of ecosystem development**

Von der Naturwissenschaftlichen Fakultät der
Gottfried Wilhelm Leibniz Universität Hannover

zur Erlangung des Grades
Doktorin der Naturwissenschaften (Dr. rer. nat.)

genehmigte Dissertation
von
Dipl.-Biol. Stephanie Turner

2018

Referent: Prof. Dr. rer. nat. Axel Schippers

Korreferenten: Prof. Dr. rer. nat. Marcus A. Horn

Prof. Dr. rer. nat. Kirsten Küsel

Tag der Promotion: 24.02.2017

Contents

Zusammenfassung	VI
Abstract	VII
List of abbreviations.....	VIII
1 Introduction.....	1
1.1 Soil as a habitat for microbial communities	1
1.1.1 Soil habitat characteristics and spatial distribution of soil microorganisms	1
1.1.2 Bacteria	4
1.1.3 Archaea	4
1.1.4 Fungi	5
1.2 Microbial nitrogen cycling – from degradation of complex nitrogen polymers to nitrogen transformations.....	6
1.2.1 Different nitrogen pools and overview of nitrogen cycling in soil	6
1.2.2 N ₂ fixation	8
1.2.3 Microbial degradation of complex nitrogen polymers.....	9
1.2.4 Nitrification	10
1.2.5 Denitrification	11
1.2.6 DNRA and anammox.....	12
1.3 Microbial pattern across a soil depth profile.....	13
1.3.1 Changing soil properties across soil depth profiles	13
1.3.2 Microbial communities along vertical soil profiles	14
1.3.3 Nitrogen mineralization and abundances of nitrogen cycling microorganisms along vertical soil profiles	14
1.4 Microbial patterns during soil and ecosystem development.....	15

1.4.1	Changing soil properties along a soil development gradient	15
1.4.2	Microbial communities along ecosystem development gradients	16
1.4.3	Nitrogen mineralization and abundances of nitrogen cycling microorganisms along ecosystem development gradients	17
1.5	The chronosequence approach	18
1.5.1	Definition, advantages and possible limitations of a chronosequence.....	18
1.5.2	Site description: Franz Josef chronosequence.....	18
1.6	Knowledge gaps and research hypotheses	22
2	Results and Discussion.....	25
2.1	<i>Archaea</i> are playing a quantitatively increasing role with increasing soil depth and soil age as compared to <i>Bacteria</i> and <i>Fungi</i> (manuscript 1).....	25
2.2	Archaeal and bacterial community composition of mineral soils considerably changes during long-term ecosystem development (manuscript 1)	27
2.3	Activities of nitrogen-hydrolyzing exoenzymes in soil profiles during progressive and retrogressive ecosystem development are not only affected by the nutrient gradients, but also by changes in soil mineralogical properties (manuscript 2)	32
2.4	Abundances and community composition of nitrogen cycling microorganisms are significantly affected by long-term ecosystem development due to the soil nutrient and mineralogical gradients (manuscript 3).....	36
2.5	Nitrogen cycling activities and nitrogen functional gene abundances are reduced due to an increasing influence of the soil mineral phase in mineral soils during long-term soil development (manuscript 4)	40
2.6	Conclusion.....	44
3	References	46
4	Manuscripts	62
4.1	List of manuscripts and authors contributions	62

4.1.1	Microbial community dynamics in soil depth profiles over 120,000 years of ecosystem development.....	62
4.1.2	Mineralogical impact on long-term patterns of soil nitrogen and phosphorus enzyme activities ...	62
4.1.3	120,000 years of soil ecosystem development results in distinct nitrogen cycling microbial communities.....	63
4.1.4	Microbial utilization of mineral-associated nitrogen in soils.....	64
4.2	Full manuscripts.....	65
4.2.1	Manuscript 1: Microbial community dynamics in soil depth profiles over 120,000 years of ecosystem development	65
4.2.2	Manuscript 2: Mineralogical impact on long-term patterns of soil nitrogen and phosphorus enzyme activities	99
4.2.3	Manuscript 3: 120,000 years of soil ecosystem development results in distinct nitrogen cycling microbial communities.....	118
4.2.4	Manuscript 4: Microbial utilization of mineral-associated nitrogen in soils	162
	List of publications	182
	Danksagung.....	183
	Persönliche Erklärung zur Dissertation.....	185
	Curriculum vitae	186

Zusammenfassung

Bodenmikroorganismen spielen eine wichtige Rolle für Ökosystemfunktionen wie den Abbau organischen Materials und die Bodenbildung, und sie sind verantwortlich für die meisten Umwandlungsprozesse des Stickstoffkreislaufs. Während der Langzeit-Entwicklung von Ökosystemen, bestehend aus der Progression und der Retrogression, verändern sich Nährstoffgehalte und Mineralogie des Bodens, die wahrscheinlich die mikrobielle Gemeinschaft und den mikrobiellen Stickstoffumsatz beeinflussen. Das Ziel dieser Doktorarbeit war es, die mikrobielle Gemeinschaft sowie den mikrobiellen Stickstoffumsatz entlang eines Langzeit-Ökosystementwicklungsgradienten zu charakterisieren und die gefundenen mikrobiellen Änderungen mit Veränderungen der Bodenparameter in Beziehung zu setzen unter besonderer Betrachtung der Mineralbodenhorizonte. Dafür wurden Bodenprofile bis zu einem Meter Tiefe entlang der 120.000 Jahre alten Franz Josef Chronosequenz (Neuseeland) untersucht.

Die Ergebnisse der qPCR Analyse zeigten, dass das Verhältnis von *Archaea* zu *Bacteria* nicht nur mit der Bodentiefe, sondern auch mit dem Bodenalter zunahm. Die Archaeengemeinschaft, welche mittels 16S rRNA Gen-Pyrosequenzierung untersucht wurde, veränderte sich deutlich mit dem Bodenalter hin zu einer Dominanz der *Bathyarchaeota*, welche bereits häufig in anderen nährstoff- und energiearmen Habitaten detektiert wurden. Diese Ergebnisse zusammen mit denen eines Mikrokosmos-Inkubationsexperiments deuten drauf hin, dass *Archaea* besser an die Mineral-induzierte Nährstofflimitation in den Unterböden angepasst sind. Dies wird anhand einer Selektion von bestimmten Taxa, besonders in älteren Böden mit einer Phosphorlimitierung, deutlich. Im Gegensatz dazu bleibt die bakterielle Gemeinschaft relativ stabil während der Langzeit-Ökosystementwicklung.

Die Aktivitäten und Abundanzen Stickstoff-umsetzender Mikroorganismen veränderten sich signifikant während der Langzeit-Ökosystementwicklung im Zusammenhang mit Veränderungen des Boden-Stickstoffgehalts und konnten in den Mineralbodenhorizonten mit mineralogischen Parametern in Beziehung gesetzt werden. Die Aktivitäten der Exoenzyme Protease und Urease wurden durch einen zunehmenden Gehalt an Eisen- und Aluminiumoxiden und Tonmineralen im Boden inhibiert. Ebenso nahmen die Abundanzen von archaischen Ammoniumoxidierern und Nitratreduzierern, welche anhand von qPCR des funktionellen Gens (*amoA* und *narG*) quantifiziert wurden, in den Unterböden des ältesten Standorts ab. Dies hing möglicherweise mit einer verminderten Substratverfügbarkeit zusammen, welche durch den zunehmenden Gehalt an Eisen- und Aluminiumoxiden und Tonmineralen verursacht wurde. Damit übereinstimmend zeigte sich bei einem Inkubationsexperiment, dass die Verfügbarkeit von Stickstoff durch Interaktionen mit Bodenmineralen herabgesetzt sein kann, aber mineral-gebundener Stickstoff dennoch eine wichtige Stickstoffquelle für Bodenmikroorganismen darstellt. Die Verfügbarkeit des mineral-gebundenen Stickstoffs hängt hauptsächlich von der Sauerstoffversorgung, den bodenmineralogischen Eigenschaften und dem entsprechenden Stickstoff-Substrattyp ab.

Zusammenfassend zeigen die Ergebnisse dieser Doktorarbeit, dass mikrobielle Gemeinschaften und der mikrobielle Stickstoffumsatz im Boden nicht nur von der initialen Boden- und Ökosystementwicklung beeinflusst werden, sondern sich auch während der Langzeitentwicklung einschließlich einer Retrogression signifikant verändern. Überdies wurde neben Kohlenstoff- und Nährstoffgehalten auch die Relevanz von Bodenmineralen für die Bodenmikrobiologie hervorgehoben.

Schlagerworte: Bodenmikrobiologie, Chronosequenz, Stickstoffumsatz

Abstract

Soil microbial communities play a key role in ecosystem functioning including organic matter degradation and soil formation and they mediate most transformation processes of nitrogen (N) cycling. During long-term ecosystem development that comprises a progressive and a retrogressive phase, soil nutrient contents and mineralogy changes, probably altering microbial communities and microbial nitrogen cycling. The aim of this thesis was to investigate microbial communities as well as microbial N cycling during long-term ecosystem development and to relate these microbial dynamics to changes in soil properties with special consideration of conditions in mineral soil horizons. Therefore, we analyzed soil profiles down to one meter depth along the 120,000 year old Franz Josef chronosequence (New Zealand).

The results of qPCR analysis revealed that the archaeal to bacterial ratio not only increased with soil depth, but also with soil age, and the archaeal community composition analyzed by pyrosequencing of the 16S rRNA gene showed a pronounced shift with soil age towards a dominance of *Bathyarchaeota* frequently detected in nutrient-poor, low-energy habitats. These results together with those of a microcosm soil incubation experiment suggest that *Archaea* might better cope with mineral-induced nutrient limitation in subsoils by the selection for specific archaeal taxa, especially at the older sites characterized by P limitation. In contrast, bacterial communities remained rather stable during long-term ecosystem development.

Activities and abundances of N cycling microorganisms significantly changed during long-term ecosystem development linked to changes in soil N content and were also related to mineralogical properties in mineral soils. Thus, the activities of the exoenzymes protease and urease were inhibited by the content of Fe and Al oxides as well as clay. Similarly, abundances of archaeal ammonia oxidizers and nitrate reducers quantified by qPCR of N functional genes (*amoA* and *narG*, respectively) were reduced in subsoils at the oldest site probably due to constrained substrate availability caused by the increasing content of Fe and Al oxides as well as clay-sized minerals. In line with these findings, the microcosm incubation experiment showed that the availability of N could be constrained by interaction with soil minerals; however, mineral-associated N provides an important N source for soil microorganisms. The availability of mineral-associated N was mainly related to the soil O₂ status, soil mineralogical characteristics and substrate type.

In summary, this thesis revealed that soil microbial communities and microbial N cycling are not only affected by early soil and ecosystem development, but also significantly change during longer time periods including a retrogressive phase. Moreover, in addition to the soil carbon and nutrient contents the relevance of the soil minerals for soil microbiology was highlighted.

Keywords: Soil microbiology, Chronosequence, Nitrogen cycling

List of abbreviations

16S rRNA	Prokaryotic small subunit (16S) ribosomal ribonucleic acid
Al	Aluminum
Anammox	Anaerobic ammonium oxidation
AOA	Ammonia-oxidizing archaea
AOB	Ammonia-oxidizing bacteria
C	Carbon
C _{mic}	Microbial biomass carbon
Comammox	Complete oxidation of ammonia to nitrate
DNA	Deoxyribonucleic acid
DNRA	Dissimilatory nitrate reduction to ammonium
Fe	Iron
Fe _{d-o}	Dithionite-citrate-extractable iron minus oxalate-extractable iron
Fe _o , Al _o	Oxalate-extractable iron and aluminum
Fe _p , Al _p	Pyrophosphate-extractable iron and aluminum
<i>FSCG</i>	<i>Forest Soil Crenarchaeotal Group</i>
HF	Heavy fraction
HPLC	High-performance liquid chromatography
LF	Light fraction
<i>MCG</i>	<i>Miscellaneous Crenarchaeotal Group</i>
MOM	Mineral-associated organic matter
N	Nitrogen
N _{mic}	Microbial biomass nitrogen
N _{min}	Inorganic nitrogen (nitrate + ammonium)
OC	Organic carbon
ON	Organic nitrogen

OP	Organic phosphorus
OTU	Operational taxonomic unit
P	Phosphorus
PCA	Principal component analysis
PCR	Polymerase chain reaction
POM	Particulate organic matter
qPCR	Quantitative PCR
RDA	Redundancy analysis
<i>SAGMCG</i>	<i>South African Gold Mine Crenarchaeotal Group 1</i>
SOM	Soil organic matter
SSU	Small subunit
TCC	Total cell counts
TN	Total nitrogen
TP	Total phosphorus
T-RF	Terminal restriction fragment
T-RFLP	Terminal restriction fragment length polymorphism
wt%	Weight percent

1 Introduction

1.1 Soil as a habitat for microbial communities

1.1.1 *Soil habitat characteristics and spatial distribution of soil microorganisms*

The soil is the most complex habitat on earth and represents the upper part of the earth's crust consisting of unconsolidated organic and mineral material. The soil habitat is characterized by several environmental factors, influencing soil microbial abundances, community composition and activities, like pH, temperature, redox regime, moisture, texture or soil organic matter (SOM) content with a high spatial variability due to the large heterogeneity in soils (Voroney & Heck 2015). There is evidence that local heterogeneity and microscale environmental gradients e.g. with soil depth cause as much or even higher variation in microbial community composition as across surface soils of different biomes (Fierer et al. 2009, Eilers et al. 2012). The soil biota consist of plants, animals and microorganisms and it was estimated that soil inhabit one third of all living organisms (Voroney & Heck 2015). Soil microorganisms comprise the three domains of life – *Archaea*, *Bacteria* and *Eukaryotes* (Fig. 1) with the latter including fungi, protozoa and micro-algae. One gram of surface soil (dry weight) contains about 10^{10} bacterial and 10^6 fungal cells with a tremendous biodiversity and could be considered as an immense biochemical gene library (Trevors 2010).

Bacteria and *Archaea* often occur each as single cells, as micro-colonies associated with decaying SOM or larger colonies of several hundred cells on soil aggregates or minerals (Fig. 2 A-C). Most *Fungi* and some *Bacteria* (e.g. *Streptomyces*) exhibit a filamentous habit and built up extensive networks of hyphae (Fig. 2 D) that are important for tapping nutrients and promoting soil aggregation. Soil microorganisms are embedded in an extracellular mucilage of microbial origin (e.g. extracellular polymeric substances, necromass) constituting a significant source of SOM and being important for SOM stabilization and aggregation (Miltner et al. 2012). Another important soil habitat and hotspot of microbial activity constitutes the rhizosphere, i.e. the zone of soil (few millimeters from the root surface) where microbial processes are influenced by the root system. Thereby, plants provide organic carbon (OC) as rhizodeposition comprising root exudates, root litter, and damaged root cells influencing bacterial communities (Dennis et al. 2010). Vice versa, microbial communities of the rhizosphere could affect plant health, e.g. by improving nutrient uptake (nitrogen, N; phosphorus, P) due to mycorrhizal fungi or N₂-fixing bacteria, or preventing the colonization by pathogenic microorganisms (Berendsen et al. 2012).

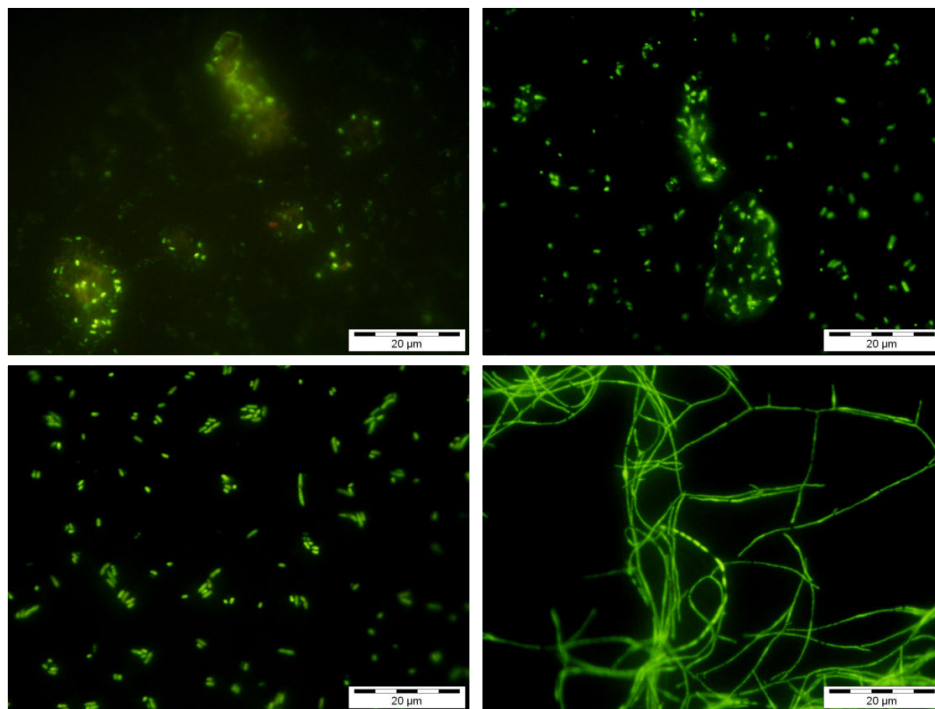


Fig. 2: Microscopic pictures of SYBR Green I stained microbial cells derived from enrichment cultures of soil samples along the Franz Josef chronosequence. (A), (B) microbial cells in micro-colonies attached to soil particles, (C) morphological diversity of soil microorganisms, (D) filamentous habit (courtesy of Gudrun Mengel-Jung).

1.1.2 Bacteria

Soil *Bacteria* are characterized by an extremely high physiological diversity with more than 150 pathways and 900 different reactions (van Elsas et al. 2007). The most abundant soil *Bacteria* belong to the phyla *Acidobacteria*, *Actinobacteria*, *Proteobacteria*, *Bacteroidetes*, *Chloroflexi* and *Firmicutes* (Fierer et al. 2009). Although *Acidobacteria* are ubiquitous and abundant in soils, there are very few cultured representatives and therefore their ecological role remains elusive. The abundance of *Acidobacteria* is negatively correlated with soil pH and this parameter is also a good predictor for their community compositions with subgroups linked to neutral pH (Jones et al. 2009). Members of the *Actinobacteria* are aerobes and heterotrophs playing a major role in SOM decomposition (Killham & Prosser 2015). Many of the cultivated bacteria belong the phylum *Proteobacteria* that is characterized by a broad metabolic diversity and is of great importance to soil carbon (C) e.g. SOM decomposition, and N cycling e.g. N₂ fixation, see chapter 1.2 (Kersters et al. 2006, Killham & Prosser 2015). The phylum *Bacteroidetes* is also very diverse, but there is evidence that soil *Bacteroidetes* are copiotrophic showing high abundances in (surface) soils with high amounts of labile SOM and being involved in the decay of SOM (Fierer et al. 2007, Eilers et al. 2012, Killham & Prosser 2015). The *Chloroflexi* are a phylum with few cultivated representatives and most soil *Chloroflexi* belong to the ‘subphylum I’ and the class *Ktedonobacteria* (Yamada & Sekiguchi 2009). For instance, the strain *Ktedonobacter racemifer* was isolated from soil and is characterized as a mesophilic, aerobic heterotroph (Cavaletti et al. 2006). Cultured representatives of soil *Firmicutes* belong to well-known genera as for example *Clostridium* and *Bacillus*. *Firmicutes* are gram-positive with aerobic or anaerobic metabolism and include endospore formers (Killham & Prosser 2015).

1.1.3 Archaea

Before the establishment of culture-independent PCR-based molecular techniques, *Archaea* were considered to be mostly extremophiles and were isolated from environments such as hot springs, salt lakes, and thermal vents (Killham & Prosser 2015). With the introduction of 16S rRNA gene analysis,

sequences affiliated with the *Crenarchaeota* were frequently detected in moderate habitats such as soils (Jurgens et al. 1997, Buckley et al. 1998, Ochsenreiter et al. 2003). Since then, the rapid increase in 16S rRNA gene sequences lead to the discovery of more and more new archaeal groups, e.g. *Thaumarchaeota*, *Bathyarchaeota*, *Lokiarchaeota* and *Hadesarchaeota* (Brochier-Armanet et al. 2008, Meng et al. 2014, Spang et al. 2015, Baker et al. 2016) and hence a fast changing archaeal phylogeny (Fig.).

Soil *Archaea* comprise on average 2% of the 16S rRNA gene sequences and there is evidence that they are predominantly oligotrophs as compared to most soil *Bacteria* (Fierer et al. 2007, Nemergut et al. 2010, Wessén et al. 2010, Chroňáková et al. 2015). Soil archaeal communities were dominated by the former *Crenarchaeota* 1.1b, now part of the phylum *Thaumarchaeota* (Bates et al. 2011). So far, all cultivated members of the phylum *Thaumarchaeota* (Group 1.1a and 1.1b) could oxidize ammonia to nitrite being the rate limiting step of the nitrification (Oton et al. 2016), but there is also evidence that *Thaumarchaeota* of the Group 1.1c could grow without performing ammonia oxidation (Weber et al. 2015). In addition to the *Thaumarchaeota*, members of the *Euryarchaeota* such as *Methanomicrobiales*, *Methanosarcinales*, *Thermoplasmatales* and *Halobacteriales* were also frequently detected in soils (Auguet et al. 2010). Whereas little is known about the role of *Thermoplasmatales* and *Halobacteriales* that were described as heterotrophs and normally isolated from geothermal, acidic or hypersaline environments, *Methanomicrobiales* and *Methanosarcinales* are methanogens and produce methane in anoxic zones of soils (Offre et al. 2013). Recent studies provide evidence that also members of the class *Thermoplasmata* are able to produce methane (Paul et al. 2012, Iino et al. 2013).

1.1.4 Fungi

Fungi are *Eukaryotes* and present in all soils. Most soil *Fungi* belong to the phyla *Ascomycota* and *Basidiomycota* with a proportion of 56 and 31%, respectively (Tedersoo et al. 2014). They interact with both living and dead organisms and are as decomposers fundamental for SOM mineralization including N and P cycling. Especially during early stages of SOM decomposition their filamentous growth form and their capacity to excrete a wide range of hydrolytic and oxidative extracellular enzymes are

advantageous for *Fungi* being the principal degraders of plant cell wall material (Taylor & Sinsabaugh 2015). The enzyme repertoire of classical decomposer *Fungi* (saprotrophs) contains e.g. phenol oxidases and peroxidases to degrade aromatic compounds such as lignin, and hydrolases and other polysaccharide-degrading enzymes to degrade cellulose, pectin and hemicellulose (Rabinovich et al. 2004). As mycorrhizal partner, most *Fungi* live in a close interaction with plant roots as either endosymbionts (arbuscular and ericoid mycorrhizal *Fungi*) or ectomycorrhizal *Fungi* (Balestrini et al. 2015). Mycorrhizal *Fungi* deliver water and mineral nutrients (N, P), thereby promoting the growth of the plants (Berendsen et al. 2012, Taylor & Sinsabaugh 2015). Further, *Fungi* produce spores that enable them the survival of harsh conditions and the dispersal over great distances by air (Taylor & Sinsabaugh 2015).

1.2 Microbial nitrogen cycling – from degradation of complex nitrogen polymers to nitrogen transformations

1.2.1 Different nitrogen pools and overview of nitrogen cycling in soil

Nitrogen can be found in inorganic and organic forms in soils with the latter residing mainly in SOM, plant biomass and microbial biomass (Fig. 3). So far, in present ecological concepts the SOM N pool is considered to be one pool without further differentiation into functionally and compositionally different fractions (Rennenberg et al. 2009, Robertson & Groffman 2015, Stein & Klotz 2016). Schimel and Bennett (2004) emphasized the compositional differences of SOM N consisting of polymers and monomers that differ in availability for soil microorganisms and plants (Rennenberg et al. 2009). However, beyond this classification into polymers and monomers, there is increasing evidence that SOM resides in different functional pools, e.g. particulate and mineral-associated organic matter (POM and MOM, respectively), possessing different availability (Schmidt et al. 2011). Soil minerals stabilize SOM via adsorption and coprecipitation affecting the turnover rates of SOM (Schmidt et al. 2011, Kleber et al. 2015).

While the role and the characteristics of OC in different SOM fractions are already well investigated (von Lützow et al. 2006, Kögel-Knabner et al. 2008, Gentsch et al. 2015), knowledge about N transformation in different functional N pools and their stabilization is scarce. Although the cycling of C and N is connected to each other via biomass production and degradation, the effect of the soil mineral characteristics on mineralization of OC and organic N (ON) differs as reported by previous studies (Knicker 2011, Heckman et al. 2013, Bimüller et al. 2014). A sorption experiment with dissolved ON and different mineral phases as well as subsoils showed that the retention of ON was smaller than that of OC (Kaiser & Zech 2000). In contrast, N containing compounds such as proteins are preferentially accumulated in stabilized SOM by metal oxides (Knicker 2011, Pronk et al. 2013). Microbial extracellular enzymes could be sorbed to soil mineral surfaces (Fig. 4) mostly resulting in inhibited activities and therefore slowing down microbial SOM degradation and mineralization (Gianfreda et al. 1992, Nannipieri & Smalla 2006, Burns et al. 2013). In addition, Dippold et al. (2014) reported that the bioavailability of sorbed alanine representing a potential substrate for soil microorganisms strongly depends on the mineral phase characteristics that acts as a sorbent with the lowest microbial utilization of alanine sorbed to an iron (Fe) oxide (goethite). Consequently, microbial N cycling could be impaired directly by the inhibition of extracellular enzyme activities or indirectly by constraining their substrate availability.

Most N transformations in soils are mediated by soil microorganisms (Robertson & Groffman 2015). The main external, natural sources of N are atmospheric deposition or microbial N₂-fixation. Fixed N is used to support biomass production and could be converted to ammonium by ammonification. During nitrification the ammonium is converted to nitrite and nitrate. Denitrification, i.e. the reduction of nitrite to N₂O or N₂, and the anammox reaction, i.e. the anaerobic ammonium oxidation with nitrite to N₂, leads each to microbially caused N losses from soil. In contrast, during the ammonification by dissimilatory nitrate reduction to ammonium (DNRA), the microbially transformed N remains in the soil. Plant and soil microorganisms compete for ammonium, nitrate and monomeric SOM ON, whereas SOM ON polymers are depolymerized by extracellular enzymes mainly derived from soil microorganisms (Rennenberg et al. 2009, Burns et al. 2013).

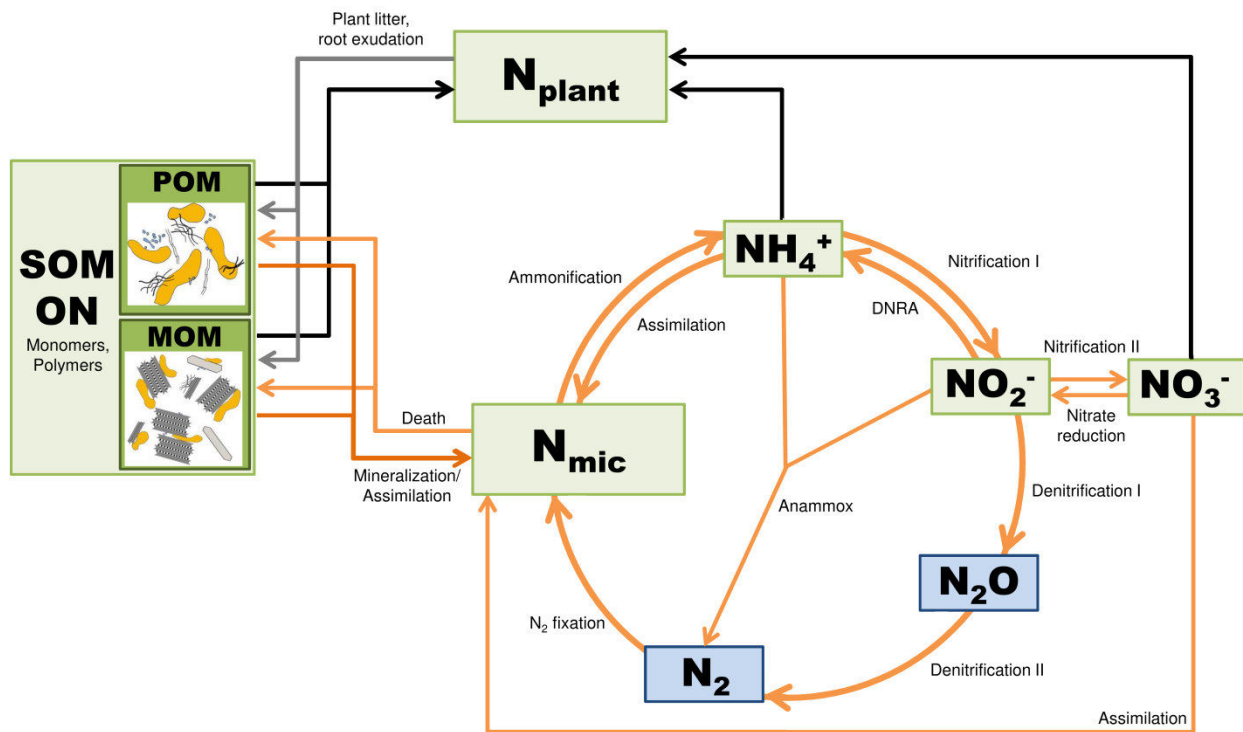


Fig. 3: Schematic overview of soil N pools and microbial N transformation. SOM organic N (ON) pool consists of ON in particulate organic matter (POM) and mineral-associated organic matter (MOM). N_{mic} represents N in microbial biomass and N_{plant} represents N in plant biomass. Microbial processes are indicated by orange arrows, competing uptake of ON, ammonium and nitrate by plants is indicated by black arrows, and plant ON input to SOM ON pool is indicated by grey arrows. Gaseous N forms are shown in blue boxes. Nitrification I and II denote ammonia oxidation and nitrite oxidation, respectively. Denitrification I denotes nitrite reduction and nitric oxide reduction and denitrification II denotes nitrous oxide reduction.

1.2.2 N_2 fixation

Atmospheric N_2 can be transformed to biologically available N species by biological N fixation representing an important N input to soils. N_2 -fixing microorganisms (diazotrophs) break the triple bond of N_2 and convert it to ammonia using the nitrogenase enzyme. This process is restricted to members of the domains *Archaea* and *Bacteria* that constitute a phylogenetically (methanogenic *Archaea*, *Proteobacteria*, *Cyanobacteria*, *Firmicutes* and *Actinobacteria*) and physiologically diverse group (Bottomley & Myrold 2015). Free-living N_2 -fixing bacteria could be autotrophic or heterotrophic with the latter being constrained by a low availability of labile C compounds (Reed et al. 2011, Davies et al. 2013). Associative N_2 -fixing bacteria use root secretions as C source and are found in the rhizosphere and the

intercellular spaces of the root cortex (Bottomley & Myrold 2015). *Cyanobacteria* and other photosynthetic bacteria are important diazotrophs in rice paddies and biological soil crusts (Whitton 2000, Belnap 2003). Symbiotic associations between N₂-fixing bacteria (rhizobia) and legumes provide the plant with N while the energy for N₂ fixation is supplied by the photosynthetic host (van der Heijden et al. 2008). Similarly, the actinobacterial genus *Frankia* forms symbiotic associations with nonleguminous plants like alder (Benson 1982).

1.2.3 Microbial degradation of complex nitrogen polymers

In soil, most N containing compounds are available as polymers, such as proteins, chitin, or peptidoglycan that could not be taken up by soil microorganisms. Therefore, the first step in the microbial degradation of N containing substrates is the depolymerization into smaller compounds by extracellular enzymes (Geisseler et al. 2010). Important enzymes that cleave N compounds are proteases, peptidases, amidase, deaminase, urease, and chitinases (Caldwell 2005). Proteases and peptidases hydrolyze proteins and peptides into smaller peptides or amino acids, whereas amidases and deaminases cleave an amino group from primary amines (Caldwell 2005, Geisseler et al. 2010). The urease catalyzes the hydrolysis of urea to CO₂ and ammonium (Sinsabaugh et al. 2000). Chitinases cleave the links between the N-acetyl-D-glucosaminide molecules of chitin (Geisseler et al. 2010).

In general, enzymes in soil could be located intracellular, periplasmatic, or extracellular (Fig. 4). Extracellular enzymes could be bound to the outer cell surface, secreted by soil microorganisms by intent, or leaking from dead, lysed cells (Burns et al. 2013). The production of enzymes costs energy as well as C and nutrients such as N and therefore is strongly regulated by the microbial cell. Consequently, extracellular enzyme activities could be used as proxies for the nutrient demand of the cells (Sinsabaugh et al. 2008).

After depolymerization, mineralization, or nitrification, soil microorganisms could take up N compounds as nitrate, ammonium or small organic N molecules. The uptake of nitrate and small organic compounds is normally depressed when high concentrations of ammonium are available. However, the

uptake of small organic compounds has the advantage of providing also C and energy in addition to N (Geisseler et al. 2010).

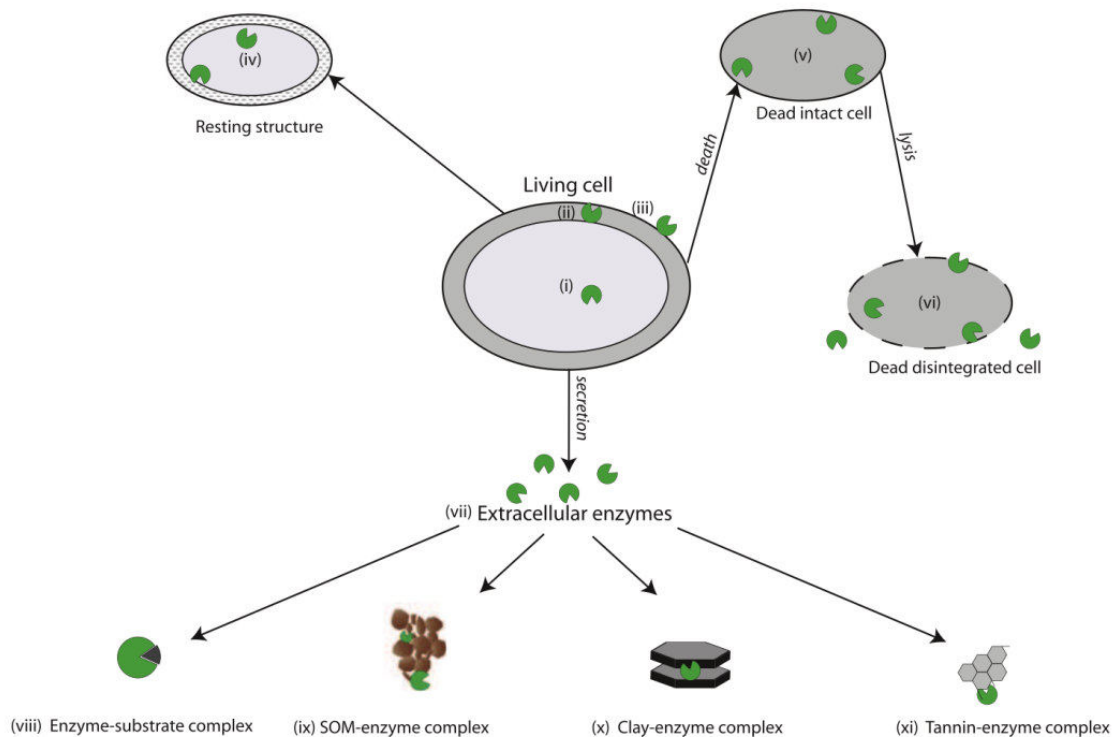


Fig. 4: Locations of enzymes in soil (intracellular (i, iv, v, vi), periplasmic (ii), or extracellular (iii, vii)) and interactions of extracellular enzymes with substrate (viii), SOM (ix), soil minerals (x), or tannins (xi) (from Burns et al. 2013).

1.2.4 Nitrification

During nitrification, microorganisms aerobically oxidize ammonia via nitrite to nitrate. Therefore, nitrification constitutes an important source of nitrate that is more mobile in soils than ammonium (Robertson & Groffman 2015). Further, nitrification causes a decrease in soil pH due to production of protons and could be a source of NO and N₂O formed as intermediates with the latter being relevant as greenhouse gas (Robertson & Groffman 2015). Nitrification is a two-step process conducted by physiologically distinct groups of microorganisms: ammonia oxidizers and nitrite oxidizers. The first step could be performed by ammonia-oxidizing *Archaea* (AOA) as well as ammonia-oxidizing *Bacteria* (AOB). All isolated AOA belong to the phylum *Thaumarchaeota* and most AOA seem to dominate

oligotrophic habitats with low ammonia concentrations (Leininger et al. 2006, Di et al. 2010). Further, there is evidence that AOA especially dominate in acidic soils with pH < 5.5 (Prosser & Nicol 2012). In a wide range of soils, AOA outnumber AOB and dominate ammonia oxidation (Prosser & Nicol 2012, Offre et al. 2013). The AOB belong to *Beta*- and *Gammaproteobacteria* with *Nitrosomonas* and *Nitrospira* common in soils (Norton 2011).

The second step of the nitrification, the oxidation of nitrite to nitrate, is performed by bacteria of different phylogenetic groups such as *Alpha*- (*Nitrobacter*), *Beta*- (*Candidatus Nitrotoga*), *Gamma*- (*Nitrococcus*) and *Deltaproteobacteria* (*Nitrospina*), and the phylum *Nitrospirae* (Ehrich et al. 1995, Robertson & Groffman 2015). Moreover, Sorokin et al. (2012) discovered a nitrite-oxidizing bacterium from a nitrifying bioreactor belonging to the phylum *Chloroflexi* that possibly also occurs in soils (Cretoiu et al. 2015).

However, in 2015 van Kessel et al. and Daims et al. discovered *Nitrospira* bacteria that are capable to perform the complete oxidation of ammonia to nitrate (comammox) and a screening of public databases revealed that *amoA* sequences closely related to this *Nitrospira* species were detected in a wide range of habitats including different soil types.

In addition to the above described autotrophic nitrifiers, several heterotrophic bacteria and fungi are capable to nitrify by oxidizing ammonia or organic forms of N. However, this heterotrophic nitrification pathway does not serve for energy production and cellular growth and seem to be only important in soils, in which autotrophic nitrifiers are inhibited (Robertson & Groffman 2015, Zhang et al. 2015).

1.2.5 Denitrification

Denitrification is a microbial process where nitrate and nitrite is sequentially reduced to gaseous NO, N₂O and N₂ being relevant as N loss point in soils and contributes to emission of the greenhouse gas N₂O (Robertson & Groffman 2015). Denitrification is carried out by a wide range of soil microorganisms including *Bacteria*, *Archaea* and *Fungi* (Bonete et al. 2008, Long et al. 2013). Most denitrifiers are

heterotrophic bacteria that use nitrate as terminal electron acceptor for respiration under oxygen-deficient conditions. Therefore, denitrification mainly occurs in water-saturated soils such as wetlands or after rainfall events when oxygen diffusion is inhibited (Robertson & Groffman 2015).

Denitrifiers can co-exist with nitrifiers and rapidly consume the produced nitrate or nitrite. This process is termed coupled nitrification-denitrification and occurs in soils where oxic and anoxic microhabitats are located close to each other, e.g. at soil aggregates or cracks (Wrage et al. 2001). This coupling of both processes could also be carried out by one organism during the so-called nitrifier-denitrification. Autotrophic ammonia oxidizers, e.g. *Nitrosomonas europaea*, conduct the nitrifier-denitrification especially under low oxygen concentrations (Colliver & Stephenson 2000) as well as heterotrophic nitrifiers under aerobic conditions (Wrage et al. 2001).

In contrast to the latter processes, during co-denitrification, N₂O and N₂ could also be formed as a hybrid N-N species by combining two different N compounds, e.g. nitrite with a co-metabolized amine (Tanimoto et al. 1992, Spott & Stange 2011). Like conventional denitrification, this process is detected in *Archaea*, *Bacteria* and *Fungi* (Aeressens et al. 1986, Tanimoto et al. 1992, Stieglmeier et al. 2014).

1.2.6 DNRA and anammox

Besides the classical N cycling pathways of nitrification, denitrification and N₂ fixation, there are more N transformations which role and relevance in soil microbial N cycling are not fully understood. Dissimilatory nitrate reduction to ammonium (DNRA; nitrate ammonification) is the anaerobic reduction of nitrate via nitrite to ammonium. Redox state and the C to nitrate ratio are important factors regulating the partitioning between DNRA and denitrification in soils (Baggs 2011, Rütting et al. 2011). DNRA rates seem to be highest in soils with high SOM content in humid regions with a high relative importance compared to denitrification especially in temperate climate (Rütting et al. 2011).

During the anaerobic ammonium oxidation (anammox), ammonium and nitrite are converted to N₂ by anammox bacteria (Robertson & Groffman 2015). These bacteria are affiliated with the phylum *Planctomycetes* and comprise genera such as *Scalindula*, *Kuenenia* and *Brocadia* (Strous 2011). Compared to marine environments and wastewater treatment, the anammox pathway is relatively

unimportant in soils because of low ammonia input and therefore denitrification dominates (Strous 2011). Only in paddy soils and wetland soils anammox bacteria were detected so far (Humbert et al. 2012, Bai et al. 2015).

1.3 Microbial pattern across a soil depth profile

1.3.1 Changing soil properties across soil depth profiles

Within a soil depth profile, soil parameters such as pH, temperature, SOM content, moisture, or nutrient contents could change drastically (Holden & Fierer 2005). The uppermost layer consists of decaying SOM from plant residues and roots comprising the organic horizon (O horizon) and the underlying SOM-enriched mineral topsoil (A horizon). Due to eluviation by water, soluble and colloidal inorganic compounds were transported from surface layers deeper into the soil profile and accumulate in the subsurface horizon (B horizon). Below the B horizon the least weathered parent material comprises the C horizon (Voroney & Heck 2015).

The content of SOM and correspondingly the contents of C and nutrients (e.g. N and organic P, OP) sharply decline with soil depth (Holden & Fierer 2005, Hansel et al. 2008). However, despite the decreasing SOM content with soil depth, subsoils (below 20 cm) harbor more than half of the total C stocks to 100 cm depth ranging from 48% to 68% between different biomes (Jobbágy & Jackson 2000). In humid regions, the content of clay is higher in subsoils (B horizon) than in topsoils (Merrill 1906). Therefore, most OC and ON in subsoils is associated with soil minerals forming mineral-organic associations (Sollins et al. 2006, Kögel-Knabner et al. 2008, Mikutta et al. 2009). In acid and near neutral soils, the main stabilization mechanisms of SOM is reported to be the interaction with amorphous Fe and aluminum (Al) oxides (Rumpel & Kögel-Knabner 2011).

1.3.2 Microbial communities along vertical soil profiles

Corresponding to the steep gradient in SOM content, abundances and activities of most microorganisms are highest in the organic topsoils and decline with depth (Taylor et al. 2002, Fierer et al. 2003, Eilers et al. 2012). While organic soil horizons are typically enriched in *Fungi* and gram-negative bacteria, the relative proportion of gram-positive bacteria, *Actinobacteria* and *Archaea* increases with depth (Fierer et al. 2003, Uroz et al. 2013). Similarly, the microbial diversity and community composition of the three taxa are also vertically stratified. The bacterial diversity declines with depth and community composition varies with soil depth showing differences between soil horizons (Hansel et al. 2008, Hartmann et al. 2009). Fungal community composition shows distinct patterns with soil depth with fungal taxa confined either to litter or organic soil horizon and a relative higher abundance of *Ascomycota* in organic compared to mineral soil horizons (Baldrian et al. 2012, Uroz et al. 2013). In contrast, the archaeal diversity is highest in deeper soil horizons, but also shows differences in community composition between soil horizons (Hansel et al. 2008, Hartmann et al. 2009).

1.3.3 Nitrogen mineralization and abundances of nitrogen cycling microorganisms along vertical soil profiles

Coinciding with the general trend of decreasing OC and ON content as well as microbial abundances with soil depth, the N mineralization rate and the activities of N-hydrolyzing extracellular enzymes also decrease (Ajwa et al. 1998, Aon & Colaneri 2001, Taylor et al. 2002, Holden & Fierer 2005, Stone et al. 2014, Pinggera et al. 2015). Depolymerized ON compounds are utilized preferentially via the direct uptake route as small organic molecules such as amino acids or small peptides by microorganisms of surface soils and subsoils likewise (Pinggera et al. 2015).

Correspondingly to activities and general microbial abundances, abundances of *nifH* genes, bacterial *amoA* genes, nitrate reductases genes (*narG* and *napA*), and denitrifying genes (*nirK* and *nirS*) decrease with depth in different soils (Mergel et al. 2001, Kandeler et al. 2009, Onodera et al. 2010, Marhan et al. 2011, Stone et al. 2015). While Mergel et al. (2001) and Stone et al. (2015) also reported a

decreasing trend for *nosZ* (nitrous oxide reductase) gene abundances, abundances slightly increase with soil depth being maximal in the B horizon of forest soil (Kandeler et al. 2009). In contrast to AOB abundances, archaeal *amoA* gene copy numbers varies with soil depth according to season (Onodera et al. 2010) and, similarly, Hansel et al. (2008) detected AOA in subsoil B and C horizons, but not in the topsoil A horizon.

Throughout the soil profile and within soil aggregates, the oxygen content can fluctuate depending on soil type and its corresponding properties such as texture or water content (Sexstone et al. 1985, Holden & Fierer 2005). Oxygen availability and the redox regime act as a switch between aerobic and anaerobic N cycling pathways and could determine whether particular N cycling microorganisms are stimulated or not (Pett-Ridge et al. 2006). Thus, differences in abundance trends with soil depth can be related to soil characteristics, e.g. the abundances of anammox bacteria (based on *hszB* gene copy numbers) that increase with soil depth in paddy soils (Bai et al. 2015), although anammox bacteria have so far been rarely detected in soil systems.

1.4 Microbial patterns during soil and ecosystem development

1.4.1 Changing soil properties along a soil development gradient

After major disturbances such as volcanic eruption or glacier retreat, ecosystem development starts involving soil formation and primary succession (Walker & del Moral 2003). This stage of progression is characterized by an increase in biomass with ongoing time (Wardle et al. 2004, Peltzer et al. 2010). After hundreds to thousands of years the progressive development leads to a maximal biomass stage (Odum 1969, Wardle et al. 2004, Peltzer et al. 2010). However, without further rejuvenating disturbances this “climax” stage is followed by a retrogressive phase. Retrogression occurs after thousands to millions of years if the ecosystem undergoes a substantial decline in ecosystem productivity, plant biomass, availability of nutrients and above- and belowground communities shifted to nutrient-stress-tolerant and slow-growing species (Vitousek & Farrington 1997, Wardle et al. 2004, Peltzer et al. 2010).

This sequence of ecosystem development is linked to pedogenesis and associated changes in nutrient availability (Fig.). Abiotic nutrient input in soils derives from atmospheric sources like precipitation or dust and parent material derived sources (Blume et al. 2010). While in young soils N tends to be scarce mainly entering in small amounts via atmospheric input, primary minerals, e.g. apatite, of the parent material provide a rich P source (Menge et al. 2012, Turner & Condon 2013). With ongoing soil and ecosystem development, N₂-fixing symbioses increase the available N pool, whereas weathering and leaching of P-containing minerals results in a depletion of P (Fig. 5; Peltzer et al. 2010, Turner & Condon 2013). Additionally, during ecosystem development a mineralogical gradient forms due to transformations of soil minerals from primary minerals via poorly crystalline minerals to secondary minerals and crystalline metal (hydr)oxides during pedogenesis (Vitousek et al. 1997). Therefore, with increasing soil age, the content of available P decreases due to the absolute loss and the protection by Fe and Al hydr(oxides) (Vitousek et al. 1997, Turner et al. 2007). Overall, young ecosystems are rather N limited, whereas with increasing age there is a shift to P limitation in older, retrogressive stages (Wardle et al. 2004, Menge et al. 2012).

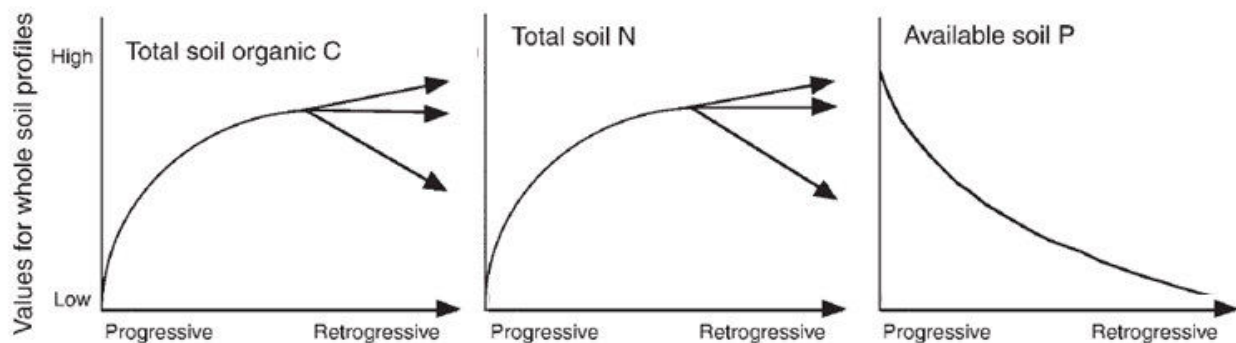


Fig. 5: Changes in C and nutrient (N, P) content during progressive and retrogressive soil development phases modified after Peltzer et al. (2010).

1.4.2 Microbial communities along ecosystem development gradients

During the early stage of ecosystem development, the colonization by pioneer microorganisms promotes soil formation. Thereby, microorganisms are responsible for biological weathering of the parent

material and create biofilms that provide interfaces for nutrient turnover (Schulz et al. 2013). With ongoing progression of the ecosystem, SOM accumulates coinciding with an increase in plant biomass aboveground as well as an increase in microbial activities and abundances belowground (Schipper et al. 2001, Richardson et al. 2004, Brankatschk et al. 2011, Turner et al. 2012, 2013, Blaško et al. 2015). Bacterial community composition changes during early progression (till ~ 100 years) accompanied by stable or increasing bacterial diversity and richness (Nemergut et al. 2007, Zumsteg et al. 2012b, Brown & Jumpponen 2014, Mateos-Rivera et al. 2016). Although archaeal community composition also changes with ongoing soil development, archaeal diversity decreases (Zumsteg et al. 2012b, Mateos-Rivera et al. 2016).

There are only a few studies that analyzed microbial communities during longer-term ecosystem development including retrogression. The bacterial community composition in topsoils along a dune chronosequence changes according to progressive and retrogressive ecosystem development stages (Jangid et al. 2013a). Similarly, along a forest chronosequence there was a shift in bacterial community composition with increasing soil age, however, with greater differences during the progressive phase (Jangid et al. 2013b). Both studies reported decreasing bacterial diversity with ongoing development. The analysis of a chronosequence derived from uplifted marine terraces varying in vegetation types also gave similar results with a compositional shift for bacterial communities in topsoils (Uroz et al. 2014). Consequently, bacterial community composition in topsoil seems to be altered by soil and ecosystem development.

1.4.3 Nitrogen mineralization and abundances of nitrogen cycling microorganisms along ecosystem development gradients

In the initial phase of soil development, the major N source derives from N deposition and promotes biomass production of pioneer (micro)organisms (Brankatschk et al. 2011, Schulz et al. 2013). The decomposition of complex SOM derived from biomass, in turn, supports N mineralization processes, as reflected by high relative activities of extracellular enzymes such as protease and chitinases

(Brankatschk et al. 2011). With ongoing ecosystem development and increasing plant coverage, N₂-fixing microbes become more and more important in N acquisition (Nemergut et al. 2007, Brankatschk et al. 2011, Schulz et al. 2013). In vegetated, more developed soils, the N cycle becomes more complex as revealed by increasing abundances of several different N pathway coding genes such as *nifH* (N₂ fixation), *amoA* (ammonia oxidation), *nirK* and *nosZ* (denitrification). Likewise, N cycle related activities such as N₂ fixation, nitrification and denitrification rates increase (Kandeler et al. 2006, Töwe et al. 2010, Brankatschk et al. 2011, Schulz et al. 2013, Zeng et al. 2016). The functional diversity of the soil microbial communities is maximal in developed soils and biomass N provides the most important ON source (Tscherko et al. 2003, Schulz et al. 2013).

1.5 The chronosequence approach

1.5.1 Definition, advantages and possible limitations of a chronosequence

A chronosequences is defined as a set of sites originated from the same parent material or substrate differing in age (Walker et al. 2010). Chronosequences provide the unique opportunity to study temporal dynamics during ecological succession and pedogenesis (soil formation) over long time periods up to millions of years with the different sites developing under similar climatic conditions (Stevens & Walker 1970, Walker et al. 2010). To study natural development processes, chronosequences should be not altered or modified by anthropogenic activities which would impede a correct interpretation of the temporal dynamics. Chronosequences should consist of more than two stages, should show a clear pattern of temporal change and several lines of evidence that verify the history and the time series. An appropriate chronosequence study should examine replicate plots within one stage to compare variation within and between development stages (Walker et al. 2010).

1.5.2 Site description: Franz Josef chronosequence

The Franz Josef chronosequence is located at the edge of the Southern Alps on the West Coast on the South Island of New Zealand (~43° S, 170° E; Fig. 6). The soils developed due to repeated advance

and retreat of the Franz Josef glacier from glacial outwash of greywacke and mica schist. They span a time scale from present to 120.000 years and the two oldest sites (60 and 120 kyr) also received Pleistocene loess depositions (Stevens 1968, Almond et al. 2001). Soils developed from initial soils with A and C horizons (0.06 kyr, Haplic Regosol), to Stagnic Regosols and Stagnic Cambisols (0.5 kyr) characterized by a starting horizon differentiation, a cumulating organic layer (O horizon), and brownish discoloration (B horizon), and to Stagnic Podzols (1 – 120 kyr) characterized by the formation of an eluvial horizon (E horizon) with increasing thickness (IUSS Working Group WRB, 2006; Fig. 7; Turner et al. 2014). Thereby, the soil horizons across the soil profile are grouped into organic topsoil (O horizon), mineral topsoil (A horizon) and subsoil (E, B, and C horizon). The mean annual temperature is 10.8 °C; precipitation at the youngest four sites (0.06 – 5 kyr) is ca. 6.500 mm and ca. 3.500 mm at the three older sites (12 – 120 kyr). Soils are covered by temperate rainforest with a general dominance of evergreen angiosperms. Woody plant diversity, vegetation cover and tree height increase through ecosystem progression, and then decline (Richardson et al. 2004).

The history of the Franz Josef chronosequence is well characterized and the sites are remote precluding disturbances by anthropogenic activities (Stevens 1968, Almond et al. 2001). Organic and mineral topsoils of the Franz Josef chronosequence are already well investigated in terms of C and nutrient (N, P, and sulfur) dynamics (e.g. Richardson et al. 2004; Turner et al. 2013; Turner et al. 2016), vegetation development (e.g. Richardson et al. 2004), and partly microbial communities and activities (e.g. Allison et al. 2007; Jangid et al. 2013b) providing valuable data for the interpretation of our own results.

Similarly to most long-term chronosequences (see chapter 1.4.1), the soils along the Franz Josef chronosequence are characterized by a C, nutrient and mineralogical gradient with highest soil OC and ON contents at the intermediate-aged sites and a sharp decline in OP and total P (TP) contents with ongoing soil development (Fig. 8; Richardson et al. 2004, Turner et al. 2014). Soil mineralogy is characterized by a change from a large portion of pedogenic Fe and Al residing in metal-humus complexes (pyrophosphate-extractable Fe and Al; Fe_p, Al_p) at the younger sites, to more poorly crystalline

Fe and Al phases (oxalate-extractable Fe and Al; Fe_o , Al_o) at intermediate-aged sites and into a dominance of crystalline Fe and clay-sized minerals (dithionite-citrate-extractable Fe minus oxalate-extractable Fe; Fe_{d-o}) at the oldest site (Turner et al. 2014). The clay content increases with soil age and the analysis of clay mineral assemblages reveals a remarkable suite of transitional phases such as vermiculite and several interstratifications with vermiculitic, smectitic, chloritic and micaceous layers developing during weathering (Turner et al. 2014, Dietel et al. 2017).

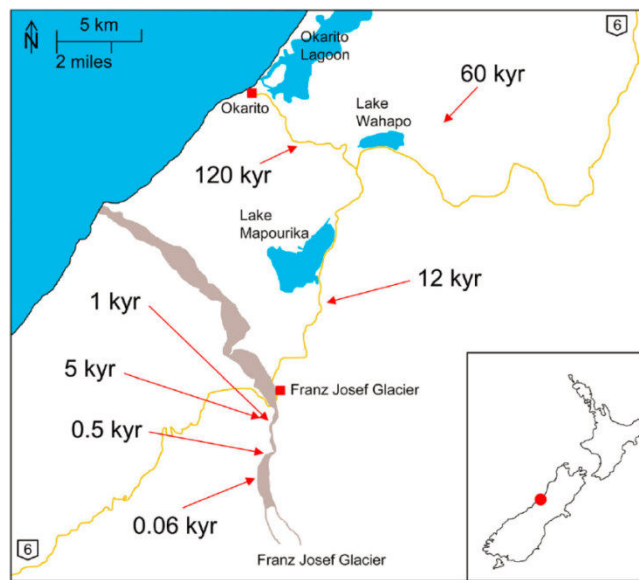


Fig. 6: Map of sampling sites along the 120 kyr old Franz Josef chronosequence modified after Dietel et al. (2017).

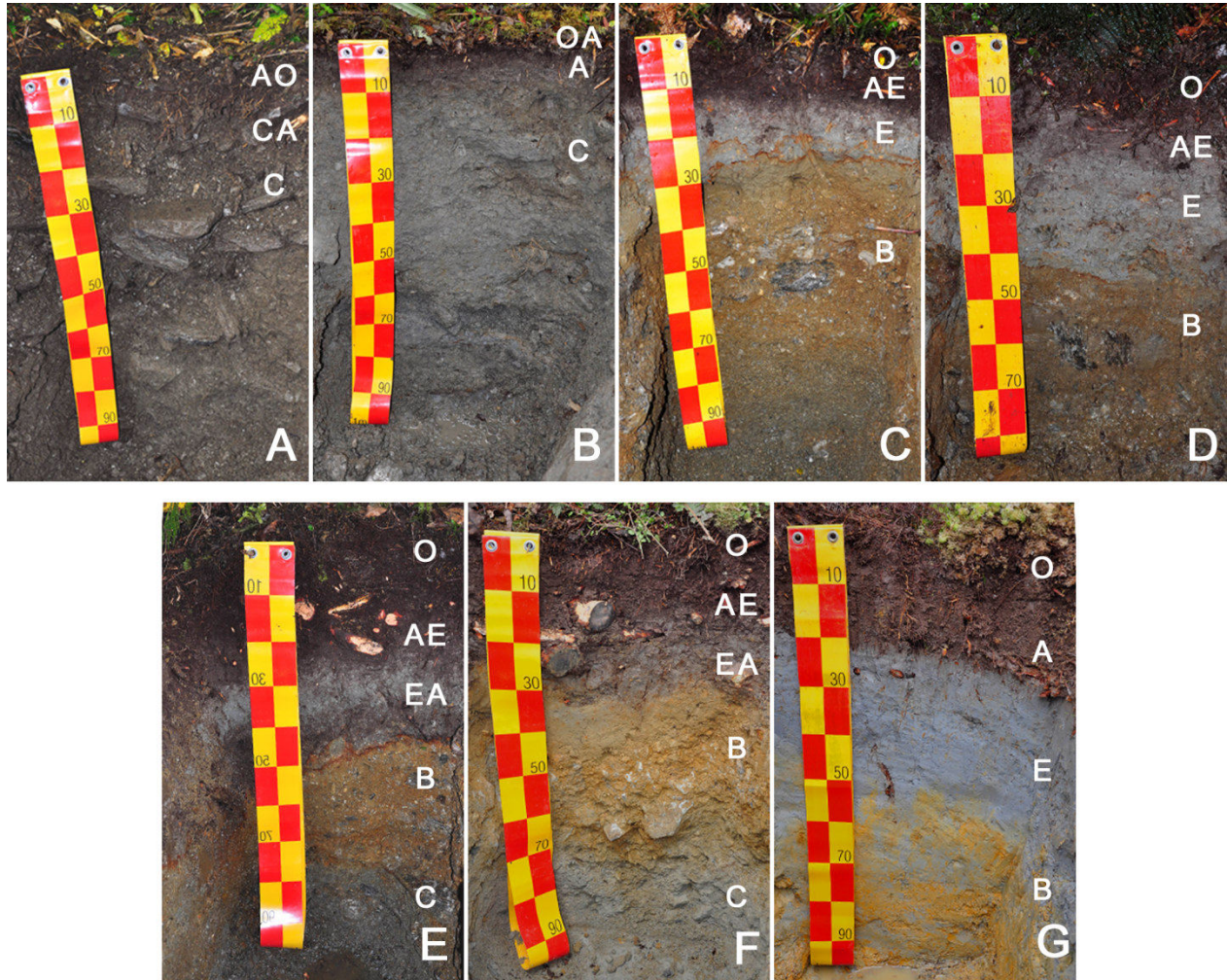


Fig. 7: Soil depth profiles of all seven sampling sites along the Franz Josef chronosequence showing soil development stages: (A) 0.06, (B) 0.5, (C) 1, (D) 5, (E) 12, (F) 60, and (G) 120 kyr modified after Turner et al. (2014). Smaller capital letters across the soil depth profile designate the soil horizons (O/OA, A/AE, E/EA, B, C).

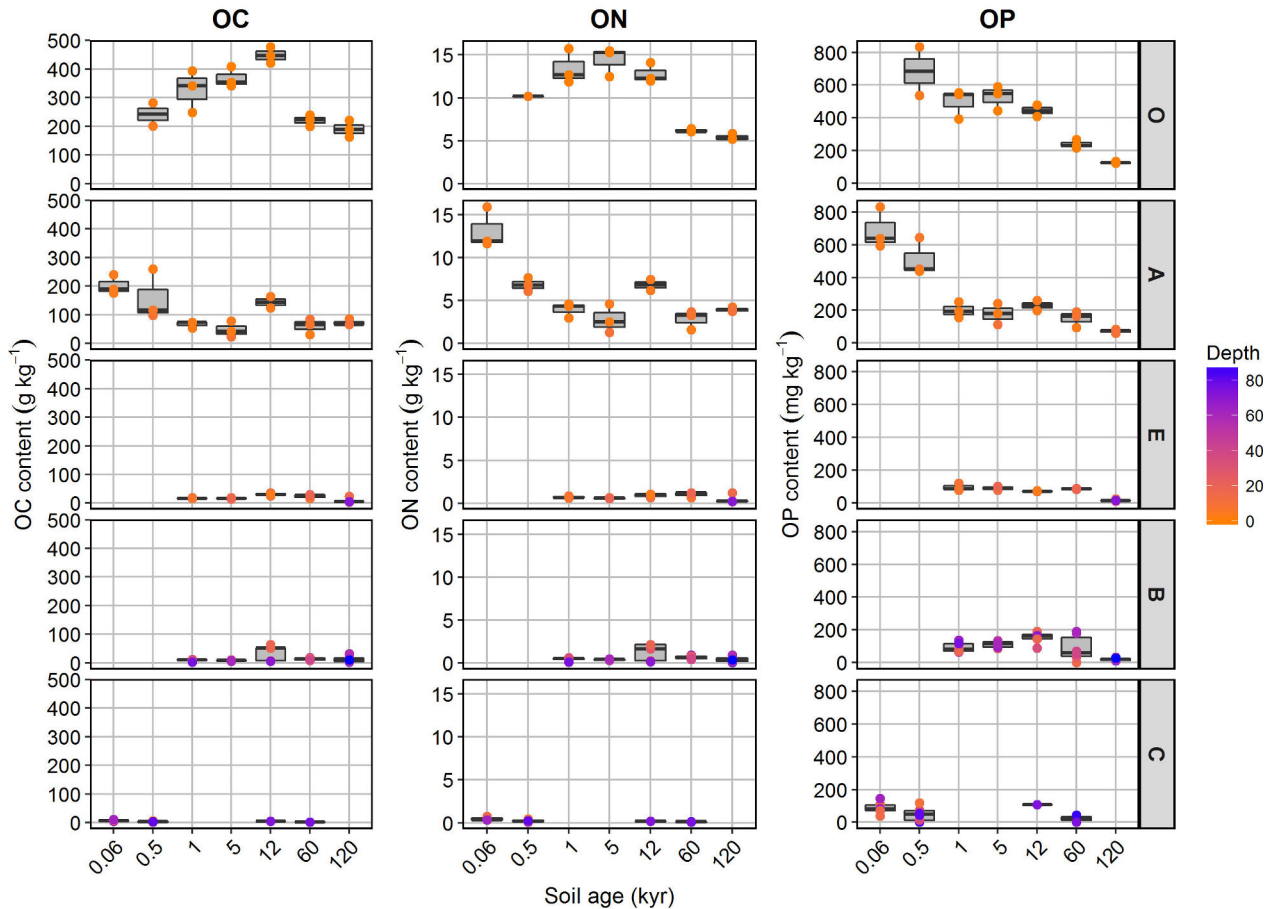


Fig. 8: The content of OC, ON and OP in each horizon cluster (O, A, E, B, and C) in soils of different ages along the Franz Josef chronosequence. The contents were shown as boxplots with single points for horizon and soil profile replicates. The color of the points indicates soil depth (cm). Data were derived from Turner et al. (2014).

1.6 Knowledge gaps and research hypotheses

Although, the dynamics of microbial communities in general, and of N cycling microorganisms in particular, are already well investigated during early soil and ecosystem development (i.e. the progressive phase) there are major knowledge gaps with regard to longer time periods that include retrogressive ecosystem development. Additionally, most studies about soil microbial patterns during ecosystem development focus on topsoils while ignoring subsoils that represent an important habitat for numerous soil microorganisms and significantly differing in soil conditions from topsoils with an increasing importance of soil mineralogical properties. Furthermore, there are several studies analyzing

the relationship between microbial communities or microbial N cycling and soil mineralogical properties in artificial systems, but studies in natural soil systems are scarce. Therefore the research questions of this thesis were: How do microbial abundances and communities develop in whole soil profiles during long-term ecosystem development including retrogression that is characterized by low nutrient (P limitation) and low substrate content? How do microbial N cycling abundances and activities develop in whole soil profiles during long-term ecosystem development? Which soil parameters shape long-term dynamics of microbial communities and microbial N cycling with special consideration of conditions in mineral soil horizons? Based on these questions, the following five main hypotheses were tested:

- I. *Archaea* are playing a quantitatively increasing role with increasing soil depth and soil age as compared to *Bacteria* and *Fungi*.
- II. Archaeal and bacterial community composition of mineral soils considerably changes during long-term ecosystem development.
- III. Activities of nitrogen-hydrolyzing exoenzymes in soil profiles during progressive and retrogressive ecosystem development are not only affected by the nutrient gradients, but also by changes in soil mineralogical properties.
- IV. Abundances and community composition of nitrogen cycling microorganisms are significantly affected by long-term ecosystem development due to the soil nutrient and mineralogical gradients.
- V. Nitrogen cycling activities and nitrogen functional gene abundances are reduced due to an increasing influence of the soil mineral phase in mineral soils during long-term soil development.

This Ph.D. thesis was part of the research project “Accumulation, transformation, and stabilization of organic nitrogen along a mineralogical soil gradient”, a cooperation between the geomicrobiology of the Bundesanstalt für Geowissenschaften und Rohstoffe (BGR) and the Institute of Soil Science of the funded by the German Research Foundation (DFG). While the Leibniz Universität

Hannover investigated soil chemical and mineralogical properties, this thesis focusses on the microbiological part of the research project.

Soil depth profiles of the Franz Josef chronosequence were analyzed for chemical soil parameters (pH, C, N, P), soil texture and mineralogical parameters (Fe and Al (hydr)oxides). Microbial abundances were measured as total cell counts (TCC) via SYBR Green I cell staining and microbial biomass via the fumigation-extraction-method. Abundances of *Archaea*, *Bacteria* and *Fungi* were quantified via qPCR of small subunit (SSU) rRNA genes and archaeal and bacterial community composition were determined by pyrosequencing of 16S rRNA genes. Activities of N-hydrolyzing extracellular enzymes were measured colorimetrically and by HPLC, and abundances of N cycling microorganisms were quantified by qPCR using marker genes for ammonia oxidation (*amoA*), nitrate reduction (*narG*), and chitin degradation (*chiA*). To elucidate which soil parameters affect microbial abundances and activities during long-term soil development a microcosm incubation experiment was conducted. Thereby, the effects of soil age, SOM (mineral-associated vs. particulate), O₂ status, and C and P additions were tested. Using a combination of activity measurements and molecular methods, microbial N transformation rates (net N mineralization, N₂O and N₂ production), abundances of SSU rRNA genes and N functional genes (qPCR), as well as archaeal and bacterial community composition (T-RFLP) were determined.

2 Results and Discussion

2.1 *Archaea* are playing a quantitatively increasing role with increasing soil depth and soil age as compared to *Bacteria* and *Fungi* (manuscript 1)

Bacterial, fungal and eukaryotic abundances were maximal in organic topsoils along the Franz Josef chronosequence and decreased with soil depth, whereas archaeal abundances were maximal in A horizons at some sites (0.5, 12, 60, and 120 kyr) as determined by qPCR of SSU rRNA gene copy numbers. Moreover, archaeal to bacterial abundance ratios increased with soil depth, while fungal to bacterial ratios decreased resulting in a relative predominance that shifted from *Fungi* to *Bacteria* to *Archaea* with increasing soil depth. Archaeal, bacterial, fungal and eukaryotic SSU rRNA gene copy numbers were positively correlated to soil OC, ON and OP contents in whole soil profiles along the Franz Josef chronosequences with stronger relationships for *Bacteria*, *Fungi* and *Eukarya*. These results for temperate rainforest soils support previous findings of a vertical stratification of microbial taxa within the soil profile for spruce forest and grassland soils (Fierer et al. 2003, Baldrian et al. 2012, Uroz et al. 2013). Stratification may be mainly related to substrate availability and preferences of microbial taxa. Thereby, *Bacteria*, *Fungi* and *Eukarya* seem to be more dependent on substrate availability that is highest in organic topsoils due to litter input. *Fungi* play a key role in the decomposition of particulate SOM (e.g. litter) by excreting a wide range of extracellular enzymes and mediate the degradation of complex compounds such as cellulose that are enriched in C (Baldrian et al. 2012, Taylor & Sinsabaugh 2015). Therefore, their abundance is positively correlated to soil C:N ratio. While *Fungi* may quantitatively dominate the litter horizon, their relative abundance decreases with soil depth with *Bacteria* and *Archaea* becoming more important (Baldrian et al. 2012, Gittel et al. 2014a). The increase of the relative quantitative importance of *Archaea* with soil depth and the negative relationship between archaeal to bacterial ratios and increasing soil C contents as reported for fertilization studies (Nemergut et al. 2010, Wessén et al. 2010, Chroňáková et al. 2015) suggest that soil *Archaea*, in particular *Thaumarchaeota*, are rather oligotrophs according to the oligotroph-copiotroph model of Fierer et al. (2007) and thus, are probably specifically adapted to

subsoil conditions. Moreover, energy limitation becomes more relevant with increasing soil depth giving presumably preference for *Archaea* over *Bacteria* as discussed in detail below (Valentine 2007).

Interestingly, the archaeal to bacterial abundance ratio not only increased with soil depth, but also with soil age in subsoils coinciding with a depletion in P and an increase in Fe and Al (hydr)oxides as well as clay-sized minerals. Results of the microcosm incubation experiment, where the influence of soil properties (O₂ status, SOM fraction, soil age and C and P addition) on microbial community dynamics was studied, indicated that bacterial abundances were influenced by all tested parameters with a strong effect of O₂ status, SOM fraction and their interaction, whereas archaeal abundances were hardly affected by these parameters. Similarly, archaeal abundances were only slightly affected by clay mineral composition and showed no change if the Fe oxide ferrihydrite was added as tested in an 18 month incubation experiment with artificial soils (Hemkemeyer et al. 2014). Moreover, *Archaea* showed slower growth rates when compared to bacterial and fungal abundances over the incubation period in this experiment. In contrast, bacterial abundances were significantly affected by mineral composition and particle size fractions with a positive effect of ferrihydrite under oxic conditions in this incubation experiment (Hemkemeyer et al. 2014). This is in line with the findings of manuscript 1 that under oxic conditions bacterial abundances were higher in the heavy fraction (HF, containing MOM) comprising a higher proportion of soil minerals and MOM. However, under anoxic conditions bacterial abundances were lower in the HF fraction indicating an inhibition of bacterial growth that may be induced by an energy and substrate limitation. While anoxic conditions generally create energy limiting conditions, SOM bound to soil minerals forming mineral-organic associations by adsorption or coprecipitation may constrain substrate availability for soil microorganisms (Kaiser & Guggenberger 2007, Heckman et al. 2013, Kleber et al. 2015). Although SOM in mineral-organic associations may be still partially available for soil microorganisms, presumably via desorption, the decomposition might be retarded (Mikutta et al. 2007, Dippold et al. 2014, Swenson et al. 2015). In contrast to *Bacteria*, Valentine (2007) hypothesized that *Archaea* are adapted to chronic energetic stress being a feature that ecologically and evolutionary distinguish *Archaea* and *Bacteria*. Their ability to inhabit extreme environments and a range of

biochemical mechanisms to adapt to these extreme conditions support this hypothesis. Another example is the CO₂ fixation pathway of AOA being highly abundant in rather common, non-extreme environments that is more energy-efficient than any other aerobic autotrophic pathway (Könneke et al. 2014). AOA could oxidize ammonia at extreme low concentrations due to a very efficient C fixation thereby explaining their ecological success in nutrient-limited environments.

Overall, the results of the microcosm incubation experiment provide insights into the factors that may cause microbial abundance patterns along the Franz Josef chronosequence. High precipitation regularly creates water-saturated conditions with low oxygen availability in these soils. Consequently, the rather anoxic conditions and the declining substrate availability due to an increasing influence of the soil mineral phase with soil depth and soil age decreases bacterial abundances. Hence, while *Bacteria* might be inhibited, *Archaea* probably better cope with these mineral-induced nutrient and substrate limitation because of their slow growth rates, their rather oligotrophic lifestyle and their hypothesized better adaptation to chronic energetic stress resulting in increasing archaeal to bacterial abundance ratios in subsoils, especially at the oldest site of the Franz Josef chronosequence.

2.2 Archaeal and bacterial community composition of mineral soils considerably changes during long-term ecosystem development (manuscript 1)

The archaeal and bacterial community composition was analyzed in selected soil samples of different horizons along the Franz Josef chronosequence via tag-encoded pyrosequencing. Due to a multitude of gradients in soil properties along the chronosequence, e.g. in nutrient (N, P) content and soil mineralogy, considerable changes in archaeal and bacterial community composition were hypothesized. Surprisingly, our results revealed that archaeal community composition showed a clear shift with soil age, whereas bacterial communities were rather stable.

The archaeal community composition at young to intermediate sites (0.5 and 5 kyr) mainly comprised members of the *Forest Soil Crenarchaeotal Group* (FSCG; Jurgens et al. 1997) and the *South*

African Gold Mine Crenarchaeotal Group 1 (SAGMCG-1; Takai et al. 2001) with 50 – 92% and 0.1 – 20%, respectively. In later stages (12 and 120 kyr) the community composition changed to a dominance of the newly proposed phylum *Bathyarchaeota* (Meng et al. 2014), formerly known as *Miscellaneous Crenarchaeotal Group (MCG)*, with a relative abundance of 46 – 74%. An analysis of the phylogenetic affiliation of our bathyarchaeotal sequences showed, that most of them were closely related to the *pSL22* cluster, a sister group of the *MCG*, that originally derived from a hot spring in Yellowstone National Park (Barns et al. 1996). The *FSCG*, originally derived from boreal forest soils, and the *SAGMCG-1* (belong to *Group 1.1a Thaumarchaeota*) including the ammonia oxidizer “*Candidatus Nitrosotalea devanaterre*” are common soil archaeal groups (Jurgens et al. 1997, Bomberg et al. 2011, Lehtovirta-Morley et al. 2011, Pester et al. 2012, Chroňáková et al. 2015, Tupinambá et al. 2016). In contrast, members of the *Bathyarchaeota* are widespread and often predominant in marine sediments (Kubo et al. 2012, Breuker et al. 2013), while studies that detected them in soils are rare, and if the group was detected the reported relative abundance was very low (< 5%) in most soils (Gittel et al. 2014b, Chroňáková et al. 2015, Tupinambá et al. 2016). Only in peatland soils and a permafrost soil they were abundant (> 20%) in several samples, and in a depth of 23 – 25 cm in the active layer of a permafrost soil up to 73% of the operational taxonomic units (OTUs) were affiliated to the *Bathyarchaeota* corresponding to the high abundances in the 120 kyr old soil of the Franz Josef chronosequence (Hawkins et al. 2014, Wei et al. 2014).

Unfortunately, there are no cultivated representatives of the *FSCG* belonging to *Group 1.1c Thaumarchaeota* and of the *Bathyarchaeota*, therefore little is known about the ecological relevance of these groups. While all cultivated representative of the *Group 1.1a* and *1.1b Thaumarchaeota* are capable of ammonia oxidation (Pester et al. 2012), there is evidence that members of *Group 1.1c Thaumarchaeota* can grow without oxidizing ammonia but instead their growth was stimulated by the addition of ON compounds such as glutamate or casamino acid in microcosms (Weber et al. 2015). *Group 1.1c Thaumarchaeota* were abundant in forest and moorland soils with a preference for lower pH, higher soil moisture and higher SOM content when compared to AOA (Oton et al. 2016). Their preference for high

SOM content suggests a role in SOM decomposition and corresponds to the higher abundances at younger to intermediate aged soils as compared to older soils, and additionally all three factors fit with their extremely high abundance (93%) in the O horizon of the 5 kyr site. Although, there are several studies aiming to reveal the physiological capabilities of the *Bathyarchaeota*, in particular of the *MCG*, they remain poorly understood, too. So far, the *MCG* are considered to be mostly heterotrophic anaerobes as revealed by carbon isotopic composition analysis and genome reconstruction of sediment *MCG* archaea (Biddle et al. 2006, Lazar et al. 2016). They are highly abundant and active in nutrient-poor and energy-limited marine subsurface sediments (Biddle et al. 2006, Fry et al. 2008) and results of genome reconstruction from single cells and metagenomes provide evidence that *MCG* archaea are capable of protein degradation possessing for example genes for extracellular peptidases and peptide- and amino acid transporters (Lloyd et al. 2013, Lazar et al. 2016). These findings fit to the high abundance of the *Bathyarchaeota* in older, P limited soils of the Franz Josef chronosequence coinciding with an increase in extracellular aminopeptidase activities and suggest that the *Bathyarchaeota* may be adapted to the low substrate and nutrient-poor conditions by degrading proteins of dead microbial biomass. At the oldest soil development stage (120 kyr) microbial biomass represents an important internal carbon and nutrient pool because the soil receives only small allochthonous SOM input compared to the soil of other ages (Turner et al. 2013; calculated from manuscript 2).

According to the results of the microcosm incubation experiment, changes in archaeal community composition during long-term soil development are associated with the SOM fraction and soil age-related soil properties. While SOM fractions (bulk soil vs. HF) differed in the proportion of soil minerals as well as substrate availability constrained by substrate-mineral interactions, the factor soil age is linked to several gradients such as soil C and nutrient contents as well as soil mineralogy. Since the addition of C and P did not significantly affect archaeal community composition, the effect of soil fraction and soil age might be related to changes in mineralogical properties. This assumption is in line with findings of fertilization studies for grassland soil summarized by Leff et al. (2015) which indicated that the archaeal community composition was not significantly altered by P additions. In contrast, different clay

minerals resulted in different archaeal community composition in the particle size fraction < 20 μm after a 18 month incubation period with artificial soil microcosms (Hemkemeyer et al. 2014). Additionally, archaeal community composition in tropical soils was best explained by two sets of soil variables: sulfur, sodium and ammonium-N, or clay, potassium, ammonium-N and nitrate-N (de Gannes et al. 2015). While emphasizing the importance of clay content, this study suggest that ammonium and nitrate content could also be responsible for the compositional shift in line with the finding of Leff et al. (2015) that N additions had a significant effect. However, Leff et al. (2015) hypothesized that this effect is associated with AOA that respond to differences in N pools, thus, these soil properties would be less important for the archaeal compositional shift at the Franz Josef chronosequence because the relative proportion of AOA on total archaeal abundances decreased at the older sites being very low compared to the younger sites (manuscript 3).

Contrary to the *Archaea*, bacterial community composition remained rather stable during long-term soil development and was dominated by *Acidobacteria*, *Chloroflexi*, *Planctomycetes*, and *Proteobacteria*. *Acidobacteria* and *Proteobacteria* are common and abundant in different soils, whereas *Chloroflexi* and *Planctomycetes* were detected in low abundances mostly < 5% (Roesch et al. 2007, Fierer et al. 2009, Uroz et al. 2013, Chroňáková et al. 2015, de Gannes et al. 2015). Although soils of the Franz Josef chronosequence are characterized by several changes in soil properties during long-term development, bacterial communities in mineral soils did not changed considerably, neither on phylum nor on genus level, corresponding to stable communities of topsoils older than 5 kyr (Jangid et al. 2013b). Similarly, bacterial communities along other long-term chronosequences also remained rather stable as reported for the Mendocino chronosequence (uplifted marine terraces, time points T2 and T3), B horizons of a dune chronosequence located in Georgia (US) and a dune chronosequence bordering on the Lake Michigan (Tarlera et al. 2008, Williams et al. 2013, Uroz et al. 2014). In contrast to drastic changes in bacterial community composition during early succession (Nemergut et al. 2007, Zumsteg et al. 2012a, Brown & Jumpponen 2014, Mateos-Rivera et al. 2016), the composition seem to remain stable in developed and retrogressive stages corresponding to changes in soil pH, that rapidly decreased from

approximately seven to four during early succession of glacier forelands, but afterwards also remained stable (Tscherko et al. 2003; Williams et al. 2013; manuscript 2). The soil pH was one of the best predictors for the bacterial community composition and also many other studies in different soils showed that pH is one of the most important factors determining bacterial community composition (Fierer et al. 2009, Rousk et al. 2010, Dini-Andreote et al. 2014, Chroňáková et al. 2015).

However, principal component analysis (PCA) and variation partitioning showed that bacterial community composition was rather linked to soil depth than soil age with slight differences in abundances of particular phyla and genera. The PCA revealed that *Planctomycetes* (*Gemmata*-affiliated sequences and unclassified 41) were highly abundant in the organic horizon fitting to their aerobic, heterotrophic lifestyle (Franzmann & Skerman 1984). A relative higher proportion in the organic horizon was observed for *Actinobacteria* (*Acidothermus*-affiliated sequences) constituting also aerobic heterotrophs that play an important role in the decomposition of organic polymers such as chitin (Beier & Bertilsson 2013, Killham & Prosser 2015). With increasing soil depth the abundance of the *Acidobacteria* (unclassified 7) tended to increase down to the B horizon in line with previous findings suggesting a rather oligotrophic lifestyle (Fierer et al. 2007, Hansel et al. 2008, Eilers et al. 2012, Chroňáková et al. 2015). The effect of soil depth on bacterial community composition could be explained by the strong effect of the O₂ status in the microcosm incubation experiment. Because soils along the Franz Josef chronosequence regularly receive high precipitation that results in water-saturated conditions with low oxygen availability and creates a steep redox gradient with soil depth.

In addition to the strong effect of the O₂ status, bacterial community composition differed significantly between SOM fractions (bulk soil vs. HF) with unique terminal restriction fragments (T-RFs) detected in each fraction. Distinct bacterial communities were also reported for the HF and light fraction (LF, containing POM) in an incubation experiment with four different fractions (rhizosphere, shoot residue, LF, and HF) and it was presumed that the selection for well adapted species may be greater in the HF than in the rhizosphere due to distinct habitat characteristics dominated by soil mineral particles and stabilized SOM (Blackwood & Paul 2003). Furthermore, there are several incubation studies with artificial

soils showing that bacterial community composition was altered by different clay minerals or Fe oxides (Babin et al. 2013, Heckman et al. 2013, Vogel et al. 2014, Steinbach et al. 2015). However, while the SOM fraction had a significant effect, soil age affected only HhaI-digested bacterial fragments exhibiting a rather weak effect. This finding is in line with bacterial community patterns along the Franz Josef chronosequence and differences between previous studies and this incubation experiment may originate from the use of natural soils with less prominent differences in mineral composition compared to artificial soils with pure minerals.

In summary, our results revealed that archaeal abundances were hardly affected by soil mineralogical properties (SOM fraction and soil age), whereas the archaeal community showed a clear soil-age related compositional shift towards a *Bathyarchaeota* predominance indicating that archaeal communities may quantitatively predominate subsoils, especially in nutrient-depleted old soils, by better coping with mineral-induced substrate limitations and by selection for taxa that are adapted to nutrient-poor, low energy habitats. In contrast, bacterial communities remained rather stable in their composition during long-term soil development, but bacterial abundances relatively decreased with soil depth and age due to a negative effect of soil minerals probably by constraining substrate availability.

2.3 Activities of nitrogen-hydrolyzing exoenzymes in soil profiles during progressive and retrogressive ecosystem development are not only affected by the nutrient gradients, but also by changes in soil mineralogical properties (manuscript 2)

The degradation of complex ON starts with the cleavage of polymers by extracellular enzymes into small molecules that could be utilized by soil microorganisms (Geisseler et al. 2010). Potential activities of N-hydrolyzing enzymes (alanine-aminopeptidase, leucine-aminopeptidase, protease, and urease) and P-hydrolyzing enzyme (phosphatase) decreased sharply with soil depth in soil profiles along the Franz Josef chronosequence. The N-hydrolyzing enzyme activities in organic topsoils were maximal at intermediate-aged soils (1 – 12 kyr), whereas the phosphatase activity increased with soil age

corresponding to previous results reported by Allison et al. (2007). Enzyme activities in organic topsoils reflect the progressive development, with maximal N-hydrolyzing enzyme activities coinciding with plant biomass maximum (Richardson et al. 2004), and retrogressive development phases, with increasing phosphatase activity matching the increasing P limitation. Similar to microbial abundances (manuscript 1), all extracellular enzyme activities were positively correlated to soil OC, ON, and OP content for soil depth profiles indicating the close relationship between activity and substrate pool content.

While potential enzyme activities on soil mass basis reflect absolute decomposition rates at ecosystem level, their normalization to the substrate pool content could provide information on nutrient demand of soil microorganisms and substrate availability (Boerner et al. 2005, Sinsabaugh et al. 2008). Except for protease, all normalized enzyme activities were strongly negatively correlated to their substrate pool content (ON or OP) in organic topsoils indicating a down-regulation if sufficient substrate is available probably due to high amounts of litter input. In contrast, in mineral soil horizons the relationship between enzyme activity and substrate content was not as strong as for the O horizon and some enzymes even showed positive correlations in particular soil horizons. Enzymes and their substrates were affected by multiple soil parameters resulting in more complex interactions in mineral soils than in the organic layer such as transformation and stabilization processes initiated by the soil mineral phase (Kaiser & Guggenberger 2000, Burns et al. 2013). However, both ON-normalized aminopeptidase activities showed a negative correlation to soil ON content also in mineral soils and were less related to soil mineralogical properties compared to the other enzyme activities suggesting that these aminopeptidases were hardly affected by the soil mineral phase. In contrast, OP-normalized phosphatase activity was negatively correlated to soil OP content not only in O horizons but also in A and E horizons, whereas there was a positive relationship in B and C horizons. As indicated by a decreasing OC:OP ratio with soil depth, soil OP may preferentially be retained by hydrous Fe and Al oxides in comparison to OC compounds as reported for sorption experiments and bacteria-derived extracellular polymeric substances (Kaiser 2001, Mikutta et al. 2011, Swenson et al. 2015). As a result soil microorganisms might up-regulate phosphatase activities to still meet their nutritional demand for P.

The ON-normalized activities of urease and protease showed no significant relationship to soil ON content in mineral soils, but instead were negatively correlated to particular soil mineralogical properties, e.g. the content of Fe and Al oxides residing in poorly crystalline minerals and metal-humus complexes ((Fe+Al)_o) or the clay content. Several laboratory studies provide evidence that enzyme activities were inhibited by clay-sized minerals or Fe and Al oxides due to adsorption to mineral surfaces and/or stabilization of enzymes and their substrates (Gianfreda et al. 1992, Bayan & Eivazi 1999). Moreover, Fe and Al oxides are considered to be the main stabilizing agents of SOM in temperate subsoils (Kögel-Knabner et al. 2008). Similarly, OP-normalized phosphatase activity was also negatively correlated to the (Fe+Al)_o content in line with previous results (Bayan & Eivazi 1999, Achat et al. 2012). In opposition to these findings, other studies with artificial and natural soils reported that the presence of clay or iron oxides could enhance enzyme activities (Bayan & Eivazi 1999, Allison 2006, Shahriari et al. 2010). This inconsistency in the literature might be related to differences in the experimental conditions with the pH being an example for one important factor determining the type and strength of the interaction between mineral surfaces and SOM (Quiquampoix et al. 1993, Kedi et al. 2013).

Profile-based enzyme activities normalized to profile stocks of the corresponding substrate pool indicate nutrient limitations in soils down to one meter depth. The ON-normalized profile-based activities of N-hydrolyzing enzymes were highest in the youngest soils revealing that belowground communities might be also N limited in line with aboveground plant communities (Richardson et al. 2004). This N limitation might be more pronounced in subsoils due to small N input as indicated by higher activities normalized to microbial biomass carbon (C_{mic}) compared to topsoils. In contrast, with ongoing ecosystem development the OP-normalized phosphatase activity increased with soil age being maximal at the two oldest retrogressive development stages revealing an increasing P limitation, thereby also matching aboveground P limitation of plant communities (Richardson et al. 2004). However, C_{mic}-normalized phosphatase activities were higher in topsoils than in subsoils suggesting that subsoil communities may be adapted to P limited conditions by more efficient P acquisition mechanisms or a down regulation of phosphatase activity due to an aggravation of P limitation by strong substrate-mineral interaction as

indicated by opposite trends of TP stocks vs. stocks of clay and Fe_{d-o} . Further, as discussed above, results of correlation analysis point to an inhibition of phosphatase activities due to high Fe and Al oxide concentrations at the older sites. Interestingly, the profile-based urease activity showed patterns matching the N-hydrolyzing enzymes but also those of the phosphatase, i.e. urease activity was maximal in young soils (0.06 and 0.5 kyr) and similar high in the two oldest soils (60 and 120 kyr). Compared with the C_{mic} -normalized activities there were also similar trends with in tendency higher values in subsoils for younger soils and in topsoils for older soils. This suggests that the urease activity not only responds to the N limitation in undeveloped soils but also to P limitation during retrogression. In soils a potential source of urea, the substrate of the urease, could be the degradation of nucleic acids such as DNA that contain phosphate compounds (Hasan 2000). The DNA concentrations in topsoils of the Franz Josef chronosequence increased up to 12 kyr and decreased in later stages, whereas the proportion of DNA on total OP content increased to ~25% at the oldest site (Turner et al. 2007). Thus, DNA degradation might represent an important P source in the older P limited soils releasing urea that stimulates the urease activity.

Overall, the results of enzyme activity measurements indicated that soil microorganisms in soil profiles along the Franz Josef chronosequence were adapted to the specific habitat conditions, especially in older nutrient-depleted soils. Microbial biomass provides an important N and P source during ecosystem retrogression (Turner et al. 2013) because of the small amount of allochthonous SOM when compared to progressive development stages. Thus, enzyme activities were up-regulated (i.e. ON-normalized aminopeptidases and urease as well as OP-normalized phosphatase) to immediately recycle nutrients hold in this biomass pool to prevent their loss e.g. by leaching due to high precipitation.

2.4 Abundances and community composition of nitrogen cycling microorganisms are significantly affected by long-term ecosystem development due to the soil nutrient and mineralogical gradients (manuscript 3)

The abundances of soil microorganisms involved in N cycling using different substrate types were quantified via qPCR of N functional genes, i.e. the archaeal and bacterial *amoA* gene for the ammonia oxidizers conducting the first step of nitrification, the *narG* gene for nitrate reducers, and the *chiA* gene for bacterial chitin degraders with chitin representing a complex ON compound common in soils. The abundances of ammonia-oxidizing prokaryotes were quantitatively dominated by the *Archaea* in soil depth profiles along the Franz Josef chronosequence, whereas bacterial ammonia oxidizers were only detected in the youngest soil (0.06 kyr). Acidic soils (pH < 5.5) were normally dominated by AOA (Prosser & Nicol 2012, Stempfhuber et al. 2015) explaining their dominance in most soils along the Franz Josef chronosequence (0.5 – 120 kyr) with a pH ranging from 3.8 to 5.6, while the pH of the youngest soil ranged from 5.8 to 6.4. However, archaeal *amoA* gene abundances were low or below detection limits in organic topsoils, while they were highest in mineral topsoils and decreased with soil depth. Archaeal *amoA* gene abundances were almost two orders of magnitude lower in the two oldest soils (60 and 120 kyr) in mineral topsoils, similar to their patterns in subsoil horizons (as discussed below).

In contrast to archaeal *amoA*, *narG* and *chiA* gene abundances showed highest values in organic topsoils increasing during ecosystem progression (0.06 to 12 kyr) and decreasing during retrogression (60 to 120 kyr). This pattern coincides with patterns of general microbial abundances (manuscript 1) and activities of N-hydrolyzing enzymes (manuscript 2, Allison et al. 2007) as well as long-term vegetation development (Richardson et al. 2004). Thus, the high amount of SOM input via plant litter at intermediate-aged sites seem to stimulate not only microbial abundances and activities in general, but also increase abundances of nitrate reducers with the *narG* gene being widespread among heterotrophs and abundances of chitin degraders being important in ON mineralization (Beier & Bertilsson 2013). In line with this finding and similar to previous studies about topsoils of glacier forelands, the abundances of

narG and *chiA* genes were strongly correlated with soil OC and ON content (Kandeler et al. 2006, Zeng et al. 2016).

To analyze the proportion of N functional gene abundances on total microbial communities, the N functional gene copy numbers were normalized to TCC. In topsoils, the TCC-normalized archaeal *amoA* gene abundances were similar to their soil mass counterparts being two orders of magnitude lower in the two oldest soils (A horizons), whereas TCC-normalized *narG* and *chiA* gene abundances were highest at these sites. However, extreme P limitation in older soils causes nutrient-poor conditions that should favor *Archaea* over *Bacteria* as shown for example by a dominance of AOA in low-ammonium habitats compared to AOB (Leininger et al. 2006, Di et al. 2010, Prosser & Nicol 2012). But with regard to P, a previous study reported that P addition in P-deficient soils did not affect archaeal *amoA* gene abundances in line with the results of the microcosm incubation experiment using A horizons of the Franz Josef chronosequence (Chen et al. 2016, manuscript 4). Similarly, *narG* gene abundances were not affected or even decreased by P addition, whereas *chiA* gene abundances were increased (Ma et al. 2016, manuscript 4). Interestingly, the phosphatase activity per C_{mic} was highest in topsoils of the 120 kyr site indicating an adaptation of topsoil microbial communities to the extreme P limited conditions by being able to use efficiently the small amounts of P input via plant litter or recycled from dead microbial biomass (Turner et al. 2013, manuscript 2). Therefore, heterotrophic bacteria including *narG* and *chiA* functional groups might constitute a higher proportion on the total microbial communities in the oldest topsoils compared to AOA.

In subsoils, as already mentioned above, archaeal *amoA* abundances also decreased in the two oldest soils, although AOA are well adapted to low-substrate and low-energy conditions prevailing in subsoils, e.g. by coupling ammonia oxidation with an highly energy-efficient CO_2 -fixation pathway (Könneke et al. 2014). With ongoing soil development, subsoils were enriched in clay content and Fe and Al oxides providing mineral surfaces that could interact with SOM. While negatively charged surfaces of clay minerals could bind the positively charged ammonium or fix it in their interlayers, Fe and Al oxides preferentially adsorb OP in comparison to OC compounds (Kaiser 2001, Mikutta et al. 2011, Nieder et al.

2011, Swenson et al. 2015). As a result, the already depleted contents of ammonium and OP in old subsoils might be additionally constrained in their availability due to the interactions with the soil minerals and therefore resulted in decreased AOA abundances. This explanation match with the negative relationship between soil clay content and archaeal *amoA* abundances as well as the positive relationship between OP content and archaeal *amoA* abundances and with findings of the microcosm incubation experiment where high contents of clay and Fe and Al oxides coincided with low archaeal *amoA* abundances (manuscript 4).

Similarly, the *narG* gene abundances showed a significant soil age effect in subsoils and were minimal at the 60 and 120 kyr site, although nitrate is highly mobile in soils and hardly interacts with soil minerals. However, due to the low SOM content subsoil microbial communities could be energy-limited (Fontaine et al. 2007). Thus, the abundances of nitrate reducers being mostly heterotrophs could be decreased by the interaction of soil minerals with the low amount of SOM resulting in constrained substrate availability, especially in the old soils of the Franz Josef chronosequence. In line with this assumption, total N (TN)-normalized *narG* gene abundances were positively correlated to soil OC and ON content, whereas they were negatively related to soil mineralogical properties such as the content of Fe_{d-o}.

In contrast, the soil mass related and TN-normalized *chiA* gene abundances remained almost constant with ongoing soil development in subsoils. While the soil age affected *chiA* gene abundances in A horizons in line with the results of the microcosm incubation experiment (manuscript 4), in subsoil horizons this age effect was less pronounced. Although the increasing content of Fe and Al oxides and other clay-sized minerals might constrain the substrate availability of chitin as an ON compound (Pronk et al. 2013, Dippold et al. 2014), thus possibly decrease *chiA* gene abundances, this result suggests that *chiA* genes may originate from inactive chitin-degraders. In soils, active chitin-degrading bacteria are often affiliated with the *Actinomycetes* (Williamson et al. 2000, Beier & Bertilsson 2013) being aerobes and spore-formers. Thus, *chiA* genes detected in subsoils horizons may derive from chitin-degraders of the overlaying topsoils horizons that were vertically transported by high precipitation and probably form spores or be inactive in subsoils due to the unfavorable conditions.

By the example of the archaeal *amoA* gene, patterns of functional community composition during long-term ecosystem development were investigated via clone libraries and resulted in five OTUs (threshold distance 0.09). Similar to changes in functional AOA community composition during early soil development (Hernández et al. 2014, Zeng et al. 2016), archaeal *amoA* community composition along the Franz Josef chronosequence changed from a dominance of OTU1 and OTU2 at the younger sites (0.5 and 5 kyr), OTU1 and OTU4 at the intermediate-aged site (12 kyr), to OTU1 and OTU3 at the oldest site (120 kyr). In comparison to the pronounced compositional shift in archaeal community composition based on the 16S rRNA gene (manuscript 1), the functional AOA community was similar in younger and older soils with OTUs 1, 2, 3, and 5 being affiliated to the *Nitrosotalea* cluster, while OTU4 was affiliated with the *Nitrososphaera* subcluster 7.2 and was also abundant in the intermediate-aged soil.

During early soil development across a glacier foreland with constant pH, functional AOA communities were linked to soil TN and C content (Zeng et al. 2016). However, a redundancy analysis (RDA) with forward selection of soil properties that explained most of the variation in functional AOA community composition along the Franz Josef chronosequence resulted in highest values for pH (24.3%, $P = 0.11$), soil age (21.6%, $P = 0.08$), and ammonium content (23.6%, $P = 0.03$). In line with this result, Tripathi et al. (2015) reported that pH and ammonium content significantly affected AOA community composition in temperate biomes. Similarly, in a Scottish soil survey with 71 environmental variables, pH and N fertilizer input explained most of AOA community composition variation (Yao et al. 2013). The occurrence of members of the *Nitrosotalea* cluster and *Nitrososphaera* subcluster is also highly dependent on soil pH; while the *Nitrosotalea* cluster is dominant in some acidic soils, particular *Nitrososphaera* subcluster show preference for specific pH ranges and could be dominant in acidic, acido-neutral, and alkaline soils (Gubry-Rangin et al. 2011, Pester et al. 2012, Stempfhuber et al. 2015).

2.5 Nitrogen cycling activities and nitrogen functional gene abundances are reduced due to an increasing influence of the soil mineral phase in mineral soils during long-term soil development (manuscript 4)

To evaluate the influence of soil properties, that changes along a long-term ecosystem development gradient, on microbial N cycling and N functional gene abundances in mineral soils a microcosm incubation experiment was conducted. Because most N in mineral soil is associated with minerals, it was tested in particular if mineral-associated N is an important bioavailable N source for soil microorganisms and what factors (soil age, O₂ status, phosphate addition and priming via cellulose addition) determine its bioavailability in comparison to bulk soil N. Therefore, soils samples were density fractionated with the HF mainly containing the mineral-associated SOM fraction.

During the 125 d incubation period the inorganic N (N_{min}) released upon mineralization of the HF was 4 – 23 times higher than the initial N_{min} content, indicating that mineral-associated N was the main source of bioavailable N for soil microorganisms in the tested A horizons. This finding was supported by positive net N mineralization rates and detectable microbial biomass N (N_{mic}) and N functional gene abundances in HF samples, as well as a tendency towards higher N₂ production and higher nitrate consumption under anoxic conditions in HF samples when compared to bulk soil. While in another short 18 h incubation experiment N was hardly incorporated in the HF (Compton & Boone 2002), results of a further long-term incubation experiment lasting for 300 d revealed a significant N mineralization in the HF (Swanston et al. 2004) in line with the findings of manuscript 4 suggesting that mineral-associated N is relevant as long-term N source for soil microorganisms.

Microbial N cycling activities and N functional gene abundances differed significantly between the HF and bulk soil samples. Interestingly, net N mineralization of HF samples was twice as high as in bulk samples corresponding to similar results for soil fractions of different forest types (Sollins et al. 1984). However, Swanston et al. (2004) measured values of net N mineralization for the HF that were half as high as for bulk soil. These differences might be explained by differences in the amount of immobilized ammonium, thus, while both fraction mineralize a considerable amount of ON, more of the produced

positively charged ammonium ion was adsorbed to negatively charged clay minerals or fixed into their interlayers in HF samples resulting in a lower bioavailability and lower microbial immobilization (Russow et al. 2008, Nieder et al. 2011). Thereby, the strength of this stabilizing effect may depend on the proportion of the HF in bulk soils as the absolute amount of minerals was higher in the HF incubations (since bulk soils still contained the LF). Hence, a varying proportion of the HF on bulk soil might explain the different results in net N mineralization with 95 wt% of HF in this experiment compared to 67 – 92 wt% of Swanston et al. (2004). In addition, Sollins et al. (1984) suggested that LF-SOM could be faster mineralized by soil microorganisms resulting in overall higher amounts of microbially immobilized N in bulk samples. Both explanations would imply higher respirations rates in bulk soils than in HF that is true for most of this incubation samples (manuscript 4).

One of the most important controls on microbial N cycling of mineral-associated N was the soil age in this incubation experiment. To account for soil age-related effects that were not connected to differences in initial C and N content, all measured, numerical parameters were normalized to initial soil C or N content. Therefore, differences between soil ages were most likely caused by the mineralogical or P gradient developing during soil pedogenesis. However, the influence of P was additionally tested by a P addition treatment and discussed below. The chosen A horizons (0.5, 5, 12, and 120 kyr) were characterized by an opposite trend in soil mineralogy when compared to mineral soil stocks up to one meter soil depth along the Franz Josef chronosequence. Young A horizon soils (0.5 and 5 kyr) possessed a higher content of clay and secondary Fe and Al phases, thus, could stabilize ON and ammonium more efficiently. In accordance with this, lower net N mineralization rates and lower archaeal *amoA* and *chiA* gene copy numbers in the younger soils (0.5 and 5 kyr) as compared to the older soils (12 and 120 kyr) suggested a decreased bioavailability of N resulting in an inhibition of microbial N cycling and related abundances due to the soil mineral phase. Correspondingly, a sorption experiment with alanine and different clay minerals and Fe oxides revealed that the bioavailability of sorbed alanine was lowest for the Fe oxides (Dippold et al. 2014). Moreover, N-containing compounds, such as proteins, were preferentially accumulated in stabilized SOM due to an interaction with metal oxides, especially at pH < 7 (Knicker

2011, Pronk et al. 2013). In contrast, net nitrification and *narG* gene copy numbers, both linked to nitrate transformation processes, were hardly affected by soil age. While ammonium ions could be constrained by interaction with soil mineral surfaces, nitrate as a negatively charged ion is even in the presence of soil minerals highly bioavailable (Heckman et al. 2013). Consequently, nitrate dependent processes and related gene abundances were hardly impacted by the soil mineral phase.

The microbial utilization of mineral-associated N was primarily controlled by the O₂ status. Most measured N cycling activities and N functional gene abundances as well as respiration rates and microbial biomass were many times higher (lower for N₂ and N₂O production) under oxic than under anoxic conditions. In general, the redox regime acts as a master control on microbial N transformation pathways by specifically inhibiting or stimulating aerobic or anaerobic processes (Pett-Ridge et al. 2006). Although, the O₂ status had a similar effect on microbial N cycling activities in bulk soil and the HF, the effect size was greater for the HF, especially for net N mineralization (and net nitrification). Additionally, for HF samples the effect of soil age was greater under anoxic conditions. These observations indicate that under anoxic conditions, where energy is limited for microorganisms, the influence of soil mineralogical properties on net N mineralization is more pronounced, because in general the utilization of mineral-associated N might be linked to energy allocation. Examples for energy-depend processes are the production of organic or inorganic acids resulting in mineral dissolution and release of SOM or the production of highly sorptive metabolites serving as substitutes (Uroz et al. 2011, Swenson et al. 2015). However, this does not apply for nitrate-consuming activities and related functional abundances as reflected by higher N₂ production and *narG* gene copy numbers under anoxic conditions in the HF as compared to bulk soil. Overall, the substrate type and characteristics (ON, ammonium or nitrate) determines how bioavailable the substrate is for soil microorganisms with the O₂ status being an important switch that controls the N pathway type and thus the preferred substrate type.

Contrary to expectations, N₂O production could only be detected in bulk samples under anoxic conditions. Because of the low initial soil nitrate concentration low N₂O production rates could be expected in general with lower values for bulk soils due to a higher C availability (reflected by higher

respiration rates) that would favor the complete reduction pathway towards N₂ (Senbayram et al. 2012). The differences between expected and measured results may be connected to the community composition of nitrate reducers. Likewise, soil-age related differences in N₂O production rates with higher values at 5 and 120 kyr may be related to differences in microbial community composition corresponding to the findings of the community fingerprinting via T-RFLP that showed a pronounced age effect for archaeal communities and a weak age effect for bacterial communities. In line with this assumption Wallenstein et al. (2006) and reference therein reported that different soils with contrasting N₂O to N₂ ratios possessed different denitrifier communities. Furthermore, there is evidence that the soil AOA *Nitrososphaera viennensis* is capable to produce N₂O via co-denitrification under oxygen-depleted conditions corresponding to archaeal *amoA* genes detected also under anoxic conditions in the incubation samples (Spott et al. 2011).

The effect of P addition was minor when compared to O₂ status and soil age, nevertheless, net N mineralization was significantly enhanced in HF samples of older, P limited soils, especially under oxic conditions. Previous studies showed that OP and TP were preferentially adsorbed by Fe and Al oxides most likely decreasing their bioavailability (Heckman et al. 2013, Swenson et al. 2015). Consequently, in the already P-depleted, older soils of the Franz Josef chronosequence P availability is aggravated by mineral interactions and, thus, P addition may mitigate P limitation in mineral-enriched HF samples thereby stimulating net N mineralization activity, whereas bulk samples were not influenced by P addition. Consistently, net N mineralization rates in soils of a pot experiment and in a field fertilization study were also stimulated by P addition (Falkiner et al. 1993; calculated from Baral et al. 2014).

Previous studies indicated that the decomposition of subsoil SOM, mainly composed of MOM, could be stimulated by the addition of an easily available C source such as cellulose; this effect is termed “priming effect” (Fontaine et al. 2007, Wild et al. 2014). Therefore, the influence of ¹³C-labeled cellulose on microbial cycling in the HF was tested by differentiating between cellulose- and SOM-derived CO₂ production. In general, mineralization of mineral-associated SOM showed a tendency to be positively primed under oxic conditions reflected by higher SOM-derived CO₂ production in C treatments as

compared to the treatment without any additions. However, net N mineralization was lower in C treatments probably due to higher microbial N immobilization (Vinten et al. 2002). Similarly, Colman & Schimel (2013) confirmed in a study with 84 mineral soils under different vegetation types, that C content was one of the most important drivers of net N mineralization with a negative relationship. Overall, while C cycling was stimulated by the cellulose amendment, the utilization of mineral-associated N was rather inhibited under oxic conditions pointing to a shift from N to a more pronounced C cycling including N immobilization (Colman & Schimel 2013). Thus, N cycling related processes may be inhibited by cellulose addition providing an easy-degradable C-rich, but N free substrate.

In summary, results of the microcosm incubation experiment revealed that the soil mineral phase could considerably reduce microbial N cycling activities and related functional abundances probably by constraining substrate availability due to SOM-mineral interactions. Nevertheless, mineral-associated N provides an important and bioavailable N source for soil microorganisms in mineral soils.

2.6 Conclusion

This thesis provided for the first time insights into microbial dynamics during long-term ecosystem development in whole soil profiles. The results revealed that microbial abundances and communities are not only changing during early ecosystem and soil development, but also during long-term development including retrogression with an increasing quantitative relevance of *Archaea* in subsoils, particularly in older P limited soils, and a pronounced compositional shift of archaeal community composition compared to rather stable bacterial communities. While archaeal abundances were hardly affected by soil age-related changes in mineralogical properties or nutrient contents, the shift in archaeal community composition was most likely linked to the mineralogical gradient along the soil chronosequence. Thus, archaeal communities might better cope with nutrient-poor, low-energy conditions combined with mineral-induced substrate limitation in subsoils and old soils due to a selection for taxa being adapted to these conditions such as for example the *Bathyarchaeota*.

Similarly, activities and abundances of N cycling microbial communities change significantly with ecosystem progression and retrogression in top- and subsoils. Most N cycling related abundances and activities were maximal at intermediate-aged sites (1 – 12 kyr) in topsoils, but decreased at older sites (60 – 120 kyr) in top- and subsoils. Further, there was strong evidence that microbial N cycling is not only affected by substrate content, but could be also decreased by the increasing content of Fe and Al oxides and other clay-sized minerals during soil development. Although (O)N is predominantly associated with soil minerals, particularly in subsoil, it is still available for microbial utilization, however, with the availability being linked to substrate type and soil mineralogy.

Overall, this thesis indicates that the ecosystem and soil development stage linked to different soil characteristics have a significant impact on microbial communities and microbial N cycling thereby affecting soil fertility and ecosystem productivity.

3 References

- Achat DL, Augusto L, Bakker MR, Gallet-Budynek A, Morel C (2012) Microbial processes controlling P availability in forest spodosols as affected by soil depth and soil properties. *Soil Biol Biochem* 44:39–48.
- Aerssens E, Tiedje JM, Averill BA (1986) Isotope labelling studies on the mechanisms of N-N bond formation in denitrification. *J Biol Chem* 261:9652–9656.
- Ajwa HA, Rice CW, Sotomayor D (1998) Carbon and nitrogen mineralization in tallgrass prairie and agricultural soil profiles. *Soil Sci Soc Am J* 62:942–951.
- Allison SD (2006) Soil minerals and humic acids alter enzyme stability: Implications for ecosystem processes. *Biogeochemistry* 81:361–373.
- Allison VJ, Condron LM, Peltzer DA, Richardson SJ, Turner BL (2007) Changes in enzyme activities and soil microbial community composition along carbon and nutrient gradients at the Franz Josef chronosequence, New Zealand. *Soil Biol Biochem* 39:1770–1781.
- Almond PC, Moar NT, Lian OB (2001) Reinterpretation of the glacial chronology of South Westland, New Zealand. *New Zeal J Geol Geophys* 44:1–15.
- Aon MA, Colaneri A. (2001) II. Temporal and spatial evolution of enzymatic activities and physico-chemical properties in an agricultural soil. *Appl Soil Ecol* 18:255–270.
- Auguet J-C, Barberan A, Casamayor EO (2010) Global ecological patterns in uncultured Archaea. *ISME J* 4:182–190.
- Babin D, et al. (2013) Metal oxides, clay minerals and charcoal determine the composition of microbial communities in matured artificial soils and their response to phenanthrene. *FEMS Microbiol Ecol* 86:3–14.
- Baggs EM (2011) Soil microbial sources of nitrous oxide: Recent advances in knowledge, emerging challenges and future direction. *Curr Opin Environ Sustain* 3:321–327.
- Bai R, et al. (2015) Activity, abundance and community structure of anammox bacteria along depth profiles in three different paddy soils. *Soil Biol Biochem* 91:212–221.
- Baker BJ, et al. (2016) Genomic inference of the metabolism of cosmopolitan subsurface Archaea, Hadesarchaea. *Nat Microbiol* 1:16002.
- Baldrian P, et al. (2012) Active and total microbial communities in forest soil are largely different and highly stratified during decomposition. *ISME J* 6:248–258.
- Balestrini R, Lumini E, Borriello R, Bianciotto V (2015) Plant-soil biota interactions. *Soil Microbiology, Ecology, and Biochemistry*, ed Paul EA (Academic Press, Amsterdam, Boston,

Heidelberg, London, New York, Oxford, Paris, San Diego, San Francisco, Singapore, Sydney, Tokyo), pp 311–338.

- Baral BR, Kuyper TW, Van Groenigen JW (2014) Liebig's law of the minimum applied to a greenhouse gas: Alleviation of P-limitation reduces soil N₂O emission. *Plant Soil* 374:539–548.
- Barns SM, Delwiche CF, Palmer JD, Pace NR (1996) Perspectives on archaeal diversity, thermophily and monophyly from environmental rRNA sequences. *Proc Natl Acad Sci USA* 93:9188–9193.
- Bates ST, et al. (2011) Examining the global distribution of dominant archaeal populations in soil. *ISME J* 5:908–917.
- Bayan MR, Eivazi F (1999) Selected enzyme activities as affected by free iron oxides and clay particle size. *Commun Soil Sci Plant Anal* 30:1561–1571.
- Beier S, Bertilsson S (2013) Bacterial chitin degradation - mechanisms and ecophysiological strategies. *Front Microbiol* 4:149.
- Belnap J (2003) The world at your feet: Desert biological soil crusts. *Front Ecol Environ* 1:181–189.
- Benson DR (1982) Isolation of *Frankia* strains from alder actinorhizal root nodules. *Appl Environ Microbiol* 44:461–465.
- Berendsen RL, Pieterse CMJ, Bakker PAHM (2012) The rhizosphere microbiome and plant health. *Trends Plant Sci* 17:478–486.
- Biddle JF, et al. (2006) Heterotrophic Archaea dominate sedimentary subsurface ecosystems off Peru. *Proc Natl Acad Sci USA* 103:3846–3851.
- Bimüller C, et al. (2014) Decoupled carbon and nitrogen mineralization in soil particle size fractions of a forest topsoil. *Soil Biol Biochem* 78:263–273.
- Blackwood CB, Paul EA (2003) Eubacterial community structure and population size within the soil light fraction, rhizosphere, and heavy fraction of several agricultural systems. *Soil Biol Biochem* 35:1245–1255.
- Blaško R, et al. (2015) Shifts in soil microbial community structure, nitrogen cycling and the concomitant declining N availability in ageing primary boreal forest ecosystems. *Soil Biol Biochem* 91:200–211.
- Blume HP, et al. (2010) *Scheffer/Schachtschabel Lehrbuch der Bodenkunde* (Spektrum Akademischer Verlag, Heidelberg).

- Boerner REJ, Brinkman JA, Smith A (2005) Seasonal variations in enzyme activity and organic carbon in soil of a burned and unburned hardwood forest. *Soil Biol Biochem* 37:1419–1426.
- Bomberg M, Münster U, Pumpanen J, Ilvesniemi H, Heinonsalo J (2011) Archaeal communities in boreal forest tree rhizospheres respond to changing soil temperatures. *Microb Ecol* 62:205–217.
- Bonete MJ, Martínez-Espinosa RM, Pire C, Zafrilla B, Richardson DJ (2008) Nitrogen metabolism in haloarchaea. *Saline Systems* 4:9.
- Bottomley PJ, Myrold DD (2015) Biological N inputs. *Soil Microbiology, Ecology, and Biochemistry*, ed Paul EA (Academic Press, Amsterdam, Boston, Heidelberg, London, New York, Oxford, Paris, San Diego, San Francisco, Singapore, Sydney, Tokyo), pp 447–470.
- Brankatschk R, Töwe S, Kleineidam K, Schloter M, Zeyer J (2011) Abundances and potential activities of nitrogen cycling microbial communities along a chronosequence of a glacier forefield. *ISME J* 5:1025–1037.
- Breuker A, Stadler S, Schippers A (2013) Microbial community analysis of deeply buried marine sediments of the New Jersey shallow shelf (IODP Expedition 313). *FEMS Microbiol Ecol* 85:578–592.
- Brochier-Armanet C, Boussau B, Gribaldo S, Forterre P (2008) Mesophilic crenarchaeota: Proposal for a third archaeal phylum, the Thaumarchaeota. *Nat Rev Microbiol* 6:245–252.
- Brown SP, Jumpponen A (2014) Contrasting primary successional trajectories of fungi and bacteria in retreating glacier soils. *Mol Ecol* 23:481–497.
- Buckley DH, Graber JR, Schmidt TM (1998) Phylogenetic analysis of nonthermophilic members of the kingdom Crenarchaeota and their diversity and abundance in soils. *Appl Environ Microbiol* 64:4333–4339.
- Burns RG, et al. (2013) Soil enzymes in a changing environment: Current knowledge and future directions. *Soil Biol Biochem* 58:216–234.
- Caldwell BA (2005) Enzyme activities as a component of soil biodiversity: A review. *Pedobiologia* 49:637–644.
- Cavaletti L, et al. (2006) New lineage of filamentous, spore-forming, gram-positive bacteria from soil. *Appl Environ Microbiol* 72:4360–4369.
- Chen Y, et al. (2016) Nitrogen mineralization as a result of phosphorus supplementation in long-term phosphate deficient soil. *Appl Soil Ecol* 106:24–32.
- Chroňáková A, et al. (2015) Response of archaeal and bacterial soil communities to changes associated with outdoor cattle overwintering. *PLoS One* 10:e0135627.

- Colliver BB, Stephenson T (2000) Production of nitrogen oxide and dinitrogen oxide by autotrophic nitrifiers. *Biotechnol Adv* 18:219–232.
- Colman BP, Schimel JP (2013) Drivers of microbial respiration and net N mineralization at the continental scale. *Soil Biol Biochem* 60:65–76.
- Compton JE, Boone RD (2002) Soil nitrogen transformations and the role of light fraction organic matter in forest soils. *Soil Biol Biochem* 34:933–943.
- Cretoiu MS, Berini F, Kielak AM, Marinelli F, van Elsas JD (2015) A novel salt-tolerant chitinase discovered by genetic screening of a metagenomic library derived from chitin-amended agricultural soil. *Appl Microbiol Biotechnol* 99:8199–8215.
- Daims H, et al. (2015) Complete nitrification by *Nitrospira* bacteria. *Nature* 528:504–509.
- Davies LO, et al. (2013) Light structures phototroph, bacterial and fungal communities at the soil surface. *PLoS One* 8:e69048.
- de Gannes V, Eudoxie G, Bekele I, Hickey WJ (2015) Relations of microbiome characteristics to edaphic properties of tropical soils from Trinidad. *Front Microbiol* 6:1045.
- Dennis PG, Miller AJ, Hirsch PR (2010) Are root exudates more important than other sources of rhizodeposits in structuring rhizosphere bacterial communities? *FEMS Microbiol Ecol* 72:313–327.
- Di HJ, et al. (2010) Ammonia-oxidizing bacteria and archaea grow under contrasting soil nitrogen conditions. *FEMS Microbiol Ecol* 72:386–394.
- Dietel J, et al. (2017) Complexity of clay mineral formation during 120,000 years of soil development along the Franz Josef chronosequence, New Zealand. *New Zeal J Geol Geophys* doi:10.1080/00288306.2016.1245668.
- Dini-Andreote F, et al. (2014) Dynamics of bacterial community succession in a salt marsh chronosequence: Evidences for temporal niche partitioning. *ISME J* 8:1989–2001.
- Dippold M, Biryukov M, Kuzyakov Y (2014) Sorption affects amino acid pathways in soil: Implications from position-specific labeling of alanine. *Soil Biol Biochem* 72:180–192.
- Ehrich S, Behrens D, Lebedeva E, Ludwig W, Bock E (1995) A new obligately chemolithoautotrophic, nitrite-oxidizing bacterium, *Nitrospira moscoviensis* sp. nov. and its phylogenetic relationship. *Arch Microbiol* 164:16–23.
- Eilers KG, Debenport S, Anderson S, Fierer N (2012) Digging deeper to find unique microbial communities: The strong effect of depth on the structure of bacterial and archaeal communities in soil. *Soil Biol Biochem* 50:58–65.

- Falkiner RA, Khanna PK, Raison RJ (1993) Effect of superphosphate addition on N mineralization in some Australian forest soils. *Aust J Soil Res* 31:285–296.
- Fierer N, Bradford MA, Jackson RB (2007) Toward an ecological classification of soil bacteria. *Ecology* 88:1354–1364.
- Fierer N, Schimel JP, Holden PA (2003) Variations in microbial community composition through two soil depth profiles. *Soil Biol Biochem* 35:167–176.
- Fierer N, Strickland MS, Liptzin D, Bradford MA, Cleveland CC (2009) Global patterns in belowground communities. *Ecol Lett* 12:1238–1249.
- Fontaine S, et al. (2007) Stability of organic carbon in deep soil layers controlled by fresh carbon supply. *Nature* 450:277–280.
- Franzmann PD, Skerman VB (1984) *Gemmata obscuriglobus*, a new genus and species of the budding bacteria. *Antonie Van Leeuwenhoek* 50:261–268.
- Fry JC, Parkes RJ, Cragg BA, Weightman AJ, Webster G (2008) Prokaryotic biodiversity and activity in the deep seafloor biosphere. *FEMS Microbiol Ecol* 66:181–196.
- Geisseler D, Horwath WR, Joergensen RG, Ludwig B (2010) Pathways of nitrogen utilization by soil microorganisms - A review. *Soil Biol Biochem* 42:2058–2067.
- Gentsch N, et al. (2015) Properties and bioavailability of particulate and mineral-associated organic matter in Arctic permafrost soils, Lower Kolyma Region, Russia. *Eur J Soil Sci* 66:722–734.
- Gianfreda L, Rao MA, Violante A (1992) Adsorption, activity and kinetic properties of urease on montmorillonite, aluminium hydroxide and Al(OH)_x-montmorillonite complexes. *Soil Biol Biochem* 24:51–58.
- Gittel A, et al. (2014a) Distinct microbial communities associated with buried soils in the Siberian tundra. *ISME J* 8:841–53.
- Gittel A, et al. (2014b) Site- and horizon-specific patterns of microbial community structure and enzyme activities in permafrost-affected soils of Greenland. *Front Microbiol* 5:541.
- Gubry-Rangin C, et al. (2011) Niche specialization of terrestrial archaeal ammonia oxidizers. *Proc Natl Acad Sci USA* 108:21206–21211.
- Hansel CM, Fendorf S, Jardine PM, Francis CA (2008) Changes in bacterial and archaeal community structure and functional diversity along a geochemically variable soil profile. *Appl Environ Microbiol* 74:1620–1633.

- Hartmann M, Lee S, Hallam SJ, Mohn WW (2009) Bacterial, archaeal and eukaryal community structures throughout soil horizons of harvested and naturally disturbed forest stands. *Environ Microbiol* 11:3045–3062.
- Hasan HAH (2000) Ureolytic microorganisms and soil fertility: A review. *Commun Soil Sci Plant Anal* 31:2565–2589.
- Hawkins AN, Johnson KW, Bräuer SL (2014) Southern Appalachian peatlands support high archaeal diversity. *Microb Ecol* 67:587–602.
- Heckman K, et al. (2013) The influence of goethite and gibbsite on soluble nutrient dynamics and microbial community composition. *Biogeochemistry* 112:179–195.
- Hemkemeyer M, et al. (2014) Artificial soil studies reveal domain-specific preferences of microorganisms for the colonisation of different soil minerals and particle size fractions. *FEMS Microbiol Ecol* 90:770–782.
- Hernández M, Dumont MG, Calabi M, Basualto D, Conrad R (2014) Ammonia oxidizers are pioneer microorganisms in the colonization of new acidic volcanic soils from South of Chile. *Environ Microbiol Rep* 6:70–79.
- Holden PA, Fierer N (2005) Microbial processes in the vadose zone. *Vadose Zo J* 4:1–21.
- Hug LA, et al. (2016) A new view of the tree of life. *Nat Microbiol* 1:16048.
- Humbert S, Zopfi J, Tarnawski S-E (2012) Abundance of anammox bacteria in different wetland soils. *Environ Microbiol Rep* 4:484–490.
- Iino T, et al. (2013) *Candidatus Methanogranum caenicola*: A novel methanogen from the anaerobic digested sludge, and proposal of *Methanomassiliicoccaceae* fam. nov. and *Methanomassiliicoccales* ord. nov., for a methanogenic lineage of the class *Thermoplasmata*. *Microbes Environ* 28:244–250.
- IUSS Working Group WRB (2006) World Reference Base for Soil Resources 2006. World Soil Resources Report No. 103 (FAO, Rome).
- Jangid K, Whitman WB, Condrón LM, Turner BL, Williams MA (2013a) Progressive and retrogressive ecosystem development coincide with soil bacterial community change in a dune system under lowland temperate rainforest in New Zealand. *Plant Soil* 367:235–247.
- Jangid K, Whitman WB, Condrón LM, Turner BL, Williams MA (2013b) Soil bacterial community succession during long-term ecosystem development. *Mol Ecol* 22:3415–3424.
- Jobbágy EG, Jackson RB (2000) The vertical distribution of soil organic carbon and its relation to climate and vegetation. *Ecol Appl* 10:423–436.

- Jones RT, et al. (2009) A comprehensive survey of soil acidobacterial diversity using pyrosequencing and clone library analyses. *ISME J* 3:442–453.
- Jurgens G, Lindström K, Saano A (1997) Novel group within the kingdom Crenarchaeota from boreal forest soil. *Appl Environ Microbiol* 63:803–805.
- Kaiser K (2001) Dissolved organic phosphorus and sulphur as influenced by sorptive interactions with mineral subsoil horizons. *Eur J Soil Sci* 52:489–493.
- Kaiser K, Guggenberger G (2000) The role of DOM sorption to mineral surfaces in the preservation of organic matter in soils. *Org Geochem* 31:711–725.
- Kaiser K, Guggenberger G (2007) Sorptive stabilization of organic matter by microporous goethite: Sorption into small pores vs. surface complexation. *Eur J Soil Sci* 58:45–59.
- Kaiser K, Zech W (2000) Sorption of dissolved organic nitrogen by acid subsoil horizons and individual mineral phases. *Eur J Soil Sci* 51:403–411.
- Kandeler E, Deiglmayr K, Tscherko D, Bru D, Philippot L (2006) Abundance of *narG*, *nirS*, *nirK*, and *nosZ* genes of denitrifying bacteria during primary successions of a glacier foreland. *Appl Environ Microbiol* 72:5957–5962.
- Kandeler E, et al. (2009) Response of total and nitrate-dissimilating bacteria to reduced N deposition in a spruce forest soil profile. *FEMS Microbiol Ecol* 67:444–454.
- Kedi B, Abadie J, Sei J, Quiquampoix H, Staunton S (2013) Diversity of adsorption affinity and catalytic activity of fungal phosphatases adsorbed on some tropical soils. *Soil Biol Biochem* 56:13–20.
- Kerstens K, et al. (2006) Introduction to the Proteobacteria. *The Prokaryotes. Volume 5: Proteobacteria: Alpha and Beta Subclasses*, eds Dworkin M, Falkow S, Rosenberg E, Schleifer K-H, Stackebrandt E (Springer, New York), pp 3–37.
- Killham K, Prosser JI (2015) The Bacteria and Archaea. *Soil Microbiology, Ecology, and Biochemistry*, ed Paul EA (Academic Press, Amsterdam, Boston, Heidelberg, London, New York, Oxford, Paris, San Diego, San Francisco, Singapore, Sydney, Tokyo), pp 41–76.
- Kleber M, et al. (2015) Mineral-organic associations: Formation, properties, and relevance in soil environments. *Adv Agron* 130:1–140.
- Knicker H (2011) Soil organic N - An under-rated player for C sequestration in soils? *Soil Biol Biochem* 43:1118–1129.
- Kögel-Knabner I, et al. (2008) Organo-mineral associations in temperate soils: Integrating biology, mineralogy, and organic matter chemistry. *J Plant Nutr Soil Sci* 171:61–82.

- Könneke M, et al. (2014) Ammonia-oxidizing archaea use the most energy-efficient aerobic pathway for CO₂ fixation. *Proc Natl Acad Sci USA* 111:8239–8244.
- Kubo K, et al. (2012) Archaea of the Miscellaneous Crenarchaeotal Group are abundant, diverse and widespread in marine sediments. *ISME J* 6:1949–1965.
- Lazar CS, et al. (2016) Genomic evidence for distinct carbon substrate preferences and ecological niches of Bathyarchaeota in estuarine sediments. *Environ Microbiol* 18:1200–1211.
- Leff JW, et al. (2015) Consistent responses of soil microbial communities to elevated nutrient inputs in grasslands across the globe. *Proc Natl Acad Sci USA* 112:10967–10972.
- Lehtovirta-Morley LE, Stoecker K, Vilcinskas A, Prosser JI, Nicol GW (2011) Cultivation of an obligate acidophilic ammonia oxidizer from a nitrifying acid soil. *Proc Natl Acad Sci USA* 108:15892–15897.
- Leininger S, et al. (2006) Archaea predominate among ammonia-oxidizing prokaryotes in soils. *Nature* 442:806–809.
- Lloyd KG, et al. (2013) Predominant archaea in marine sediments degrade detrital proteins. *Nature* 496:215–218.
- Long A, Heitman J, Tobias C, Philips R, Song B (2013) Co-occurring anammox, denitrification, and codenitrification in agricultural soils. *Appl Environ Microbiol* 79:168–176.
- Ma W, et al. (2016) Response of microbial functional groups involved in soil N cycle to N, P and NP fertilization in Tibetan alpine meadows. *Soil Biol Biochem* 101:195–206.
- Marhan S, et al. (2011) Abundance and activity of nitrate reducers in an arable soil are more affected by temporal variation and soil depth than by elevated atmospheric [CO₂]. *FEMS Microbiol Ecol* 76:209–219.
- Mateos-Rivera A, et al. (2016) The effect of temperature change on the microbial diversity and community structure along the chronosequence of the sub-arctic glacier forefield of Styggedalsbreen (Norway). *FEMS Microbiol Ecol* 92:fnw038.
- Meng J, et al. (2014) Genetic and functional properties of uncultivated MCG archaea assessed by metagenome and gene expression analyses. *ISME J* 8:650–659.
- Menge DNL, Hedin LO, Pacala SW (2012) Nitrogen and phosphorus limitation over long-term ecosystem development in terrestrial ecosystems. *PLoS One* 7:e42045.
- Mergel A, Schmitz O, Mallmann T, Bothe H (2001) Relative abundance of denitrifying and dinitrogen-fixing bacteria in layers of forest soil. *FEMS Microbiol Ecol* 36:33–42.
- Merrill GP (1906) *A treatise on rocks, rock-weathering and soils* (The MacMillan Company, New York).

- Mikutta R, et al. (2007) Biodegradation of forest floor organic matter bound to minerals via different binding mechanisms. *Geochim Cosmochim Acta* 71:2569–2590.
- Mikutta R, et al. (2009) Biogeochemistry of mineral-organic associations across a long-term mineralogical soil gradient (0.3–4100 kyr), Hawaiian Islands. *Geochim Cosmochim Acta* 73:2034–2060.
- Mikutta R, Zang U, Chorover J, Haumaier L, Kalbitz K (2011) Stabilization of extracellular polymeric substances (*Bacillus subtilis*) by adsorption to and coprecipitation with Al forms. *Geochim Cosmochim Acta* 75:3135–3154.
- Miltner A, Bombach P, Schmidt-Brücken B, Kästner M (2012) SOM genesis: Microbial biomass as a significant source. *Biogeochemistry* 111:41–55.
- Nannipieri P, Smalla K (2006) *Nucleic acids and proteins in soil*, eds Nannipieri P, Smalla K (Springer-Verlag, Berlin, Heidelberg, New York).
- Nemergut DR, et al. (2007) Microbial community succession in an unvegetated, recently deglaciated soil. *Microb Ecol* 53:110–122.
- Nemergut DR, Cleveland CC, Wieder WR, Washenberger CL, Townsend AR (2010) Plot-scale manipulations of organic matter inputs to soils correlate with shifts in microbial community composition in a lowland tropical rain forest. *Soil Biol Biochem* 42:2153–2160.
- Nieder R, Benbi DK, Scherer HW (2011) Fixation and defixation of ammonium in soils: A review. *Biol Fertil Soils* 47:1–14.
- Norton JM (2011) Diversity and environmental distribution of ammonia-oxidizing bacteria. *Nitrification*, eds Ward BB, Arp DJ, Klotz MG (ASM Press, Washington), pp 39–55.
- Ochsenreiter T, Selezi D, Quaiser A, Bonch-Osmolovskaya L, Schleper C (2003) Diversity and abundance of Crenarchaeota in terrestrial habitats studied by 16S RNA surveys and real time PCR. *Environ Microbiol* 5:787–797.
- Odum EP (1969) The strategy of ecosystem development. *Science* 164:262–270.
- Offre P, Spang A, Schleper C (2013) Archaea in biogeochemical cycles. *Annu Rev Microbiol* 67:437–457.
- Onodera Y, Nakagawa T, Takahashi R, Tokuyama T (2010) Seasonal change in vertical distribution of ammonia-oxidizing archaea and bacteria and their nitrification in temperate forest soil. *Microbes Environ* 25:28–35.
- Oton EV, Quince C, Nicol GW, Prosser JI, Gubry-Rangin C (2016) Phylogenetic congruence and ecological coherence in terrestrial Thaumarchaeota. *ISME J* 10:85–96.

- Paul K, Nonoh JO, Mikulski L, Brune A (2012) “*Methanoplasmatales*,” *Thermoplasmatales*-related archaea in termite guts and other environments, are the seventh order of methanogens. *Appl Environ Microbiol* 78:8245–8253.
- Peltzer DA, et al. (2010) Understanding ecosystem retrogression. *Ecol Monogr* 80:509–529.
- Pester M, et al. (2012) *amoA*-based consensus phylogeny of ammonia-oxidizing archaea and deep sequencing of *amoA* genes from soils of four different geographic regions. *Environ Microbiol* 14:525–539.
- Pett-Ridge J, Silver WL, Firestone MK (2006) Redox fluctuations frame microbial community impacts on N-cycling rates in a humid tropical forest soil. *Biogeochemistry* 81:95–110.
- Pinggera J, Geisseler D, Piepho HP, Joergensen RG, Ludwig B (2015) Effect of substrate quality on the N uptake routes of soil microorganisms in different soil depths. *Pedobiologia* 58:211–218.
- Pronk GJ, Heister K, Kögel-Knabner I (2013) Is turnover and development of organic matter controlled by mineral composition? *Soil Biol Biochem* 67:235–244.
- Prosser JI, Nicol GW (2012) Archaeal and bacterial ammonia-oxidisers in soil: The quest for niche specialisation and differentiation. *Trends Microbiol* 20:523–531.
- Quiquampoix H, Staunton S, Baron M-H, Ratcliffe RG (1993) Interpretation of the pH dependence of protein adsorption on clay mineral surfaces and its relevance to the understanding of extracellular enzyme activity in soil. *Colloids Surfaces A Physicochem Eng Asp* 75:85–93.
- Rabinovich ML, Bolobova AV, Vasil’chenko LG (2004) Fungal decomposition of natural aromatic structures and xenobiotics: A review. *Appl Biochem Microbiol* 40:1–17.
- Reed SC, Cleveland CC, Townsend AR (2011) Functional ecology of free-living nitrogen fixation: A contemporary perspective. *Annu Rev Ecol Evol Syst* 42:489–512.
- Rennenberg H, et al. (2009) Nitrogen balance in forest soils: Nutritional limitation of plants under climate change stresses. *Plant Biol* 11:4–23.
- Richardson SJ, Peltzer DA, Allen RB, McGlone MS, Parfitt RL (2004) Rapid development of phosphorus limitation in temperate rainforest along the Franz Josef soil chronosequence. *Oecologia* 139:267–276.
- Robertson GP, Groffman PM (2015) Nitrogen transformations. *Soil Microbiology, Ecology, and Biochemistry*, ed Paul EA (Academic Press, Amsterdam, Boston, Heidelberg, London, New York, Oxford, Paris, San Diego, San Francisco, Singapore, Sydney, Tokyo), pp 421–446.
- Roesch LFW, et al. (2007) Pyrosequencing enumerates and contrasts soil microbial diversity. *ISME J* 1:283–290.

- Rousk J, et al. (2010) Soil bacterial and fungal communities across a pH gradient in an arable soil. *ISME J* 4:1340–1351.
- Rumpel C, Kögel-Knabner I (2011) Deep soil organic matter - a key but poorly understood component of terrestrial C cycle. *Plant Soil* 338:143–158.
- Russow R, Spott O, Stange CF (2008) Evaluation of nitrate and ammonium as sources of NO and N₂O emissions from black earth soils (Haplic Chernozem) based on ¹⁵N field experiments. *Soil Biol Biochem* 40:380–391.
- Rütting T, Boeckx P, Müller C, Klemmedtsson L (2011) Assessment of the importance of dissimilatory nitrate reduction to ammonium for the terrestrial nitrogen cycle. *Biogeosciences* 8:1779–1791.
- Schimel JP, Bennett J (2004) Nitrogen mineralization: Challenges of a changing paradigm. *Ecology* 85:591–602.
- Schipper LA, Degens BP, Sparling GP, Duncan LC (2001) Changes in microbial heterotrophic diversity along five plant successional sequences. *Soil Biol Biochem* 33:2093–2103.
- Schmidt MWI, et al. (2011) Persistence of soil organic matter as an ecosystem property. *Nature* 478:49–56.
- Schulz S, et al. (2013) The role of microorganisms at different stages of ecosystem development for soil formation. *Biogeosciences* 10:3983–3996.
- Senbayram M, Chen R, Budai A, Bakken L, Dittert K (2012) N₂O emission and the N₂O/(N₂O+N₂) product ratio of denitrification as controlled by available carbon substrates and nitrate concentrations. *Agric Ecosyst Environ* 147:4–12.
- Sexstone AJ, Revsbech NP, Parkin TB, Tiedje JM (1985) Direct measurement of oxygen profiles and denitrification rates in soil aggregates. *Soil Sci Soc Am J* 49:645–651.
- Shahriari F, Higashi T, Tamura K (2010) Effects of clay addition on soil protease activities in Andosols in the presence of cadmium. *Soil Sci Plant Nutr* 56:560–569.
- Sinsabaugh RL, Reynolds H, Long TM (2000) Rapid assay for amidohydrolase (urease) activity in environmental samples. *Soil Biol Biochem* 32:2095–2097.
- Sinsabaugh RL, et al. (2008) Stoichiometry of soil enzyme activity at global scale. *Ecol Lett* 11:1252–1264.
- Sollins P, Spycher G, Glassman CA (1984) Net nitrogen mineralization from light- and heavy-fraction soil organic matter. *Soil Biol Biochem* 16:31–37.
- Sollins P, et al. (2006) Organic C and N stabilization in a forest soil: Evidence from sequential density fractionation. *Soil Biol Biochem* 38:3313–3324.

- Sorokin DY, et al. (2012) Nitrification expanded: Discovery, physiology and genomics of a nitrite-oxidizing bacterium from the phylum *Chloroflexi*. *ISME J* 6:2245–2256.
- Spang A, et al. (2015) Complex archaea that bridge the gap between prokaryotes and eukaryotes. *Nature* 521:173–179.
- Spott O, Stange CF (2011) Formation of hybrid N₂O in a suspended soil due to co-denitrification of NH₂OH. *J Plant Nutr Soil Sci* 174:554–567.
- Spott O, Russow R, Stange CF (2011) Formation of hybrid N₂O and hybrid N₂ due to codenitrification: First review of a barely considered process of microbially mediated N-nitrosation. *Soil Biol Biochem* 43:1995–2011.
- Stein LY, Klotz MG (2016) The nitrogen cycle. *Curr Biol* 26:R94–R98.
- Steinbach A, et al. (2015) Clay minerals and metal oxides strongly influence the structure of alkane-degrading microbial communities during soil maturation. *ISME J* 9:1687–1691.
- Stempfhuber B, et al. (2015) pH as a driver for ammonia-oxidizing archaea in forest soils. *Microb Ecol* 69:879–883.
- Stevens PR (1968) A chronosequence of soils near the Franz Josef glacier. *PhD thesis Univ Canterbury, New Zeal.*
- Stevens PR, Walker TW (1970) The chronosequence concept and soil formation. *Quarterly Rev Biol* 45:333–350.
- Stieglmeier M, et al. (2014) Aerobic nitrous oxide production through N-nitrosating hybrid formation in ammonia-oxidizing archaea. *ISME J* 8:1135–1146.
- Stone MM, DeForest JL, Plante AF (2014) Changes in extracellular enzyme activity and microbial community structure with soil depth at the Luquillo Critical Zone Observatory. *Soil Biol Biochem* 75:237–247.
- Stone MM, Kan J, Plante AF (2015) Parent material and vegetation influence bacterial community structure and nitrogen functional genes along deep tropical soil profiles at the Luquillo Critical Zone Observatory. *Soil Biol Biochem* 80:273–282.
- Strous M (2011) Beyond denitrification: Alternative routes to dinitrogen. *Nitrogen Cycling in Bacteria: Molecular Analysis*, ed Moir JW (Caister Academic Press, Norfolk), pp 123–134.
- Swanston C, et al. (2004) Long-term effects of elevated nitrogen on forest soil organic matter stability. *Biogeochemistry* 70:227–250.
- Swenson TL, Bowen BP, Nico PS, Northen TR (2015) Competitive sorption of microbial metabolites on an iron oxide mineral. *Soil Biol Biochem* 90:34–41.

- Takai K, Moser DP, DeFlaun M, Onstott TC, Fredrickson JK (2001) Archaeal diversity in waters from deep South African gold mines. *Appl Environ Microbiol* 67:5750–5760.
- Tanimoto T, Hatano K, Kim D, Uchiyama H, Shoun H (1992) Co-denitrification by the denitrifying system of the fungus *Fusarium oxysporum*. *FEMS Microbiol Lett* 93:177–180.
- Tarlera S, Jangid K, Ivester AH, Whitman WB, Williams MA (2008) Microbial community succession and bacterial diversity in soils during 77 000 years of ecosystem development. *FEMS Microbiol Ecol* 64:129–140.
- Taylor JP, Wilson B, Mills MS, Burns RG (2002) Comparison of microbial numbers and enzymatic activities in surface soils and subsoils using various techniques. *Soil Biol Biochem* 34:387–401.
- Taylor LD, Sinsabaugh RL (2015) The soil fungi: Occurrence, phylogeny, and ecology. *Soil Microbiology, Ecology, and Biochemistry*, ed Paul EA (Academic Press, Amsterdam, Boston, Heidelberg, London, New York, Oxford, Paris, San Diego, San Francisco, Singapore, Sydney, Tokyo).
- Tedersoo L, et al. (2014) Global diversity and geography of soil fungi. *Science* 346:1256688.
- Töwe S, et al. (2010) Abundance of microbes involved in nitrogen transformation in the rhizosphere of *Leucanthemopsis alpina* (L.) HEYWOOD grown in soils from different sites of the Damma glacier forefield. *Microb Ecol* 60:762–770.
- Trevors JT (2010) One gram of soil: A microbial biochemical gene library. *Antonie Van Leeuwenhoek* 97:99–106.
- Tripathi BM, et al. (2015) Soil pH and biome are both key determinants of soil archaeal community structure. *Soil Biol Biochem* 88:1–8.
- Tscherko D, Rustemeier J, Richter A, Wanek W, Kandeler E (2003) Functional diversity of the soil microflora in primary succession across two glacier forelands in the Central Alps. *Eur J Soil Sci* 54:685–696.
- Tupinambá DD, et al. (2016) Archaeal community changes associated with cultivation of Amazon forest soil with oil palm. *Archaea* 2016:Article ID 3762159.
- Turner BL, Condrón LM (2013) Pedogenesis, nutrient dynamics, and ecosystem development: The legacy of T.W. Walker and J.K. Syers. *Plant Soil* 367:1–10.
- Turner BL, et al. (2016) Sulfur dynamics during long-term ecosystem development. *Biogeochemistry* 128:281–305.
- Turner BL, Condrón LM, Richardson SJ, Peltzer DA, Allison VJ (2007) Soil organic phosphorus transformations during pedogenesis. *Ecosystems* 10:1166–1181.

- Turner BL, Condron LM, Wells A, Andersen KM (2012) Soil nutrient dynamics during podzol development under lowland temperate rain forest in New Zealand. *Catena* 97:50–62.
- Turner BL, et al. (2013) Soil microbial biomass and the fate of phosphorus during long-term ecosystem development. *Plant Soil* 367:225–234.
- Turner S, et al. (2014) Mineralogical impact on long-term patterns of soil nitrogen and phosphorus enzyme activities. *Soil Biol Biochem* 68:31–43.
- Uroz S, Tech JJ, Sawaya NA, Frey-Klett P, Leveau JHJ (2014) Structure and function of bacterial communities in ageing soils: Insights from the Mendocino ecological staircase. *Soil Biol Biochem* 69:265–274.
- Uroz S, et al. (2013) Functional assays and metagenomic analyses reveals differences between the microbial communities inhabiting the soil horizons of a Norway spruce plantation. *PLoS One* 8:e55929.
- Uroz S, et al. (2011) Bacterial weathering and its contribution to nutrient cycling in temperate forest ecosystems. *Res Microbiol* 162:820–831.
- Valentine DL (2007) Adaptations to energy stress dictate the ecology and evolution of the Archaea. *Nat Rev Microbiol* 5:316–323.
- van der Heijden MGA, Bardgett RD, Van Straalen NM (2008) The unseen majority: Soil microbes as drivers of plant diversity and productivity in terrestrial ecosystems. *Ecol Lett* 11:296–310.
- van Elsas JD, Torsvik V, Hartmann A, Øvreås L, Jansson JK (2007) The bacteria and archaea in soil. *Modern Soil Microbiology*, eds van Elsas JD, Jansson JK, Trevors JT (CRC Press, Boca Raton, London, New York), pp 83–106.
- van Kessel MAHJ, et al. (2015) Complete nitrification by a single microorganism. *Nature* 528:555–559.
- Vinten AJA, Whitmore AP, Bloem J, Howard R, Wright F (2002) Factors affecting N immobilisation/mineralisation kinetics for cellulose-, glucose- and straw-amended sandy soils. *Biol Fertil Soils* 36:190–199.
- Vitousek PM, et al. (1997) Soil and ecosystem development across the Hawaiian Islands. *GSA Today* 7:1–8.
- Vitousek PM, Farrington H (1997) Nutrient limitation and soil development: Experimental test of a biogeochemical theory. *Biogeochemistry* 37:63–75.
- Vogel C, et al. (2014) Establishment of macro-aggregates and organic matter turnover by microbial communities in long-term incubated artificial soils. *Soil Biol Biochem* 79:57–67.

- von Lützow M, et al. (2006) Stabilization of organic matter in temperate soils: Mechanisms and their relevance under different soil conditions - a review. *Eur J Soil Sci* 57:426–445.
- Voroney RP, Heck RJ (2015) The soil habitat. *Soil Microbiology, Ecology, and Biochemistry*, ed Paul EA (Academic Press, Amsterdam, Boston, Heidelberg, London, New York, Oxford, Paris, San Diego, San Francisco, Singapore, Sydney, Tokyo).
- Walker LR, del Moral R (2003) *Primary succession and ecosystem rehabilitation* (Cambridge University Press, Cambridge).
- Walker LR, Wardle DA, Bardgett RD, Clarkson BD (2010) The use of chronosequences in studies of ecological succession and soil development. *J Ecol* 98:725–736.
- Wallenstein MD, Myrold DD, Firestone M, Voytek M (2006) Environmental controls on denitrifying communities and denitrification rates: Insights from molecular methods. *Ecol Appl* 16:2143–2152.
- Wardle DA, Walker LR, Bardgett RD (2004) Ecosystem properties and forest decline in contrasting long-term chronosequences. *Science* 305:509–513.
- Weber EB, Lehtovirta-Morley LE, Prosser JI, Gubry-Rangin C (2015) Ammonia oxidation is not required for growth of group 1.1c soil Thaumarchaeota. *FEMS Microbiol Ecol* 91:fiv001.
- Wei S, et al. (2014) Diversity and distribution of Archaea community along a stratigraphic permafrost profile from Qinghai-Tibetan Plateau, China. *Archaea* 2014: Article ID 240817.
- Wessén E, Hallin S, Philippot L (2010) Differential responses of bacterial and archaeal groups at high taxonomical ranks to soil management. *Soil Biol Biochem* 42:1759–1765.
- Whitton BA (2000) Soils and rice-fields. *The Ecology of Cyanobacteria*, eds Whitton B, Potts M (Kluwer Academic Publishers, New York, Boston, Dordrecht, London, Moscow), pp 233–255.
- Wild B, et al. (2014) Input of easily available organic C and N stimulates microbial decomposition of soil organic matter in arctic permafrost soil. *Soil Biol Biochem* 75:143–151.
- Williams MA, Jangid K, Shanmugam SG, Whitman WB (2013) Bacterial communities in soil mimic patterns of vegetative succession and ecosystem climax but are resilient to change between seasons. *Soil Biol Biochem* 57:749–757.
- Williamson N, Brian P, Wellington EMH (2000) Molecular detection of bacterial and streptomycete chitinases in the environment. *Antonie Van Leeuwenhoek* 78:315–321.
- Wrage N, Velthof GL, van Beusichem ML, Oenema O (2001) Role of nitriier denitrication in the production of nitrous oxide. *Soil Biol Biochem* 33:1723–1732.

- Yamada T, Sekiguchi Y (2009) Cultivation of uncultured *Chloroflexi* subphyla: Significance and ecophysiology of formerly uncultured *Chloroflexi* “subphylum I” with natural and biotechnological relevance. *Microbes Environ* 24:205–216.
- Yao H, et al. (2013) Multi-factorial drivers of ammonia oxidizer communities: Evidence from a national soil survey. *Environ Microbiol* 15:2545–2556.
- Zeng J, et al. (2016) Primary succession of nitrogen cycling microbial communities along the deglaciated forelands of Tianshan Mountain, China. *Front Microbiol* 7:1353.
- Zhang J, Wang J, Zhong W, Cai Z (2015) Organic nitrogen stimulates the heterotrophic nitrification rate in an acidic forest soil. *Soil Biol Biochem* 80:293–295.
- Zumsteg A, Bernasconi SM, Zeyer J, Frey B (2012a) Microbial community and activity shifts after soil transplantation in a glacier forefield. *Appl Geochemistry* 26:326–329.
- Zumsteg A, et al. (2012b) Bacterial, archaeal and fungal succession in the forefield of a receding glacier. *Microb Ecol* 63:552–564.

4 Manuscripts

4.1 List of manuscripts and authors contributions

4.1.1 Microbial community dynamics in soil depth profiles over 120,000 years of ecosystem development

Stephanie Turner, Robert Mikutta, Sandra Meyer-Stüve, Georg Guggenberger, Frank Schaarschmidt, Cassandre S. Lazar, Reiner Dohrmann, Axel Schippers

Frontiers in Microbiology 8 (2017) 874

<https://doi.org/10.3389/fmicb.2017.00874>

Authors contributions:

Axel Schippers, Robert Mikutta, and Georg Guggenberger designed this study. Robert Mikutta, Sandra Meyer-Stüve, and Stephanie Turner performed soil sampling. Stephanie Turner conducted DNA extraction, qPCR, PCR, and T-RFLP analysis. Sandra Meyer-Stüve and Stephanie Turner conducted the microcosm incubation experiment. Stephanie Turner analyzed the data with input from Frank Schaarschmidt (statistics) and Cassandre S. Lazar (archaeal taxonomy), and wrote the manuscript. All authors discussed the data and reviewed the manuscript.

4.1.2 Mineralogical impact on long-term patterns of soil nitrogen and phosphorus enzyme activities

Stephanie Turner, Axel Schippers, Sandra Meyer-Stüve, Georg Guggenberger, Norman Gentsch, Reiner Dohrmann, Leo M. Condron, Andre Eger, Peter C. Almond, Duane A. Peltzer, Sarah J. Richardson, Robert Mikutta

Soil Biology & Biochemistry 68 (2014) 31-43

<http://dx.doi.org/10.1016/j.soilbio.2013.09.016>

Authors contributions:

Robert Mikutta, Axel Schippers, and Georg Guggenberger designed this study. Leo M. Condrón, Peter C. Almond, Duane A. Peltzer, and Sarah J. Richardson helped with preparation of the sampling and provided access to the sampling sites. Robert Mikutta, Norman Gentsch, Andre Eger, Sandra Meyer-Stüve, and Stephanie Turner performed soil sampling. Sandra Meyer-Stüve performed measurements of soil parameters. Stephanie Turner conducted measurements of microbial biomass and enzyme activities. Stephanie Turner analyzed the data with the help of Sandra Meyer-Stüve. Stephanie Turner, Axel Schippers, Sandra Meyer-Stüve, Georg Guggenberger, Norman Gentsch, Reiner Dohrmann, and Robert Mikutta discussed the data. Stephanie Turner wrote the manuscript with the help of Robert Mikutta and Axel Schippers. All authors reviewed the manuscript.

4.1.3 120,000 years of soil ecosystem development results in distinct nitrogen cycling microbial communities

Stephanie Turner, Robert Mikutta, Sandra Meyer-Stüve, Georg Guggenberger, Frank Schaarschmidt, Reiner Dohrmann, Axel Schippers

Prepared for submission to *Applied and Environmental Microbiology*

Authors contributions:

Axel Schippers, Robert Mikutta, and Georg Guggenberger designed this study. Robert Mikutta, Sandra Meyer-Stüve, and Stephanie Turner performed soil sampling. Stephanie Turner conducted DNA

extraction, qPCR, and PCR analysis. Stephanie Turner analyzed the data with the help of Frank Schaarschmidt (statistics), and wrote the manuscript. All authors discussed the data and reviewed the manuscript.

4.1.4 Microbial utilization of mineral-associated nitrogen in soils

Stephanie Turner ¹, Sandra Meyer-Stüve ¹, Axel Schippers, Georg Guggenberger, Frank Schaarschmidt, Birgit Wild, Andreas Richter, Reiner Dohrmann, Robert Mikutta

¹ These authors contributed equally to this work.

Soil Biology & Biochemistry 104 (2017) 185-196

<http://dx.doi.org/10.1016/j.soilbio.2016.10.010>

Authors contributions:

Robert Mikutta, Axel Schippers and Georg Guggenberger designed this study. Robert Mikutta performed soil sampling. Sandra Meyer-Stüve and Stephanie Turner conducted the microcosm incubation experiment. Sandra Meyer-Stüve performed measurements of soil parameters. Stephanie Turner performed DNA extraction and qPCR analysis. Birgit Wild and Andreas Richter conducted ¹³C measurements. Sandra Meyer-Stüve performed the calculations on the gas data and Birgit Wild performed the calculations on the ¹³C data. Stephanie Turner and Sandra Meyer-Stüve performed statistical analyses with the help of Frank Schaarschmidt. Stephanie Turner wrote the manuscript with the help of Sandra Meyer-Stüve. All authors discussed the data and reviewed the manuscript.

4.2 Full manuscripts

4.2.1 Manuscript 1: Microbial community dynamics in soil depth profiles over 120,000 years of ecosystem development



Microbial Community Dynamics in Soil Depth Profiles Over 120,000 Years of Ecosystem Development

Stephanie Turner¹, Robert Mikutta², Sandra Meyer-Stüve³, Georg Guggenberger³, Frank Schaarschmidt⁴, Cassandre S. Lazar⁵, Reiner Dohrmann⁶ and Axel Schippers^{1*}

¹ Geomicrobiology, Federal Institute for Geosciences and Natural Resources, Hanover, Germany, ² Soil Science and Soil Protection, Martin Luther University Halle-Wittenberg, Halle, Germany, ³ Institute of Soil Science, Leibniz Universität Hannover, Hanover, Germany, ⁴ Institute of Biostatistics, Leibniz Universität Hannover, Hanover, Germany, ⁵ Aquatic Geomicrobiology, Institute of Ecology, Friedrich Schiller University Jena, Jena, Germany, ⁶ Technical Mineralogy and Clay Mineralogy, Federal Institute for Geosciences and Natural Resources, Hanover, Germany

OPEN ACCESS

Edited by:

Mark Alexander Lever,
ETH Zurich, Switzerland

Reviewed by:

Gary M. King,
Louisiana State University,
United States
Tatiana A. Vishnivetskaya,
University of Tennessee at Knoxville,
United States

*Correspondence:

Axel Schippers
axel.schippers@bgr.de

Specialty section:

This article was submitted to
Extreme Microbiology,
a section of the journal
Frontiers in Microbiology

Received: 25 October 2016

Accepted: 01 May 2017

Published: 19 May 2017

Citation:

Turner S, Mikutta R, Meyer-Stüve S,
Guggenberger G, Schaarschmidt F,
Lazar CS, Dohrmann R and
Schippers A (2017) Microbial
Community Dynamics in Soil Depth
Profiles Over 120,000 Years
of Ecosystem Development.
Front. Microbiol. 8:874.
doi: 10.3389/fmicb.2017.00874

Along a long-term ecosystem development gradient, soil nutrient contents and mineralogical properties change, therefore probably altering soil microbial communities. However, knowledge about the dynamics of soil microbial communities during long-term ecosystem development including progressive and retrogressive stages is limited, especially in mineral soils. Therefore, microbial abundances (quantitative PCR) and community composition (pyrosequencing) as well as their controlling soil properties were investigated in soil depth profiles along the 120,000 years old Franz Josef chronosequence (New Zealand). Additionally, in a microcosm incubation experiment the effects of particular soil properties, i.e., soil age, soil organic matter fraction (mineral-associated vs. particulate), O₂ status, and carbon and phosphorus additions, on microbial abundances (quantitative PCR) and community patterns (T-RFLP) were analyzed. The archaeal to bacterial abundance ratio not only increased with soil depth but also with soil age along the chronosequence, coinciding with mineralogical changes and increasing phosphorus limitation. Results of the incubation experiment indicated that archaeal abundances were less impacted by the tested soil parameters compared to *Bacteria* suggesting that *Archaea* may better cope with mineral-induced substrate restrictions in subsoils and older soils. Instead, archaeal communities showed a soil age-related compositional shift with the *Bathyarchaeota*, that were frequently detected in nutrient-poor, low-energy environments, being dominant at the oldest site. However, bacterial communities remained stable with ongoing soil development. In contrast to the abundances, the archaeal compositional shift was associated with the mineralogical gradient. Our study revealed, that archaeal and bacterial communities in whole soil profiles are differently affected by long-term soil development with archaeal communities probably being better adapted to subsoil conditions, especially in nutrient-depleted old soils.

Keywords: *Archaea*, *Bacteria*, *Bathyarchaeota*, chronosequence, soil depth, subsoil, pyrosequencing, qPCR

INTRODUCTION

Soil microbial communities mediate key processes in soil ecosystem functioning including organic matter (OM) degradation, nutrient cycling, and mineral weathering. During the early stage of pedogenesis heterotrophic and phototrophic pioneer microorganisms are responsible for biological weathering of the bedrock material and create interfaces for OM and nutrient turnover, e.g., in biofilms (Tscherko et al., 2003; Nemergut et al., 2007; Schulz et al., 2013; Haynes, 2014). Thereby they provide favorable conditions for the colonization by plants (Schulz et al., 2013). With ongoing soil development and ecosystem progression, an increasing plant biomass causes an accumulation of OM that is accompanied by an increase in microbial cell numbers, biomass and activity of heterotrophic microorganisms (Richardson et al., 2004; Brankatschk et al., 2011; Turner et al., 2014). The archaeal community composition showed a shift during the first 110-years of soil development at a receding Swiss glacier (Zumsteg et al., 2012) and Nicol et al. (2005) reported changes within the phylum *Crenarchaeota* during 9500 years of succession for an Austrian glacier foreland. Similarly, many studies reported that the bacterial community composition considerably changed during progression with highest bacterial species turnover rates during the first years (Nemergut et al., 2007; Schütte et al., 2009; Wu et al., 2012; Zumsteg et al., 2012; Jangid et al., 2013a,b).

A soil chronosequence, i.e., soils of different ages that derived from the same parent material under similar climatic conditions, provides the unique opportunity for investigating microbial patterns with regard to soil development (Stevens and Walker, 1970). While microbial function and community composition dynamics during the development of young to intermediate-aged soils are already well investigated (Tscherko et al., 2003; Brankatschk et al., 2011; Zumsteg et al., 2012; Schulz et al., 2013), the knowledge about long-term dynamics is limited. There are a few studies analyzing bacterial communities of topsoils over several thousand years of ecosystem development including not only progressive but also retrogressive stages. Retrogression occurs after thousands to millions years when the ecosystem undergoes a decline in nutrient availability, productivity, and plant biomass (Peltzer et al., 2010). The diversity of bacterial communities decreased during retrogression coinciding with a depletion of soil phosphorus (P) (Jangid et al., 2013a,b; Uroz et al., 2014). However, there is a lack of information about archaeal community composition dynamics during retrogression.

Soil chronosequences are also an excellent tool to identify the environmental parameters that shape the microbial community composition during soil development. Most studies found distinct bacterial communities along the soil development gradient that were linked to changes in soil pH, carbon (C), and nutrient concentrations such as nitrogen (N) and P, or the C:N ratio (Zumsteg et al., 2012; Jangid et al., 2013a; Uroz et al., 2014; Freedman and Zak, 2015). In contrast, archaeal communities seem to be related to plant cover and N content (Zumsteg et al., 2012).

While most of these studies focus on topsoil communities it is still poorly understood how subsoil communities develop with

ongoing soil age and which parameters are important in shaping these communities. Subsoils considerably differ in environmental conditions compared to topsoils, e.g., the concentrations of C and nutrients steeply decrease with soil depth (Hansel et al., 2008; Turner et al., 2014; Stone et al., 2015). Accordingly, subsoils harbor distinct microbial communities adapted to these energy and substrate limited conditions (Blume et al., 2002; Fierer et al., 2003; Hansel et al., 2008; Hartmann et al., 2009). Furthermore, the content of iron (Fe) and aluminum (Al) (hydr)oxides and clay minerals increase not only with increasing soil depth, but also most notably with increasing soil age (Tarlera et al., 2008; Mikutta et al., 2009; Turner et al., 2014). Tarlera et al. (2008) investigated bacterial communities of subsoil B horizons along a 77,000-years dune chronosequence and found a strong relationship between community structure and soil age, but did not further analyze the relationship to specific soil properties. Sorption of OM and nutrients such as P to reactive minerals may restrict substrate availability, particularly in subsoil environments, thus intensifying substrate limitation and potentially facilitate microbial communities adapted to these conditions. Further, the presence of particulate OM entering the topsoil as aboveground litter or roots may also induce differences in microbial community composition in comparison to subsoil, which are dominated by OM associated with minerals (Mikutta et al., 2009; Kleber et al., 2015).

Therefore, the main research questions of this study were (i) how microbial abundances and community composition develop in whole soil profiles along a long-term soil development gradient, and (ii) how microbial communities are shaped by soil properties during soil development with special consideration of microbial communities in mineral soils. To address these questions we investigated microbial abundances via quantitative PCR (qPCR) and community patterns via pyrosequencing of archaeal and bacterial 16S rRNA genes in soils along the 120,000 (120 kyr) years old Franz Josef chronosequence, New Zealand. The Franz Josef chronosequence gives the valuable opportunity to study patterns of long-term ecosystem development and is already well investigated in terms of vegetation and topsoil bacterial communities (Richardson et al., 2004; Jangid et al., 2013b), thus, providing background information for data interpretation. In addition, this soil chronosequence formed a C and nutrient gradient with highest C and N contents at the intermediate-aged sites and a sharp decline in total P content with ongoing soil development (Richardson et al., 2004; Turner et al., 2014). Further, the chronosequence is characterized by a mineralogical gradient that is characterized by an increase in Fe and Al (hydr)oxides and clay-sized minerals with soil age (Turner et al., 2014). High precipitation creates regularly water-saturated conditions in the soils of the chronosequence resulting in low oxygen availability and changes in the redox regime. Due to the complexity of environmental gradients (C, nutrients and soil mineralogy) along the Franz Josef chronosequence we additionally conducted a microcosm incubation experiment to disentangle the effects of the different soil properties on microbial communities. Therefore, we investigated microbial abundances via qPCR and microbial community patterns via T-RFLP and compared these between the different experimental incubation

treatments, i.e., soil age, soil OM fraction (mineral-associated vs. particulate), O₂ status, and C and P additions, covering the most relevant soil parameters that changes along the soil chronosequence.

MATERIALS AND METHODS

Site Description and Soil Sampling

Soils of the Franz Josef chronosequence (~43°S, 170°E) have developed due to glacier advance and retreat from greywacke and mica schist and are located on the West Coast of the South Island of New Zealand (Almond et al., 2001). The area is characterized by humid temperate climate with high mean annual precipitation (3500–6500 mm) and is covered by rainforest (Richardson et al., 2004).

Seven sites ranging from 0.06 to 120 kyr were sampled in January 2012 (Supplementary Figure S1; Stevens, 1968; Almond et al., 2001). At each site, three soil profiles (replicates) up to one meter depth were excavated and each horizon was sampled. Details of site characteristics and soil properties are given in Turner et al. (2014). Soil profiles contain organic topsoil (O horizon), mineral topsoil (A horizon), and subsoils with an eluvial horizon (E horizon), mineral subsoil (B horizon), and the parent material for soil genesis (C horizon); the respective horizons per site are shown in **Figure 1**. For molecular analyses,

soil samples were taken with a sterile lab spoon, frozen and stored at –20°C until analysis. For the microcosm incubation experiment, A horizons of four selected sites (0.5, 5, 12, and 120 kyr) were sampled in February 2014. Soil samples were kept at <8°C prior to incubation.

Nucleic Acid Extraction and Quantification of Small Subunit (SSU) rRNA Genes

Nucleic acids of all soil samples were extracted in triplicate (or in duplicate for the microcosm incubation experiment) using the FastDNA® Spin Kit for Soil (MP Biomedicals, Santa Ana, CA, United States) with modifications according to Webster et al. (2003) and DNA extracts were pooled.

Quantification of small subunit (SSU) rRNA genes of *Archaea*, *Bacteria*, *Fungi*, and *Eukarya* were performed by qPCR for all soil samples derived from the sampling in 2012. For the qPCR a StepOnePlus™ Real-Time PCR System (Applied Biosystems, Life Technologies, Carlsbad, CA, United States) was used with either TaqMan® (*Bacteria* according to Nadkarni et al., 2002 and *Eukarya*) or SYBR® Green I chemistry (all others). All qPCRs contained 5 μL mastermix, 1 μL BSA (3 g L⁻¹; Sigma–Aldrich, St. Louis, MO, United States), primers (**Table 1**), 1 μL DNA template and filled to the final volume of 10 μL with dH₂O. As mastermixes we used Platinum SYBR Green qPCR SuperMix-UDG with ROX (Life Technologies, Carlsbad, CA, United States)

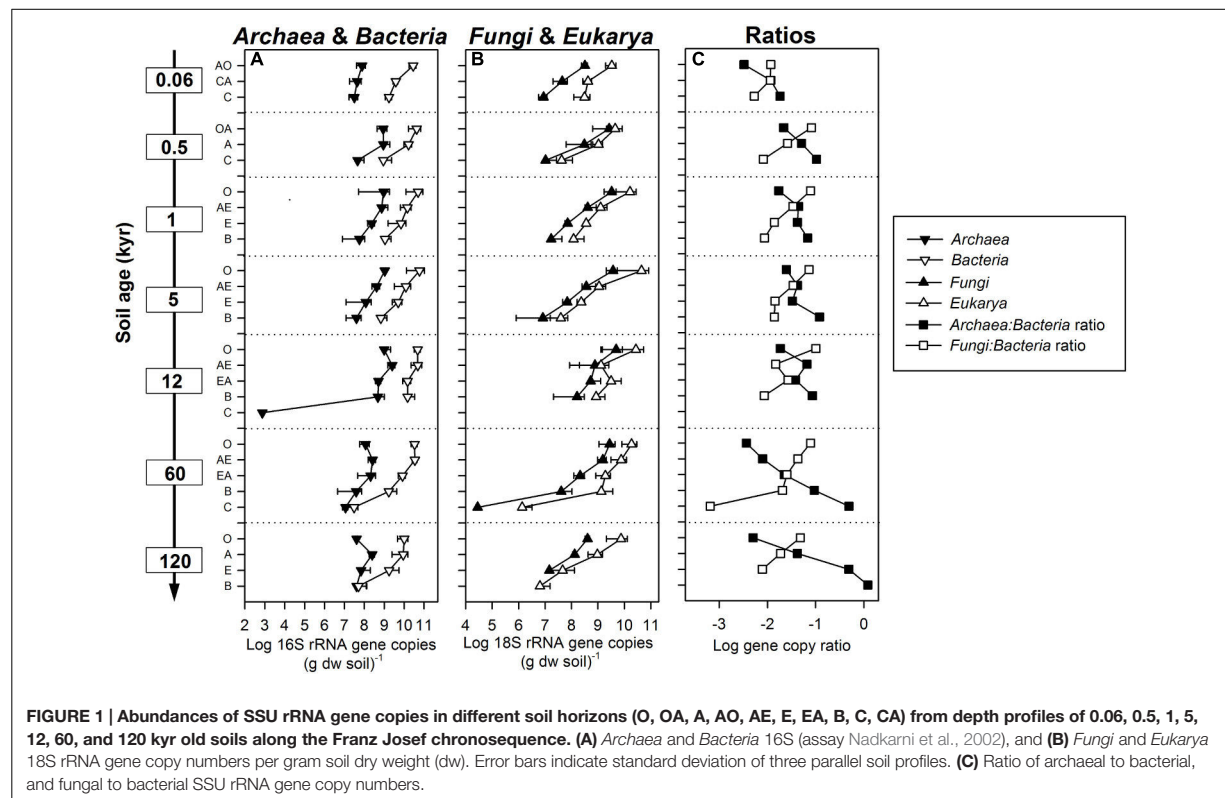


TABLE 1 | Primers and conditions for qPCR assays.

Primer	Sequences (5' – 3') & qPCR conditions	Primer concentration (μM)	Efficiency (%)	Reference
Archaeal 16S rRNA gene				
Arch915F Arch1059R	AGG AAT TGG CGG GGG AGC AC GCC ATG CAC CWC CTC T 95°C-5 min; 40x: 95°C-15 s, 60°C-45 s; 95°C-45 s	0.4	94.2–96.9	Kubo et al., 2012
Bacterial 16S rRNA gene				
Bac340F Bac806R Bac probe	TCC TAC GGG AGG CAG CAG T GGA CTA CCA GGG TAT CTA ATC CTG TT FAM-CGT ATT ACC GCG GCT GCT GGC AC-TAMRA 50°C-2 min, 95°C-10 min; 40x: 95°C-15 s, 60°C-1 min	0.1	87.8–91.5	Nadkarni et al., 2002
U1048F U1371	GTG ITG CAI GGI IGT CGT CA ACG TCI TCC ICI CCT TCC TC 95°C-7 min; 40x: 95°C-30 s, 60.5°C-30 s, 72°C-40 s; 95°C-45 s	0.25	93.1–95.5	Gray et al., 2011
Fungal SSU 18S rRNA gene				
nu-SSU-0817-F nu-SSU-1196-R	TTA GCA TGG AAT AAT RRA ATA GGA TCT GGA CCT GGT GAG TTT CC 95°C-10 min; 40x: 95°C-1 min, 56°C-1 min, 72°C-1 min; 95°C-1 min	0.5	94.5–97.8	Borneman and Hartin, 2000
Eukaryotic 18S rRNA gene				
VIC	Probe and primers by Applied Biosystems 50°C-2 min, 95°C-10 min; 40x: 95°C-15 s, 60°C-1 min	0.05	90.3–93.9	Applied Biosystems, 2002

for *Archaea* and *Bacteria* (Gray et al., 2011), PerfeCTa qPCR ToughMix ROX (Quanta Biosciences, Gaithersburg, MD, United States) for *Bacteria* (Nadkarni et al., 2002) and *Eukarya*, and FastStart Universal SYBR Green Master (ROX) (Roche, Rotkreuz, Switzerland) for *Fungi*. Standards were made from purified PCR product obtained from whole genome extracted from pure cultures: *Methanosarcina barkeri* (*Archaea*), *Escherichia coli* (*Bacteria* – Nadkarni et al., 2002), *Pseudomonas stutzeri* (*Bacteria* – Gray et al., 2011), and *Fusarium oxysporum* (*Fungi*). For the *Eukarya* assay we used fish sperm DNA as standard. For SYBR® Green I assays the product specificity was confirmed by melt curve analysis and the product size was verified by agarose gel electrophoresis. Template DNA was used in three dilutions to check for inhibition by co-extracted PCR inhibitors. Standard DNA, template DNA, and non-template control were run in three replicates. Abundances were reported in SSU rRNA gene copy numbers per gram dry weight of soil. Gene copy numbers of the incubation experiment were normalized to initial soil fraction organic C (OC) content (Supplementary Table S1) to account for the variability of the OC content in initial soil samples allowing a comparison of incubation experiment derived differences.

Tag-Encoded Pyrosequencing of Archaeal and Bacterial 16S rRNA Genes

Archaeal and bacterial 16S rRNA genes of selected soil samples (sampling in 2012; Supplementary Figure S2) were amplified

with the tag-encoded primer pairs Arch344f/Arch915r (Stahl and Amann, 1991; Sørensen et al., 2004) for *Archaea* and Bac341f/Bac785r (Herlemann et al., 2011) for *Bacteria*. All PCRs were performed using a total volume of 50 μL containing 5 μL of 10 \times polymerase buffer, 10 μL dNTPs (each 1 mM; Fermentas, Thermo Fisher Scientific, Waltham, MA, United States), 3 μL bovine serum albumin (3 g L⁻¹), 2.5 μL of each primer (10 μM), 0.5 μL 1.25 U polymerase (*Pfu* DNA Polymerase, Promega, Madison, WI, United States), 24.5 μL dH₂O and 2 μL template DNA. Touch-down PCR was performed with the following conditions: 95°C for 1.5 min, 10 touch-down cycles of 95°C for 1 min, 62°C (*Archaea*) and 65°C (*Bacteria*) for 30 s (decreasing by 1°C in each cycle), 72°C for 2 min, and 25 cycles of 95°C for 1 min, 52°C (*Archaea*) and 55°C (*Bacteria*) for 30 s, 72°C for 2 min, followed by 72°C for 5 min. The PCR products were checked for correct fragment size using agarose gel electrophoresis, cleaned up with the QIAquick PCR Purification Kit (QIAGEN, Hilden, Germany), and pooled in equimolar amounts. Adaptor ligation and sequencing of archaeal and bacterial amplicons were conducted by GATC Biotech (Konstanz, Germany) with the GS FLX System (Roche, Basel, Switzerland).

Sequences were sorted according to primers and tags, denoised according to Quince et al. (2009) and trimmed with mothur 1.29 (Schloss et al., 2009). Briefly, sequences with ≥ 1 mismatch to primer or tag sequence, ≥ 1 ambiguity or ≥ 8 homopolymers were removed. Tags were removed and sequences

were aligned with SINA 1.2.11 (Pruesse et al., 2012). Chimeric sequences were identified using the UCHIME algorithm (Edgar et al., 2011) implemented in the mothur program package and removed. Remaining sequences were clustered to operational taxonomic units (OTUs) at 97% sequence identity level and *Bacteria* were classified with SILVA database release 115 (Quast et al., 2013). Richness estimator (Chao1) and Shannon diversity index were calculated for archaeal and bacterial OTUs using mothur.

The phylogenetic 16S rRNA gene trees for the phyla *Bathyarchaeota*, *Woesearchaeota*, *Thaumarchaeota* and *Euryarchaeota* were calculated with ARB (Ludwig et al., 2004) using the neighbor-joining method based on Jukes–Cantor distances. Therefore, 16S rRNA gene sequences were aligned with SINA (Pruesse et al., 2012).

Soil Microcosm Incubation Experiment

To evaluate the effect of specific soil characteristics (O_2 status, soil fraction, soil age, C, and P addition) on microbial abundances and community composition we set up a microcosm incubation experiment with soils of the Franz Josef chronosequence (Supplementary Figure S3; Turner et al., 2017). Therefore, we used different soil fractions (bulk soil, mineral-associated OM, and particulate OM) of A horizons of four soil ages (0.5, 5, 12, and 120 kyr). For soil density fractionation, 25 g of soil were dispersed in 125 mL sodium polytungstate solution ($\rho = 1.6 \text{ g cm}^{-3}$; Cerli et al., 2012) and sonicated for 9 min 38 s with 60 J mL^{-1} with an ultrasonic device (LABSONIC®, Sartorius Stedim Biotech GmbH, Göttingen, Germany). The lighter, particulate OM fraction (light fraction, LF) was separated from the heavy mineral-associated OM fraction (heavy fraction, HF) by decantation after deposition for 1 h and centrifugation for 10 min at 3500 g. To minimize possible negative effects of the sodium polytungstate on microbial activities (Blackwood and Paul, 2003; Crow et al., 2007), both fractions were washed with deionized water until the electrical conductivity was less than $50 \mu\text{S cm}^{-1}$, and freeze dried resulting in approximately 95 wt% of HF and 2 wt% of LF. For initial OC and total N concentrations see Supplementary Table S1. Toxic effects caused by tungsten residues in the fractionated samples could be ruled out because of similar mineralization rates of bulk soil compared to density fractions (Gentsch et al., 2015).

For each microcosm, 10 g (bulk or HF) or 1 g (LF) dried soil fraction sample were filled up to 20 g with sterile quartz powder ($<125 \mu\text{m}$, Carl Roth GmbH + Co. KG, Karlsruhe, Germany) into 125 mL serum vials. To evaluate the influence of C and P additions we tested different treatments in bulk soil and the HF: without any addition (wo), with NaH_2PO_4 (P; $500 \mu\text{g PO}_4\text{-P g}^{-1}$ soil fraction), cellulose (C; $40 \text{ mg cellulose-C g}^{-1}$ soil fraction C) or the addition of both (CP). The C and P treatments were not tested for the LF because we focused on the comparison between bulk soil vs. the HF and further had only very little amounts of LF material. Controls consisted of 20 g quartz powder only.

To further counteract the possible negative effect of the fractionation procedure on microbial activity, we inoculated each incubation sample with 3 mL of a soil slurry with an active,

indigenous microbial community. Soil slurries consisted of fresh, wet soil of the corresponding sampling site (0.5, 5, 12, and 120 kyr) suspended in sterile Hoagland solution (without a P or N source, soil weight to volume ratio = 1:10). Samples were then adjusted to 60% water-holding capacity with sterile distilled water and carefully homogenized with a spatula. Replicate samples were incubated under oxic and anoxic conditions to analyze the effect of O_2 status. For oxic incubation, serum vials were closed with polyethylene wool to allow gas exchange. Anoxic vials were fitted with septa and flushed repeatedly with helium. All samples were pre-incubated at 15°C for 10 days for equilibration and afterward the cellulose was added and the main-incubation started. For maintaining high humidity in oxic vials, a tray of water was placed into the incubator and the water content was checked every few days and, if necessary, readjusted. The loss of water in anoxic vials was negligible during incubation. All combinations of the tested factors (O_2 status, soil fraction, soil age, and C and P addition) were prepared in triplicate resulting together with the controls in 222 incubation samples. After 125 days of incubation, all vials were sampled destructively for end-point molecular analyses including qPCR (assays for *Archaea*, *Bacteria* and *Fungi* as described above) and terminal restriction fragment length polymorphism (T-RFLP). Samples were frozen and stored at -20°C until analysis.

Community Profiling of Incubation Samples via T-RFLP

Archaeal and bacterial community composition of incubation samples were analyzed via T-RFLP rather than pyrosequencing because for the incubation experiment the focus was on community patterns and a lower microbial diversity was expected than in the original soil samples. For amplification, DNA extracts were purified and concentrated with PowerClean® Pro DNA Clean-Up Kit (MO BIO Laboratories, Carlsbad, CA, United States). Archaeal 16S rRNA genes were amplified with primer pair Cy5-labeled 20F (Massana et al., 1997) and 915R (Stahl and Amann, 1991) and bacterial 16S rRNA genes with primer pair Cy5-labeled 8F (Frank et al., 2007) and 907R (Muyzer et al., 1995). The 25 μL PCR reaction volume contained 5 μL OneTaq® Standard Reaction Buffer (New England Biolabs, Ipswich, MA, United States), 5 μL dNTPs (each 1 mM; Fermentas, Thermo Fisher Scientific, Waltham, MA, United States), 1.5 μL BSA (3 g L^{-1}), 0.6 μL (*Archaea*) or 0.4 μL (*Bacteria*) of each primer ($10 \mu\text{M}$), 0.125 μL OneTaq® Hot Start DNA Polymerase ($5 \text{ U } \mu\text{L}^{-1}$), 1–2.5 μL sample DNA and was filled up with dH_2O . The thermal cycling protocol was 95°C for 5 min, 30 cycles of 95°C for 30 s, 57°C (*Archaea*) or 52°C (*Bacteria*) for 30 s, 68°C for 1 min 10 s and the final extension at 68°C for 10 min on a Biometra TProfessional Thermocycler (Analytik Jena AG, Jena, D). The PCR products length was checked on an agarose gel and digested with HaeIII and RsaI for *Archaea* or HaeIII and HhaI for *Bacteria* (all restriction enzymes were purchased from Thermo Scientific, Carlsbad, MA, United States) for 2 h at 37°C . Restriction fragments (T-RFs) were analyzed on a capillary sequencer (Beckman Coulter, GenomeLab™ GeXP, CEQ8000, Fullerton, CA, United States).

The T-RFLP data was noise filtered and aligned via T-REX (Culman et al., 2009).

For data analysis, T-RFs with a fragment size <65 or >600 bp were discarded. Relative abundances of T-RFs were calculated based on peak areas and only T-RFs with a relative abundance of $\geq 3\%$ in all samples were included in further analysis.

Data Analysis and Statistics

Soil properties of the Franz Josef chronosequence were analyzed by Turner et al. (2014) on the same samples and were used for statistical analysis (Supplementary Table S2). Gene copy numbers of the chronosequence samples were determined for every soil horizon and for the figures mean values were calculated for each horizon cluster (O, A, E, B, and C; $n = 28$). For statistical analysis we used all individual data points ($n = 101$). To explore the relationship between soil properties and SSU rRNA gene copy numbers we calculated Spearman rank order correlation coefficients with R (version 3.2.3; R Core Team, 2015).

The effects of soil age, horizon, age \times horizon interaction and depth within a horizon on SSU rRNA gene copy numbers were analyzed as fixed effects in a linear mixed effects model ('lmer' function of the 'lme4' package; Bates et al., 2015). Therefore, SSU rRNA gene copy number data were log-transformed because they ranged across several orders of magnitude, were right-skewed and showed increasing variance with increasing means. The variance between individual profiles was included as random effect to account for repeated measures within the same profile. The inspection of initial model residuals revealed that variances differed between topsoil (O, A) and subsoil (E, B, C) horizon clusters despite log-transformation. Thus, separate models were fitted to topsoil and subsoil data subsets. The main effects and interaction were tested in ANOVA following the model fit, all pairwise comparisons (Tukey-Test) of soil age groups within horizon clusters were performed based on least square means, after centering depth at each age \times horizon clusters' mean depth (package 'lsmeans'; Lenth, 2015).

Multivariate statistics for pyrosequencing community data was performed with Canoco 5 (v5.02; ter Braak and Šmilauer, 2012) on relative proportions of archaeal groups and bacterial genera. To illustrate differences in microbial communities between the samples, we conducted a principal component analysis (PCA) and used the parameters soil age and soil depth as supplementary variables. To assess the conditional (unique) effect of soil age and soil depth on microbial community composition we used variation partitioning and Monte Carlo permutation test (99,999 permutations). Redundancy analysis (RDA) with interactive forward selection and Monte Carlo permutation test (99,999 permutations) was used to identify the effect of soil properties that explained a significant proportion of variation in the microbial community composition. All tests were considered as significant at $P < 0.05$.

For the incubation experiment data set (bulk vs. HF samples), the main effects of O₂ status, soil fraction, soil age, P and C addition on SSU rRNA gene copy numbers were determined by a five-way ANOVA including their interactions with R. Therefore, the measured parameters and residuals were checked for normal-distribution and log-transformed if necessary. Since we got

significant results for almost all five factors for several parameters, we used a random effect model including the five factors and their two-way interactions to estimate the variance components using the 'lmer' function of the 'lme4' package (Bates et al., 2015) for determining the relative importance of each factor. Because in this relatively simple model the O₂ status appeared to be the most important factor for the variation in most microbial abundance patterns, we also used variance component estimation in a more complex random effect model including the remaining four factors and their four-way interactions for the oxic and anoxic data subset.

To explore how the tested factors affect the archaeal and bacterial community composition in the incubation experiment we conducted a non-metric multidimensional scaling (NMDS) with Bray-Curtis distance measure and two dimensions based on relative T-RF abundances in Canoco 5. To test for significant differences in community composition (bulk vs. HF samples) between the levels of each factor we used a multiresponse permutation procedure (MRPP) with Bray-Curtis distance and 99,999 permutations. The MRPP is implemented in the vegan package (Oksanen et al., 2015) in R and generates the chance-corrected within group agreement statistic A. Values of A close to 0 correspond to no systematic differences between the levels of the tested factor, whereas values close to 1 indicate that items within each factor level are nearly identical, i.e., the tested factors define clearly different groups with mostly homogeneous community composition within a group.

Sequence Deposition

Archaeal and bacterial 16S rRNA gene raw reads were deposited in NCBI Sequence Read Archive (SRA) under the BioProject ID PRJNA299489.

RESULTS

Abundances of Archaea, Bacteria, Fungi and Eukarya along the Soil Chronosequence

Archaeal, bacterial, fungal, and eukaryotic SSU rRNA gene copy numbers were determined by qPCR (Figures 1A,B). Overall, in O horizons the copy numbers of all four taxa peaked at the intermediate-aged sites (1–12 kyr; Supplementary Table S3) and decreased with soil depth at all sites. With regard to soil depth, the maximum of the archaeal gene copy number was not always in O horizons as for all other groups but at some sites in A horizons (0.5, 12, 60, and 120 kyr). In subsoil horizons all SSU gene copy numbers showed an age effect with significant lower abundances at the oldest site except for the *Archaea* (Supplementary Table S3). The sum of archaeal and bacterial 16S rRNA gene copy numbers was positively correlated to total cell counts determined by Turner et al. (2014) ($r = 0.91$, $P < 0.001$). Interestingly, the ratio of *Archaea* to *Bacteria* not only increased with soil depth but also significantly with soil age in subsoils (Figure 1C and Supplementary Table S3). In contrast, the fungal to bacterial abundance ratio decreased with soil depth and was lowest at the youngest and the oldest site throughout the soil profile. All SSU

TABLE 2 | Spearman rank order correlation coefficients for SSU rRNA gene copy numbers g⁻¹ dry weight soil and soil properties of the soil chronosequence.

	OC	ON	OP	pH
Archaea	0.76	0.77	0.55	-0.75
Bacteria	0.89	0.89	0.73	-0.73
Fungi	0.88	0.88	0.66	-0.79
Eukarya	0.86	0.85	0.62	-0.71

All correlations were significant ($P < 0.001$).

rRNA gene copy numbers were highly positively correlated with soil OC, organic N (ON), ammonium and organic P (OP) content and negatively with pH (Table 2 and Supplementary Table S4). Correlations between gene abundances and soil parameters such as the total P and nitrate content, or mineralogical properties such as particle size and content of pedogenic Fe and Al phases were weaker (Supplementary Table S4).

Archaeal and Bacterial Community Composition along the Soil Chronosequence

The archaeal and bacterial community composition was analyzed using tag-encoded pyrosequencing of 16S rRNA genes. The pyrosequencing yielded a total of 592,752 reads, which were quality-filtered and then clustered to 2208 archaeal and 28,482 bacterial OTUs at 97% sequence identity level. The archaeal community composition was dominated by the *Forest Soil Crenarchaeotal Group* (FSCG, belong to *Group 1.1c*; Jurgens et al., 1997), the *South African Gold Mine Crenarchaeotal Group 1* (SAGMCG-1; Takai et al., 2001), both belonging to the *Thaumarchaeota* (Supplementary Figure S4), and the newly proposed phylum *Bathyarchaeota* (Meng et al., 2014), formerly known as *Miscellaneous Crenarchaeotal Group* (MCG) (Figure 2A). Interestingly, most sequences that belong to the *Bathyarchaeota* were affiliated with sequences of the pSL22 cluster, a sister group of the MCG, and only a few were closely related to the MCG, subgroup 6 (Figure 3). Furthermore, archaeal communities comprised members of the *Euryarchaeota* (e.g., *Thermoplasmatales*, *Rice Cluster I* and *Methanomicrobia*; Supplementary Figure S5) and *Woesearchaeota* (*Rice Cluster V*; Figure 3), however, both constituting only <1% of the total archaeal community. Archaeal diversity and richness decreased with increasing soil age (Supplementary Table S5).

There was a clear compositional shift with soil age characterized by a FSCG dominance at the young to intermediate-aged soils to a high abundance of the *Bathyarchaeota* at the older sites (Figure 2C). To examine the unique effect of soil age and soil depth on archaeal community composition we conducted variation partitioning and the results emphasized the stronger effect of soil age accounting for 17.8% of total adjusted variation compared to the effect of soil depth with 14.3% (both $P < 0.05$). The effect of soil properties on the archaeal community composition was analyzed by RDA using forward selection. The content of OP and pyrophosphate-extractable Fe (Fe_p), representing Fe in metal-organic complexes, explained 75.8 and

9.5% of the total variation of archaeal community composition, respectively (both $P < 0.05$).

Compared to the *Archaea*, the bacterial community remained quite stable with ongoing soil development and the most abundant phyla across all samples were *Acidobacteria*, *Chloroflexi*, *Planctomycetes*, and *Proteobacteria* (Figure 2B). A PCA of the relative abundances of bacterial genera confirmed that samples did not cluster according to soil age (Figure 2D). This finding was confirmed by variation partitioning showing that the conditional effect of soil age and soil depth separately was not significant, but explained together (including their interaction) 10.3% of the bacterial community variation ($P = 0.052$). A RDA of relative proportions of bacterial genera with forward selection of soil properties showed that the content of nitrate and silt explained together a proportion of 39.2% of total adjusted variation (both $P < 0.05$). Instead of nitrate and silt content also pH (if picked first in the forward selection) can be a good predictor for community composition explaining 21.2% ($P < 0.001$) of the total variation. Similar to *Archaea*, bacterial diversity and richness also decreased with soil age (Supplementary Table S5).

Incubation Experiment: Abundances of Archaea, Bacteria and Fungi

The variation in SSU rRNA gene copy numbers could be mainly explained by the O₂ status for *Bacteria* and *Fungi*, but not for *Archaea* (Figures 4A–C, 5). For bacterial 16S rRNA gene copy numbers the soil fraction was the second most important control with the effect depending on the O₂ status (Figure 5): Under oxic conditions bacterial 16S rRNA gene copy numbers were higher for HF samples, whereas under anoxic conditions copy numbers were higher for bulk samples (Figure 4B). For the LF, all SSU rRNA gene copy numbers were similar or lower compared to bulk and HF samples with the greatest differences for *Bacteria* (Figures 4A–C). However, P and C addition did not significantly affect archaeal 16S rRNA gene copy numbers, whereas bacterial and fungal copy numbers mostly increased due to C and P addition in both bulk and HF samples, especially under oxic conditions (Figures 4A–C and Supplementary Tables S6, S7). The archaeal to bacterial abundance ratios showed higher values for HF samples under anoxic conditions, but were relatively similar under oxic conditions (Figure 4D). The C and CP treatment in HF samples resulted in higher fungal to bacterial abundance ratios (Figure 4E). The results of the variance component estimation with the more complex random effect model for the oxic and anoxic data subsets showed that despite the significance of three-way factor interactions (ANOVA), most variation in microbial abundance patterns could be explained by the effect of single factors or their two-way interactions (Supplementary Tables S6–S8).

Incubation Experiment: Archaeal and Bacterial Community Composition

Archaeal and bacterial community composition were analyzed via T-RFLP, each with two restriction enzymes resulting overall in 31 (HaeIII) and 23 T-RFs (RsaI) for *Archaea*, and 54 (HaeIII)

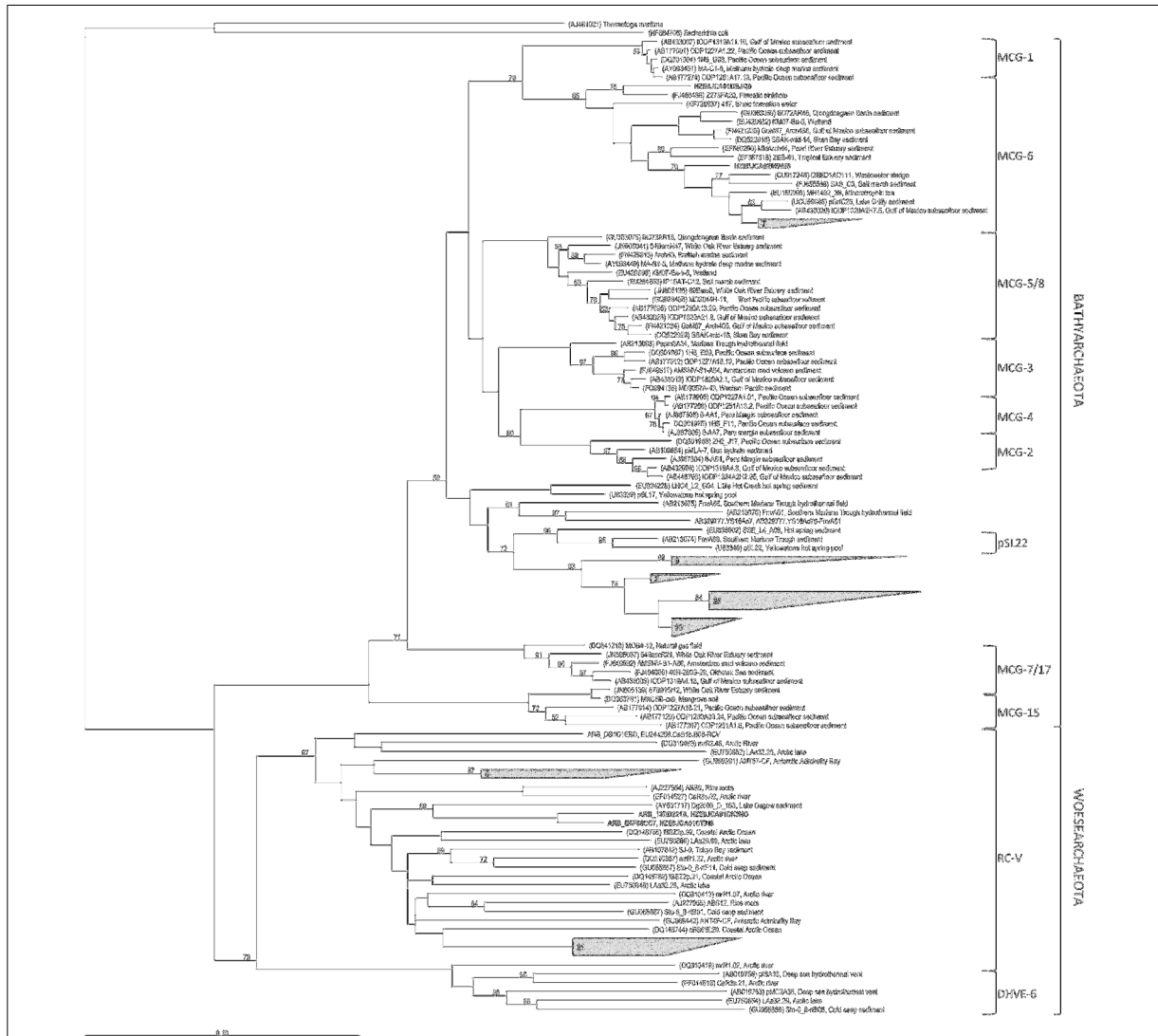


FIGURE 3 | Phylogenetic affiliation of *Bathyarchaeota* and *Woesearchaeota* 16S rRNA gene sequences from soils along the Franz Josef chronosequence (in bold or grouped as gray-shaded form including the number of the respective sequences). Bootstrap values (in percent) are based on 1000 replicates (values below 50% are not shown). The scale bar indicates 10% estimated phylogenetic divergence.

and 46 T-RFs (HhaI) for *Bacteria*. Both were significantly affected by the soil fraction (bulk vs. HF; **Table 3**) and showed T-RFs that were unique for the respective fraction (Supplementary Table S9). Besides the soil fraction, the site age mainly affected the archaeal community composition followed by a slight effect of the O₂ status (**Figure 6A**, **Table 3**, and Supplementary Figure S6A). However, archaeal communities of LF samples were only little affected by soil age and partially clustered to samples of a different soil age. On the contrary, the bacterial community composition showed distinct clusters for oxic and anoxic conditions (**Figure 6B**, **Table 3**, and Supplementary Figure S6B). Archaeal as well as bacterial community compositions

were not significantly affected by the addition of P or C (**Table 3**).

DISCUSSION

Our study provides the first insight into the dynamics of microbial abundances and communities in soil depth profiles over long-term ecosystem development including retrogression. Using the Franz Josef chronosequence gave us the unique opportunity to analyze community patterns of the soil microbiota linked to pedogenesis in an undisturbed

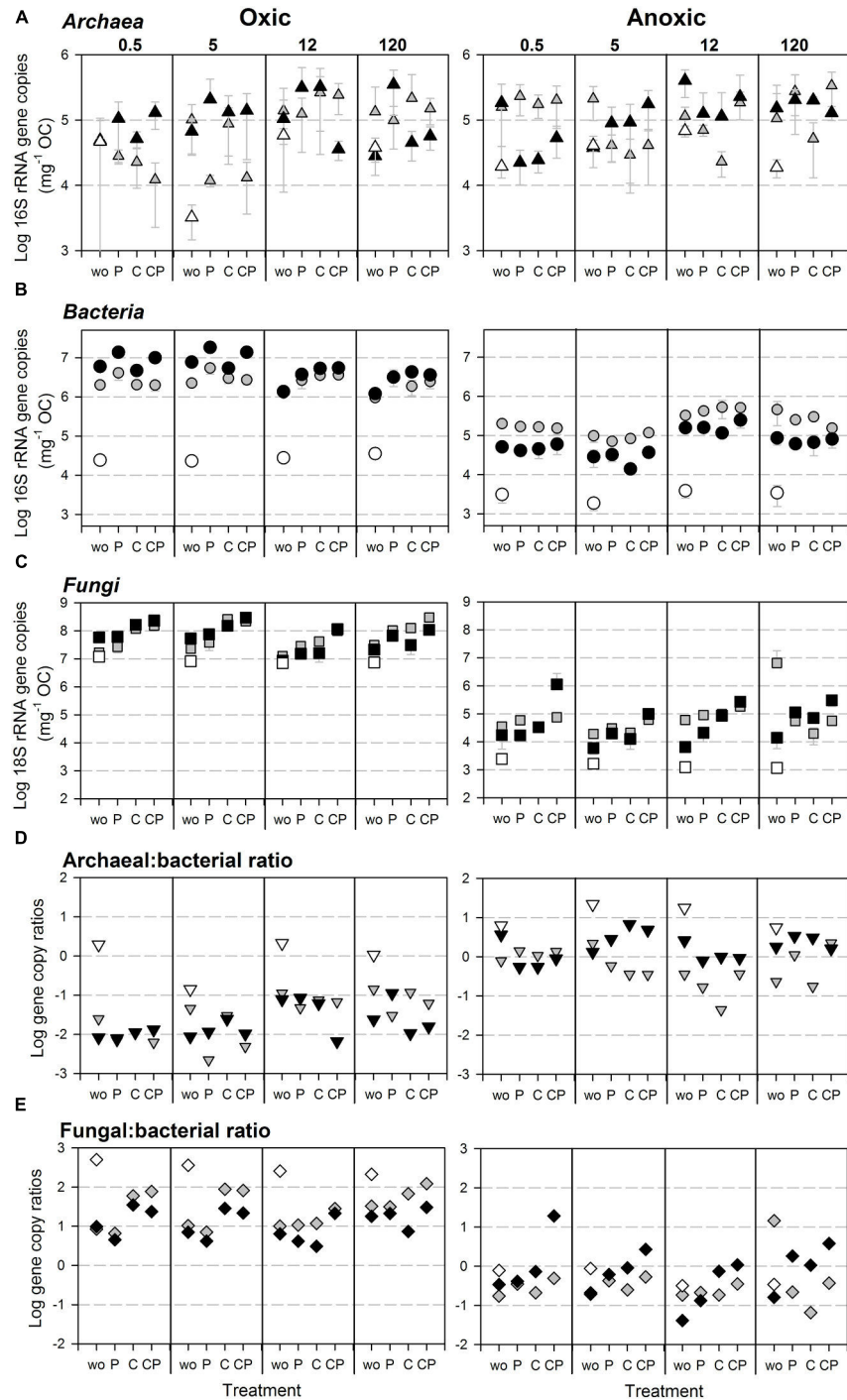


FIGURE 4 | Abundances of SSU rRNA gene copies normalized to initial OC content in the soil microcosm incubation experiment for (A) *Archaea*, (B) *Bacteria* (assay Gray et al., 2011), and (C) *Fungi* as well as (D) archaeal to bacterial, and (E) fungal to bacterial SSU rRNA gene copy ratios under oxic (Left) and anoxic (Right) conditions. Gray shades of symbols indicate soil fraction: bulk (gray), HF (black), and LF (white, only wo-treatment). Every plot shows gene copy numbers of the differently aged soils (0.5, 5, 12, and 120 kyr), each with the four treatments (wo, P, C, and CP). Error bars indicate standard deviation of three parallel incubation samples.

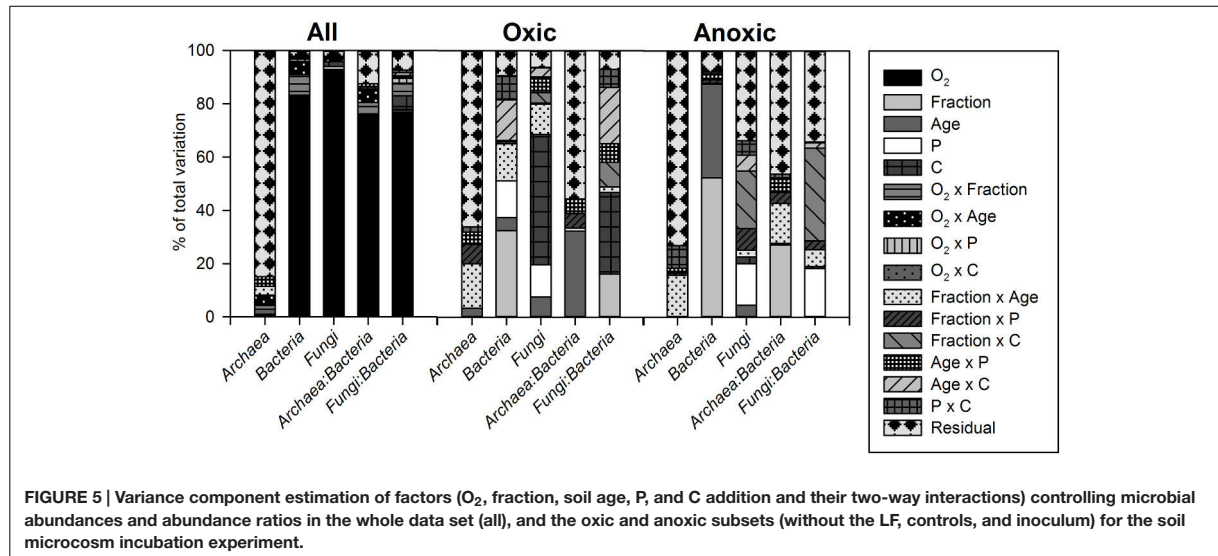


FIGURE 5 | Variance component estimation of factors (O_2 , fraction, soil age, P, and C addition and their two-way interactions) controlling microbial abundances and abundance ratios in the whole data set (all), and the oxic and anoxic subsets (without the LF, controls, and inoculum) for the soil microcosm incubation experiment.

soil environment. To explore the relevance of specific soil properties for microbial patterns during long-term ecosystem development, we set up a microcosm incubation experiment. While such experiments cannot entirely reflect the conditions in natural soil, they provide valuable insights into the interactions between individual soil characteristics and soil microbiota.

The soils along the Franz Josef chronosequence are covered by rainforest (Richardson et al., 2004) that provides, especially at the intermediate-aged sites (1–12 kyr), a large input of OM to topsoil horizons causing a high microbial biomass, high enzymatic activities (Turner et al., 2014), and a maximum of archaeal, bacterial, fungal, and eukaryotic SSU rRNA gene copy numbers in organic horizons at these sites (Figures 1A,B and Supplementary Table S3). This link between vegetation and belowground microbiota was supported by correlation analysis showing a strong relationship between soil OC, ON and OP contents, and microbial activities and abundances (microbial biomass, total cell counts, and SSU rRNA gene copy numbers) for whole soil profiles along the chronosequence (Table 2; Turner et al., 2014).

TABLE 3 | Effects of the different factors on microbial community composition in the soil microcosm incubation experiment (bulk and HF, without the LF) as revealed by multi-response permutation procedure (MRPP).

	A (O_2)	A (Fraction)	A (Site age)	A (P)	A (C)
Archaea (HaeIII)	0.047	0.026	0.220	−0.008	−0.007
Archaea (Rsal)	0.063	0.050	0.138	−0.004	−0.011
Bacteria (HaeIII)	0.178	0.048	0.028	0.008	−0.007
Bacteria (Hhal)	0.186	0.048	0.045	0.004	−0.007

A is the within-group agreement statistic, significant results at $P < 0.01$ are typed in bold.

Archaea rather than Bacteria Predominate Subsoils, Especially at Older Development Stages

The *Archaea* to *Bacteria* abundance ratio was lowest in the organic horizon and increased with soil depth pointing to a relative predominance of *Archaea* in subsoils (Figure 1C). Additionally, bacterial, fungal, and eukaryotic abundances were maximal in the organic horizon, whereas archaeal abundances were highest in mineral A horizons at some sites. These observations were in line with findings for a spruce forest, where a higher abundance of *Archaea* was determined via metagenomics for the mineral soil horizon compared to the organic horizon (Uroz et al., 2013). Archaeal 16S rRNA gene copy numbers in a soil profile of a boreal peatland even increased in the upper 50 cm and then remained almost stable to a depth of 175 cm (Lin et al., 2014). Accordingly, *Bacteria* and *Fungi* seem to dominate the OM-rich layer (O horizon) being responsible for the decomposition of particulate OM while the *Archaea* seem to be better adapted to subsoil conditions where OM generally becomes less available due to a multitude of soil environmental factors, including sorption to and stabilization by minerals (Schmidt et al., 2011; Kleber et al., 2015). Fertilization and manipulation studies have shown that archaeal to bacterial abundance ratios are negatively related to increasing soil C contents suggesting that soil *Archaea* might be rather oligotrophs (Fierer et al., 2007; Nemergut et al., 2010; Wessén et al., 2010; Chroňáková et al., 2015).

Interestingly, the *Archaea* to *Bacteria* abundance ratio not only increased with soil depth but also with soil age pointing to an increasing relative quantitative importance of *Archaea* in long-term soil development coinciding with a P-limitation and an increase in Fe and Al (hydr)oxides as well as other clay-sized minerals at older stages (Turner et al., 2014). However, our results of the incubation experiment showed that archaeal

abundances were hardly affected by soil fraction (bulk vs. HF), soil age (including the mineralogical gradient) as well as C and P addition (Figure 5 and Supplementary Table S6) showing that archaeal abundances were rather stable under the tested conditions. Based on an 18-months incubation experiment with artificial soils, Hemkemeyer et al. (2014) also reported only a weak influence of the clay mineral composition on archaeal abundances with no effect of the addition of the Fe oxide ferrihydrite. In addition, archaeal abundances increased slower than *Bacteria* or *Fungi* over the 18 months indicating slower growth rates and a better adaptation to nutrient-poor conditions. In general, the distribution across extreme habitats and a range of biochemical mechanisms to cope with extreme conditions suggest that the adaptation to chronic energetic stress is a crucial factor that ecologically and evolutionary distinguish *Archaea* from *Bacteria* (Valentine, 2007).

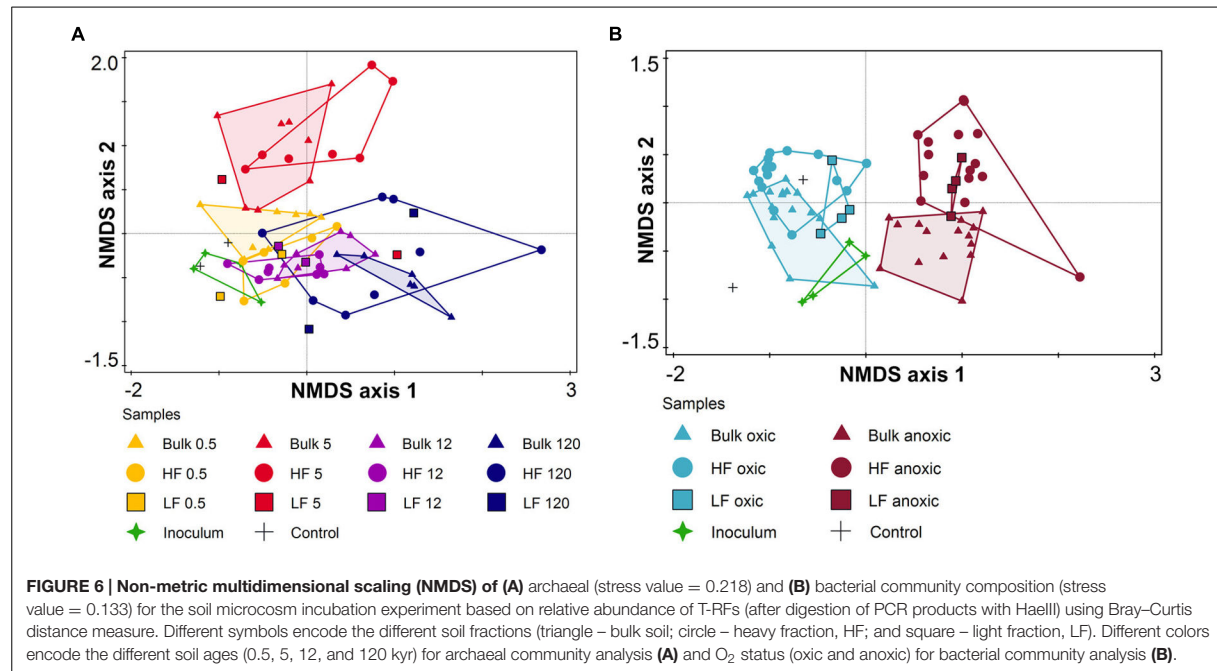
In contrast, bacterial abundances were significantly impacted by almost all tested factors in our incubation experiment (Supplementary Table S6) with the largest effects of the O₂ status and the soil fraction (Figure 5). Similarly, Hemkemeyer et al. (2014) reported a pronounced effect of mineral composition and particle size fraction on bacterial abundances with a positive effect of ferrihydrite (oxic conditions). Our results indicate that the O₂ status determined whether bacterial abundances were increased or decreased in HF samples. While under oxic condition bacterial abundances were higher in HF samples compared to bulk samples, under anoxic conditions they were lower maybe due to energy limitation that constrained the *Bacteria* in using mineral-associated OM (Figures 4B,D).

Taken together, the results of our microcosm incubation experiment revealed factors that possibly drive the abundance patterns at the Franz Josef chronosequence, i.e., O₂ status and soil fraction for bacterial abundances, whereas archaeal abundances were hardly affected by the tested factors. High precipitation regularly creates water-saturated conditions with low oxygen availability in these soils. Consequently, the rather anoxic conditions and the increasing influence of the soil mineral phase with soil depth and soil age decreases bacterial abundances. Additionally, soil minerals such as Fe and Al oxides and other clay-sized minerals, e.g., vermiculite, could impair the substrate availability for soil microorganisms due to the formation of mineral-organic associations by adsorption and coprecipitation (Kaiser and Guggenberger, 2007; Heckman et al., 2013; Kleber et al., 2015; Dietel et al., 2017) and thereby creating or intensifying nutrient-limited conditions. However, substrates bound to mineral surfaces are partly still available for microbial utilization depending on the sorption-desorption properties of the bound substrates, but their decomposition is retarded (Mikutta et al., 2007; Dippold et al., 2014). Thus, while *Bacteria* might be inhibited, *Archaea* probably better cope with this mineral-induced nutrient and substrate limitation because of their slow growth rates, their rather oligotrophic lifestyle and their hypothesized better adaptation to chronic energetic stress resulting in increasing archaeal to bacterial abundance ratios in subsoils, especially at the oldest site of the Franz Josef chronosequence.

A decreasing fungal to bacterial ratio with soil depth along the Franz Josef chronosequence (Figure 1C) and higher ratios in LF samples compared to HF and bulk samples under oxic conditions in our incubation experiment (Figure 4E) point to a predominance of *Fungi* in habitats enriched in particulate OM (i.e., leaf and root litter) and with a high oxygen availability. These findings match with previous studies reporting relatively higher fungal abundance in soils with litter or soil macroaggregates (250–2000 μm, contain particulate OM) as compared to *Bacteria* (Baldrian et al., 2012; Smith et al., 2014). Noteworthy, under anoxic conditions we detected higher fungal to bacterial ratios for the C and CP treatment of the HF with almost similar SSU rRNA gene copy numbers for both taxa (Figures 4B,C,E). Accordingly, *Fungi* may survive adverse conditions as spores, but their abundance could increase even in anoxic habitats dominated by mineral-associated OM if there is an easy-degradable C source such as cellulose available. This observation corresponds to findings of Wild et al. (2014) for subsoil horizons that were amended with different ¹³C-labeled substrates with a significant, positive effect of glucose and amino acids on fungal abundance.

Shift in Archaeal Community Composition with Ongoing Soil Development

The increasing archaeal to bacterial abundance ratio with soil age was accompanied by a clear compositional shift of the archaeal community (Figure 2A). At young to intermediate-aged soils the archaeal community composition was characterized by the occurrence of common soil groups as the *FSCG* and *SAGMCG-1* belonging to the phylum *Thaumarchaeota*. Surprisingly, at the oldest, P-limited site, the *Bathyarchaeota* were dominant with a proportion of up to 74%. Most of our sequences were affiliated with the pSL22 cluster (Figure 3), originally derived from a hot spring in Yellowstone National Park (Barns et al., 1996) and clustered to sequences derived from hydrothermal vents or other hot springs with no cultivated representatives. However, some of our bathyarchaeotal sequences were affiliated with sequences of the *MCG* subgroup 6 derived from marine and freshwater sediments, subsurface or wastewater sludge, thus, representing a rather widespread subgroup. So far *Bathyarchaeota* mostly comprising the *MCG* (Meng et al., 2014), that were reported to be one of the most abundant and at the same time one of the most active groups in nutrient-poor, low energy environments like marine subsurface sediments (Fry et al., 2008; Breuker et al., 2013; Figure 3). There are only a few studies, mainly about waterlogged soils, reporting the *MCG* constituting a mentionable proportion of the archaeal soil community (summarized by Kubo et al., 2012 in the Supplementary Information). In peatland soils of the Appalachian Mountains not only *Archaea* of the *Group 1.1c* and *SAGMCG-1* were detected but also *MCG* with a proportion of 37% (Hawkins et al., 2014). Another study about permafrost soils analyzed the archaeal community in different soil depths and reported that 26–73% of the sequences were affiliated to *MCG*-OTUs corresponding to our high proportions (Wei et al., 2014).



Unfortunately, little is known about the physiological capabilities of the *Bathyarchaeota* because there are no cultivated representatives so far. The *MCG* archaea are considered to be mainly heterotrophic anaerobes (Biddle et al., 2006; Lazar et al., 2016) and *MCG* cells of the marine subsurface encoded extracellular protein-degrading enzymes such as aminopeptidases, thus, seem to be able to degrade persistent detrital matter comprised of cell wall components (Lloyd et al., 2013; Lazar et al., 2016). This assumption would be in line with an increase of aminopeptidase activities at the oldest site (Turner et al., 2014) suggesting that *Bathyarchaeota* at the oldest site may be adapted to the substrate and nutrient-poor conditions and are probably able to degrade proteins of dead microbial biomass that comprises an important internal carbon and nutrient pool at this soil development stage receiving only a small allochthonous OM input compared to the younger soil ages (Turner et al., 2013; calculated from Turner et al., 2014).

The archaeal community composition shift in soils of the Franz Josef chronosequence was related to soil age (Figure 2C) that is accompanied by a mineralogical and P gradient. Although the sample number for this pyrosequencing analysis was relatively low ($n = 9$), the age-related archaeal community composition shift matched with the T-RFLP results of our incubation experiment: The archaeal community composition was significantly affected by soil age and soil fraction, too (Figure 6A). Hemkemeyer et al. (2014) also reported an effect of different clay minerals on archaeal community composition in the particle size fraction $<20 \mu\text{m}$ after 18 months of incubation. In contrast, the addition of C or P had no impact on the archaeal community composition (Table 3) consistent with findings of fertilization studies that showed that the archaeal community

composition was not impacted by P addition (Leff et al., 2015). These results indicated that the age-related shift in archaeal community composition probably is caused by differences in soil mineralogical properties instead of changes in C or P contents.

Bacterial Communities Remained Stable over Long-Term Soil Development

In contrast to the clear age-related compositional shift of the archaeal community, the bacterial community did not change considerably (Figures 2B,D). Our results revealed that neither on phylum nor on genus level a restructuring of the bacterial community composition took place in mineral soils over long-term soil development. Similarly, Jangid et al. (2013b) reported stable bacterial communities in topsoils of the Franz Josef chronosequence older than 5 kyr and this observation was also described for other long-term soil chronosequences such as the Mendocino chronosequence (uplifted marine terraces, time points T2 and T3), B horizons of a dune chronosequence located in Georgia (United States), and a dune chronosequence bordering on the Lake Michigan (Tarlera et al., 2008; Williams et al., 2013; Uroz et al., 2014). Thus, bacterial communities seem to change drastically during early succession, but then remain relatively stable despite of changing mineralogical composition and the nutrient gradients. This observation could be linked to the rapidly decreasing soil pH, from approximately seven to four, during early succession of glacier forelands (Tschirko et al., 2003; Williams et al., 2013; Turner et al., 2014); pH is considered to be one of the most important factors structuring bacterial community composition (Fierer et al., 2009; Dini-Andreote et al., 2014). This explanation is also in line with our observation that

the pH is one of the best predictors for bacterial community composition at the Franz Josef chronosequence.

The results of the incubation experiment showed that the O₂ status was the most important controlling parameter for bacterial community composition if the pH remained stable during long-term soil development (Figure 6B and Table 3). This observation corresponds to our findings at the Franz Josef chronosequence where bacterial community composition was rather influenced by soil depth forming a steep redox gradient in these regularly water-saturated soils (Figure 2D).

Besides O₂ status, bacterial community composition differed significantly between soil fractions (Table 3) and T-RFs that were unique for either bulk or HF samples were detected (Supplementary Table S9). Blackwood and Paul (2003) also conducted a soil fractionation experiment and analyzed the bacterial community composition in four different fractions. They reported distinct communities for the HF and the LF concluding that these fractions provided distinct soil habitats due to different characteristics of the soil matrix and the OM within each fraction. They presumed that the selection for well adapted species may be greater in the HF compared to other fractions like the rhizosphere.

There are several studies reporting a significant effect of mineral composition such as different clay minerals or Fe oxides on bacterial communities in incubation experiments with artificial soils (Babin et al., 2013; Heckman et al., 2013; Vogel et al., 2014; Steinbach et al., 2015). On the contrary, we detected only a slight soil age effect for bacterial T-RFLP profiles analyzed with HhaI (Table 3). This difference may be related to the use of natural soils in our study which featured less pronounced differences in mineralogical compositions compared to artificial soils consisting of pure minerals used in other studies.

CONCLUSION

Our study provides first insights in patterns of microbial communities in soil depth profiles along the long-term ecosystem development gradient of the Franz Josef chronosequence. The archaeal to bacterial abundance ratio increased not only with soil depth, but also with soil age with archaeal abundances being less impacted by the mineral-associated soil fraction and soil age than *Bacteria*. Moreover, pyrosequencing results revealed that *Archaea* and *Bacteria* show different patterns in relation to soil age: archaeal communities were clearly affected by soil age linked to changes in soil mineralogical properties, whereas bacterial community composition remained stable. Overall, our results indicate, that archaeal communities may relatively predominate

REFERENCES

- Almond, P. C., Moar, N. T., and Lian, O. B. (2001). Reinterpretation of the glacial chronology of South Westland, New Zealand. *N. Z. J. Geol. Geophys.* 44, 1–15. doi: 10.1080/00288306.2001.9514917
- Applied Biosystems (2002). *TaqMan® Ribosomal RNA Control Reagents. VIC™ Probes. Protocol*. Foster City, CA: Applied Biosystems
- Babin, D., Ding, G.-C., Pronk, G. J., Heister, K., Kögel-Knabner, I., and Smalla, K. (2013). Metal oxides, clay minerals and charcoal determine the composition

subsoils, especially in nutrient-depleted old soils, by better coping with mineral-induced substrate limitations and due to changes in community composition to taxa (i.e., *Bathyarchaeota*) that are adapted to nutrient-poor, low energy habitats.

Further research is necessary to gain a better understanding of the processes and general patterns associated with long-term soil development and the particular role of microorganisms being of utmost importance for nutrient cycling. Special attention should be paid to the impact of mineral-organic associations on soil microbial communities and the underlying mechanisms controlling this interaction.

AUTHOR CONTRIBUTIONS

AS, RM, and GG designed this study. RM, SM-S, and ST performed soil sampling. ST and SM-S conducted laboratory work. ST analyzed the data with input from FS (statistics) and CL (archaeal taxonomy), and wrote the manuscript. All authors discussed the data and revised the manuscript.

FUNDING

This research was funded by the German Science Foundation (DFG), grants MI 1377/5-2 and SCHI 535/11-2 to RM and AS, respectively.

ACKNOWLEDGMENTS

We greatly acknowledge Norman Gentsch, Andre Eger, Roger Michael Klatt and Leo M. Condron for the help with preparation and realization of the sampling, Peter C. Almond, Duane A. Peltzer and Sarah J. Richardson for access to the sampling sites, Daria Frohloff and Gudrun Mengel-Jung for help with the DNA extraction of incubation samples, Cornelia Struckmeyer for laboratory support, Marco Blöthe for support with pyrosequencing data analysis, Sabrina Hedrich for support with T-RFLP, and Christian Siebenbürgen for help with graphical issues.

SUPPLEMENTARY MATERIAL

The Supplementary Material for this article can be found online at: <http://journal.frontiersin.org/article/10.3389/fmicb.2017.00874/full#supplementary-material>

- of microbial communities in matured artificial soils and their response to phenanthrene. *FEMS Microbiol. Ecol.* 86, 3–14. doi: 10.1111/1574-6941.12058
- Baldrian, P., Kolařík, M., Štursová, M., Kopecký, J., Valášková, V., Větrovský, T., et al. (2012). Active and total microbial communities in forest soil are largely different and highly stratified during decomposition. *ISME J.* 6, 248–258. doi: 10.1038/ismej.2011.95
- Barns, S. M., Delwiche, C. F., Palmer, J. D., and Pace, N. R. (1996). Perspectives on archaeal diversity, thermophily and monophyly from environmental rRNA

- sequences. *Proc. Natl. Acad. Sci. U.S.A.* 93, 9188–9193. doi: 10.1073/pnas.93.17.9188
- Bates, D., Mächler, M., Bolker, B., and Walker, S. C. (2015). Fitting linear mixed-effects models using lme4. *J. Stat. Softw.* 67, 1–48.
- Biddle, J. F., Lipp, J. S., Lever, M. A., Lloyd, K. G., Sørensen, K. B., Anderson, R., et al. (2006). Heterotrophic Archaea dominate sedimentary subsurface ecosystems off Peru. *Proc. Natl. Acad. Sci. U.S.A.* 103, 3846–3851. doi: 10.1073/pnas.0600035103
- Blackwood, C. B., and Paul, E. A. (2003). Eubacterial community structure and population size within the soil light fraction, rhizosphere, and heavy fraction of several agricultural systems. *Soil Biol. Biochem.* 35, 1245–1255. doi: 10.1016/S0038-0717(03)00188-3
- Blume, E., Bischoff, M., Reichert, J. M., Moorman, T., Konopka, A., and Turco, R. F. (2002). Surface and subsurface microbial biomass, community structure and metabolic activity as a function of soil depth and season. *Appl. Soil Ecol.* 20, 171–181. doi: 10.1016/S0929-1393(02)00025-2
- Borneman, J., and Hartin, R. J. (2000). PCR Primers that amplify fungal rRNA genes from environmental samples. *Appl. Environ. Microbiol.* 66, 4356–4360. doi: 10.1128/AEM.66.10.4356-4360.2000
- Brankatschk, R., Töwe, S., Kleineidam, K., Schloter, M., and Zeyer, J. (2011). Abundances and potential activities of nitrogen cycling microbial communities along a chronosequence of a glacier forefield. *ISME J.* 5, 1025–1037. doi: 10.1038/ismej.2010.184
- Breuker, A., Stadler, S., and Schippers, A. (2013). Microbial community analysis of deeply buried marine sediments of the New Jersey shallow shelf (IODP Expedition 313). *FEMS Microbiol. Ecol.* 85, 578–592. doi: 10.1111/1574-6941.12146
- Cerli, C., Celi, L., Kalbitz, K., Guggenberger, G., and Kaiser, K. (2012). Separation of light and heavy organic matter fractions in soil – Testing for proper density cut-off and dispersion level. *Geoderma* 170, 403–416. doi: 10.1016/j.geoderma.2011.10.009
- Chroňáková, A., Schloter-Hai, B., Radl, V., Endesfelder, D., Quince, C., Elhottová, D., et al. (2015). Response of archaeal and bacterial soil communities to changes associated with outdoor cattle overwintering. *PLoS ONE* 10:e0135627. doi: 10.1371/journal.pone.0135627
- Crow, S. E., Swanston, C. W., Lajtha, K., Brooks, J. R., and Keirstead, H. (2007). Density fractionation of forest soils: methodological questions and interpretation of incubation results and turnover time in an ecosystem context. *Biogeochemistry* 85, 69–90. doi: 10.1007/s10533-007-9100-8
- Culman, S. W., Bukowski, R., Gauch, H. G., Cadillo-Quiroz, H., and Buckley, D. H. (2009). T-REX: software for the processing and analysis of T-RFLP data. *BMC Bioinformatics* 10:171. doi: 10.1186/1471-2105-10-171
- Dietel, J., Dohrmann, R., Guggenberger, G., Meyer-Stüve, S., Turner, S., Schippers, A., et al. (2017). Complexity of clay mineral formation during 120,000 years of soil development along the Franz Josef chronosequence, New Zealand. *N. Z. J. Geol. Geophys.* 60, 23–35. doi: 10.1080/00288306.2016.1245668
- Dini-Andreote, F., de Cássia Pereira e Silva, M., Triado-Margarit, X., Casamayor, E. O., van Elsas, J. D., and Salles, J. F. (2014). Dynamics of bacterial community succession in a salt marsh chronosequence: evidences for temporal niche partitioning. *ISME J.* 8, 1989–2001. doi: 10.1038/ismej.2014.54
- Dippold, M., Biryukov, M., and Kuzuyakov, Y. (2014). Sorption affects amino acid pathways in soil: implications from position-specific labeling of alanine. *Soil Biol. Biochem.* 72, 180–192. doi: 10.1016/j.soilbio.2014.01.015
- Edgar, R. C., Haas, B. J., Clemente, J. C., Quince, C., and Knight, R. (2011). UCHIME improves sensitivity and speed of chimera detection. *Bioinformatics* 27, 2194–2200. doi: 10.1093/bioinformatics/btr381
- Fierer, N., Allen, A. S., Schimel, J. P., and Holden, P. A. (2003). Controls on microbial CO₂ production: a comparison of surface and subsurface soil horizons. *Glob. Chang. Biol.* 9, 1322–1332. doi: 10.1046/j.1365-2486.2003.00663.x
- Fierer, N., Bradford, M. A., and Jackson, R. B. (2007). Toward an ecological classification of soil bacteria. *Ecology* 88, 1354–1364.
- Fierer, N., Strickland, M. S., Liptzin, D., Bradford, M. A., and Cleveland, C. C. (2009). Global patterns in belowground communities. *Ecol. Lett.* 12, 1238–1249. doi: 10.1111/j.1461-0248.2009.01360.x
- Frank, D. N., Amand, A. L. S., Feldman, R. A., Boedeker, E. C., Harpaz, N., and Pace, N. R. (2007). Molecular-phylogenetic characterization of microbial community imbalances in human inflammatory bowel diseases. *Proc. Natl. Acad. Sci. U.S.A.* 104, 13780–13785.
- Freedman, Z., and Zak, D. R. (2015). Soil bacterial communities are shaped by temporal and environmental filtering: evidence from a long-term chronosequence. *Environ. Microbiol.* 17, 3208–3218. doi: 10.1111/1462-2920.12762
- Fry, J. C., Parkes, R. J., Cragg, B. A., Weightman, A. J., and Webster, G. (2008). Prokaryotic biodiversity and activity in the deep seafloor biosphere. *FEMS Microbiol. Ecol.* 66, 181–196. doi: 10.1111/j.1574-6941.2008.00566.x
- Gentsch, N., Mikutta, R., Shibistova, O., Wild, B., Schneckler, J., Richter, A., et al. (2015). Properties and bioavailability of particulate and mineral-associated organic matter in Arctic permafrost soils, Lower Kolyma Region, Russia. *Eur. J. Soil Sci.* 66, 722–734. doi: 10.1111/ejss.12269
- Gray, N. D., Sherry, A., Grant, R. J., Rowan, A. K., Hubert, C. R. J., Callbeck, C. M., et al. (2011). The quantitative significance of Syntrophaceae and syntrophic partnerships in methanogenic degradation of crude oil alkanes. *Environ. Microbiol.* 13, 2957–2975. doi: 10.1111/j.1462-2920.2011.02570.x
- Hansel, C. M., Fendorf, S., Jardine, P. M., and Francis, C. A. (2008). Changes in bacterial and archaeal community structure and functional diversity along a geochemically variable soil profile. *Appl. Environ. Microbiol.* 74, 1620–1633. doi: 10.1128/AEM.01787-07
- Hartmann, M., Lee, S., Hallam, S. J., and Mohn, W. W. (2009). Bacterial, archaeal and eukaryal community structures throughout soil horizons of harvested and naturally disturbed forest stands. *Environ. Microbiol.* 11, 3045–3062. doi: 10.1111/j.1462-2920.2009.02008.x
- Hawkins, A. N., Johnson, K. W., and Bräuer, S. L. (2014). Southern Appalachian peatlands support high archaeal diversity. *Microb. Ecol.* 67, 587–602. doi: 10.1007/s00248-013-0352-7
- Haynes, R. J. (2014). “Nature of the belowground ecosystem and its development during pedogenesis,” in *Advances in Agronomy*, Vol. 172, ed. D. L. Sparks (Amsterdam: Academic Press), 43–109.
- Heckman, K., Welty-Bernard, A., Vazquez-Ortega, A., Schwartz, E., Chorover, J., and Rasmussen, C. (2013). The influence of goethite and gibbsite on soluble nutrient dynamics and microbial community composition. *Biogeochemistry* 112, 179–195. doi: 10.1007/s10533-012-9715-2
- Hemkemeyer, M., Pronk, G. J., Heister, K., Kögel-Knabner, I., Martens, R., and Tebbe, C. C. (2014). Artificial soil studies reveal domain-specific preferences of microorganisms for the colonisation of different soil minerals and particle size fractions. *FEMS Microbiol. Ecol.* 90, 770–782. doi: 10.1111/1574-6941.12436
- Herlemann, D. P., Labrenz, M., Jürgens, K., Bertilsson, S., Wanek, J. J., and Andersson, A. F. (2011). Transitions in bacterial communities along the 2000 km salinity gradient of the Baltic Sea. *ISME J.* 5, 1571–1579. doi: 10.1038/ismej.2011.41
- Jangid, K., Whitman, W. B., Condrón, L. M., Turner, B. L., and Williams, M. A. (2013a). Progressive and retrogressive ecosystem development coincide with soil bacterial community change in a dune system under lowland temperate rainforest in New Zealand. *Plant Soil* 367, 235–247. doi: 10.1007/s11104-013-1720-2
- Jangid, K., Whitman, W. B., Condrón, L. M., Turner, B. L., and Williams, M. A. (2013b). Soil bacterial community succession during long-term ecosystem development. *Mol. Ecol.* 22, 3415–3424. doi: 10.1111/mec.12325
- Jürgens, G., Lindström, K., and Saano, A. (1997). Novel group within the kingdom Crenarchaeota from boreal forest soil. *Appl. Environ. Microbiol.* 63, 803–805.
- Kaiser, K., and Guggenberger, G. (2007). Sorptive stabilization of organic matter by microporous goethite: sorption into small pores vs. surface complexation. *Eur. J. Soil Sci.* 58, 45–59. doi: 10.1111/j.1365-2389.2006.00799.x
- Kleber, M., Eusterhues, K., Keiluweit, M., Mikutta, C., Mikutta, R., and Nico, P. S. (2015). Mineral-organic associations: formation, properties, and relevance in soil environments. *Adv. Agron.* 130, 1–140. doi: 10.1016/bs.agron.2014.10.005
- Kubo, K., Lloyd, K. G., F Biddle, J., Amann, R., Teske, A., and Knittel, K. (2012). Archaea of the Miscellaneous Crenarchaeotal Group are abundant, diverse and widespread in marine sediments. *ISME J.* 6, 1949–1965. doi: 10.1038/ismej.2012.37
- Lazar, C. S., Baker, B. J., Seitz, K., Hyde, A. S., Dick, G. J., Hinrichs, K.-U., et al. (2016). Genomic evidence for distinct carbon substrate preferences and ecological niches of Bathyarchaeota in estuarine sediments. *Environ. Microbiol.* 18, 1200–1211. doi: 10.1111/1462-2920.13142

- Leff, J. W., Jones, S. E., Prober, S. M., Barberán, A., Borer, E. T., Firn, J. L., et al. (2015). Consistent responses of soil microbial communities to elevated nutrient inputs in grasslands across the globe. *Proc. Natl. Acad. Sci. U.S.A.* 112, 10967–10972. doi: 10.1073/pnas.1508382112
- Lenth, R. (2015). *Lsmmeans: Least-Squares Means*. Available at: <https://CRAN.R-project.org/package=lsmmeans>
- Lin, X., Tfaily, M. M., Steinweg, J. M., Chanton, P., Esson, K., Yang, Z. K., et al. (2014). Microbial community stratification linked to utilization of carbohydrates and phosphorus limitation in a boreal peatland at Marcell Experimental Forest, Minnesota, United States. *Appl. Environ. Microbiol.* 80, 3518–3530. doi: 10.1128/AEM.00205-14
- Lloyd, K. G., Schreiber, L., Petersen, D. G., Kjeldsen, K. U., Lever, M. A., Steen, A. D., et al. (2013). Predominant archaea in marine sediments degrade detrital proteins. *Nature* 496, 215–218. doi: 10.1038/nature12033
- Ludwig, W., Strunk, O., Westram, R., Richter, L., Meier, H., Yadhukumar, et al. (2004). ARB: a software environment for sequence data. *Nucleic Acids Res.* 32, 1363–1371. doi: 10.1093/nar/gkh293
- Massana, R., Murray, A. E., Preston, C. M., and DeLong, E. F. (1997). Vertical distribution and phylogenetic characterization of marine planktonic Archaea in the Santa Barbara Channel. *Appl. Environ. Microbiol.* 63, 50–56.
- Meng, J., Xu, J., Qin, D., He, Y., Xiao, X., and Wang, F. (2014). Genetic and functional properties of uncultivated MCG archaea assessed by metagenome and gene expression analyses. *ISME J.* 8, 650–659. doi: 10.1038/ismej.2013.174
- Mikutta, R., Mikutta, C., Kalbitz, K., Scheel, T., Kaiser, K., and Jahn, R. (2007). Biodegradation of forest floor organic matter bound to minerals via different binding mechanisms. *Geochim. Cosmochim. Acta* 71, 2569–2590. doi: 10.1016/j.gca.2007.03.002
- Mikutta, R., Schaumann, G. E., Gildemeister, D., Bonneville, S., Kramer, M. G., Chorover, J., et al. (2009). Biogeochemistry of mineral-organic associations across a long-term mineralogical soil gradient (0.3–4100 kyr), Hawaiian Islands. *Geochim. Cosmochim. Acta* 73, 2034–2060. doi: 10.1016/j.gca.2008.12.028
- Muyzer, G., Teske, A., Wirsén, C. O., and Jannasch, H. W. (1995). Phylogenetic relationships of Thiomicrospira species and their identification in deep-sea hydrothermal vent samples by denaturing gradient gel electrophoresis of 16S rDNA fragments. *Arch. Microbiol.* 164, 165–172. doi: 10.1007/BF02529967
- Nadkarni, M. A., Martin, F. E., Jacques, N. A., and Hunter, N. (2002). Determination of bacterial load by real-time PCR using a broad range (universal) probe and primer set. *Microbiology* 148, 257–266. doi: 10.1128/JCM.40.5.1698
- Nemergut, D. R., Anderson, S. P., Cleveland, C. C., Martin, A. P., Miller, A. E., Seimon, A., et al. (2007). Microbial community succession in an unvegetated, recently deglaciated soil. *Microb. Ecol.* 53, 110–122. doi: 10.1007/s00248-006-9144-7
- Nemergut, D. R., Cleveland, C. C., Wieder, W. R., Washenberger, C. L., and Townsend, A. R. (2010). Plot-scale manipulations of organic matter inputs to soils correlate with shifts in microbial community composition in a lowland tropical rain forest. *Soil Biol. Biochem.* 42, 2153–2160. doi: 10.1016/j.soilbio.2010.08.011
- Nicol, G. W., Tscherko, D., Embley, T. M., and Prosser, J. I. (2005). Primary succession of soil Crenarchaeota across a receding glacier foreland. *Environ. Microbiol.* 7, 337–347. doi: 10.1111/j.1462-2920.2004.00698.x
- Oksanen, J., Blanchet, F. G., Kindt, R., Legendre, P., Minchin, P. R., O'Hara, R. B., et al. (2015). *Vegan: Community Ecology Package. R Package Version 2.3-2*. Available at: <https://CRAN.R-project.org/package=vegan>
- Peltzer, D. A., Wardle, D. A., Allison, V. J., Baisden, W. T., Bardgett, R. D., Chadwick, O. A., et al. (2010). Understanding ecosystem retrogression. *Ecol. Monogr.* 80, 509–529. doi: 10.1890/09-1552.1
- Pruesse, E., Peplies, J., and Glöckner, F. O. (2012). SINA: accurate high-throughput multiple sequence alignment of ribosomal RNA genes. *Bioinformatics* 28, 1823–1829. doi: 10.1093/bioinformatics/bts252
- Quast, C., Pruesse, E., Yilmaz, P., Gerken, J., Schweer, T., Yarza, P., et al. (2013). The SILVA ribosomal RNA gene database project: improved data processing and web-based tools. *Nucleic Acids Res.* 41, D590–D596. doi: 10.1093/nar/gks1219
- Quince, C., Lanzén, A., Curtis, T. P., Davenport, R. J., Hall, N., Head, I. M., et al. (2009). Accurate determination of microbial diversity from 454 pyrosequencing data. *Nat. Methods* 6, 639–641. doi: 10.1038/nmeth.1361
- R Core Team (2015). *R: A Language and Environment for Statistical Computing*. Vienna: R Foundation for Statistical Computing.
- Richardson, S. J., Peltzer, D. A., Allen, R. B., McGlone, M. S., and Parfitt, R. L. (2004). Rapid development of phosphorus limitation in temperate rainforest along the Franz Josef soil chronosequence. *Oecologia* 139, 267–276. doi: 10.1007/s00442-004-1501-y
- Schloss, P. D., Westcott, S. L., Ryabin, T., Hall, J. R., Hartmann, M., Hollister, E. B., et al. (2009). Introducing mothur: open-source, platform-independent, community-supported software for describing and comparing microbial communities. *Appl. Environ. Microbiol.* 75, 7537–7541.
- Schmidt, M. W. L., Torn, M. S., Abiven, S., Dittmar, T., Guggenberger, G., Janssens, I. A., et al. (2011). Persistence of soil organic matter as an ecosystem property. *Nature* 478, 49–56. doi: 10.1038/nature10386
- Schulz, S., Brankatschk, R., Dümig, A., Kögel-Knabner, I., Schloter, M., and Zeyer, J. (2013). The role of microorganisms at different stages of ecosystem development for soil formation. *Biogeosciences* 10, 3983–3996. doi: 10.5194/bg-10-3983-2013
- Schütte, U. M. E., Abdo, Z., Bent, S. J., Williams, C. J., Schneider, M. G., Solheim, B., et al. (2009). Bacterial succession in a glacier foreland of the High Arctic. *ISME J.* 3, 1258–1268. doi: 10.1111/j.1365-294X.2009.04479.x
- Smith, A. P., Marin-Spiotta, E., de Graaff, M. A., and Balser, T. C. (2014). Microbial community structure varies across soil organic matter aggregate pools during tropical land cover change. *Soil Biol. Biochem.* 77, 292–303. doi: 10.1016/j.soilbio.2014.05.030
- Sørensen, K., Lauer, A., and Teske, A. (2004). Archaeal phylotypes in a metal-rich and low-activity deep subsurface sediment of the Peru Basin, ODP Leg 201, Site 1231. *Geobiology* 2, 151–161. doi: 10.1111/j.1472-4677.2004.00028.x
- Stahl, D. A., and Amann, R. (1991). "Development and application of nucleic acid probes in bacterial systematics," in *Nucleic acid Techniques in Bacterial Systematics*, eds E. Stackebrandt and M. Goodfellow (New York, NY: John Wiley & Sons Ltd), 205–248.
- Steinbach, A., Schulz, S., Giebler, J., Schulz, S., Pronk, G. J., Kögel-Knabner, I., et al. (2015). Clay minerals and metal oxides strongly influence the structure of alkane-degrading microbial communities during soil maturation. *ISME J.* 9, 1687–1691. doi: 10.1038/ismej.2014.243
- Stevens, P., and Walker, T. (1970). The chronosequence concept and soil formation. *Q. Rev. Biol.* 45, 333–350.
- Stevens, P. R. (1968). *A Chronosequence of Soils Near the Franz Josef Glacier*. dissertation thesis, University of Canterbury, Christchurch.
- Stone, M. M., Kan, J., and Plante, A. F. (2015). Parent material and vegetation influence bacterial community structure and nitrogen functional genes along deep tropical soil profiles at the Luquillo Critical Zone Observatory. *Soil Biol. Biochem.* 80, 273–282. doi: 10.1016/j.soilbio.2014.10.019
- Takai, K., Moser, D. P., DeFlaun, M., Onstott, T. C., and Fredrickson, J. K. (2001). Archaeal diversity in waters from deep South African gold mines. *Appl. Environ. Microbiol.* 67, 5750–5760. doi: 10.1128/AEM.67.21.5750
- Tarlera, S., Jangid, K., Ivester, A. H., Whitman, W. B., and Williams, M. A. (2008). Microbial community succession and bacterial diversity in soils during 77 000 years of ecosystem development. *FEMS Microbiol. Ecol.* 64, 129–140. doi: 10.1111/j.1574-6941.2008.00444.x
- ter Braak, C. J. F., and Šmilauer, P. (2012). *Canoco Reference Manual and User's Guide: Software for Ordination, Version 5.0*. Ithaca: Microcomputer Power.
- Tscherko, D., Rustemeier, J., Richter, A., Wanek, W., and Kandeler, E. (2003). Functional diversity of the soil microflora in primary succession across two glacier forelands in the Central Alps. *Eur. J. Soil Sci.* 54, 685–696. doi: 10.1046/j.1365-2389.2003.00570.x
- Turner, B. L., Lambers, H., Condrón, L. M., Cramer, M. D., Leake, J. R., Richardson, A. E., et al. (2013). Soil microbial biomass and the fate of phosphorus during long-term ecosystem development. *Plant Soil* 367, 225–234. doi: 10.1007/s11104-012-1493-z
- Turner, S., Meyer-Stüve, S., Schippers, A., Guggenberger, G., Schaarschmidt, F., Wild, B., et al. (2017). Microbial utilization of mineral-associated nitrogen in soils. *Soil Biol. Biochem.* 104, 185–196. doi: 10.1016/j.soilbio.2016.10.010
- Turner, S., Schippers, A., Meyer-Stüve, S., Guggenberger, G., Gentsch, N., Dohrmann, R., et al. (2014). Mineralogical impact on long-term patterns of soil nitrogen and phosphorus enzyme activities. *Soil Biol. Biochem.* 68, 31–43. doi: 10.1016/j.soilbio.2013.09.016
- Uroz, S., Ioannidis, P., Lengelle, J., Cébron, A., Morin, E., Buée, M., et al. (2013). Functional assays and metagenomic analyses reveals differences between the

- microbial communities inhabiting the soil horizons of a Norway spruce plantation. *PLoS ONE* 8:e55929. doi: 10.1371/journal.pone.0055929
- Uroz, S., Tech, J. J., Sawaya, N. A., Frey-Klett, P., and Leveau, J. H. J. (2014). Structure and function of bacterial communities in ageing soils: insights from the Mendocino ecological staircase. *Soil Biol. Biochem.* 69, 265–274. doi: 10.1016/j.soilbio.2013.11.002
- Valentine, D. L. (2007). Adaptations to energy stress dictate the ecology and evolution of the Archaea. *Nat. Rev. Microbiol.* 5, 316–323. doi: 10.1038/nrmicro1619
- Vogel, C., Babin, D., Pronk, G. J., Heister, K., Smalla, K., and Kögel-Knabner, I. (2014). Establishment of macro-aggregates and organic matter turnover by microbial communities in long-term incubated artificial soils. *Soil Biol. Biochem.* 79, 57–67. doi: 10.1016/j.soilbio.2014.07.012
- Webster, G., Newberry, C. J., Fry, J. C., and Weightman, A. J. (2003). Assessment of bacterial community structure in the deep sub-seafloor biosphere by 16S rDNA-based techniques: a cautionary tale. *J. Microbiol. Methods* 55, 155–164. doi: 10.1016/S0167-7012(03)00140-4
- Wei, S., Cui, H., He, H., Hu, F., Su, X., and Zhu, Y. (2014). Diversity and distribution of Archaea community along a stratigraphic permafrost profile from Qinghai-Tibetan Plateau, China. *Archaea* 2014:240817. doi: 10.1155/2014/240817
- Wessén, E., Hallin, S., and Philippot, L. (2010). Differential responses of bacterial and archaeal groups at high taxonomical ranks to soil management. *Soil Biol. Biochem.* 42, 1759–1765. doi: 10.1016/j.soilbio.2010.06.013
- Wild, B., Schneckner, J., Alves, R. J. E., Barsukov, P., Bárta, J., Capek, P., et al. (2014). Input of easily available organic C and N stimulates microbial decomposition of soil organic matter in arctic permafrost soil. *Soil Biol. Biochem.* 75, 143–151. doi: 10.1016/j.soilbio.2014.04.014
- Williams, M. A., Jangid, K., Shanmugam, S. G., and Whitman, W. B. (2013). Bacterial communities in soil mimic patterns of vegetative succession and ecosystem climax but are resilient to change between seasons. *Soil Biol. Biochem.* 57, 749–757. doi: 10.1016/j.soilbio.2012.08.023
- Wu, X., Zhang, W., Liu, G., Yang, X., Hu, P., Chen, T., et al. (2012). Bacterial diversity in the foreland of the Tianshan No. 1 glacier, China. *Environ. Res. Lett.* 7:014038. doi: 10.1088/1748-9326/7/1/014038
- Zumsteg, A., Bernasconi, S. M., Zeyer, J., and Frey, B. (2012). Microbial community and activity shifts after soil transplantation in a glacier forefield. *Appl. Geochemistry* 26, 326–329. doi: 10.1016/j.apgeochem.2011.03.078

Conflict of Interest Statement: The authors declare that the research was conducted in the absence of any commercial or financial relationships that could be construed as a potential conflict of interest.

Copyright © 2017 Turner, Mikutta, Meyer-Stüve, Guggenberger, Schaarschmidt, Lazar, Dohrmann and Schippers. This is an open-access article distributed under the terms of the Creative Commons Attribution License (CC BY). The use, distribution or reproduction in other forums is permitted, provided the original author(s) or licensor are credited and that the original publication in this journal is cited, in accordance with accepted academic practice. No use, distribution or reproduction is permitted which does not comply with these terms.



Supplementary Material

Microbial Community Dynamics in Soil Depth Profiles over 120,000 Years of Ecosystem Development

Stephanie Turner, Robert Mikutta, Sandra Meyer-Stüve, Georg Guggenberger, Frank Schaarschmidt, Cassandre Sara Lazar, Reiner Dohrmann, Axel Schippers*

* **Correspondence:** Axel Schippers, Axel.Schippers@bgr.de

1 Supplementary Tables and Figures

1.1 Supplementary Tables

Table S1 Initial concentrations of organic carbon (OC) and total nitrogen (TN) per g soil fraction of samples used for the soil incubation experiment (Turner et al., 2017).

Site age (kyr)	Fraction	OC (mg g ⁻¹)	TN (mg g ⁻¹)
0.5	Bulk	144.2	7.9
5		137.3	7.7
12		77.7	3.6
120		65.5	3.6
0.5	HF	126.1	6.7
5		99.8	5.5
12		63.7	3.0
120		57.1	3.1
0.5	LF	403.5	14.0
5		409.5	14.1
12		387.9	11.9
120		381.8	10.5

Table S2 Physico-chemical and soil mineralogical properties of soil horizons along the Franz Josef chronosequence (Turner et al., 2014). Soil horizons used for the incubation experiment are highlighted in green. Hor. – horizon, OC – organic carbon, ON – organic nitrogen, TP – total phosphorus, Fe_d – dithionite-extractable Fe phases representing poorly crystalline and crystalline Fe oxides as well as Fe-humus-complexes, (Fe+Al)_o – oxalate-extractable Fe and Al phases representing poorly crystalline minerals and metal-humus-complexes, Fe_{d-o} – difference between dithionite-extractable Fe and oxalate-extractable Fe representing crystalline Fe phases, (Fe+Al)_p – Fe and Al from organic complexes.

Site age (kyr)	Hor.	pH	OC (g kg ⁻¹)	ON (g kg ⁻¹)	TP (mg kg ⁻¹)	(Fe+Al) _o (g kg ⁻¹)	Fe _d (g kg ⁻¹)	(Fe+Al) _p (g kg ⁻¹)	Fe _{d-o} (g kg ⁻¹)	Clay (%)	Silt (%)	Sand (%)
0.06	AO	5.8	201.5	13.2	1103	4.2	3.3	4.3	0.4	11	31	58
0.06	CA	6.0	7.3	0.5	686	2.3	2.9	1.1	1.1	3	17	80
0.06	C	6.4	7.2	0.4	804	2.7	3.6	1.7	1.5	6	31	63
0.5	OA	4.5	241.7	10.2	785	ND	ND	11.6	ND	ND	ND	ND
0.5	A	4.7	158.4	6.9	583	7	3.6	7.7	0.0	17	55	28
0.5	C	5.6	3.6	0.2	744	1.7	1.3	1.5	0.1	5	46	49
1	O	3.9	327.6	13.4	544	ND	ND	2.9	ND	ND	ND	ND
1	AE	4.1	66.6	4.0	220	2.4	1.3	3.6	0.1	12	58	30
1	E	4.7	17.2	0.7	103	3.2	2.0	3.3	0.6	12	55	33
1	B	5.3	9.5	0.5	272	8.5	6.8	5.5	1.1	5	43	52
5	O	3.9	367.9	14.4	681	ND	ND	2.3	ND	ND	ND	ND
5	AE	4.3	47.3	2.8	195	2.7	1.9	1.4	0.4	13	56	30
5	E	4.9	16.6	0.6	100	4.2	3.2	1.8	0.6	13	58	29
5	B	5.1	8.1	0.4	231	8.5	7.2	2.2	1.1	6	51	43
12	O	3.8	448.1	12.8	499	ND	ND	1.2	ND	ND	ND	ND
12	AE	4.1	143.6	6.8	244	1.6	0.6	1.2	0.0	7	56	36
12	EA	4.5	30.5	0.9	76	1.4	0.7	0.9	0.4	5	52	43
12	B	5.0	36.4	1.3	328	13.4	8.2	4.7	2.6	9	34	57
12	C	5.5	4.7	0.2	664	6.6	0.8	0.6	0.3	8	28	64
60	O	4.0	220.3	6.2	296	ND	ND	1.6	ND	ND	ND	ND
60	AE	4.1	60.4	2.9	161	1.7	0.7	1	0.2	11	68	20
60	EA	4.7	24.0	1.0	92	5.9	3.8	3.1	0.5	14	67	19
60	B	5.1	13.3	0.7	137	13.9	9.4	3.9	1.8	16	59	25
60	C	5.5	2.2	0.1	591	2.6	1.2	0.9	0.5	7	43	50
120	O	4.4	190.4	5.4	136	ND	ND	0.6	ND	ND	ND	ND
120	A	4.2	72.1	4.0	78	0.5	0.2	0.5	0.0	10	77	13
120	E	4.9	7.7	0.4	16	2.9	2.3	1.7	1.4	12	74	13
120	B	5.2	12.5	0.4	77	7.8	24.7	4	22.0	20	51	29

ND = not determined

Table S3 Results of the Tukey's post hoc test following the two-way ANOVA (soil age, horizon, their interaction and depth as a covariate) on microbial abundances along soil profiles of the Franz Josef chronosequence determined by qPCR (Figure 1). Letters indicate differences in abundances between different soil ages within each horizon (horizontal direction). Equal letters denote that the abundances not significantly differed from each other (Tukey test, $P < 0.05$).

	Soil age (kyr)						
	0.06	0.5	1	5	12	60	120
<i>Archaea</i>							
O	-	ab	a	a	a	ab	b
A	a	ab	ab	ab	b	a	a
E	-	-	a	a	a	a	a
B	-	-	a	a	a	a	a
C	a	a	-	-	b	a	-
<i>Bacteria</i>							
O	-	ab	a	a	a	ab	b
A	abc	abc	abc	ab	c	ac	b
E	-	-	a	ab	a	a	b
B	-	-	ab	ab	a	ab	b
C	a	ab	-	-	-	b	-
<i>Fungi</i>							
O	-	ab	a	a	a	ab	b
A	ab	ab	ab	a	ab	b	a
E	-	-	a	ab	a	a	b
B	-	-	a	a	a	a	a
C	a	ab	-	-	-	b	-
<i>Eukarya</i>							
O	-	a	a	a	a	a	a
A	ab	ab	ab	a	ab	b	ab
E	-	-	ab	ab	a	a	b
B	-	-	ab	ab	ab	a	b
C	a	ab	-	-	-	b	-
<i>Archaea:Bacteria</i>							
O	-	a	a	a	a	a	a
A	a	bc	bc	bc	b	ac	bc
E	-	-	ab	a	ab	a	b
B	-	-	a	a	a	a	b
C	a	b	-	-	-	b	-
<i>Fungi:Bacteria</i>							
O	-	a	a	a	a	a	a
A	a	a	a	a	a	a	a
E	-	-	a	a	a	a	a
B	-	-	ab	ab	ab	a	b
C	a	a	-	-	-	a	-

Table S4 Spearman rank order correlation coefficients for SSU rRNA gene copy numbers g⁻¹ dry weight soil and soil chemical and mineralogical properties of the soil chronosequence. Significant results at P < 0.01 are typed in bold.

	NO ₃ ⁻	NH ₄ ⁺	TP	(Fe+Al) _o	Fe _d	(Fe+Al) _p	Fe _{d-o}	Clay	Silt	Sand
<i>Archaea</i>	0.19	0.56	-0.02	-0.20	-0.23	0.18	-0.33	0.14	0.23	-0.20
<i>Bacteria</i>	0.36	0.69	0.18	-0.17	-0.27	0.08	-0.44	0.13	0.14	-0.09
<i>Fungi</i>	0.40	0.78	0.08	-0.16	-0.28	0.00	-0.38	0.31	0.33	-0.31
<i>Eukarya</i>	0.42	0.76	0.06	-0.06	-0.14	0.04	-0.30	0.30	0.24	-0.22

Table S5 Number of archaeal and bacterial observed OTUs, richness estimator, and diversity index of the 16S rRNA gene sequences of samples along the Franz Josef chronosequence.

Sample	Archaea			Bacteria		
	No. OTUs ¹	Chao1 ²	H ³	No. OTUs ¹	Chao1 ²	H ³
0.5_CB	323	745 (603-959)	3.10 (3.04-3.17)	635	2134 (1748-2653)	5.54 (5.45-5.62)
5_O	239	565 (441-765)	2.60 (2.54-2.67)	922	4272 (3507-5264)	6.28 (6.21-6.35)
5_AE	288	685 (541-911)	3.12 (3.06-3.18)	500	1359 (1116-1697)	5.20 (5.12-5.29)
5_E	177	410 (308-590)	2.56 (2.51-2.62)	454	1276 (1030-1629)	5.08 (5.00-5.16)
5_B	199	442 (343-609)	2.62 (2.57-2.68)	456	1429 (1134-1853)	5.13 (5.06-5.10)
12_EA	343	1029 (799-1374)	2.77 (2.70-2.84)	498	1319 (1087-1642)	5.18 (5.10-5.27)
12_B	n.d.	n.d.	n.d.	501	1815 (1424-2374)	5.21 (5.13-5.29)
120_E1	225	608 (459-852)	2.26 (2.19-2.32)	361	812 (662-1036)	4.89 (4.81-4.96)
120_E2	163	358 (275-503)	1.69 (1.63-1.75)	219	552 (421-767)	3.68 (3.59-3.77)
120_B	176	419 (314-603)	1.82 (1.75-1.89)	267	850 (626-1214)	4.18 (4.09-4.26)

¹ Number of observed OTUs² Chao1 richness estimator with higher and lower 95% confidence interval in parentheses.³ Shannon diversity index with higher and lower 95% confidence interval in parentheses.

n.d. no data

Table S6 Effects of the different factors on microbial abundances in the soil microcosm incubation experiment (bulk and HF, without the LF) as revealed by five-way ANOVA with significant interactions. Frac – fraction.

	O ₂	Fraction	Site age	P	C	Significant interactions
<i>Archaea</i>	*	n.s.	***	n.s.	n.s.	O ₂ ×Age*, Age×P*, O ₂ ×Frac×Age***, O ₂ ×Frac×P**, O ₂ ×P×C***, Frac×Age×C*, Frac×Age×P**
<i>Bacteria</i> ¹	***	***	***	***	n.s.	O ₂ ×Frac***, O ₂ ×Age***, O ₂ ×P***, Frac×Age***, Frac×P***, Age×C***, O ₂ ×Frac×Age***, O ₂ ×Age×P*, O ₂ ×Age×C***, O ₂ ×P×C***, Frac×Age×C*, Frac×P×C*
<i>Fungi</i> ¹	***	n.s.	**	***	***	O ₂ ×Age***, O ₂ ×C*, Frac×Age**, Frac×P**, Frac×C**, Age×C**, O ₂ ×Frac×Age**, O ₂ ×Frac×P*, O ₂ ×Frac×C***, O ₂ ×Age×P*
<i>Archaea:Bacteria</i> ¹	***	**	**	n.s.	n.s.	O ₂ ×Frac***, O ₂ ×Age***, O ₂ ×P*, Age×P**, O ₂ ×Frac×Age**, O ₂ ×Frac×P**, Frac×Age×P*, Frac×Age×C*, Frac×P×C*
<i>Fungi:Bacteria</i> ¹	***	n.s.	***	***	***	O ₂ ×Frac***, O ₂ ×P***, Frac×C**, Age×C***, P×C**, O ₂ ×Frac×Age**, O ₂ ×Frac×C***, O ₂ ×Age×C**

*** P < 0.001, ** 0.001 < P < 0.01; * 0.01 < P < 0.05; n.s. – not significant (P > 0.05).

¹ data not normal-distributed, see Table S7 for analysis of normal-distributed oxic and anoxic data subset.

Table S7 Results of four-way ANOVA with significant interactions for the oxic and anoxic subsets of the soil incubation experiment (HF vs. bulk samples, without the LF). Frac – fraction.

	Fraction	Site age	P	C	Significant interactions
<i>Bacteria</i> oxic	***	***	***	**	Frac×Age***, Age×C***, P×C***, Frac×Age×P*
<i>Bacteria</i> anoxic	***	***	n.s.	n.s.	Frac×P**, Age×P**, P×C**, Frac×P×C*
<i>Fungi</i> oxic	n.s.	***	***	***	Frac×Age***, Frac×P*, Frac×C***, Age×P***, Age×C***, Frac×Age×C*, Frac×P×C***, Age×P×C*
<i>Fungi</i> anoxic	n.s.	***	***	***	Frac×P**, Frac×C***, Age×C*, P×C*
<i>Archaea:Bacteria</i> oxic	n.s.	***	*	n.s.	Frac×P*, Frac×Age×C*
<i>Archaea:Bacteria</i> anoxic	***	***	n.s.	n.s.	Frac×Age**, Frac×P*, Age×P*, Frac×Age×C*
<i>Fungi:Bacteria</i> oxic	***	***	**	***	Frac×Age***, Frac×C***, Age×P***, Age×C***, P×C***, Frac×Age×P**, Frac×Age×C***, Frac×P×C**, Age×P×C***
<i>Fungi:Bacteria</i> anoxic	***	*	***	***	Frac×Age*, Frac×C***

*** $P < 0.001$, ** $0.001 < P < 0.01$; * $0.01 < P < 0.05$; n.s. – not significant ($P > 0.05$).

Table S8 Results of variance component estimation of factors (fraction, soil age, P and C addition and their four-way interactions) controlling microbial abundances and abundance ratios in the oxic and anoxic subsets (without the LF, controls and inoculum) for the soil microcosm incubation experiment.

	% of total variation				
Oxic	<i>Archaea</i>	<i>Bacteria</i>	<i>Fungi</i>	<i>Archaea:Bacteria</i>	<i>Fungi:Bacteria</i>
Fraction	0	33	0	0	17
Age	6	5	9	31	1
P	0	14	12	2	0
C	0	0	50	0	32
Fraction × Age	10	13	10	0	0
Fraction × P	1	1	0	3	0
Fraction × C	0	0	2	0	8
Age × P	0	0	5	3	5
Age × C	0	15	2	0	19
P × C	0	9	0	0	5
Fraction × Age × P	14	0	0	5	0
Fraction × Age × C	3	0	2	5	1
Fraction × P × C	5	0	2	1	0
Age × P × C	0	0	2	0	2
Fraction × Age × P × C	0	3	0	0	5
Residual	62	8	4	49	3
Anoxic	<i>Archaea</i>	<i>Bacteria</i>	<i>Fungi</i>	<i>Archaea:Bacteria</i>	<i>Fungi:Bacteria</i>
Fraction	0	53	0	29	0
Age	0	35	5	3	0
P	0	0	16	0	18
C	0	0	3	0	1
Fraction × Age	10	0	2	10	6
Fraction × P	0	1	8	1	3
Fraction × C	0	0	21	0	35
Age × P	0	2	0	0	0
Age × C	0	0	6	0	2
P × C	7	0	5	0	0
Fraction × Age × P	5	0	0	4	0
Fraction × Age × C	0	1	1	0	0
Fraction × P × C	0	1	0	0	0
Age × P × C	0	0	0	0	0
Fraction × Age × P × C	20	0	0	17	1
Residual	58	7	34	36	34

Table S9 Total number of T-RFs and number of T-RFs that were unique either in bulk, HF, or LF samples of the soil incubation experiment (without inoculum and control).

	Total	Bulk	HF	LF
Archaea (HaeIII)	31	3	3	1
Archaea (RsaI)	23	8	1	0
Bacteria (HaeIII)	52	5	6	0
Bacteria (HhaI)	44	7	4	1

1.2 Supplementary Figures

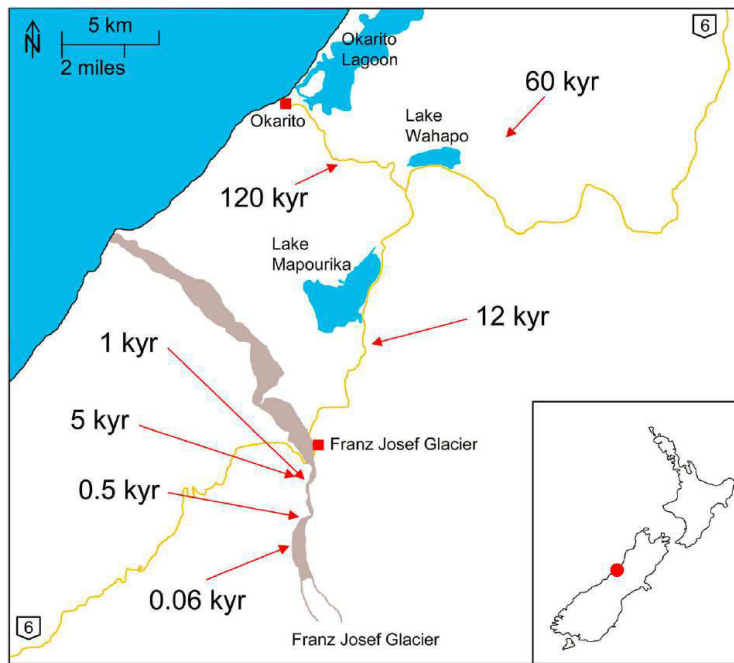


Figure S1 Map of sampling sites along the 120 kyr old Franz Josef chronosequence modified after Dietel et al. (2017).

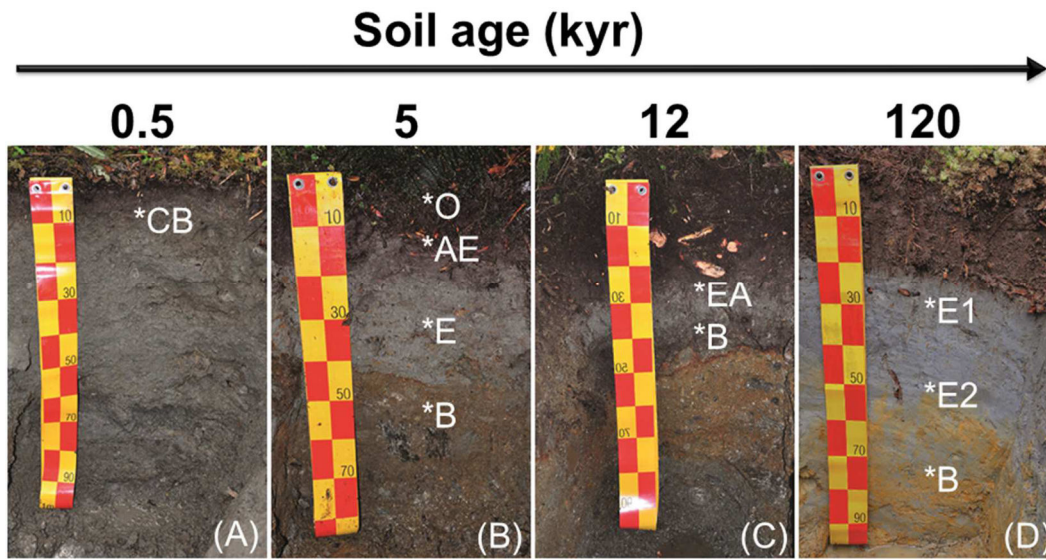


Figure S2 Soil profiles at four sampling sites along the Franz Josef chronosequence of (A) 0.5, (B) 5, (C) 12, and (D) 120 kyr soil age. Asterisks mark horizons that were analyzed by pyrosequencing.

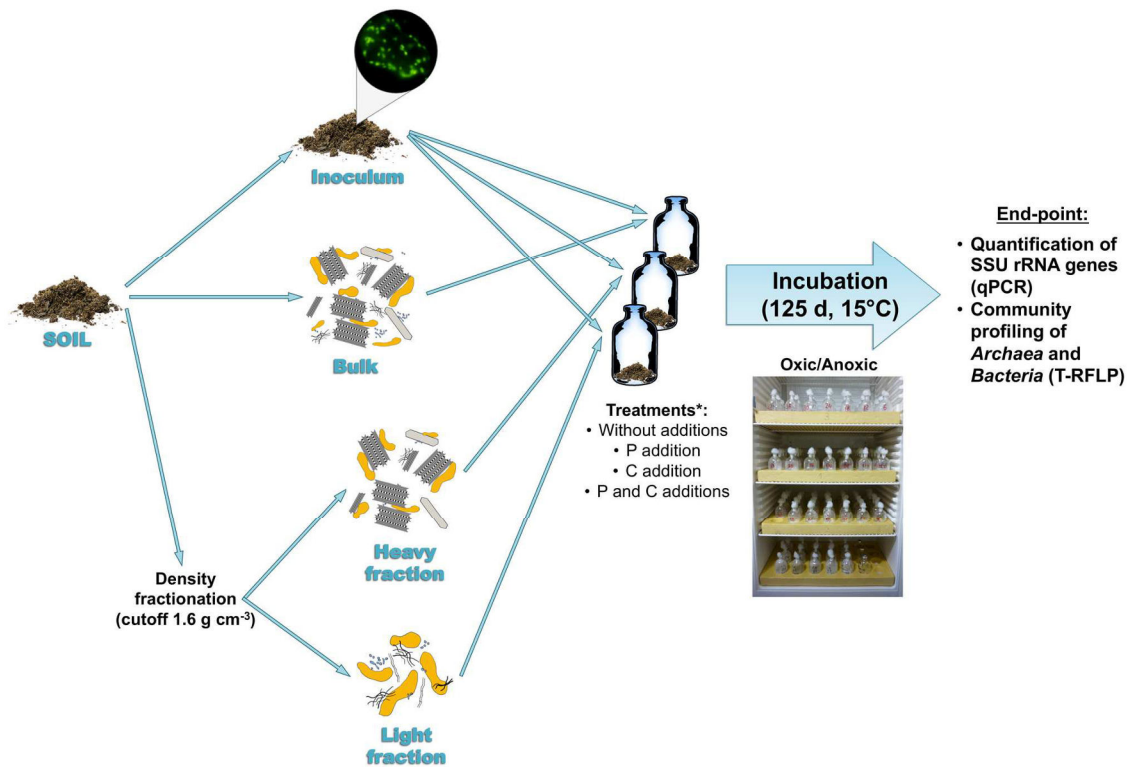


Figure S3 Schematic overview of the microcosm incubation experiment setup modified after Turner et al. (2017). *The C and P treatments were not tested for the light fraction samples. Photographs courtesy of Christian Siebenbürgen and Norman Gentsch.

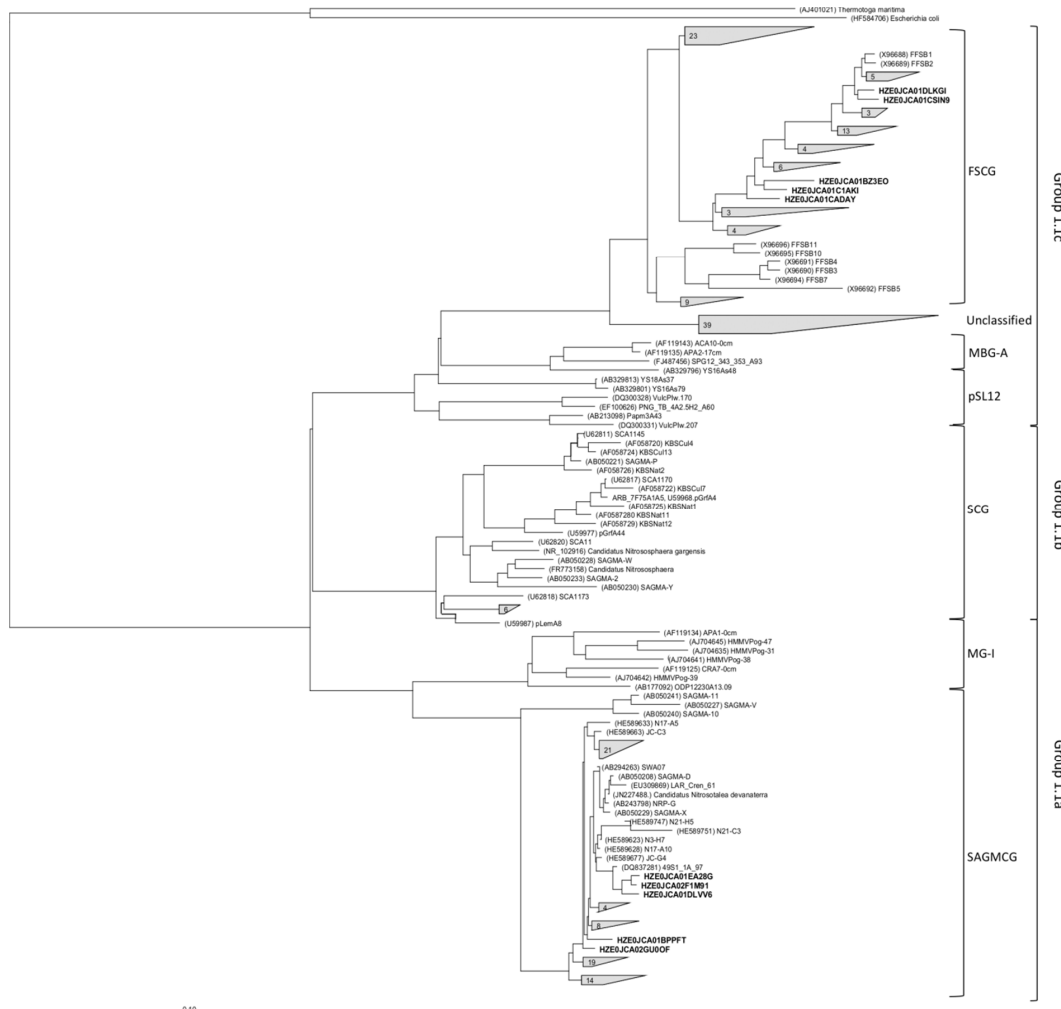


Figure S4 Phylogenetic affiliation of *Thaumarchaeota* 16S rRNA gene sequences from soils along the Franz Josef chronosequence (in bold or grouped). The scale bar indicates 10% estimated phylogenetic divergence.

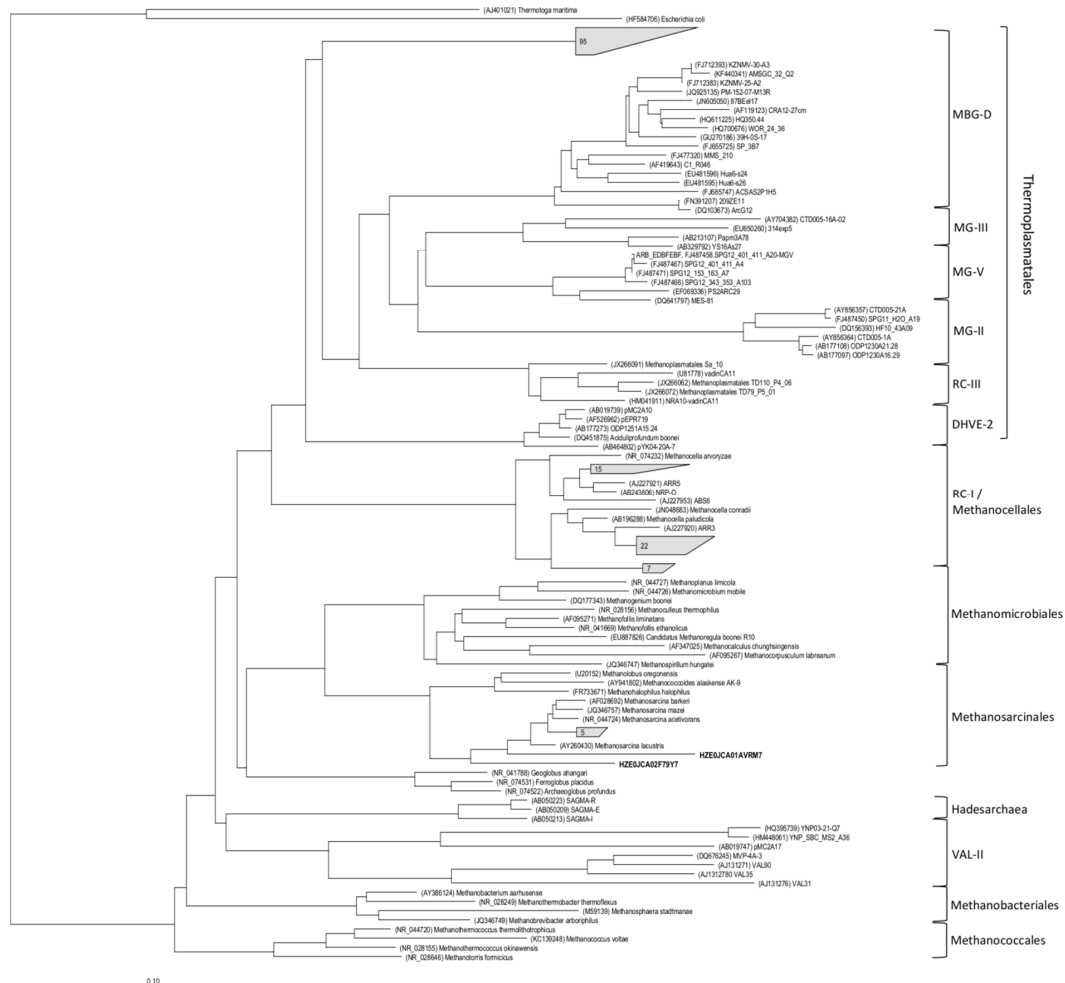


Figure S5 Phylogenetic affiliation of *Euryarchaeota* 16S rRNA gene sequences from soils along the Franz Josef chronosequence (in bold or grouped). The scale bar indicates 10% estimated phylogenetic divergence.

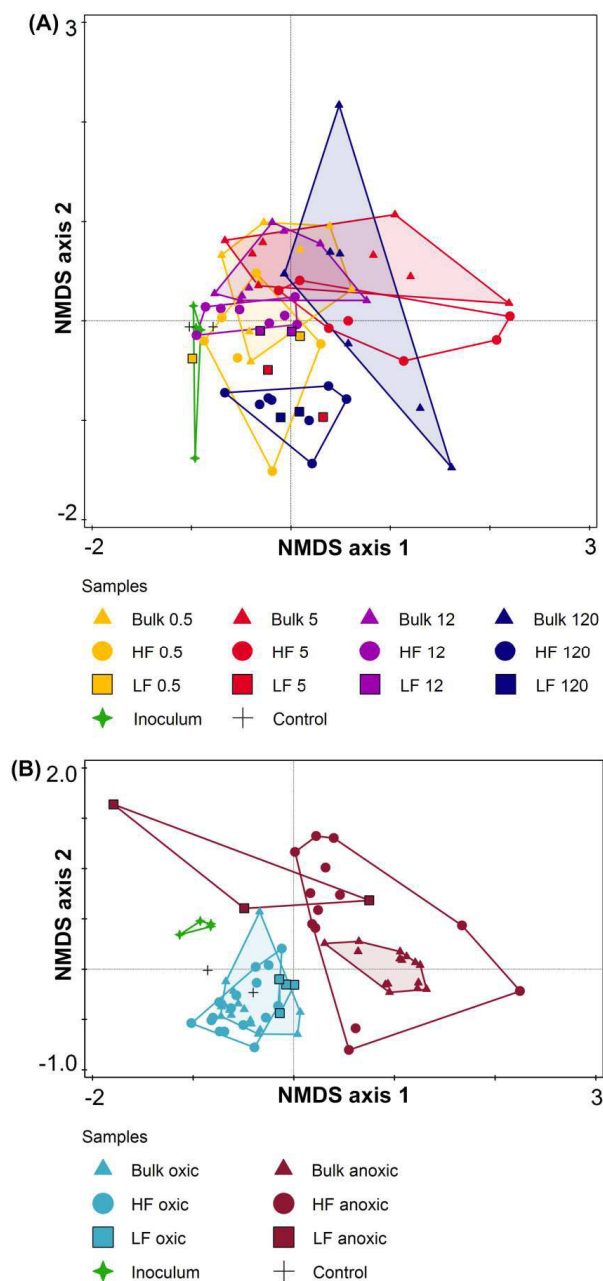


Figure S6 Non-metric multidimensional scaling (NMDS) of **(A)** archaeal (stress value = 0.120) and **(B)** bacterial community composition (stress value = 0.100) for the soil microcosm incubation experiment based on relative abundance of T-RFs (after digestion of PCR products with *RsaI* or *HhaI*, respectively) using Bray-Curtis distance measure. Different symbols encode the different soil fractions (triangle – bulk soil; circle - heavy fraction, HF; and square – light fraction, LF). Different colors encode the different soil ages (0.5, 5, 12, and 120 kyr) for archaeal community analysis **(A)** and O₂ status (oxic and anoxic) for bacterial community analysis **(B)**.

References

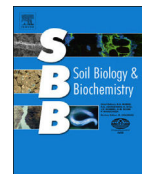
- Dietel, J., Dohrmann, R., Guggenberger, G., Meyer-Stüve, S., Turner, S., Schippers, A., et al. (2017). Complexity of clay mineral formation during 120,000 years of soil development along the Franz Josef chronosequence, New Zealand. *New Zeal. J. Geol. Geophys.* 60, 23–35. doi:10.1080/00288306.2016.1245668.
- Turner, S., Meyer-Stüve, S., Schippers, A., Guggenberger, G., Schaarschmidt, F., Wild, B., et al. (2017). Microbial utilization of mineral-associated nitrogen in soils. *Soil Biol. Biochem.* 104, 185–196. doi:10.1016/j.soilbio.2016.10.010.
- Turner, S., Schippers, A., Meyer-Stüve, S., Guggenberger, G., Gentsch, N., Dohrmann, R., et al. (2014). Mineralogical impact on long-term patterns of soil nitrogen and phosphorus enzyme activities. *Soil Biol. Biochem.* 68, 31–43. doi:10.1016/j.soilbio.2013.09.016.

4.2.2 *Manuscript 2: Mineralogical impact on long-term patterns of soil nitrogen and phosphorus enzyme activities*



Contents lists available at ScienceDirect

Soil Biology & Biochemistry

journal homepage: www.elsevier.com/locate/soilbio

Mineralogical impact on long-term patterns of soil nitrogen and phosphorus enzyme activities



Stephanie Turner^a, Axel Schippers^a, Sandra Meyer-Stüve^b, Georg Guggenberger^b, Norman Gentsch^b, Reiner Dohrmann^a, Leo M. Condron^c, Andre Eger^c, Peter C. Almond^c, Duane A. Peltzer^d, Sarah J. Richardson^d, Robert Mikutta^{b,*}

^a Bundesanstalt für Geowissenschaften und Rohstoffe, Stilleweg 2, 30655 Hannover, Germany

^b Leibniz Universität Hannover, Institut für Bodenkunde, Herrenhäuser Str. 2, 30419 Hannover, Germany

^c Agriculture and Life Sciences, Lincoln University, PO Box 85084, Lincoln 7647, Christchurch, New Zealand

^d Landcare Research, PO Box 69040, Lincoln 7640, Canterbury, New Zealand

ARTICLE INFO

Article history:

Received 6 July 2013

Received in revised form

6 September 2013

Accepted 12 September 2013

Available online 24 September 2013

Keywords:

Soil chronosequence

N- and P-hydrolyzing enzymes

Mineralogical composition

Fe and Al oxides

Clay

N- and P-limitation

Microbial biomass

Cell counts

Enzyme activities

Pedon

ABSTRACT

During long-term ecosystem development, both soil mineralogical composition and nutrient contents change, thus possibly altering microbial nutrient cycling by constraining substrate accessibility. In addressing the mineral impact on nitrogen (N) and phosphorus (P) cycling, we determined microbial abundances, activities of N-hydrolyzing (aminopeptidases, protease, urease) and P-hydrolyzing (phosphatase) enzymes and the potential substrate availability as well as their physicochemical and mineralogical controls in whole soil profiles along the 120 kyr-old Franz Josef chronosequence (New Zealand). Pedogenic soil iron (Fe) and aluminum (Al) resided initially (<1 kyrs) in metal-humus complexes, changed to poorly crystalline Fe and Al at intermediate-aged sites (1–12 kyrs) and into dominance of clay and crystalline Fe oxides at the oldest site. Despite this, organic C (OC) and organic N (ON) stocks increased only slightly with soil age, whereas organic P (OP) stocks decreased continuously. In organic layers, enzyme activities were mainly regulated by ON and OP concentrations, whereas in mineral soils, mineral–enzyme relations were more complex and included both, direct and indirect effects. Protease, urease, and phosphatase activities were inhibited by mineral interactions, especially with poorly crystalline Fe and Al oxides, whereas aminopeptidases were less affected by mineralogical properties. On a pedon basis, most N-hydrolyzing enzyme activities per ON stocks responded negatively to increasing stocks of poorly crystalline Fe and Al minerals, but were also affected by the C:N ratio of labile organic substrates. Profile-based phosphatase activities per OP stock were highest at the oldest sites having the largest stocks of clay and crystalline Fe oxides. Overall, our study indicates that long-term mineral changes create distinct patterns of nutrient accumulation and N- and P-enzyme activities at both horizon and pedon scale, with a variable extent of the mineralogical effect for the different N-hydrolyzing enzymes.

© 2013 Published by Elsevier Ltd.

1. Introduction

Extracellular enzyme activities drive many soil ecosystem functions and also provide a useful tool to monitor microbial activity. Soil microorganisms excrete extracellular enzymes to degrade complex organic compounds into small utilizable molecules for microbial assimilation. This process is considered to be the rate limiting step in the decomposition of organic matter (OM) and

nutrient mineralization (Sinsabaugh, 1994). The enzyme production is regulated by the environmental nutrient status because it is both energy intensive and requires nitrogen (N) and therefore indicates microbial nutrient demand (Sinsabaugh et al., 2008). This is reflected by the negative relationship between extracellular enzyme activity and the availability of assimilable nutrients (Olander and Vitousek, 2000; Allison and Vitousek, 2005; Allison et al., 2007). Therefore, enzyme activities depend on enzyme stability itself and the accessibility and quality of potential substrates.

What remains poorly understood is how enzyme activities are altered by abiotic factors such as the mineralogical soil composition (Allison, 2006; Marinari and Vittori Antisari, 2010; Achat et al.,

* Corresponding author. Tel.: +49 511 762 3561.

E-mail address: mikutta@ifbk.uni-hannover.de (R. Mikutta).

2012). Variation in soil mineral assemblage can cause a differential accumulation and stabilization of organic forms of carbon (OC), nitrogen (ON), and phosphorus (OP) (Mikutta et al., 2009, 2010; Vincent et al., 2012). Soil enzyme activities can also be affected directly by mineralogical composition. For example, enzymes can be stabilized against degradation and proteolysis by clay minerals, whereas their activities can be inhibited due to sorption onto the surface of clay minerals (Nannipieri and Smalla, 2006) or enhanced by the presence of allophane (Allison, 2006). Besides direct effects, minerals can exert several indirect effects on enzyme activity. Organic substrates can be adsorbed onto mineral surfaces (Kalbitz et al., 2005; Mikutta et al., 2007) or complexed and precipitated with iron (Fe) or aluminum (Al) (Nierop et al., 2002; Scheel et al., 2007), thus, resulting in a reduced bioavailability (Allison and Jastrow, 2006). Organic matter strongly bound to minerals is typically less accessible to microorganisms (Kaiser et al., 2007), whereas the presence of an easily desorbable OM pool promotes microbial activity (Mikutta et al., 2007). These strong organo-mineral interactions, particular in subsoil horizons, can deplete concentrations of dissolved nutrients (ON, OP) in the soil solution, potentially causing an up-regulation of enzyme activities. The mineralogical composition of soil, however, changes with ongoing weathering and soil formation and results in varying interaction processes with soil OM (Torn et al., 1997; Mikutta et al., 2009, 2010). Most studies of enzyme activities have focused on topsoil horizons (Allison et al., 2007; Baldrian et al., 2008), and little is known about the dynamics of ON and OP in relation to microbial activity on a pedon scale, even though a large fraction of soil OM is contained in mineral subsoil horizons (Kaiser and Guggenberger, 2000; Moore and Turunen, 2004).

Here, we test whether the activities of N- and P-hydrolyzing enzymes depend solely on N and P abundances, or are altered throughout soil development because of shifts in mineral assemblage from primary silicates to more protective minerals like poorly crystalline and crystalline Fe and Al phases (Torn et al., 1997; Mikutta et al., 2009). We used a chronosequence to test these ideas because it is a powerful space-for-time approach for assessing changes in soil properties and processes (Stevens and Walker, 1970; Wardle et al., 2004). During long-term soil development nutrient concentrations change. Nitrogen limits during primary succession and accumulates over time due to atmospheric inputs and biological N₂-fixation while P is initially high and becomes increasingly scarce as a result of weathering of P-containing minerals and leaching (Walker and Syers, 1976; Crews et al., 1995; Peltzer et al., 2010). We hypothesize that changing mineralogical properties with soil age, directly and indirectly control microbial N and P enzyme activities. Specifically, we focus on enzyme regulation mechanisms in whole soil pedons, including organic and mineral horizons, in relation to nutrient concentrations and their potential accessibilities. For that, we determined microbial abundances and activities of N- and P-hydrolyzing enzymes and investigated their controls based on soil physicochemical and mineralogical properties along the 120 kyr-old Franz Josef soil chronosequence in New Zealand (Stevens, 1968; Almond et al., 2001). Storage of OC, ON, and OP along the sequence were analyzed and the potential substrate availability of OM was tested in desorption experiments.

2. Material and methods

2.1. Sites and soil sampling

The Franz Josef chronosequence is located on the West Coast on the South Island of New Zealand (~43° S, 170° E). The soils developed due to repeated glacial advance and retreat from greywacke and mica schist spanning a time scale from present to

120 kyrs. The two oldest sites also received loess depositions (Stevens, 1968; Almond et al., 2001). The mean annual temperature is 10.8 °C; precipitation at the youngest four sites is ca. 6500 mm and ca. 3500 mm at the three older sites. Soils are covered by temperate rainforest with a general dominance of evergreen angiosperms. Woody plant diversity, vegetation cover and tree height increase through ecosystem progression, and then decline (Richardson et al., 2004).

Soil samples from seven sites were collected in January 2012. From three randomly chosen profiles per site, every genetic horizon was sampled to a soil depth of 1 m, thus, three site replicates were available for laboratory analyses. For determination of soil bulk density and soil moisture, samples were taken with 100 cm³ cylinders. For total cell counts, a 1-mL fresh soil mini-core taken by a truncated syringe was fixed with 2% (vol./vol.) formaldehyde in 0.9% NaCl solution and shaken vigorously. All soil samples for microbial analysis were kept at <4 °C prior to analysis.

2.2. Soil parameters

Moist soil material was sieved through a 2-mm sieve and subsequently air-dried. Samples taken with 100 cm³ cylinders were dried at 60 °C to a constant weight to calculate bulk density and soil moisture. Soil pH was measured in distilled water (1:2.5; wt./vol.). Total C (TC) and total N (TN) contents were measured by a CNS analyzer (Vario EL III; Elementar Analysensysteme GmbH, Hanau, Germany). Soil samples did not contain carbonate due to the acidic conditions, therefore TC was equivalent to OC. Inorganic N ([N_{min}] = [NO₃⁻] + [NH₄⁺]) was extracted from field moist samples with 1 M KCl (1:10 wt./vol.), kept frozen until analysis and was determined photometrically (SAN-plus, Skalar Analytical B.V., Breda, The Netherlands). Organic N was calculated as the difference between TN and N_{min}. Total P (TP) and OP contents of soils were analyzed using the ignition method of Saunders and Williams (1955) with photometric detection of the blue P-molybdate complex at 880 nm (Schinner et al., 1993). Selective extractions of oxalate-extractable Fe and Al (Fe_o, Al_o) and dithionite–citrate–bicarbonate-extractable Fe (Fe_d) were performed on bulk soil samples according to Schlichting et al. (1995). Acid oxalate dissolves Fe and Al from poorly crystalline minerals and metal–humus-complexes while dithionite–citrate–bicarbonate extracts pedogenically formed Fe phases including poorly crystalline and crystalline Fe oxides as well as Fe–humus complexes. The difference between dithionite–citrate–bicarbonate extractable Fe and oxalate oxalate-extractable Fe represents crystalline Fe phases (Fe_{d-o}). Extraction of Fe and Al from organic complexes (Fe_p, Al_p) was accomplished with 0.1 M sodium pyrophosphate (Na₄P₂O₇, pH 9.5) at a solid-to-solution ratio of 1:50. Solutions were flocculated with 5 mL of 0.05 M MgSO₄ and 5-mL aliquots were centrifuged at 300,000 g for 6 h. Fe and Al concentrations in extraction solutions were measured by inductively coupled plasma atomic-emission spectroscopy (Varian 725-ES, Varian Inc., Palo Alto, California, United States). Particle size distribution of horizons was determined after removal of Fe oxides and OM by standard pipette analysis (Schlichting et al., 1995).

2.3. Potential substrate availability

In order to test the potential availability of OM for enzymatic reactions, two desorption experiments were conducted. First, field moist soil samples were extracted with 0.5 M K₂SO₄ (1:4 wt./vol.) for OC and TN. The K₂SO₄-extractable fraction was considered to be a highly bioavailable OM pool (Balsler and Firestone, 2005). Second, dry soil samples were extracted with 0.1 M NaH₂PO₄ (1:25 wt./vol.) for 17 h, centrifuged (30 min, 3500 g) and filtered (0.45 μm, polyvinylidene difluoride membrane). The OC and TN contents of the

Table 1Physico-chemical properties, soil property ratios, total cell counts (TCC), microbial biomass carbon (C_{mic}), and microbial biomass nitrogen (N_{mic}) at each site. Hor. – horizon.

Site age (kyrs)	Hor.	pH (H ₂ O)	OC (g kg ⁻¹)	ON (g kg ⁻¹)	Nmin (g kg ⁻¹)	TP (mg kg ⁻¹)	OP (mg kg ⁻¹)	OC:TP	OC:OP	ON:TP	TCC (cells × 10 ⁷ g ⁻¹)	C_{mic} (μg C g ⁻¹)	N_{mic} (μg N g ⁻¹)
0.06	AO	5.8	201.5	13.2	0.10	1103	688	183	293	12	8517	1229	335
0.06	CA	6.0	7.3	0.5	0.02	686	73	11	100	1	189	113	28
0.06	C	6.4	7.2	0.4	0.03	804	101	9	71	0	74	38	9
0.5	OA	4.5	241.7	10.2	0.11	785	685	308	353	13	4209	1222	217
0.5	A	4.7	158.4	6.9	0.04	583	512	272	309	12	2499	352	60
0.5	C	5.6	3.6	0.2	0.02	744	47	5	78	0	42	7	3
1	O	3.9	327.6	13.4	0.07	544	497	603	660	25	7334	3261	458
1	AE	4.1	66.6	4.0	0.03	220	200	303	333	18	497	570	94
1	E	4.7	17.2	0.7	0.03	103	94	166	184	7	403	106	18
1	B	5.3	9.5	0.5	0.02	272	92	35	103	2	75	26	4
5	O	3.9	367.9	14.4	0.13	681	527	540	698	21	6647	2621	441
5	AE	4.3	47.3	2.8	0.03	195	178	243	267	14	513	304	42
5	E	4.9	16.6	0.6	0.03	100	88	166	189	6	449	79	11
5	B	5.1	8.1	0.4	0.02	231	110	35	74	2	36	9	2
12	O	3.8	448.1	12.8	0.10	499	444	898	1010	26	11,962	2281	381
12	AE	4.1	143.6	6.8	0.05	244	228	589	629	28	2110	1126	168
12	EA	4.5	30.5	0.9	0.02	76	71	400	430	12	176	188	18
12	B	5.0	36.4	1.3	0.02	328	151	111	241	4	260	174	19
12	C	5.5	4.7	0.2	0.01	664	107	7	44	0	37	n.d.	n.d.
60	O	4.0	220.3	6.2	0.05	296	237	744	928	21	1091	1626	286
60	AE	4.1	60.4	2.9	0.04	161	149	375	405	18	2331	1427	222
60	EA	4.7	24.0	1.0	0.03	92	84	260	285	11	431	196	28
60	B	5.1	13.3	0.7	0.03	137	87	97	153	5	158	58	10
60	C	5.5	2.2	0.1	0.02	591	21	4	102	0	5	35	1
120	O	4.4	190.4	5.4	0.07	136	126	1402	1512	40	976	2022	371
120	A	4.2	72.1	4.0	0.05	78	73	922	991	51	390	1586	227
120	E	4.9	7.7	0.4	0.03	16	14	479	564	25	12	116	10
120	B	5.2	12.5	0.4	0.04	77	19	161	648	5	31	n.d.	2

n.d. = not detected.

filtrates were measured by a TOC analyser (LiquiTOC trace, Elementar Analysensysteme GmbH, Hanau, Germany). Operationally, the NaH₂PO₄-fraction was considered to include easy available and reversibly mineral-bound OM, whereas the NaH₂PO₄-resistant fraction was considered to be most stable being either strongly bound to minerals (Kaiser and Guggenberger, 2007) or located in particulate OM structures.

2.4. Microbial biomass and total cell counts

Microbial biomass C and N were determined by the fumigation–extraction-method (Vance et al., 1987). Organic C content of the K₂SO₄-extracts was measured by a TOC analyser (high TOC II, Elementar Analysensysteme GmbH, Hanau, Germany). Microbial biomass C was calculated with $k_{EC} = 0.45$ (Joergensen, 1996) and expressed as μg C per gram dry soil. Ninhydrin-reactive N was measured in the same K₂SO₄-extracts according to Joergensen and Brookes (1990). Microbial biomass N was calculated as $N_{mic} = 5 \times [\text{Ninhydrin-reactive N}]$ and expressed as μg N per gram dry soil.

For total cell counts, a subsample of each formaldehyde-fixed soil sample was sonicated, stained with SYBR Green I (Invitrogen) and embedded with moviol on black polycarbonate membrane filters (0.2 μm, Nuclepore, Whatman) (Lunau et al., 2005). The stained cells on the filters were counted by using epifluorescence microscopy.

2.5. Enzyme activities

The potential activities of five enzymes involved in the hydrolysis of N and P compounds were assessed for each horizon in three

analytical replicates: protease, urease, alanine aminopeptidase (ala-AP), leucine aminopeptidase (leu-AP), and phosphatase.

Protease and urease activities were determined colorimetrically according to Schinner et al. (1993). For protease measurement, field-moist soil was incubated with sodium caseinate as substrate. The activity was expressed as tyrosine equivalents per gram dry soil per 2 h. Urease activity was determined by adding urea solution as substrate to field-moist soil. The absorbance was measured at 690 nm and urease activity was expressed as N equivalents per gram dry soil per 2 h.

The activities of ala-AP, leu-AP, and phosphatase were measured by HPLC using fluorogenic substrates. The method described by Stemmer (2004) was modified and allowed a simultaneous analysis of multiple enzymes. 7-amino-4-methylcoumarin derivatives (L-ala-7-AMC and L-leu-7-AMC) and a 4-methylumbelliferone derivative (4-MU-phosphate) were used as substrates. The substrates were pre-dissolved in dimethyl sulfoxide. The assay buffer was adjusted to pH 5.0 with NaOH. For the incubation experiment 0.5 g field-moist soil and 10 mL diluted assay buffer (1:5) were sonicated for 1 min. The three substrates were added to the soil-buffer-suspension and the assay was incubated at 30 °C for 3 h. Changing substrate concentrations over time (0, 1, 2, 3 h) were measured by removing a subsample of 400 μL from the assay, stopping the reaction with 1 mL methanol and 2 mL KH₂PO₄ buffer (25 mM, pH 6.1) and extracting non-hydrolyzed substrate derivatives and free 4-MU and 7-AMC. The supernatant of the extracted solution was filtered (0.2 μm membrane filter) and injected into the HPLC system.

HPLC analyses were carried out using an Agilent 1200 (Agilent Technologies, Santa Clara, California, United States) system with thermostated autosampler (40 °C). Separation took place on a Zorbax Eclipse Plus C18 pre-column (4.6 × 12.5 mm, 5 μm) and a

Zorbax Eclipse Plus C18 column (4.6 × 250 mm, 5 μm) at a flow rate of 0.8 mL min⁻¹ and an oven temperature of 40 °C. The mobile phase A was KH₂PO₄ buffer (25 mM, pH 6.1, 0.45 μm filtered) and the mobile phase B was methanol. Non-hydrolyzed substrate derivatives and free 4-MU and 7-AMC were detected with a diode array detector at a wavelength of 320 nm. The activities of both aminopeptidases (APs) and phosphatase were expressed as nmol substrate per gram dry soil per h.

All measured enzyme activities were also expressed on a soil ON content basis for N-hydrolyzing enzymes and on a soil OP content basis for phosphatase as well as on a C_{mic} basis.

2.6. Data analysis

Data for the genetic horizons of whole soil profiles were separated into the main horizons O, A, E, B and C depending on site age. Profile-based stocks (PS) of soil properties were calculated from all sampled horizons to depth of 1 m as follows:

$$PS = \sum_{h=1}^H a_h = \sum_{h=1}^H [c_h \times BD_h \times (100 - \%G_h) \times z_h] \quad (1)$$

where

- a_h = soil property stock in each horizon
- h = horizon number = 1, ..., H (where H = horizon, that contains the depth of 1 m)
- c_h = soil parameter concentration in horizon h
- BD_h = bulk density in horizon h
- $\%G_h$ = gravel content (%) in horizon h
- z_h = horizon thickness, for horizon number H only until a depth of 1 m.

Site specific enzyme activities were calculated on a pedon basis according to Equation (1). To relate profile-based enzyme activities to substrate stocks (ON, OP) their ratio was calculated and expressed as mmol h⁻¹ kg⁻¹ for leu-AP, ala-AP and phosphatase; g tyrosine 2 h⁻¹ kg⁻¹ for protease and g N 2 h⁻¹ kg⁻¹ for urease.

We used Pearson product–moment correlation with a significance threshold of $P < 0.05$ to analyze the relationship between microbial abundances, enzyme activities and soil properties based on log transformed data with SigmaPlot 12.3 (Systat Software Inc., 2011–2012, San Jose, California, United States). In rare cases when neither untransformed nor log-transformed data were normal distributed, correlations were checked with Spearman's rank correlation coefficient.

3. Results

3.1. Soil properties

Soils shifted from Haplic Regosols at the youngest site (Fig. S1a), to Stagnic Regosols and Stagnic Cambisols at the 0.5 kyr site (Fig. S1b), and to Stagnic Podzols at the older sites (Fig. S1c–g) (IUSS Working Group WRB, 2006). At the intermediate-aged and older sites (>1 kyr), soils exhibited thick E horizons resulting from a combination of redoximorphic conditions and eluviation of OM, clay, Fe and Al. Soil pH ranged from 3.8 to 6.4 and increased with soil depth whereas topsoil pH decreased with site age (Table 1). Soil OC and ON concentrations were highly correlated ($r = 0.99$, $P < 0.001$) and sharply declined with soil depth at all sites. In O horizons, the OC content increased towards the 12 kyr site (448 g kg⁻¹) and subsequently declined, whereas the ON content was ~13 g kg⁻¹ until 12 kyr

Table 2
Mineralogical properties of soil horizons at each site. Hor. – horizon.

Site age (kyrs)	Hor.	Fe _o (g kg ⁻¹)	Fe _d (g kg ⁻¹)	Fe _p (g kg ⁻¹)	Al _o (g kg ⁻¹)	Al _p (g kg ⁻¹)	Fe _{d-o} (g kg ⁻¹)	Clay (%)	Silt (%)	Sand (%)
0.06	AO	2.9	3.3	2.4	1.3	1.9	0.4	11	31	58
0.06	CA	1.8	2.9	0.8	0.5	0.3	1.1	3	17	80
0.06	C	2.2	3.6	1.3	0.5	0.4	1.5	6	31	63
0.5	OA	ND	ND	6.7	ND	4.9	ND	ND	ND	ND
0.5	A	4.5	3.6	4.3	2.5	3.4	0.0	17	55	28
0.5	C	1.2	1.3	0.6	0.5	0.9	0.1	5	46	49
1	O	ND	ND	1.2	ND	1.7	ND	ND	ND	ND
1	AE	1.3	1.3	2.1	1.1	1.5	0.1	12	58	30
1	E	1.4	2.0	1.2	1.8	2.1	0.6	12	55	33
1	B	5.7	6.8	2.4	2.8	3.1	1.1	5	43	52
5	O	ND	ND	0.7	ND	1.6	ND	ND	ND	ND
5	AE	1.5	1.9	0.8	1.2	0.6	0.4	13	56	30
5	E	2.6	3.2	0.9	1.6	0.9	0.6	13	58	29
5	B	6.1	7.2	0.9	2.4	1.3	1.1	6	51	43
12	O	ND	ND	0.3	ND	0.9	ND	ND	ND	ND
12	AE	0.6	0.6	0.4	1.0	0.8	0.0	7	56	36
12	EA	0.4	0.7	0.2	1.0	0.7	0.4	5	52	43
12	B	5.6	8.2	1.0	7.8	3.7	2.6	9	34	57
12	C	0.5	0.8	0.0	6.1	0.6	0.3	8	28	64
60	O	ND	ND	0.3	ND	1.3	ND	ND	ND	ND
60	AE	0.5	0.7	0.3	1.2	0.7	0.2	11	68	20
60	EA	3.3	3.8	1.4	2.6	1.7	0.5	14	67	19
60	B	7.7	9.4	1.2	6.2	2.7	1.8	16	59	25
60	C	0.7	1.2	0.1	1.9	0.8	0.5	7	43	50
120	O	ND	ND	0.1	ND	0.5	ND	ND	ND	ND
120	A	0.2	0.2	0.2	0.3	0.3	0.0	10	77	13
120	E	0.8	2.3	0.4	2.1	1.3	1.4	12	74	13
120	B	2.6	24.7	1.9	5.2	2.1	22.0	20	51	29

ND = not determined.

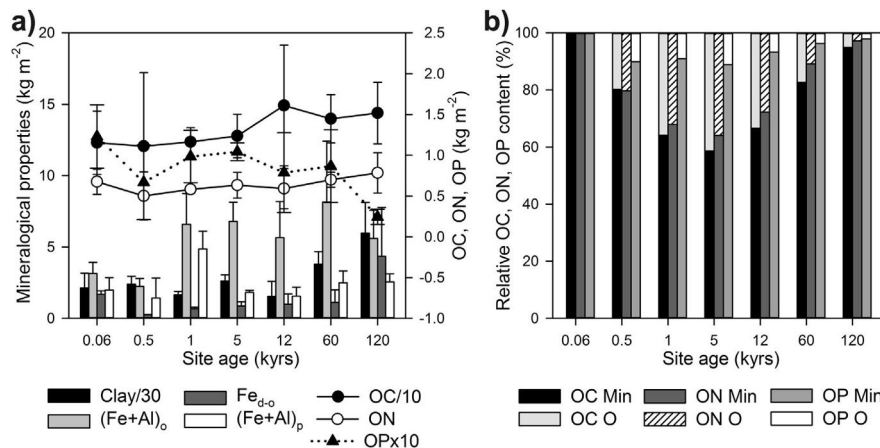


Fig. 1. (a) Profile-based nutrient and mineralogical stocks of mineral soils along the Franz Josef soil chronosequence. Error bars indicate standard deviation of three parallel profiles. (b) Relative content of OC, ON and OP in organic (O) and mineral soil (Min).

and also declined in later stages. The Nmin content ranged from 0.01 to 0.13 g kg⁻¹ and decreased with soil depth. Total P and OP contents declined with increasing soil age resulting in increasing OC:TP, OC:OP, and ON:TP ratios, whereas these ratios decreased with soil depth.

Iron and Al oxides were enriched in B horizons, where Fe_o and Al_o contents, originating from poorly crystalline Fe and Al minerals and Fe/Al-humus complexes, peaked at the 60 and 12 kyr sites, respectively (Table 2). In contrast, the Fe_d content sharply increased to 24.7 g kg⁻¹ at the 120 kyr site. Thus, the highest Fe_{d-o} value at this site indicates an enrichment of crystalline Fe oxides with soil age. The Fe_{d-o} content was negatively related to soil OC ($r = -0.46$, $P = 0.038$) and ON content ($r = -0.50$, $P = 0.020$) in mineral horizons. Iron and Al in metal-humus complexes generally decreased with site age in most horizons. Soil texture changed from sand at the youngest site to a silt prevalence with increasing soil age. The average clay content accounted for ~10%, increased with soil age in the B horizon to 20% and was positively correlated to both OC:TP ($r = 0.60$, $P = 0.003$) and OC:OP ratio ($r = 0.53$, $P = 0.011$).

On a pedon basis, OC and ON stocks in mineral soils down to 1 m depth increased slightly with soil age, whereas the OP stocks declined (Fig. 1a). The presence of reactive Fe and Al phases changed during pedogenesis in that the profile-based stocks of poorly crystalline Fe and Al phases and Fe/Al-humus complexes peaked at the intermediate-aged sites (1–60 kyrs) and declined slightly thereafter due to the formation of more crystalline minerals. At the younger stages (0.06–1 kyrs), a greater proportion of pedogenic soil Fe and Al resided in metal-humus complexes ($((\text{Fe}+\text{Al})_p:(\text{Fe}+\text{Al})_o \text{ ratio} > 0.63)$), whereas at later stages soils were enriched in poorly crystalline Fe and Al minerals such as ferrihydrite and Al hydroxides ($((\text{Fe}+\text{Al})_p:(\text{Fe}+\text{Al})_o \text{ ratio} < 0.46)$). Profile-based OC stocks were positively correlated to profile-based Al_o stocks ($r = 0.83$, $P = 0.021$), whereas profile-based ON stocks were positively correlated to profile-based Fe_{d-o} stocks ($r = 0.95$, $P = 0.001$). The profile-based clay stocks increased with site age from 64 to 179 kg m⁻² and tended to be related to profile-based ON stocks ($r = 0.71$, $P = 0.073$), but not to OC stocks. The relative proportion of profile-based OC, ON, and OP stocks in the mineral soils changed over time due to the variable contribution of organic layers, and were lowest at the 5 kyr site with 59, 64, and 89% (Fig. 1b).

3.2. Potential substrate availability

The K₂SO₄-extractable OC fractions accounted for ~1.5% of total soil OC and increased with depth and soil age, while the NaH₂PO₄-extractable OC proportions accounted for ~4% and showed the same trends (Fig. S2a). In contrast, K₂SO₄- and NaH₂PO₄-extractable TN proportions (~1% and ~5% of soil TN, respectively) rarely changed with site age, but also increased with soil depth in most cases (Fig. S2b).

On a pedon basis, K₂SO₄- and NaH₂PO₄-extractable OC and TN stocks of organic layers peaked at the intermediate-aged sites (Fig. 2a and b) similar to the soil OC and ON stocks (Fig. 1b). The K₂SO₄- and NaH₂PO₄-extractable OC stocks in mineral soils were minimal at the 0.06 and 12 kyr site and increased thereafter. The behavior of K₂SO₄-extractable TN stocks with soil age was similar to the OC stocks, whereas the NaH₂PO₄-extractable TN stocks were relatively constant over time with a minimum at the 12 kyr site. For mineral soils, the OC:TN ratios of the extractable OM fractions tended to increase over time with the highest ratio being observed for K₂SO₄-extractable OM at the 120 kyr site (Fig. 2c). The NaH₂PO₄-extractable OC stocks were positively correlated to (Fe + Al)_o content ($r = 0.81$, $P = 0.029$), while K₂SO₄-extractable OC stocks were positively correlated to Al_o ($r = 0.76$, $P = 0.047$) and Al_p content ($r = 0.79$, $P = 0.036$). Furthermore, K₂SO₄-extractable TN stocks were positively correlated to Al_o content ($r = 0.80$, $P = 0.031$).

3.3. Microbial biomass and total cell counts

In general, total cell counts, C_{mic} and N_{mic} decreased with soil depth (Table 1). Total cell counts ranged from 5.5×10^7 to 1.2×10^{11} cells per gram of soil and were positively correlated to C_{mic} ($r = 0.84$, $P < 0.001$) and N_{mic} ($r = 0.91$, $P < 0.001$). Along the soil chronosequence, total cell counts and microbial biomass peaked at intermediate-aged sites (1–12 kyrs) in the O horizon whereas there was an inverse trend in the A horizons.

3.4. Enzyme activities

Enzyme activities decreased sharply with soil depth at all sites (Fig. S3a–e). The leu-AP and ala-AP activity patterns were nearly equal regarding soil depth and site age (Fig. S3a and b). In the organic layer, activities of enzymes involved in hydrolyzing N-

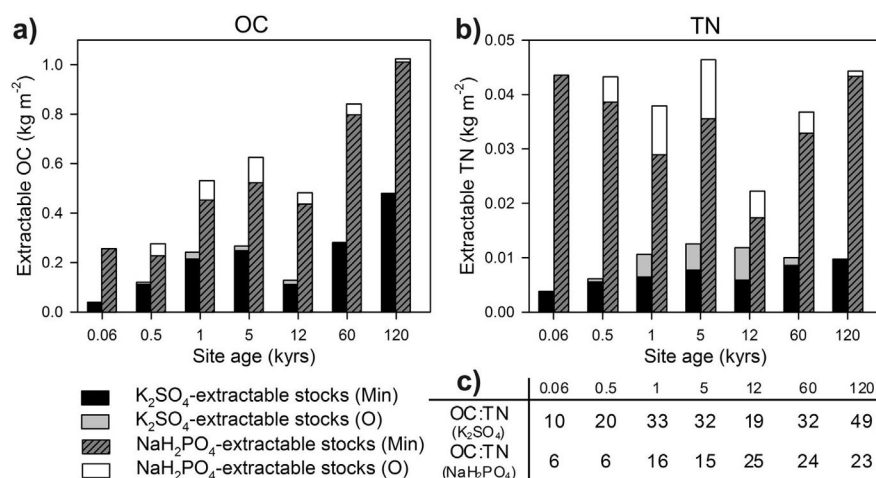


Fig. 2. Profile-based K₂SO₄- and NaH₂PO₄-extractable OC (a) and TN stocks (b) in organic (O) and mineral soils (Min) and their OC:TN ratios for mineral soils (c) along the Franz Josef soil chronosequence.

containing compounds (APs, protease, urease) peaked at intermediate-aged sites (1–12 kyr), coinciding with the highest microbial abundances (Table 1). In contrast, activity of phosphatase increased with soil age in both, O and A horizons (Fig. S3e). In eluvial and subsoil horizons, enzyme activities were low or below the detection limit, especially in most C-horizons. In E and B horizons, AP activities were relatively higher than the other enzyme activities. Activities of N-hydrolyzing enzymes and phosphatase were positively correlated with soil OC and ON contents (Table S1). The correlation between phosphatase activities and soil OP content differed between horizons.

The ON- and OP-normalized enzyme activities incorporate the soil nutrient content. Both ON-normalized AP activities increased with soil depth at most sites and were considerably higher for the eluvial and subsoil horizons of the three youngest sites (Fig. 3a and b). Activities were low at intermediate-aged sites and henceforward slightly increased in eluvial and subsoil horizons with site age. In contrast, ON-normalized protease activities showed maxima at both the 0.06 and 12 kyr sites (Fig. 3c). The ON-normalized urease activities decreased with soil depth and peaked in the CA horizon at the youngest site as well as in topsoil horizons at the two oldest sites (Fig. 3d). The OP-normalized phosphatase activities showed a decline with soil depth and a steady increase with site age (Fig. 3e).

In contrast to AP activities on a soil mass basis (Table S1), ON-normalized APs were negatively correlated with soil ON content (Fig. 4a and b), and this relationship was strongest in O horizons while there was a greater variation in mineral soil horizons. The relationship did not hold for ON-normalized protease activity (Fig. 4c). The relationship between ON-normalized urease activity and soil ON content was positive in O horizons but variable in mineral soils (Fig. 4d). Correlations between OP-normalized phosphatase activities and soil OP concentrations were negatively in O, A and E horizons, whereas in the deeper horizons a positive relationship was found (Fig. 4e).

Furthermore, ON- and OP-normalized enzyme activities in mineral soils were correlated with mineralogical properties. Protease activities decreased with increasing clay as well as Al_o content (Fig. 5a and b). Urease activities were negatively linked to Al_o and (Fe+Al)_o contents (Fig. 5c and d) and phosphatase activities dropped upon increasing Fe_o and (Fe + Al)_o contents (Fig. 5e and f).

Enzyme activities expressed per C_{mic} reflect activities per cell. The AP and protease activities per C_{mic} were higher in eluvial

and subsoil than in topsoil horizons (Fig. S4a–c), especially at the three youngest sites, corresponding to their activities per ON. Phosphatase activities per C_{mic} showed the reverse trend with higher activities in topsoils for most sites (Fig. S4e), thus, largely resembling OP-normalized activities. In contrast, C_{mic} normalized urease activities showed no clear trend regarding soil depth (Fig. S4d) and therefore differed from activities per ON.

Profile-based activities of APs were lowest at the 5 kyr site (Fig. 6a). Profile-based protease activity was maximal at the 0.06 and 12 kyr sites, whereas urease activity was lowest at the latter (Fig. 6b). Profile-based ON:TP ratio increased with site age indicating the well-documented shift from N- to P-limitation in whole soil profiles. In contrast to the N-hydrolyzing enzymes, profile-based phosphatase activity increased with soil age (Fig. 6c) and was negatively correlated to TP ($r = -0.87, P = 0.01$), but positively correlated to clay stocks ($r = 0.98, P < 0.001$) and crystalline Fe stocks ($r = 0.86, P = 0.01$).

3.5. Microbial abundances and enzyme activities related to potential substrate availability

Microbial abundances (C_{mic}, N_{mic}, and total cell counts) were positively correlated to K₂SO₄- and NaH₂PO₄-extractable OC and TN contents. Both extractable OC and TN contents tended to be negatively related to ON-normalized AP activities (Table 3). In contrast, OP-normalized phosphatase activity was positively correlated to both, K₂SO₄- and NaH₂PO₄-extractable OC and TN contents, but ON-normalized urease activity was only positively related to NaH₂PO₄-extractable OC and TN contents. These correlations differed among horizons (data not shown) similar to the observed relationship to soil OP and ON content (Fig. 4d and e). No significant relationship was detected for ON-normalized protease activity.

For mineral soils, profile-based leu-AP activity tended to be positively related to NaH₂PO₄-extractable TN stocks ($r = 0.69, P = 0.084$), while profile-based urease activity was positively correlated to these TN stocks ($r = 0.85, P = 0.016$) (Fig. 6a and b). Profile-based protease activity was negatively correlated to K₂SO₄-extractable OC stocks ($r = -0.79, P = 0.033$), whereas profile-based phosphatase activity was positively correlated to NaH₂PO₄-extractable OC ($r = 0.88, P = 0.009$) (Fig. 6c).

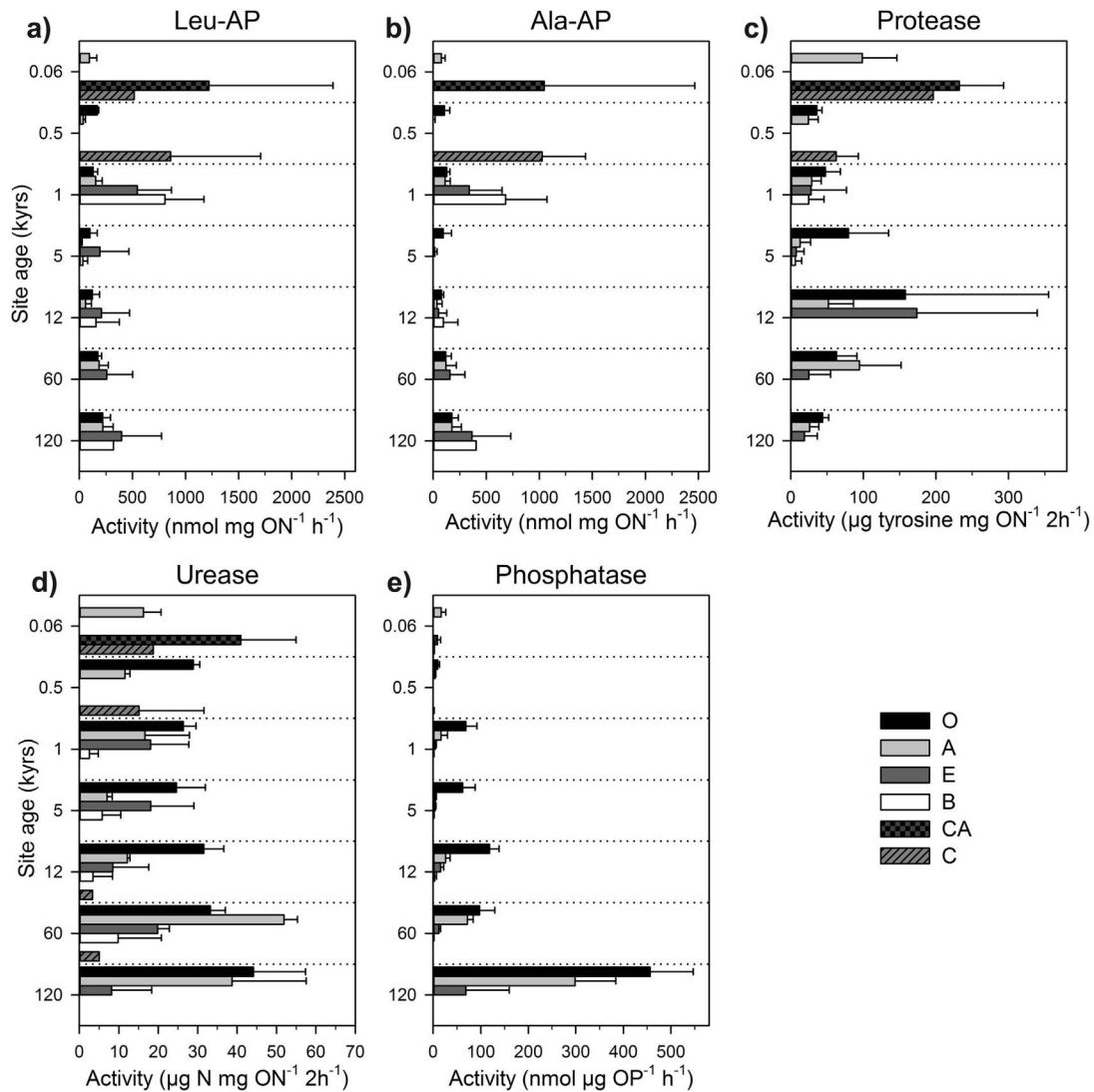


Fig. 3. Enzyme activities per mg soil ON or μg soil OP in soil profiles along the Franz Josef soil chronosequence. Error bars indicate standard deviation.

4. Discussion

4.1. Soil development

Mineralogical properties changed over 120 kyrs of soil development. Secondary poorly crystalline and crystalline hydrous Fe and Al oxides as well as clay contents became enriched with soil age (Fig. 1a, Table 2). The latter might partly be ascribed to Pleistocene loess deposition at the two oldest sites (Almond et al., 2001). Interestingly, given the variation of field repetitions, profile-based OC and ON stocks only weakly responded to mineralogical and textural variations (Fig. 1a) compared to correlations reported by other studies (see below). However, the presence of poorly crystalline Al phases positively affected OC accumulation, which is in line with other studies reporting a relationship between poorly crystalline Fe and Al oxides and OC stocks in acidic soils (Torn et al., 1997; Masiello et al., 2004) and ON storage (based on data of

Masiello et al., 2004; Mikutta et al., 2010). Profile-based OC and ON stocks increased slightly towards older soils that contained more crystalline Fe and Al oxides and clay (Fig. 1a). In contrast, OP stocks decreased, reflecting the proceeding weathering of P-containing minerals with time.

Although environmental conditions (high OM input, high precipitation and soil leaching) and the presence of protective minerals should foster the accumulation and stabilization of OM in mineral soils at the intermediate-aged sites (Torn et al., 1997; Masiello et al., 2004; Mikutta et al., 2010), relatively less OC, ON, and OP was bound in the mineral soil compared to organic layers (Fig. 1a and b). This suggests that the net accumulation rate in organic layers at these sites exceeded those of OC, ON, and OP in the mineral soil due to a relatively large biomass production. Additionally, organic compounds leached from topsoils may be partly removed due to interflow in the E horizon and, therefore, would not accumulate in the underlying B horizons. This suggests a partial

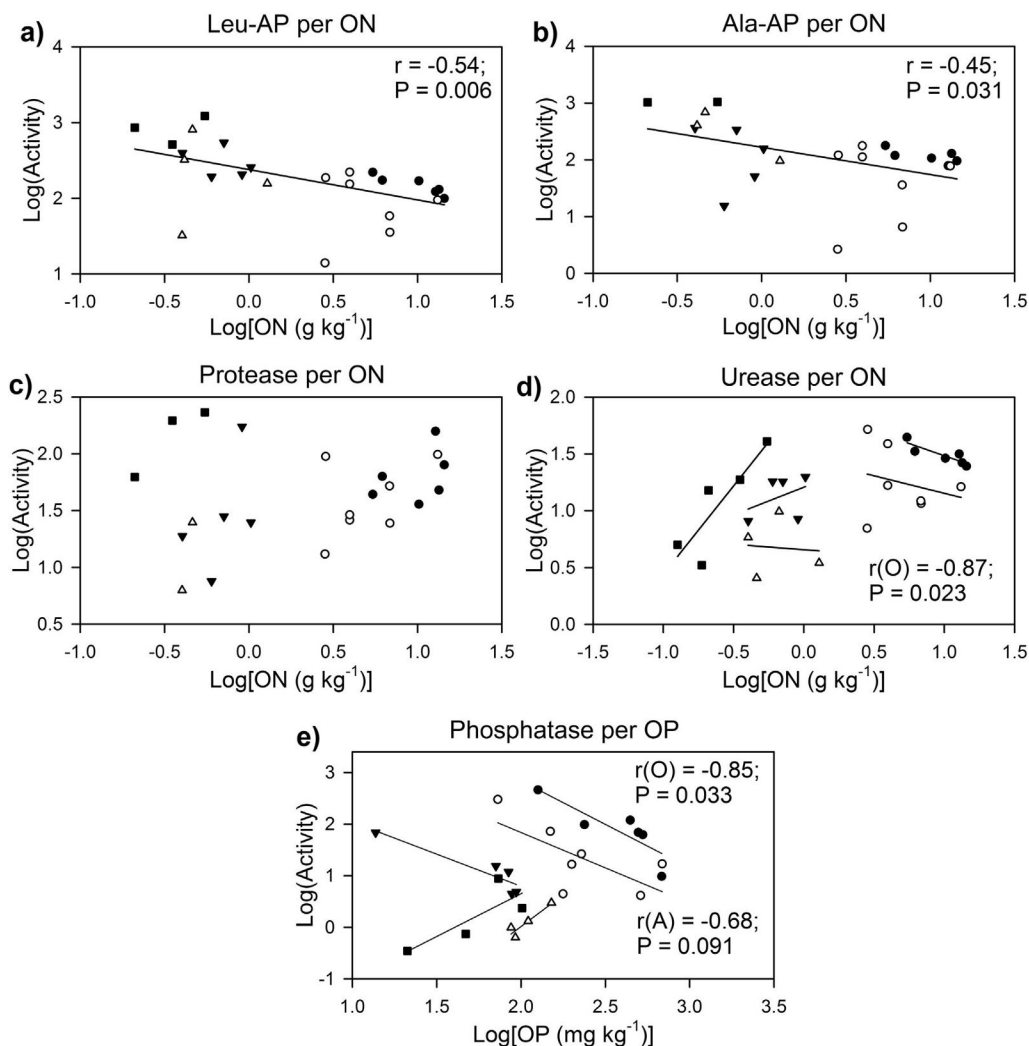


Fig. 4. Relationship between ON- or OP-normalized enzyme activities and soil ON or OP concentrations (both log-transformed). For APs regression lines were generated from data of all horizons and for urease and phosphatase regression lines were generated for each horizon: ● – O horizon, ○ – A horizon, ▼ – E horizon, △ – B horizon and ■ – C horizon. AP activities are expressed as nmol substrate mg soil ON⁻¹ h⁻¹, Protease activity is expressed as μg tyrosine mg soil ON⁻¹ 2 h⁻¹, urease activity is expressed as μg N mg soil ON⁻¹ 2 h⁻¹, and phosphatase activity is expressed as nmol substrate μg soil OP⁻¹ h⁻¹.

decoupling of top- and subsoil environments and a lack of strong correlations between OC and ON stocks with mineral parameters.

4.2. Potential substrate availability

The extraction with NaH₂PO₄ and K₂SO₄ gave evidence that much less than 13% of total soil OC and TN contents were potentially available (Fig. S2a and b). Particular the increase of NaH₂PO₄-extractable OC and TN proportions with soil depth and age suggests that this extractable OM was reversibly bound to variable-charge minerals like hydrous Fe and Al oxides or clay edges and was released upon ligand exchange with phosphate (Kaiser and Zech, 1999). Despite this, the NaH₂PO₄-extractable OC and TN fractions were surprisingly small given the fact that ~30% of goethite-associated OC was desorbed in a comparable laboratory experiment (Kaiser and Guggenberger, 2007). Accordingly, most OC and N compounds in these soils, particular in the subsoils, are held in a strongly mineral-bound fraction and are most likely protected

against rapid microbial decay (Mikutta et al., 2007) or enzymatic hydrolysis.

4.3. Microbial abundances and enzyme activities in organic soil layers

High OM input at intermediate-aged sites stimulated microbial growth and decomposition of litter and was reflected by higher microbial abundances (Table 1) and N-hydrolyzing enzyme activities on soil mass basis (Fig. S3a–d). Retrogressive P-limitation (>12 kyrs) coincided with a decline in microbial abundances (Table 1), decreasing activities of N-hydrolyzing enzymes, but increasing phosphatase activity (Fig. S3a–e). Similar patterns have been observed in other soil chronosequences developed on different parent materials (Wardle et al., 2004).

Expressing enzyme activities on substrate basis reveals regulation mechanism and possible nutrient limitation during soil

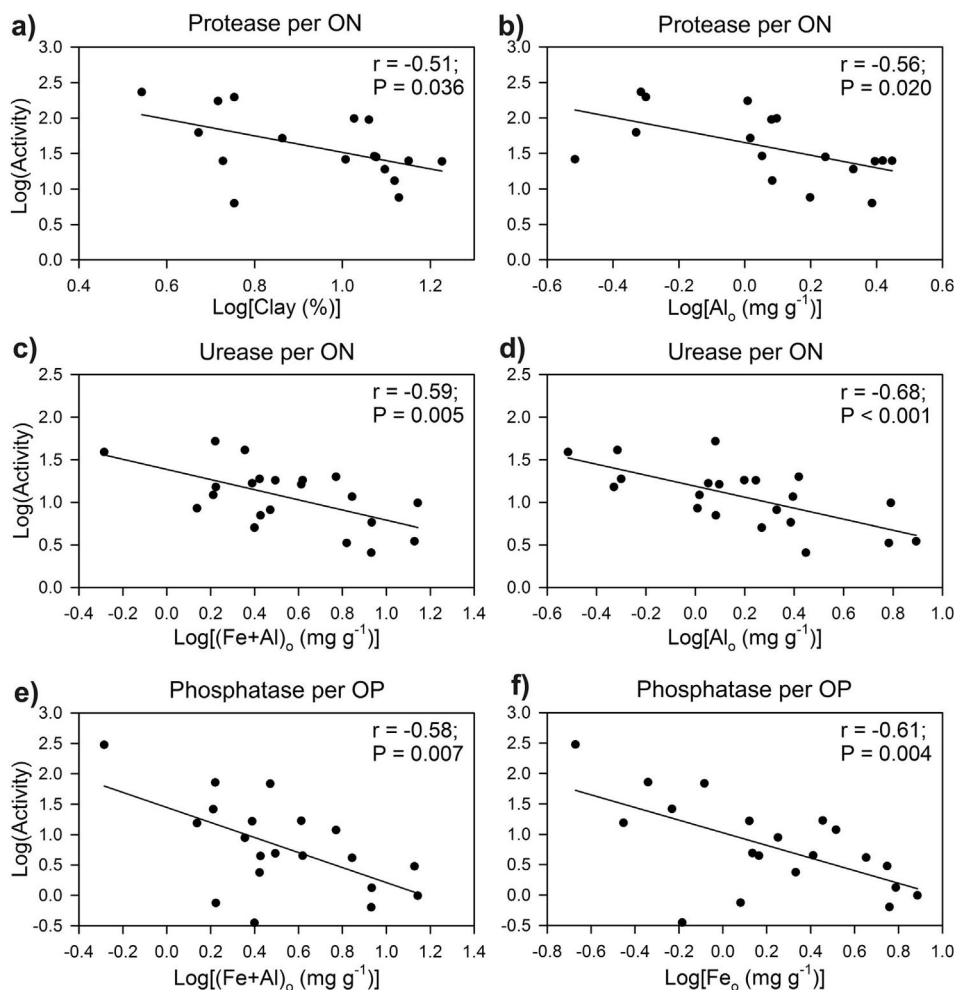


Fig. 5. Relationship between ON- or OP-normalized enzyme activities and mineralogical properties (both log-transformed) in mineral soils. Protease activity is expressed as μg tyrosine mg soil $\text{ON}^{-1} 2 \text{ h}^{-1}$, urease activity is expressed as μg N mg soil $\text{ON}^{-1} 2 \text{ h}^{-1}$, and phosphatase activity is expressed as μmol substrate μg soil $\text{OP}^{-1} \text{ h}^{-1}$.

development. Activities of N-hydrolyzing enzymes on soil mass basis differed from ON-normalized activities (Fig. 3a–d) because the former were disguised by a strong element gradient and an associated shift in microbial abundances along the chronosequence. Regulation of enzyme activities in organic soil layers mainly appears to depend on nutrient concentration. ON-normalized AP activities and urease activity showed a strong negative correlation to soil ON content (Fig. 4a, b, and d), suggesting a down-regulation if sufficient ON is available. Similarly, OP-normalized phosphatase activity was negatively correlated with OP content resulting in higher activities with increasing P-limitation (Fig. 4e). This relationship was also detected for most ON-normalized enzyme activities and K_2SO_4 - and NaH_2PO_4 -extractable OC and TN contents (Table 3), suggesting that these extractable fractions represent an important substrate source for enzymatic reactions.

However, no such down-regulation mechanism was detected for the ON-normalized protease activity (Fig. 4c), potentially because of variations in substrate specificity and regulation mechanisms of different protease classes, e.g. endo- and exoaminopeptidases (Vranova et al., 2013).

4.4. Microbial abundances and enzyme activities in mineral soil

Soil OC, ON, and OP concentrations in mineral soil were on average more than 50% lower than in organic layers (Table 1), coinciding with a very low potential substrate availability (Fig. S2a and b). As a result, microbial abundances and enzyme activities on soil mass basis were much lower than in organic layers (Table 1, Fig. S3a–e), indicating a decrease of absolute microbial activity in eluvial and subsoil horizons.

In mineral soil, regulation of enzyme activities was more complex because both, enzymes and their substrates are subject to several transformation and stabilization processes, including their interaction with minerals (Kaiser and Guggenberger, 2000). Interestingly, the relationship between ON-normalized enzyme activities and soil ON concentrations differed between horizons and also between enzymes (Fig. 4a–d). For APs we found a negative relationship just as in the organic layers. Thus, the same down-regulation mechanism seems to occur also in mineral soil, but the broader variance suggests additional interactions with other factors than ON content. The relative higher activities in subsoil horizons (Fig. S3a and b) and the missing correlation to mineralogical

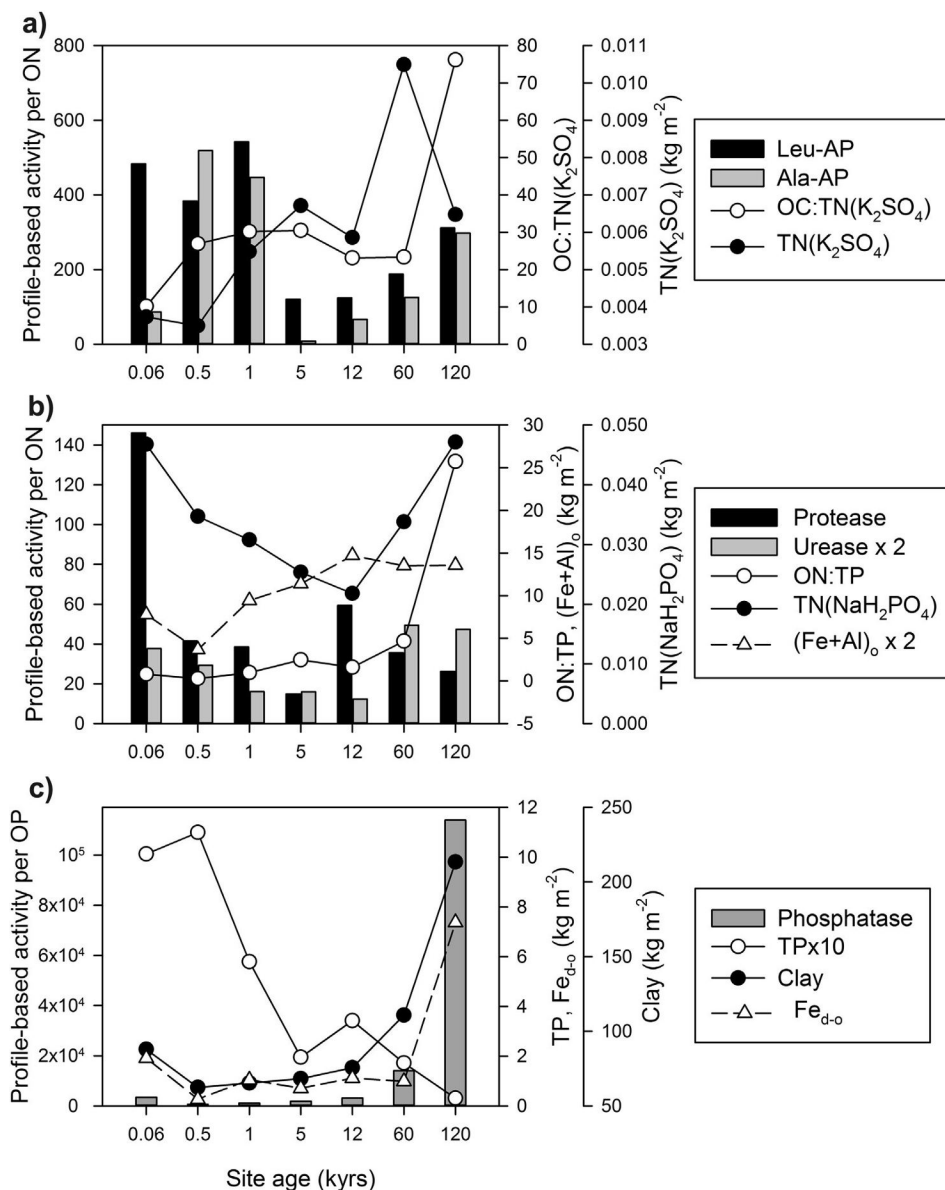


Fig. 6. Profile-based enzyme activities per ON or OP stocks in relation to profile-based soil property stocks along the Franz Josef soil chronosequence in mineral soils for one profile per site. (a) Profile-based leu-AP and ala-AP per ON stocks ($\text{mmol h}^{-1} \text{kg}^{-1}$) in relation to profile-based OC:TN ratio of K_2SO_4 -extractable contents and profile-based K_2SO_4 -extractable TN stocks; (b) profile-based protease and urease activities per ON stocks (protease: $\text{g tyrosine } 2 \text{ h}^{-1} \text{kg}^{-1}$, urease: $\text{g N } 2 \text{ h}^{-1} \text{kg}^{-1}$) in relation to profile-based soil ON:TP ratio, profile-based NaH_2PO_4 -extractable TN stocks, and profile-based $(\text{Fe}+\text{Al})_0$ stocks, and (c) profile-based phosphatase activity per OP stock ($\text{mmol h}^{-1} \text{kg}^{-1}$) in relation to profile-based TP, $\text{Fe}_{\text{d-o}}$, and clay stocks.

parameters indicate that the AP activities were less influenced by the investigated soil mineralogical properties. The OP-normalized phosphatase activity was negatively correlated to soil OP content in A and E horizons, but not in B and C horizons (Fig. 4f). Decreasing OC:OP ratios with soil depth (Table 1) may suggest a preferred retention of OP over that of OC especially by hydrous Fe and Al oxides, which has been observed in sorption experiments with dissolved OP (Kaiser, 2001) and bacteria-derived extracellular polymeric substances (Mikutta et al., 2011). As a consequence of the stronger interactions with OP compounds, more phosphatase per

substrate might be released by microorganisms. In contrast, ON-normalized protease and urease activity were not related to soil ON content in the mineral soil. Instead, these ON-normalized activities were correlated with mineralogical properties (Fig. 5a–d).

Increasing clay content associated with decreasing levels of ON-normalized protease activity suggests an inhibition of activity (Fig. 5a). In laboratory experiments with artificial enzyme–clay-complexes, enzyme activities were reduced after adsorption of enzymes onto clay surfaces (Gianfreda et al., 1991, 1992). Likewise, Bayan and Eivazi (1999) observed a general reduction of enzyme

Table 3

Pearson correlation coefficient matrix for ON- and OP-normalized enzyme activities and K₂SO₄- and NaH₂PO₄-extractable OC and TN content based on log-transformed data. *P*-value and *n* in parentheses. Significant relationships are indicated by bold font ($r > 0.5$; $P < 0.05$).

	Leu-AP/ON (nmol mg ON ⁻¹ h ⁻¹)	Ala-AP/ON (nmol mg ON ⁻¹ h ⁻¹)	Phosphatase/OP (nmol μg OP ⁻¹ h ⁻¹)	Protease/ON (μg tyrosine mg ON ⁻¹ 2 h ⁻¹)	Urease/ON (μg N mg ON ⁻¹ 2 h ⁻¹)
OC (NaH ₂ PO ₄) (g kg ⁻¹)	-0.52 (0.008, 25)	-0.39 (0.069, 23)	0.59 (0.002, 26)	-0.06 (0.772, 23)	0.40 (0.038, 27)
TN (NaH ₂ PO ₄) (g kg ⁻¹)	-0.51 (0.010, 25)	-0.41 (0.049, 23)	0.66 (<0.001, 26)	0.18 (0.410, 23)	0.58 (0.002, 27)
OC (K ₂ SO ₄) (g kg ⁻¹)	-0.43 (0.031, 25)	-0.32 (0.134, 23)	0.51 (0.008, 26)	-0.38 (0.074, 23)	0.24 (0.233, 27)
TN (K ₂ SO ₄) (g kg ⁻¹)	-0.46 (0.023, 25)	-0.41 (0.052, 23)	0.66 (<0.001, 26)	0.07 (0.758, 23)	0.47 (0.014, 27)

activities due to clay-sized minerals and a relationship between lower activities and the presence of finer clay fractions.

Similar to the enzyme-clay-relations, the (Fe+Al)_o content, mainly representing poorly crystalline Fe and Al minerals, was negatively correlated to ON-normalized protease and urease activities as well as OP-normalized phosphatase activity (Fig. 5b–f). Those minerals are considered to be the main stabilizing agents of OM in temperate acidic subsoils (Kögel-Knabner et al., 2008; Achat et al., 2012) and therefore may stabilize protease, urease and phosphatase or impair access to their substrates. These processes could alter enzyme activities and generally result in lower activities compared to those of free enzymes (Rao and Gianfreda, 2000; Gianfreda et al., 2002). A reduction of activity in the presence of Fe oxides was also reported for alkaline phosphatase (Bayan and Eivazi, 1999). Similarly, Fe and Al and other trace metals inhibit the activity of β-glucosaminidase (Ekenler and Tabatabai, 2002) and asparaginase (Frankenberger and Tabatabai, 1991).

On the contrary, other studies with artificial and natural soils have demonstrated that the presence of clay or iron oxides enhanced particular enzyme activities (Bayan and Eivazi, 1999; Allison, 2006; Shahriari et al., 2010). Hence, there is little consistency in literature related to mineral-enzyme interaction, likely caused by differences in experimental conditions such as pH. The latter exerts a strong control on the interaction between enzymes and mineral surfaces by influencing the surface affinity and associated binding strength as well as the conformation of the enzyme (Quiquampoix et al., 1993; Kedi et al., 2013).

Generally, our data on enzyme activities in natural soils support the view that protective soil minerals such as poorly crystalline Fe and Al phases and clay minerals reduce most enzyme activities through interactions with both enzymes and substrates. However, the magnitude of these interactions varies between individual mineral phases and also among the enzymes and substrates considered. Although, soil mineralogical parameters appear to trigger enzyme regulation by limiting or providing access to organic substrates, this was not reflected by the extraction approach for the assessment of substrate accessibilities.

4.5. Enzyme activities normalized to microbial biomass and pedon scale

The C_{mic}-normalized enzyme activities of APs and protease were higher in eluvial and subsoil horizons than in topsoil horizons indicating a higher microbial activity per cell (Fig. S4a–c). Similarly, Blume et al. (2002) also detected highest activities normalized to microbial abundances in deeper soil (0.5–0.9 m). These higher activities of N-hydrolyzing enzymes suggest that microbes in eluvial and subsoil horizons, especially at the younger sites, were rather N-limited (Fig. S4a–c). In contrast, C_{mic}-normalized phosphatase activity decreased with soil depth (Fig. S4e). This indicates that the subsoil microbial community is more efficient or adapted for P cycling as OP concentrations were small and P compounds were fixed to secondary minerals at the older sites. A different pattern existed for C_{mic}-normalized urease activity, in that eluvial

and subsoil horizon activities on the younger sites were higher or equal to topsoil activities, whereas at the three older sites topsoil activities were higher (Fig. S4d). This suggests that urease activity was regulated by soil ON as well as OP content or rather responded to N- and P-limitation. A potential source of urea in soils is the degradation of nucleic acids (Hasan, 2000), which would also release P compounds. The topsoil DNA concentration increased with soil age and decreased after a maximum at the 0.5–12 kyr sites, whereas the proportion of DNA to total OP increased with site age to ~25% (Turner et al., 2007). Therefore, DNA became an important, but also limited source of OP at the older sites and stimulated urease activity.

Enzyme activities on a pedon basis normalized to ON and OP stocks reflect nutrient limitations during long-term ecosystem development for whole soil profiles. Profile-based activities of N-hydrolyzing enzymes differed from each other with respect to soil age (Fig. 6a and b). Nitrogen-limitation at younger sites, as described for forest development by Richardson et al. (2004), seems to extend also to the belowground ecosystem and is reflected in higher profile-based activities of APs (0.06–1 kyrs), protease (only 0.06 kyrs), and urease (0.06–0.5 kyrs). Maximal aboveground biomass (Richardson et al., 2004) and larger N allocation as suggested by the high extractable ON stocks in O horizons at intermediate-aged sites (Fig. 2a and b) probably compensate N limitation in topsoils. For subsoils, the narrow OC:TN ratio of labile OM as estimated by K₂SO₄ extraction of fresh mineral soil suggests a lower N demand (Fig. 2c). Further, low enzymatic activities were likely facilitated by the sorption of OM or enzymes to protective poorly crystalline Fe and Al oxides (Fig. 6a and b). These processes resulted in an overall reduced pedon-based N hydrolytic activity at intermediate-aged sites. At the two oldest sites, less OM was extracted from the organic layers (Fig. 2a and b), thus pointing towards a lower input of C and N into mineral soil, and also the OC:TN ratio (5–10 versus 80) of this OM at the oldest site was much wider (data not shown). Similarly, the OC:TN ratio of the easily extractable OM in the mineral soil was wider (Fig. 2c). In microbial ecology, as rule of thumb, substrate C:N ratios of >~25 force microorganisms to invest into N mining and thus enzyme production to maintain their N demands (Robertson and Groffman, 2007). The wide C:N ratios of the K₂SO₄-extractable OM pool (32 and 49), therefore, help to explain the higher N profile-based activities of APs and urease at the oldest sites.

In contrast, phosphatase showed a consistent trend along the soil chronosequence that reflects the P-limitation gradient induced by secondary minerals. Increases in stocks of crystalline Fe and clay-sized minerals along with decreasing profile-based TP stocks caused a higher investment of microorganisms in P acquisition (Fig. 6c).

Overall, our data indicate a long-term mineralogical impact on N-hydrolyzing and P-hydrolyzing enzymes and their substrates during soil formation at both the horizon level and for whole profiles. The strength of these mineralogical effects differs among N-hydrolyzing enzymes, whereas there is a strong mineralogical influence on P content and phosphatase activity. This could be

explained by the relatively more complex interactions involved with N, whereby ON is distributed among several substance classes (Sinsabaugh et al., 2008) and secondary soil minerals can interact differently with contrasting ON pools (Mikutta et al., 2010).

4.6. Conclusions

This study demonstrates that long-term changes in mineral assemblage differently impacts N and P cycling in natural soil ecosystems. Although regulation of enzyme activities in organic layers depends primarily on ON and OP concentrations, interactions in mineral soil were more complex and include both, direct and indirect effects. Aminopeptidases seem to be less affected by mineralogical properties, whereas protease, urease and phosphatase activities were inhibited likely by sorptive interactions with clay-sized minerals including poorly crystalline Fe and Al oxides. On a pedon basis, the accumulation of poorly crystalline Fe and Al oxides at intermediate-aged soils results in slower ON turnover, whereas increasing crystalline Fe oxides and clay content coincided with higher phosphatase activity due to substrate limitation. Beside direct protection of substrates and enzymes by minerals, the quality of the soil solution, reflected by the OC:TN ratio of the labile K_2SO_4 -extractable OM, also appears important for the regulation of N enzymatic activities. Our results imply that soil forming processes alter long-term nutrient cycling during ecosystem development and highlight the role of soil minerals in regulating nutrient supply for microorganisms and plants, and ultimately many soil ecosystem processes.

Acknowledgments

We are grateful to Detlef Spier for HPLC measurements, and Gudrun Mengel-Jung for laboratory support. Furthermore, we acknowledge the help of Ulrike Pieper, Heike Steffen, Pieter Wiese, and Roger-Michael Klatt. Funding was provided by the German Science Foundation (DFG), grants MI 1377/5-1 and SCHI 535/11-1 to R.M. and A.S. The authors declare no conflicts of interest.

Appendix A. Supplementary data

Supplementary data related to this article can be found at <http://dx.doi.org/10.1016/j.soilbio.2013.09.016>.

References

- Achat, D.L., Augusto, L., Bakker, M.R., Gallet-Budynek, A., Morel, C., 2012. Microbial processes controlling P availability in forest spodosols as affected by soil depth and soil properties. *Soil Biol. Biochem.* 44, 39–48.
- Allison, S.D., 2006. Soil minerals and humic acids alter enzyme stability: implications for ecosystem processes. *Biogeochemistry* 81, 361–373.
- Allison, S.D., Jastrow, J.D., 2006. Activities of extracellular enzymes in physically isolated fractions of restored grassland soils. *Soil Biol. Biochem.* 38, 3245–3256.
- Allison, S.D., Vitousek, P.M., 2005. Responses of extracellular enzymes to simple and complex nutrient inputs. *Soil Biol. Biochem.* 37, 937–944.
- Allison, V.J., Condon, L.M., Peltzer, D.A., Richardson, S.J., Turner, B.L., 2007. Changes in enzyme activities and soil microbial community composition along carbon and nutrient gradients at the Franz Josef chronosequence, New Zealand. *Soil Biol. Biochem.* 39, 1770–1781.
- Almond, P.C., Moar, N.T., Lian, O.B., 2001. Reinterpretation of the glacial chronology of South Westland, New Zealand. *N. Z. J. Geol. Geophys.* 44, 1–15.
- Baldrian, P., Trögl, J., Frouz, J., Šnajdr, J., Valášková, V., Merhautová, V., Cajthaml, T., Herinková, J., 2008. Enzyme activities and microbial biomass in topsoil layer during spontaneous succession in spoil heaps after brown coal mining. *Soil Biol. Biochem.* 40, 2107–2115.
- Balser, T.C., Firestone, M.K., 2005. Linking microbial community composition and soil processes in a California annual grassland and mixed-conifer forest. *Biogeochemistry* 73, 395–415.
- Bayan, M., Eivazi, F., 1999. Selected enzyme activities as affected by free iron oxides and clay particle size. *Commun. Soil Sci. Plant Anal.* 30, 1561–1571.
- Blume, E., Bischoff, M., Reichert, J.M., Moorman, T., Konopka, A., Turco, R.F., 2002. Surface and subsurface microbial biomass, community structure and metabolic activity as a function of soil depth and season. *Appl. Soil Ecol.* 20, 171–181.
- Crews, T.E., Kitayama, K., Fownes, J.H., Riley, R.H., Herbert, D.A., Mueller-Dombois, D., Vitousek, P.M., 1995. Changes in soil phosphorus fractions and ecosystem dynamics across a long chronosequence in Hawaii. *Ecology* 76, 1407–1424.
- Ekenler, M., Tabatabai, M.A., 2002. Effects of trace elements on β -glucosaminidase activity in soils. *Soil Biol. Biochem.* 34, 1829–1832.
- Frankenberger, W.T., Tabatabai, M.A., 1991. Factors affecting L-asparaginase activity in soils. *Biol. Fertil. Soils* 11, 1–5.
- Gianfreda, L., Rao, M., Sannino, F., Saccomandi, F., Violante, A., 2002. Enzymes in soil: properties, behavior and potential applications. *Dev. Soil Sci.* 28B, 301–327.
- Gianfreda, L., Rao, M., Violante, A., 1992. Adsorption, activity and kinetic properties of urease on montmorillonite, aluminium hydroxide and Al(OH)₃-montmorillonite complexes. *Soil Biol. Biochem.* 24, 51–58.
- Gianfreda, L., Rao, M.A., Violante, A., 1991. Invertase (β -fructosidase): effects of montmorillonite, Al-hydroxide and Al(OH)₃-montmorillonite complex on activity and kinetic properties. *Soil Biol. Biochem.* 23, 581–587.
- Hasan, H., 2000. Ureolytic microorganisms and soil fertility: a review. *Commun. Soil Sci. Plant Anal.* 31, 2565–2589.
- IUSS Working Group WRB, 2006. World Reference Base for Soil Resources. World Soil Resources Report No. 103, second ed. FAO, Rome.
- Joergensen, R., 1996. The fumigation-extraction method to estimate soil microbial biomass: calibration of the k_{EC} value. *Soil Biol. Biochem.* 28, 25–31.
- Joergensen, R., Brookes, P., 1990. Ninhydrin-reactive nitrogen measurements of microbial biomass in 0.5 M K_2SO_4 soil extracts. *Soil Biol. Biochem.* 22, 1023–1027.
- Kaiser, K., 2001. Dissolved organic phosphorus and sulphur as influenced by sorptive interactions with mineral subsoil horizons. *Eur. J. Soil Sci.* 52, 489–493.
- Kaiser, K., Guggenberger, G., 2000. The role of DOM sorption to mineral surfaces in the preservation of organic matter in soils. *Org. Geochem.* 31, 711–725.
- Kaiser, K., Guggenberger, G., 2007. Sorptive stabilization of organic matter by microporous goethite: sorption into small pores vs. surface complexation. *Eur. J. Soil Sci.* 58, 45–59.
- Kaiser, K., Mikutta, R., Guggenberger, G., 2007. Increased stability of organic matter sorbed to ferrihydrite and goethite on aging. *Soil Sci. Soc. Am. J.* 71, 711–719.
- Kaiser, K., Zech, W., 1999. Release of natural organic matter sorbed to oxides and a subsoil. *Soil Sci. Soc. Am. J.* 63, 1157–1166.
- Kalbitz, K., Schwesig, D., Rethemeyer, J., Matzner, E., 2005. Stabilization of dissolved organic matter by sorption to the mineral soil. *Soil Biol. Biochem.* 37, 1319–1331.
- Kedi, B., Abadie, J., Sei, J., Quiquampoix, H., Staunton, S., 2013. Diversity of adsorption affinity and catalytic activity of fungal phosphatases adsorbed on some tropical soils. *Soil Biol. Biochem.* 56, 13–20.
- Kögel-Knabner, I., Guggenberger, G., Kleber, M., Kandeler, E., Kalbitz, K., Scheu, S., Eusterhues, K., Leinweber, P., 2008. Organo-mineral associations in temperate soils: integrating biology, mineralogy, and organic matter chemistry. *J. Plant Nutr. Soil Sci.* 171, 61–82.
- Lunau, M., Lemke, A., Walther, K., Martens-Habbena, W., Simon, M., 2005. An improved method for counting bacteria from sediments and turbid environments by epifluorescence microscopy. *Environ. Microbiol.* 7, 961–968.
- Marinari, S., Vittori Antisari, L., 2010. Effect of lithological substrate on microbial biomass and enzyme activity in brown soil profiles in the northern Apennines (Italy). *Pedobiologia* 53, 313–320.
- Masiello, C.A., Chadwick, O.A., Southon, J., Torn, M.S., Harden, J.W., 2004. Weathering controls on mechanisms of carbon storage in grassland soils. *Glob. Biogeochem. Cycles* 18. <http://dx.doi.org/10.1029/2004GB002219>.
- Mikutta, R., Kaiser, K., Dörr, N., Vollmer, A., Chadwick, O.A., Chorover, J., Kramer, M.G., Guggenberger, G., 2010. Mineralogical impact on organic nitrogen across a long-term soil chronosequence (0.3–4100 kyr). *Geochim. Cosmochim. Acta* 74, 2142–2164.
- Mikutta, R., Mikutta, C., Kalbitz, K., Scheel, T., Kaiser, K., Jahn, R., 2007. Biodegradation of forest floor organic matter bound to minerals via different binding mechanisms. *Geochim. Cosmochim. Acta* 71, 2569–2590.
- Mikutta, R., Schaumann, G.E., Gildemeister, D., Bonneville, S., Kramer, M.G., Chorover, J., Chadwick, O.A., Guggenberger, G., 2009. Biogeochemistry of mineral-organic associations across a long-term mineralogical soil gradient (0.3–4100 kyr), Hawaiian Islands. *Geochim. Cosmochim. Acta* 73, 2034–2060.
- Mikutta, R., Zang, U., Chorover, J., Haumaier, L., Kalbitz, K., 2011. Stabilization of extracellular polymeric substances (*Bacillus subtilis*) by adsorption to and coprecipitation with Al forms. *Geochim. Cosmochim. Acta* 75, 3135–3154.
- Moore, T.R., Turunen, J., 2004. Carbon accumulation and storage in mineral subsoil beneath peat. *Soil Sci. Soc. Am. J.* 68, 690–696.
- Nannipieri, P., Smalla, K., 2006. *Nucleic Acids and Proteins in Soil*. Springer-Verlag, Berlin, Heidelberg, New York.
- Nierop, K.G.J., Jansen, B., Verstraten, J.M., 2002. Dissolved organic matter, aluminium and iron interactions: precipitation induced by metal/carbon ratio, pH and competition. *Sci. Total Environ.* 300, 201–211.
- Olander, L., Vitousek, P., 2000. Regulation of soil phosphatase and chitinase activity by N and P availability. *Biogeochemistry* 49, 175–190.
- Peltzer, D.A., Wardle, D.A., Allison, V.J., Baisden, T.W., Bardgett, R.D., Chadwick, O.A., Condon, L.M., Parfitt, R.L., Porder, S., Richardson, S.J., Turner, B.L., Vitousek, P.M., Walker, J., Walker, L.R., 2010. Understanding ecosystem retrogression. *Ecol. Monogr.* 80, 509–529.

- Quiquampoix, H., Staunton, S., Baron, M., Ratcliffe, R., 1993. Interpretation of the pH dependence of protein adsorption on clay mineral surfaces and its relevance to the understanding of extracellular enzyme activity in soil. *Colloids Surf. A Physicochem. Eng. Asp.* 75, 85–93.
- Rao, M.A., Gianfreda, L., 2000. Properties of acid phosphatase–tannic acid complexes formed in the presence of Fe and Mn. *Soil Biol. Biochem.* 32, 1921–1926.
- Richardson, S.J., Peltzer, D.A., Allen, R.B., McGlone, M.S., Parfitt, R.L., 2004. Rapid development of phosphorus limitation in temperate rainforest along the Franz Josef soil chronosequence. *Oecologia* 139, 267–276.
- Robertson, G.P., Groffman, P.M., 2007. Nitrogen transformations. In: Paul, E.A. (Ed.), *Soil Microbiology, Ecology, and Biochemistry*, third ed. Academic Press, pp. 341–364.
- Saunders, W., Williams, E., 1955. Observations on the determination of total organic phosphorus in soils. *J. Soil Sci.* 6, 254–267.
- Scheel, T., Dörfler, C., Kalbitz, K., 2007. Precipitation of dissolved organic matter by aluminum stabilizes carbon in acidic forest soils. *Soil Sci. Soc. Am. J.* 71, 64–74.
- Schinner, F., Öhlinger, R., Kandeler, E., Margesin, R., 1993. *Bodenbiologische Arbeitsmethoden*, 2. Auflage. Springer-Verlag, Berlin, Heidelberg, New York, London, Paris, Tokyo, Hong Kong, Barcelona, Budapest.
- Schlichting, E., Blume, H.-P., Stahr, K., 1995. *Bodenkundliches Praktikum. Eine Einführung in pedologisches Arbeiten für Ökologen, insbesondere Land- und Forstwirte und für Geowissenschaftler*, 2., neubea. Auflage. Blackwell-Verlag, Berlin.
- Shahriari, F., Higashi, T., Tamura, K., 2010. Effects of clay addition on soil protease activities in Andosols in the presence of cadmium. *Soil Sci. Plant Nutr.* 56, 560–569.
- Sinsabaugh, R., 1994. Enzymic analysis of microbial pattern and process. *Biol. Fertil. Soils* 17, 69–74.
- Sinsabaugh, R.L., Lauber, C.L., Weintraub, M.N., Ahmed, B., Allison, S.D., Crenshaw, C., Contosta, A.R., Cusack, D., Frey, S., Gallo, M.E., Gartner, T.B., Hobbie, S.E., Holland, K., Keeler, B.L., Powers, J.S., Stursova, M., Takacs-Vesbach, C., Waldrop, M.P., Wallenstein, M.D., Zak, D.R., Zeglin, L.H., 2008. Stoichiometry of soil enzyme activity at global scale. *Ecol. Lett.* 11, 1252–1264.
- Stemmer, M., 2004. Multiple-substrate enzyme assays: a useful approach for profiling enzyme activity in soils? *Soil Biol. Biochem.* 36, 519–527.
- Stevens, P., Walker, T., 1970. The chronosequence concept and soil formation. *Q. Rev. Biol.* 45, 333–350.
- Stevens, P.R., 1968. *A Chronosequence of Soils Near the Franz Josef Glacier* (Ph.D. thesis). University of Canterbury, New Zealand.
- Torn, M., Trumbore, S., Chadwick, O., Vitousek, P., Hendricks, D., 1997. Mineral control of soil organic carbon storage and turnover. *Nature* 389, 170–173.
- Turner, B.L., Condon, L.M., Richardson, S.J., Peltzer, D.A., Allison, V.J., 2007. Soil organic phosphorus transformations during pedogenesis. *Ecosystems* 10, 1166–1181.
- Vance, E., Brookes, P., Jenkinson, D., 1987. An extraction method for measuring soil microbial biomass C. *Soil Biol. Biochem.* 19, 703–707.
- Vincent, A.G., Schleucher, J., Gröbner, G., Vestergren, J., Persson, P., Jansson, M., Giesler, R., 2012. Changes in organic phosphorus composition in boreal forest humus soils: the role of iron and aluminium. *Biogeochemistry* 108, 485–499.
- Vranova, V., Rejsek, K., Formanek, P., 2013. Proteolytic activity in soil: a review. *Appl. Soil Ecol.* 70, 23–32.
- Walker, T.W., Syers, J.K., 1976. The fate of phosphorus during pedogenesis. *Geoderma* 15, 1–19.
- Wardle, D., Walker, L., Bardgett, R., 2004. Ecosystem properties and forest decline in contrasting long-term chronosequences. *Science* 305, 509–513.

1 **Supplementary material**

2

3 **Table S1**

4 Pearson correlation coefficient matrix for enzyme activities (on soil mass basis) and soil OC,

5 ON, and OP contents based on log-transformed data. P-value and n in parentheses.

	OC (g kg ⁻¹)	ON (g kg ⁻¹)	OP (mg kg ⁻¹)
Leu-AP	0.71	0.71	0.56
(nmol g ⁻¹ h ⁻¹)	(< 0.001, 25)	(< 0.001, 25)	(0.004, 25)
Ala-AP	0.52	0.53	0.41
(nmol g ⁻¹ h ⁻¹)	(0.012, 23)	(0.009, 23)	(0.051, 23)
Phosphatase	0.91	0.90	0.63*
(nmol g ⁻¹ h ⁻¹)	(< 0.001, 26)	(< 0.001, 26)	(< 0.001, 26)
Protease	0.85	0.865	0.73
(µg tyrosine g ⁻¹ 2h ⁻¹)	(< 0.001, 23)	(< 0.001, 23)	(< 0.001, 23)
Urease	0.93	0.95	0.72
(µg N g ⁻¹ 2h ⁻¹)	(< 0.001, 27)	(< 0.001, 27)	(< 0.001, 27)

6 * r(O horizon) = -0.54 (P = 0.274, n = 6),

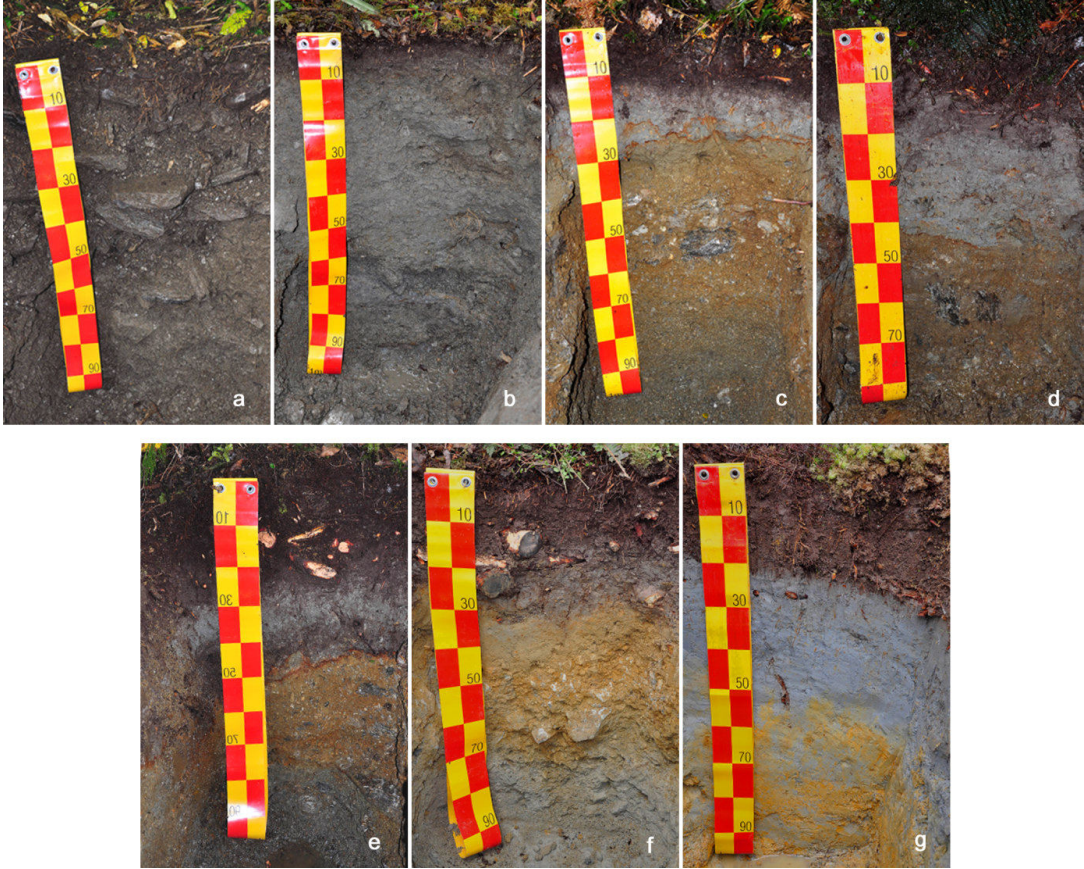
7 r(A horizon) = -0.26 (P = 0.570, n = 7),

8 r(E horizon) = -0.61 (P = 0.273, n = 5),

9 r(B horizon) = 0.93 (P = 0.069, n = 4),

10 r(C horizon) = 0.87 (P = 0.126, n = 4)

11



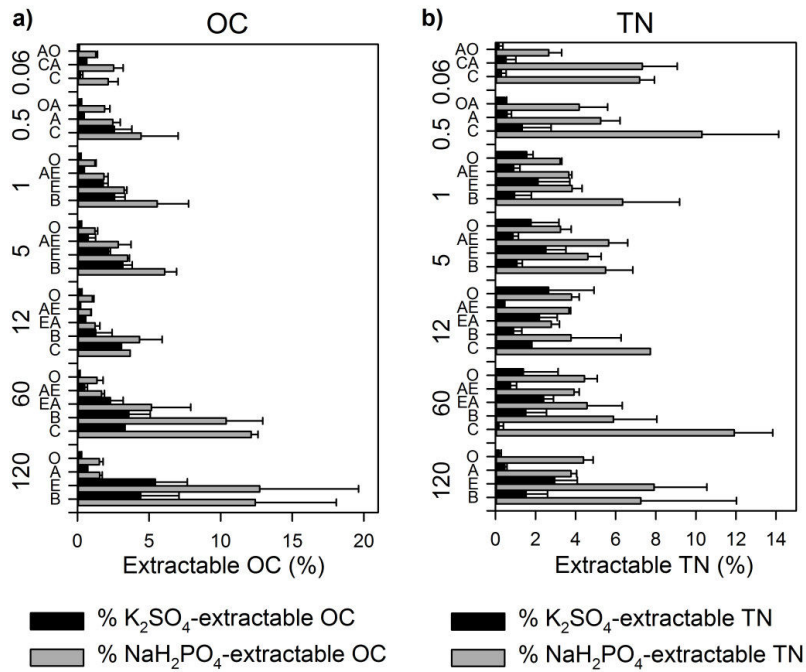
12

13 **Fig. S1.** Depth profiles of all seven sampling sites along the Franz Josef soil chronosequence

14 showing soil development stages: (a) 0.06 kyrs, (b) 0.5 kyrs, (c) 1 kyrs, (d) 5 kyrs, (e) 12 kyrs,

15 (f) 60 kyrs and (g) 120 kyrs.

16

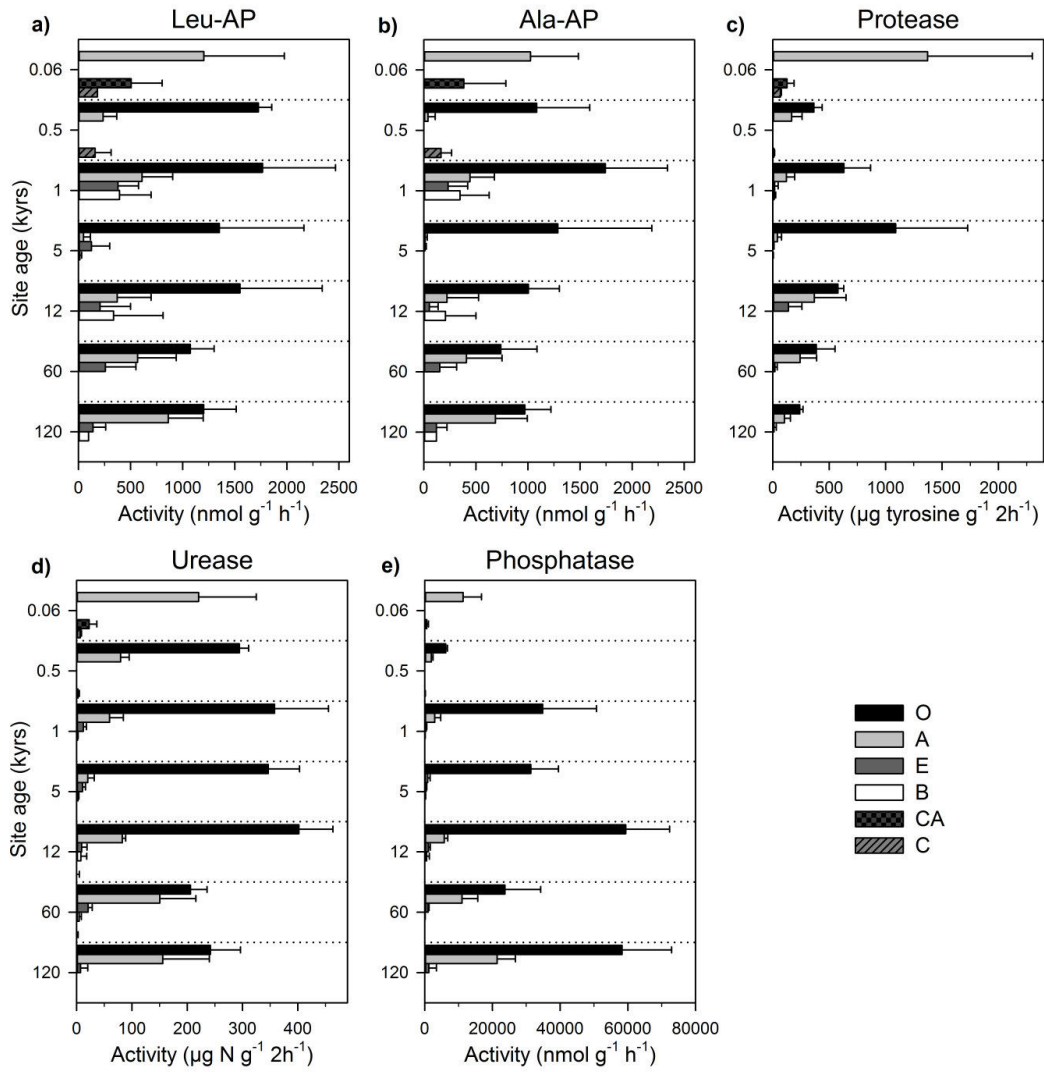


17

18 **Fig. S2.** Proportions of K_2SO_4 - and NaH_2PO_4 -extractable OC (a) and TN contents (b) in soil

19 profiles along the Franz Josef chronosequence. Error bars indicate standard deviation.

20

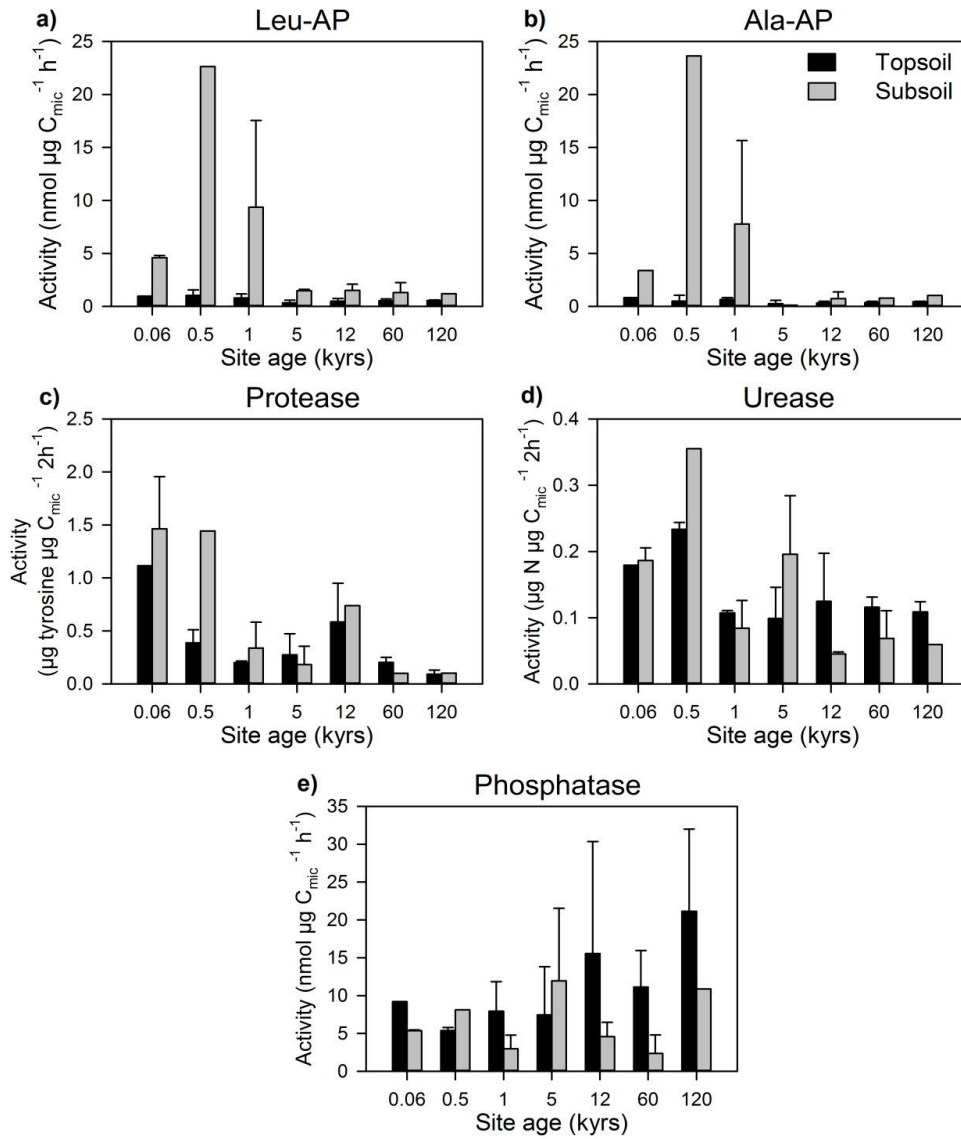


21

22 **Fig. S3.** Enzyme activities per gram dry soil in soil profiles along the Franz Josef soil
 23 chronosequence. Error bars indicate standard deviation.

24

25



26

27 **Fig. S4.** Enzyme activities per $\mu\text{g C}_{\text{mic}}$ in topsoil horizons (O and A) versus eluvial and
 28 subsoil horizons (E, B, C) at the different stages of the Franz Josef soil chronosequence. Error
 29 bars indicate standard deviation.

30

4.2.3 Manuscript 3: 120,000 years of soil ecosystem development results in distinct nitrogen cycling microbial communities

120,000 Years of Soil Ecosystem Development Results in Distinct Nitrogen Cycling Microbial Communities

Stephanie Turner,^{a,#,*} Robert Mikutta,^b Sandra Meyer-Stüve,^c Georg Guggenberger,^c Frank Schaarschmidt,^d Reiner Dohrmann,^e Axel Schippers^a

Geomicrobiology, Federal Institute for Geosciences and Natural Resources (BGR), Hannover, Germany ^a;
Soil Science and Soil Protection, Martin-Luther-Universität Halle-Wittenberg, Halle (Saale), Germany ^b;
Institute of Soil Science, Leibniz Universität Hannover, Hannover, Germany ^c; Institute of Biostatistics,
Leibniz Universität Hannover, Hannover, Germany ^d; Technical Mineralogy and Clay Mineralogy, Federal
Institute for Geosciences and Natural Resources (BGR), Hannover, Germany ^e

Running head: Nitrogen Cycling Communities Along Soil Chronosequence

#Address correspondence to Stephanie Turner, sturner.bio@gmail.com

*Present address: Stephanie Turner, Centre for Ecology and Evolution in Microbial Model Systems (EEMiS), Linnaeus University, Kalmar, Sweden

ABSTRACT

Soil microorganisms are key players of the nitrogen (N) cycle by mediating most N transformation processes and play an important role in soil development. While the dynamics of N cycling microorganisms during initial soil development are already well investigated, knowledge about their patterns during long-term ecosystem development is restricted. In this study, N functional genes of ammonia-oxidizers (*amoA*), nitrate reducers (*narG*), and chitin degraders (*chiA*) were determined via quantitative PCR and functional community composition of archaeal ammonia-oxidizers was analyzed via clone libraries (*amoA*) in soil depth profiles along the 120,000 year old Franz Josef chronosequence (New Zealand). The results showed that N functional gene abundances change significantly during long-term soil development. In organic topsoils, *narG* and *chiA* gene abundances increased from young to intermediate-aged soils and then decreased following progressive and retrogressive development of the vegetation. While the proportion of the archaeal *amoA* gene abundance to total cell counts decreased in the oldest phosphorus-limited topsoils, the proportion of *narG* and *chiA* gene abundances remained constant. In subsoils, archaeal *amoA* and *narG* gene abundances also decreased with ecosystem retrogression coinciding with the increasing content of iron and aluminum oxides and other clay-sized minerals. However, *chiA* gene abundances were hardly affected by soil age. The analysis of the archaeal *amoA* community revealed a compositional shift during long-term ecosystem development. Our study provides evidence that the dynamics of N cycling microorganisms in top- and subsoils are significantly affected by long-term ecosystem development and suggests a potential role of the mineral phase in subsoils.

IMPORTANCE

Nitrogen cycling microbial communities are of particular importance for soil ecosystems because of their relevance for soil productivity and plant growth. Recent studies revealed the dynamics of N cycling microbial communities during the early stage of ecosystem and soil development. Soil microorganisms import and provide N into the young soil system as an important macronutrient for biomass production and facilitate the establishment of plant communities. However, the dynamics of N

cycling microbial communities during long-term ecosystem development including the retrogressive phase are poorly understood. Thus, our study extends the ecological understanding of N cycling community dynamics during long-term soil development and analyzes the influence of different soil and mineralogical properties on these dynamics in top- and subsoils. Our results reveal that abundance patterns of N cycling microbial communities not only change during early ecosystem development but also over long-term time period with differences between the different N cycling traits and for top- and subsoils.

INTRODUCTION

In soil ecosystems, microbial communities act as key players of nitrogen (N) cycling by mediating most N transformation processes. During the early stage of pedogenesis, e.g. after glacier retreat, the parental material is colonized by pioneer microorganisms that are responsible for biological weathering and create interfaces for nutrient turnover, e.g. in biofilms (Schulz et al., 2013). At the initial stage of soil development most N derives from N deposition that supports microbial biomass production and facilitate the establishment of plant communities (Brankatschk et al., 2011; Schulz et al., 2013). Biomass, in turn, stimulates N mineralization processes, e.g. the decomposition of soil organic matter (SOM), as reflected by high relative protease and chitinase activities.

With increasing plant coverage, N₂-fixing microorganisms become more and more important in N acquisition as revealed by higher *nifH* gene abundances and N₂-fixation rates (Brankatschk et al., 2011; Nemergut et al., 2007; Schulz et al., 2013). Percentages of genes for nitrate reducers (*narG*) and denitrifiers (*nirK*) in relation to 16S rRNA gene abundances were higher as compared to later stages (Kandeler et al., 2006). The N cycle in the vegetated, more developed soils becomes more complex as reflected by increasing abundances of N₂-fixers (*nifH*), ammonia-oxidizers (*amoA*), and denitrifiers (*nirK* and *nosZ*) as well as increasing N cycle related activities such as N₂-fixation, nitrification and denitrification rates (Brankatschk et al., 2011; Kandeler et al., 2006; Schulz et al., 2013; Töwe et al., 2010). The functional diversity of the soil microbial communities is highest in developed soils and the composition of N functional communities such as N₂-fixing bacteria (*nifH*), archaeal and bacterial ammonia-oxidizers (*amoA*), and denitrifiers (*nosZ*) is significantly affected by soil age (Schulz et al., 2013; Tschierko et al., 2003; Zeng et al., 2016).

To analyze such dynamics of N cycling microorganisms during soil development, a chronosequence approach provides the unique opportunity of investigating at the same time soils of different age but derived from the same parent material under similar climatic conditions (Stevens and Walker, 1970). While abundances and activities of N cycling microorganisms during ecosystem progression development in soils are already well investigated (Brankatschk et al., 2011; Kandeler et al.,

2006; Tscherko et al., 2003; Zeng et al., 2016), the knowledge about the long-term patterns including retrogressive development stages is limited. Retrogression, i.e. the decline in ecosystem productivity and plant biomass, occurs after thousands to millions years of ecosystem development due to a decreasing nutrient availability (Peltzer et al., 2010) and coincides with a decrease in microbial biomass and activities (Allison et al., 2007; Turner et al., 2014; Wardle et al., 2004). Moreover, information is scarce about microbial N cycling in deeper soil horizons and how they develop with ongoing soil age, because most of the previous studies focus on topsoil microbial patterns (Brankatschk et al., 2011; Nemergut et al., 2007; Töwe et al., 2010; Tscherko et al., 2003).

Additionally, soil chronosequences are an excellent tool to identify the soil parameters that may drive N functional abundance and diversity patterns during soil development. Previous studies about N cycling microbial communities during primary succession reported that abundances of protein degraders (*aprA*), chitin degraders (*chiA*), archaeal ammonia oxidizers (*amoA*), nitrate reducers (*narG*) and denitrifiers (*nirK* and *nosZ*) were positively related to the organic carbon (OC) content, N content and pH (only *narG*) (Brankatschk et al., 2011; Kandeler et al., 2006). The N functional community composition was mainly correlated to soil total C and TN content (Zeng et al., 2016). A microcosm incubation experiment with soils of a long-term chronosequence showed that microbial N cycling activities and N functional gene abundances were significantly affected by soil mineralogical properties with the effect varying between different N substrate types, i.e. ON, ammonium or nitrate (Turner et al., 2017a).

With increasing soil age, especially in subsoils, the contents of iron (Fe) and aluminum (Al) (hydr)oxides and other clay-sized minerals increase and might interact with the microbial community, e.g. by constraining substrate availability due to sorption to soil minerals (Dippold et al., 2014; Mikutta et al., 2009; Tarlera et al., 2008; Turner et al., 2014). While nitrate is highly mobile in soils, ammonium could be sorbed to clay surfaces or fixed into clay interlayers and N-containing compounds such as proteins are accumulated in SOM that is stabilized by metal oxides (Knicker, 2011; Nieder et al., 2011; Pronk et al., 2013). The O₂ content could also considerably change with soil depth depending on water saturation and soil texture (Holden and Fierer, 2005; Lüdemann et al., 2000). Oxygen availability and thereby the redox

regime greatly impacts microbial N cycling by acting as a switch between oxic and anoxic N cycling pathways (Pett-Ridge et al., 2006).

Therefore, our main research questions were (i) how do N functional abundances and community composition change during long-term soil development including retrogression in top- vs. subsoils and (ii) which soil properties potentially influence N functional abundances and community composition dynamics? To clarify these questions we determined abundances of functional marker genes for N cycling microorganisms (archaeal and bacterial *amoA*, *narG* and *chiA*) by qPCR and we investigated the N functional community composition by the example of archaeal ammonia oxidizers (AOA) along the 120,000 year old Franz Josef soil chronosequence (New Zealand). In addition, we analyzed the relationship between microbial patterns and soil parameters including chemical and mineralogical soil characteristics. We hypothesize that (i) topsoil abundances of N cycling microorganisms follow patterns of progressive and retrogressive ecosystem development similar to general microbial abundances and vegetation due to changing SOM and nutrient contents, (ii) depending on their substrate type subsoil abundances of N cycling microorganisms might be affected by soil mineralogical properties in accordance with results of laboratory incubation experiments (Turner et al, 2017a), i.e. gene abundances related to ammonium and ON transformation are reduced by an increasing content of clay-sized minerals and Fe and Al oxides with soil age due to constrained substrate availability, and (iii) similar to N functional community composition during early soil development, archaeal *amoA* functional community composition changes during long-term ecosystem development.

RESULTS

Abundances of N functional genes

Abundances of all N functional genes, i.e. archaeal and bacterial *amoA*, *narG*, and *chiA*, decreased with soil depth by up to five orders of magnitude (Fig. 1, Fig. S1). The N functional gene abundances in organic and mineral topsoils (O and A horizon, respectively) were relatively similar with low variation, while abundances in subsoil horizons (E, B, and C horizons) showed a large variability.

Further, almost all N functional gene abundances were significantly affected by the type of soil horizon in top- and subsoils, and additionally by soil depth in subsoils (Table 2). Archaeal *amoA* genes were detected in almost all mineral soil horizons along the Franz Josef chronosequence with highest numbers in mineral topsoils, whereas they were low or even below detection limit in some organic topsoils (5, 60 and 120 kyr; Fig. 1). The archaeal *amoA* gene copy numbers were one to two orders of magnitude lower in older mineral topsoils (60 and 120 kyr) as compared to the young to intermediate-aged ones. Bacterial *amoA* genes were only detected in the youngest soil (0.06 kyr) in the AO and CA horizons (Fig. S1). Gene copy numbers of *narG* and *chiA* were highest in organic topsoils and were significantly affected by soil age (Fig. 1, Table 2). Both abundances were maximal at 5 kyr (and 0.5 kyr for *narG*) in organic topsoils and then decreased with soil age, whereas in mineral topsoils both decreased until 5 kyr, were then one order of magnitude higher at 12 and 60 kyrs, and again decreased being lowest at the 120 kyr site similar to values at the 5 kyr site (Fig. 1). In subsoils, the archaeal *amoA* gene abundance was significantly affected by soil age and decreased in E and B horizons with increasing soil age (Fig. 1, Table 2). Subsoil *narG* gene copy numbers also significantly changed with soil age being lowest at the 120 kyr site, whereas *chiA* gene copy numbers showed only a weak age effect with lower abundances at the 120 kyr site only in E horizons.

Archaeal *amoA* gene copy numbers were positively correlated with archaeal 16S rRNA gene copy numbers ($r = 0.64$, $P < 0.001$). Gene copy numbers of *narG* and *chiA* were highly positively correlated with bacterial rRNA gene copy numbers ($r = 0.97$, $P < 0.001$ and $r = 0.96$, $P < 0.001$, respectively). All N functional gene copy numbers were positively correlated with soil OC, TN, ON and OP content with stronger relationships for *narG* and *chiA* compared to archaeal *amoA* (Table 3). However, archaeal *amoA* gene copy numbers were not correlated to the ammonium content. Similarly, *narG* gene copy numbers were stronger correlated to the ON content than to the content of their substrate nitrate.

Abundances of N functional genes normalized to TCC and TN

Similar to soil mass related archaeal *amoA* gene abundances, the TCC-normalized numbers were one to two orders of magnitude lower in mineral topsoils of the two oldest sites than of the younger sites (Fig. 2). While the TCC-normalized *narG* gene abundances were significantly affected by soil age in topsoils, TCC-normalized *chiA* gene abundances remained almost constant during soil development (Table 2). However, both were highest at the two oldest sites (Fig. 2). Subsoil TCC-normalized archaeal *amoA* abundance decreased with soil age in B horizons, whereas TCC-normalized *narG* and *chiA* gene abundances showed no soil age effect (Table 2).

The subsoil TN-normalized archaeal *amoA* and *narG* gene abundances were significantly affected by soil age showing a decrease with increasing soil age (Table 2, Fig. S2). A PCA of TN-normalized N functional gene abundances with the best-fitting soil properties as supplementary variables revealed that soil mineralogical properties such as the content of Fe oxides and clay-sized minerals were important parameters fitting best the variation gradients of the N functional gene abundances (Fig. 3). Moreover, the archaeal *amoA* gene abundance was negatively related to soil clay content, while *narG* and *chiA* gene abundances were positively related to OC content and negatively related to content of Fe oxides and clay. Spearman correlation coefficients that were calculated for mineral topsoil and subsoils indicated a predominant negative relationship between N functional gene abundances and soil mineralogical properties in subsoils (Table S2). Further, archaeal *amoA* gene abundances were positively correlated to the OP and the sand content, while *narG* gene abundances were positively correlated to the ON and the OC content and negatively to the pH.

Functional community composition of AOA (*amoA*)

The functional community composition of AOA was determined via sequencing of clone libraries of the functional marker gene *amoA* and resulted in five OTUs (threshold distance 0.15). The archaeal *amoA* community composition changed with soil age with a dominance of OTU1 and OTU2 at the two younger sites, OTU1 and OTU4 at the intermediate-aged site (12 kyr), to OTU1 and OTU3 at the

oldest site (Fig. 4). Clustering of the archaeal *amoA* sequences at a threshold distance of 0.05 resulted in 20 OTUs with similar age-related patterns of functional community composition as compared to the threshold distance of 0.15 (Fig. S3). Most archaeal *amoA* OTUs were related to ‘*Candidatus Nitrosotalea devanaterra*’ (OTU1 and OTU3) or the *Nitrosotalea* cluster (OTU2), whereas the OTU4 was affiliated with *Nitrososphaera* subcluster 7.2 (Table S3, Fig. S4). The closest cultivated representatives to OTU4 and OTU5 were ‘*Candidatus Nitrososphaera evergladensis* SR1’ (sequence identity of 79%) and ‘*Nitrosopumilus maritimus* isolate SF_AOA_A07’ (sequence identity of 81%), respectively (Table S3).

DISCUSSION

Abundances of N cycling microorganisms in topsoils along the chronosequence

To elucidate the dynamics of N cycling microorganisms over 120 kyr of soil development, we quantified N functional marker genes (*amoA*, *narG*, and *chiA*) via qPCR (Fig. 1). Overall, archaea rather than bacteria quantitatively dominate the ammonia-oxidizers in soils at the Franz Josef chronosequence (Fig. S1). With decreasing soil pH the AOA may outcompete the AOB at pH < 5.5 (Prosser and Nicol, 2012; Stempfhuber et al., 2015) and therefore bacterial *amoA* genes were only detected at the youngest site with pH ~ 6 (Turner et al., 2014). Generally low archaeal *amoA* gene abundances in organic topsoils along the chronosequence (Fig. 1) may be explained by an inhibition of AOA due to high ammonium concentration derived from high SOM mineralization rates (Norman and Barrett, 2014). Even though there was no significant soil age effect in topsoils (Table 2), the archaeal *amoA* gene abundances in mineral topsoils (A horizon) were lower at the two oldest sites compared to the younger soils, similar to subsoil patterns (see below; Fig. 1).

In contrast to archaeal *amoA*, *narG* and *chiA* gene copy numbers were highest in organic topsoils, thereby increasing towards intermediate-aged soils (progression) and then decreasing during retrogressive ecosystem development (Fig. 1) matching patterns of general microbial abundances, extracellular N hydrolyzing enzyme activities, and vegetation development (Allison et al., 2007; Richardson et al., 2004; Turner et al., 2014, 2017b). The ability for nitrate reduction as first step of

denitrification or dissimilatory nitrate reduction to ammonium (DNRA) is widespread among heterotrophic microorganism, while chitin-degrading bacteria play an important role in the mineralization of ON (Beier and Bertilsson, 2013). Thus, also abundances of nitrate reducers (*narG*) and chitin degraders (*chiA*) seem to be stimulated directly and indirectly by the high SOM input via plant litter at intermediate-aged soils (Richardson et al., 2004). This observation is supported by the strong positive correlations between *narG* and *chiA* gene copy numbers and the soil OC and ON content in complete soil profiles of the Franz Josef chronosequence (Table 3). Similarly, previous studies reported that the OC and ON content are one of the most important soil properties determining N functional gene abundances in topsoils of glacier forelands (Kandeler et al., 2006; Zeng et al., 2016).

The relative gene abundance of archaeal *amoA* normalized to total DNA content was constant during early soil development of a Swiss glacier till 2000 yr (Brankatschk et al., 2011). In contrast, during long-term soil development at the Franz Josef chronosequence the ratio of archaeal *amoA* gene copy numbers to TCC was almost two orders of magnitude lower at the older sites as compared to intermediate-aged soils in mineral topsoils (Fig. 2). Topsoils at the oldest development stage are highly P depleted (OC:TP ratio 922-1402; Turner et al., 2014) causing a high level of chronic nutrient stress. Different studies reported contrasting effects of P content on AOA abundance. Whereas P addition resulted in a decrease or unchanged AOA abundances in grassland soils, their abundance increased in an incubation experiment with fertilized forest soil (Ma et al., 2016; Norman and Barrett, 2014; Zhang et al., 2013). In contrast, in P deficient soils AOA abundances showed no significant changes due to P addition in a pot experiment and also in a microcosm incubation experiment with A horizons of the Franz Josef chronosequence (Chen et al., 2016; Turner et al., 2017a). These results suggest that P is not the decisive factor determining AOA abundance patterns in old topsoils.

Former studies showed that relative abundances of *narG* gene copy numbers normalized to total DNA content decreased during early soil development (Kandeler et al., 2006), whereas relative abundances of *chiA* gene copy numbers remained constant (Brankatschk et al., 2011). Although topsoils become increasingly P depleted during long-term development, the ratios of *narG* and *chiA* gene copy

numbers to TCC were highest at 60 or 120 kyr (Fig. 2). Abundances of *narG* gene seem to be relatively unaffected by P depletion because there is evidence that P addition leads to a decrease or unchanged abundances, even in P limited soils (Ma et al., 2016; Turner et al., 2017a). However, *chiA* gene copy numbers were increased due to P addition in an incubation experiment with A horizon soils of the Franz Josef chronosequence suggesting a potential P limitation of chitin-degrading bacteria (Turner et al., 2017a). High phosphatase activities per microbial biomass in the 120 kyr topsoil of the Franz Josef chronosequence indicated that topsoil microbial communities are adapted to P limitation, thus, could efficiently use the small amounts of available P entering as plant residues or recycled from microbial biomass (Turner et al., 2013, 2014). In addition, topsoil communities might be not energy-limited because there is still a considerable SOM input via plant litter from the aboveground forest (Richardson et al., 2004). Therefore, heterotrophic bacteria, including *narG* and *chiA* functional groups, might be favored compared to AOA in these topsoils despite the extreme P limitation.

Abundances of N cycling microorganisms in subsoils along the chronosequence

In low-substrate and SOM-depleted mineral soil horizons, archaeal *amoA* genes were abundant and widespread throughout the progressive ecosystem development (Fig. 1) demonstrating their adaptation to oligotrophic habitats, e.g. by an energy-efficient CO₂-fixation pathway (Könneke et al., 2014; Norman and Barrett, 2014). Nevertheless, similar to mineral topsoil patterns, subsoil archaeal *amoA* gene copy numbers decreased during ecosystem retrogression. Subsoils, especially B horizons, at older development stages were enriched in Fe and Al oxides and other clay-sized minerals with the latter offering negatively charged surfaces that could bind positively charged ions such as ammonium or fix them into the clay interlayers (Nieder et al., 2011). The incubation experiment analyzing differently-aged soil samples of the Franz Josef chronosequence reported lower archaeal *amoA* gene copy numbers coinciding with higher contents of Fe and Al oxides and clay-sized minerals (Turner et al., 2017a). In line with this explanation, TN-normalized archaeal *amoA* gene abundances in the present study were negatively related to soil clay content (Fig. 3, Table S2) suggesting that soil minerals may constrain

substrate availability for AOA, consequently resulting in a decrease of archaeal *amoA* gene abundances and ratios to TCC during retrogression in subsoils.

In contrast to the results of the incubation experiment where *narG* gene abundances were not significantly affected by soil age (Turner et al., 2017a), in the present study the *narG* gene abundances on soil mass basis and normalized to TN were lower at 60 and 120 kyr in subsoil horizons with an significant effect of soil age (Fig. 1, Fig. S2, Table 2). However, for the incubation experiment soil samples of A horizons were used and apparently showed a different trend than subsoil horizon. While subsoil microbial communities could be energy-limited (Fontaine et al., 2007), a general decrease of SOM in connection with a constrained SOM availability due to mineral interaction (especially in B horizons) may inhibit heterotrophic microorganisms in subsoils, particularly at old development stages at the Franz Josef chronosequence. Thus, while the substrate nitrate most likely is not affected by soil-age related changes in mineralogical characteristics, nitrate reducers as predominantly heterotrophic microorganisms might be inhibited due to the decreased SOM availability. This hypothesis is supported by positive correlations between TN-normalized *narG* abundances and soil OC and ON, whereas TN-normalized *narG* abundances were negatively related to soil mineralogical properties (Fig. 3, Table S2).

Although chitin degraders are also heterotrophs and results of the incubation experiment revealed that *chiA* gene abundances were affected by soil age (Turner et al., 2017a), the soil mass basis and TN-normalized *chiA* gene abundances remained relatively constant during progression and retrogression in subsoils in the present study (Fig. 1, Fig. S2). However, this effect seem to be less pronounced in subsoil horizons (Table 2). In soils, active bacterial chitin-degraders were often affiliated with the *Actinomyces* that are mostly aerobes and produce spores (Beier and Bertilsson, 2013). Hence, *chiA* genes detected in subsoil horizon may be transferred from the overlaying topsoil by the high precipitation (Richardson et al., 2004) and *chiA* gene copy numbers may mainly derive from inactive chitin-degraders or spores formed due to unfavorable conditions. Consequently, these inactive chitin-degraders may be hardly affected by the changing soil properties.

Functional community composition of AOA along the chronosequence

Previous studies revealed that the functional AOA community composition significantly changed during early soil development after glacier retreat or volcanic eruption (Hernández et al., 2014; Zeng et al., 2016). Our results indicated that the functional AOA community composition also changed during long-term soil development corresponding to the compositional shift of total archaeal communities (Fig. 4; Turner et al., 2017b). However, compared to total archaeal communities, the compositional changes in the functional AOA community were less pronounced showing similar communities in young and old soils with most *amoA* sequences being affiliated with the *Nitrosotalea* cluster with ‘*Candidatus Nitrosotalea devanaterre*’ originally isolated from an acidic agricultural soil (Lehtovirta-Morley et al., 2011). The OTU4 that was abundant at the 12 kyr site was affiliated with *Nitrososphaera* subcluster 7.2 (Fig. S4), similar to the dominant subcluster reported for a tropical rain forest soil (Pester et al., 2012).

CONCLUSION

Our study indicated that the abundances of N cycling microorganisms considerably change during long-term ecosystem development. In organic topsoils, *narG* and *chiA* gene abundances, representing mostly heterotrophs, increased during ecosystem progression and declined in retrogression matching patterns of vegetation development, SOM input, and general microbial abundances. The proportion of *narG* and *chiA* gene abundances to TCC even remained constant suggesting an adaptation of topsoil communities to increasing P limitation as reflected by high phosphatase activity. In contrast, archaeal *amoA* gene abundances were decreased in most organic topsoils and the proportion of archaeal *amoA* genes to TCC in mineral topsoils declined during retrogression. In subsoils, pedogenesis-associated changes such as the increasing content of Fe and Al oxides as well as other clay-sized minerals may decrease archaeal *amoA* gene abundances at the retrogressive stage probably by constraining the substrate availability. Similarly, *narG* abundances decreased in the oldest subsoils because most nitrate reducers do not only require nitrate but also organic compounds that also might be sequestered by soil minerals. However, *chiA* gene abundances were hardly affected by soil age in subsoils. In accordance with patterns

of short-term development, the functional community composition of AOA slightly changed during long-term ecosystem development.

In summary, our results revealed that the abundance of each N functional gene was differently affected in top- and subsoils by long-term soil development that is not only linked to changes in C and nutrients contents, but also to a mineralogical gradient. Thus, to gain a better understanding of the dynamics of N cycling microorganisms, further N functional genes should be investigated in soil profiles at different long-term chronosequences.

MATERIAL AND METHODS

Site description and soil sampling

The Franz Josef chronosequence (~43° S, 170° E) is located on the West Coast of the South Island of New Zealand and is characterized by humid temperate climate with high mean annual precipitation of 3500 – 6500 mm (Richardson et al., 2004). Soil development started from greywacke and mica schist with the retreat of the Franz Josef glacier and the chronosequences comprises soils covering a time scale of 120,000 years (120 kyr) until present (Almond et al., 2001; Stevens, 1968). Seven sites with soil ages ranging from 0.06 to 120 kyr were sampled in January 2012 and at each site three soil profiles (replicates) up to one meter depth were excavated and each genetic horizon was sampled. Soil depth profiles contain organic topsoils (O horizon), mineral topsoils (A horizon), and subsoils with eluvial horizons (E horizon), mineral subsoils (B horizon) and parent material (C horizon); the respective horizons per site are listed in Table S1. Details on site characteristics and soil properties are given in Table S1 based on (Turner et al., 2014). For molecular analyses, soil samples were frozen and stored at -20°C until analysis.

Soil pH ranges from 3.8 to 6.4 with highest values in the youngest soil (0.06 kyr) and increasing values with soil depth (Table S1). The soils are characterized by a C, nutrient and mineralogical gradient with highest soil OC and ON contents at the intermediate-aged sites and a sharp decline in total P (TP) content with ongoing soil development (Table S1; Richardson et al., 2004). The soil mineral composition

is characterized by an increasing content of clay-sized minerals, changes in the clay mineral assemblage, and a shift from a large portion of pedogenic Fe and Al residing in metal-humus complexes (pyrophosphate-extractable Fe and Al; Fe_p, Al_p) at the younger sites, to more poorly crystalline Fe and Al phases (oxalate-extractable Fe and Al; Fe_o, Al_o) at intermediate-aged sites and into a dominance of crystalline Fe and clay-sized minerals (dithionite-citrate-extractable Fe minus oxalate-extractable Fe; Fe_d, Al_d) at the oldest site (Table S1; Dietel et al., 2016). The soils are covered by rainforest that is dominated by evergreen angiosperms and the vegetation shows progressive and retrogressive development phases (Richardson et al., 2004). The total cell counts (TCC) were determined by SYBR Green I staining of formaldehyde-fixed soil samples and ranged from 5.5×10^7 to 1.2×10^{11} cells per gram of soil and were highest at intermediate-aged soils in organic topsoils (Table S1).

Nucleic acid extraction and quantification of functional marker genes

Nucleic acids of soil samples were extracted in triplicate according to the manufacturer's protocol (FastDNA® Spin Kit for Soil, MP Biomedicals, Santa Ana, CA, US) with some modifications (Webster et al., 2003).

To characterize the abundance of different N cycling microorganisms using different substrates (ammonium, nitrate, and ON), we quantified marker genes for ammonia oxidation as the first step of nitrification (archaeal and bacterial *amoA*), for nitrate reduction (*narG*), and for bacterial chitin degradation (*chiA*), with chitin representing a complex ON compound common in soils, via qPCR as described previously (Turner et al., 2017a). Briefly, qPCR was performed by using a StepOnePlus™ Real-Time PCR System (Applied Biosystems, Life Technologies, Carlsbad, CA, US) and SYBR® Green I chemistry (Table 1). For the archaeal *amoA* and *chiA* assays we used FastStart Universal SYBR Green Master (ROX) (Roche, Rotkreuz, Switzerland), for bacterial *amoA* assay we used Platinum SYBR Green qPCR SuperMix-UDG with ROX (Life Technologies, Carlsbad, CA, US), and for *narG* assay we used ABsolute QPCR SYBR Green ROX Mix (Thermo Scientific, Waltham, MA, US). Product specificity was confirmed by melt curve analysis and the amplicon size was verified by agarose gel electrophoresis.

Template DNA was used in three dilutions (1:10, 1:100, and 1:1000) to reduce the effect of co-extracted PCR inhibitors. Standards were made from purified PCR products obtained from either environmental DNA of soil samples (archaeal *amoA*), an environmental bacterial ammonia oxidizer clone (bacterial *amoA*), or genomic DNA of pure cultures (*narG*, *chiA*). For the calibration curve, standard DNA was used in seven dilutions ranging from 1 to 10^7 gene copies μL^{-1} . Standard DNA, template DNA, and non-template control were run in three replicates. Abundances were reported in gene copy numbers per gram dry weight (dw) of soil.

Clone libraries of archaeal ammonia oxidizers

Archaeal *amoA* genes of selected samples were amplified according to the qPCR protocol in triplicate (Table 1) to analyze the functional diversity of archaeal ammonia oxidizers. The PCR was carried out in a 25- μL reaction volume containing DreamTaq PCR Master Mix (2 \times) (Life Technologies, Thermo Scientific, Carlsbad, MA, US) without SYBR® Green I. The PCR products were pooled and cleaned up with the QIAquick PCR Purification Kit (QIAGEN, Hilden, Germany). Purified PCR products were cloned and 96 clones per sample were sequenced by Microsynth AG (Balgach, Switzerland).

Contigs were constructed from overlapping forward and reverse sequences in Geneious 8.1.5 (Biomatters Ltd, Auckland, New Zealand) resulting in 808 sequences and processed with mothur 1.35.1 (Schloss et al., 2009). Sequences with ≥ 1 ambiguity, < 600 bp or > 635 bp sequence length, or ≥ 1 mismatch to primer sequence were removed. The remaining sequences were imported in Geneious, *in silico* translated amino acid sequences containing stoppcodons were removed, and remaining nucleotide sequences were aligned using ClustalW with default settings. For archaeal *amoA* sequences a species threshold of 85% sequence identity was recommended (Pester et al., 2012). Therefore, aligned sequences were clustered to operational taxonomic units (OTUs) at 85% sequence identity using mothur. Phylogenetic tree construction was done in MEGA 6.06 (Tamura et al., 2013) using one representative sequence per OTU. For comparison, archaeal *amoA* OTUs were also clustered at 95% sequence identity threshold.

Data analysis and statistics

While N functional gene abundances on soil mass basis represented abundances at ecosystem scale, we normalized N functional gene abundances to TCC to examine the proportion of N functional genes to total prokaryotic abundances during long-term soil development. Thus, the TCC-normalized N functional gene abundances reflect the proportion of N functional groups to the total microbial community. Correlation analysis (see above) revealed that soil TN content was the main driver of N functional gene abundances. Therefore, we normalized N functional gene abundances to soil TN content to elucidate the effect of soil properties other than TN content. Soil properties, TCC, and archaeal and bacterial 16S rRNA gene abundances have been determined on the same soil samples of the Franz Josef chronosequence (Turner et al., 2014, 2017b) and were used for statistical analyses.

The effects of soil age, horizon, age \times horizon interaction and depth within horizon on the log-transformed N functional gene abundances were analyzed as fixed effects in a linear mixed effects model using the 'lmer' function of the 'lme4' package (Bates et al., 2015) in R (version 3.2.3; R Core Team). The variance between the three individual soil profiles per site was included as random effect to account for repeated measures within the same site. The inspection of initial model residuals revealed that variances differed between topsoil (O, A) and subsoil (E, B, C) horizon clusters despite log-transformation. Thus, separate models were fitted to topsoil and subsoil subsets. The main effects and interaction were tested in ANOVA following the model fit, all pairwise comparisons (Tukey-Test) of soil age groups within horizon clusters were performed based on least square means, after centering depth at each age \times horizon clusters' mean depth (package 'lsmeans', Lenth, 2015). To examine the relationship between soil properties, archaeal and bacterial 16S rRNA gene abundances, and N functional gene abundances, we calculated Spearman rank order correlation coefficients with R.

To investigate the patterns of TN-normalized N functional gene abundances in mineral soils along the Franz Josef chronosequence we used a principal component analysis (PCA) on log-transformed and centered data in Canoco 5 (version 5.02; ter Braak and Šmilauer, 2012). The six best-fitting soil

properties were used as supplementary variables to illustrate their relationship to the N functional gene abundances.

Accession number(s)

The OTU sequences of archaeal *amoA* clone libraries were deposited in Genbank under accession numbers KY315819 to KY315823.

ACKNOWLEDGMENTS

This research was funded by the German Science Foundation (DFG), grants MI 1377/5-2 and SCHI 535/11-2 to R.M. and A.S., respectively. We greatly acknowledge Norman Gentsch, Andre Eger, and Leo M. Condrón for the help with preparation and realization of the sampling, Peter C. Almond, Duane A. Peltzer and Sarah J. Richardson for access to the sampling sites, Cornelia Struckmeyer for laboratory support, and Christian Siebenbürgen for help with graphical issues. The AOB standard for qPCR was kindly provided by the ‘Aquatic Geomicrobiology’ Group, University of Jena, Germany, and the *chiA* qPCR standard was kindly provided by the ‘Environmental Microbiology’ Group, TU Bergakademie Freiberg, Germany.

We declare no conflict of interest.

REFERENCES

- Allison, V. J., Condrón, L. M., Peltzer, D. A., Richardson, S. J., and Turner, B. L. (2007). Changes in enzyme activities and soil microbial community composition along carbon and nutrient gradients at the Franz Josef chronosequence, New Zealand. *Soil Biol. Biochem.* 39, 1770–1781. doi:10.1016/j.soilbio.2007.02.006.
- Almond, P. C., Moar, N. T., and Lian, O. B. (2001). Reinterpretation of the glacial chronology of South Westland, New Zealand. *New Zeal. J. Geol. Geophys.* 44, 1–15. doi:10.1080/00288306.2001.9514917.

- Bates, D., Mächler, M., Bolker, B., and Walker, S. C. (2015). Fitting linear mixed-effects models using lme4. *J. Stat. Softw.* 67, 1–48.
- Beier, S., and Bertilsson, S. (2013). Bacterial chitin degradation – mechanisms and ecophysiological strategies. *Front. Microbiol.* 4, 149. doi:10.3389/fmicb.2013.00149.
- Brankatschk, R., Töwe, S., Kleineidam, K., Schloter, M., and Zeyer, J. (2011). Abundances and potential activities of nitrogen cycling microbial communities along a chronosequence of a glacier forefield. *ISME J.* 5, 1025–1037. doi:10.1038/ismej.2010.184.
- Bru, D., Sarr, A., and Philippot, L. (2007). Relative abundances of proteobacterial membrane-bound and periplasmic nitrate reductases in selected environments. *Appl. Environ. Microbiol.* 73, 5971–5974. doi:10.1128/AEM.00643-07.
- Chen, Y., Sun, T.-T., Qian, H.-Y., Fan, J.-B., He, Y.-Q., and Sun, B. (2016). Nitrogen mineralization as a result of phosphorus supplementation in long-term phosphate deficient soil. *Appl. Soil Ecol.* 106, 24–32. doi:10.1016/j.apsoil.2016.04.019.
- Di, H. J., Cameron, K. C., Shen, J.-P., Winefield, C. S., O’Callaghan, M., Bowatte, S., et al. (2010). Ammonia-oxidizing bacteria and archaea grow under contrasting soil nitrogen conditions. *FEMS Microbiol. Ecol.* 72, 386–394. doi:10.1111/j.1574-6941.2010.00861.x.
- Dietel, J., Dohrmann, R., Guggenberger, G., Meyer-Stüve, S., Turner, S., Schippers, A., et al. (2016). Complexity of clay mineral formation during 120,000 years of soil development along the Franz Josef chronosequence, New Zealand. *New Zeal. J. Geol. Geophys.* 0, 1–13. doi:10.1080/00288306.2016.1245668.

- Dippold, M., Biryukov, M., and Kuzyakov, Y. (2014). Sorption affects amino acid pathways in soil: Implications from position-specific labeling of alanine. *Soil Biol. Biochem.* 72, 180–192. doi:10.1016/j.soilbio.2014.01.015.
- Fontaine, S., Barot, S., Barré, P., Bdioui, N., Mary, B., and Rumpel, C. (2007). Stability of organic carbon in deep soil layers controlled by fresh carbon supply. *Nature* 450, 277–280. doi:10.1038/nature06275.
- Francis, C. A., Roberts, K. J., Beman, J. M., Santoro, A. E., and Oakley, B. B. (2005). Ubiquity and diversity of ammonia-oxidizing archaea in water columns and sediments of the ocean. *Proc. Natl. Acad. Sci. U. S. A.* 102, 14683–14688. doi:10.1073/pnas.0506625102.
- Gubry-Rangin, C., Hai, B., Quince, C., Engel, M., Thomson, B. C., James, P., et al. (2011). Niche specialization of terrestrial archaeal ammonia oxidizers. *Proc. Natl. Acad. Sci. U. S. A.* 108, 21206–21211. doi:10.1073/pnas.1109000108.
- Hernández, M., Dumont, M. G., Calabi, M., Basualto, D., and Conrad, R. (2014). Ammonia oxidizers are pioneer microorganisms in the colonization of new acidic volcanic soils from South of Chile. *Environ. Microbiol. Rep.* 6, 70–79. doi:10.1111/1758-2229.12109.
- Holden, P. A., and Fierer, N. (2005). Microbial processes in the vadose zone. *Vadose Zo. J.* 4, 1–21. doi:10.2136/vzj2005.0001.
- Kaiser, K. (2001). Dissolved organic phosphorus and sulphur as influenced by sorptive interactions with mineral subsoil horizons. *Eur. J. Soil Sci.* 52, 489–493. doi:10.1046/j.1365-2389.2001.00396.x.
- Kandeler, E., Deiglmayr, K., Tschirko, D., Bru, D., and Philippot, L. (2006). Abundance of *narG*, *nirS*, *nirK*, and *nosZ* genes of denitrifying bacteria during primary successions of a glacier foreland. *Appl. Environ. Microbiol.* 72, 5957–5962. doi:10.1128/AEM.00439-06.

- Knicker, H. (2011). Soil organic N - An under-rated player for C sequestration in soils? *Soil Biol. Biochem.* 43, 1118–1129. doi:10.1016/j.soilbio.2011.02.020.
- Könneke, M., Schubert, D. M., Brown, P. C., Hügler, M., Standfest, S., Schwander, T., et al. (2014). Ammonia-oxidizing archaea use the most energy-efficient aerobic pathway for CO₂ fixation. *Proc. Natl. Acad. Sci. U. S. A.* 111, 8239–8244. doi:10.1073/pnas.1402028111.
- Lehtovirta-Morley, L. E., Stoecker, K., Vilcinskas, A., Prosser, J. I., and Nicol, G. W. (2011). Cultivation of an obligate acidophilic ammonia oxidizer from a nitrifying acid soil. *Proc. Natl. Acad. Sci. U. S. A.* 108, 15892–15897. doi:10.1073/pnas.1107196108.
- Leininger, S., Urich, T., Schloter, M., Schwark, L., Qi, J., Nicol, G. W., et al. (2006). Archaea predominate among ammonia-oxidizing prokaryotes in soils. *Nature* 442, 806–809. doi:10.1038/nature04983.
- Lenth, R. (2015). lsmeans: least-squares means. <https://CRAN.R-project.org/package=lsmeans>.
- Lüdemann, H., Arth, I., and Liesack, W. (2000). Spatial changes in the bacterial community structure along a vertical oxygen gradient in flooded paddy soil cores. *Appl. Environ. Microbiol.* 66, 754–762. doi:0099-2240/00.
- Ma, W., Jiang, S., Assemien, F., Qin, M., Ma, B., Xie, Z., et al. (2016). Response of microbial functional groups involved in soil N cycle to N, P and NP fertilization in Tibetan alpine meadows. *Soil Biol. Biochem.* 101, 195–206. doi:10.1016/j.soilbio.2016.07.023.
- Mikutta, R., Schaumann, G. E., Gildemeister, D., Bonneville, S., Kramer, M. G., Chorover, J., et al. (2009). Biogeochemistry of mineral-organic associations across a long-term mineralogical soil gradient (0.3-4100 kyr), Hawaiian Islands. *Geochim. Cosmochim. Acta* 73, 2034–2060. doi:10.1016/j.gca.2008.12.028.

-
- Mikutta, R., Zang, U., Chorover, J., Haumaier, L., and Kalbitz, K. (2011). Stabilization of extracellular polymeric substances (*Bacillus subtilis*) by adsorption to and coprecipitation with Al forms. *Geochim. Cosmochim. Acta* 75, 3135–3154. doi:10.1016/j.gca.2011.03.006.
- Nemergut, D. R., Anderson, S. P., Cleveland, C. C., Martin, A. P., Miller, A. E., Seimon, A., et al. (2007). Microbial community succession in an unvegetated, recently deglaciated soil. *Microb. Ecol.* 53, 110–122. doi:10.1007/s00248-006-9144-7.
- Nicolaisen, M. H., Risgaard-Petersen, N., Revsbech, N. P., Reichardt, W., and Ramsing, N. B. (2004). Nitrification-denitrification dynamics and community structure of ammonia oxidizing bacteria in a high yield irrigated Philippine rice field. *FEMS Microbiol. Ecol.* 49, 359–369. doi:10.1016/j.femsec.2004.04.015.
- Nieder, R., Benbi, D. K., and Scherer, H. W. (2011). Fixation and defixation of ammonium in soils: A review. *Biol. Fertil. Soils* 47, 1–14. doi:10.1007/s00374-010-0506-4.
- Norman, J. S., and Barrett, J. E. (2014). Substrate and nutrient limitation of ammonia-oxidizing bacteria and archaea in temperate forest soil. *Soil Biol. Biochem.* 69, 141–146. doi:10.1016/j.soilbio.2013.11.003.
- Peltzer, D. A., Wardle, D. A., Allison, V. J., Baisden, W. T., Bardgett, R. D., Chadwick, O. A., et al. (2010). Understanding ecosystem retrogression. *Ecol. Monogr.* 80, 509–529. doi:10.1890/09-1552.1.
- Pester, M., Rattei, T., Flechl, S., Gröngroft, A., Richter, A., Overmann, J., et al. (2012). *amoA*-based consensus phylogeny of ammonia-oxidizing archaea and deep sequencing of *amoA* genes from soils of four different geographic regions. *Environ. Microbiol.* 14, 525–539. doi:10.1111/j.1462-2920.2011.02666.x.

- Pett-Ridge, J., Silver, W. L., and Firestone, M. K. (2006). Redox fluctuations frame microbial community impacts on N-cycling rates in a humid tropical forest soil. *Biogeochemistry* 81, 95–110. doi:10.1007/s10533-006-9032-8.
- Pronk, G. J., Heister, K., and Kögel-Knabner, I. (2013). Is turnover and development of organic matter controlled by mineral composition? *Soil Biol. Biochem.* 67, 235–244. doi:10.1016/j.soilbio.2013.09.006.
- Prosser, J. I., and Nicol, G. W. (2012). Archaeal and bacterial ammonia-oxidisers in soil: the quest for niche specialisation and differentiation. *Trends Microbiol.* 20, 523–531. doi:10.1016/j.tim.2012.08.001.
- R Core Team (2015). R: A language and environment for statistical computing. R Foundation for Statistical Computing, Vienna, Austria.
- Richardson, S. J., Peltzer, D. A., Allen, R. B., McGlone, M. S., and Parfitt, R. L. (2004). Rapid development of phosphorus limitation in temperate rainforest along the Franz Josef soil chronosequence. *Oecologia* 139, 267–276. doi:10.1007/s00442-004-1501-y.
- Schloss, P. D., Westcott, S. L., Ryabin, T., Hall, J. R., Hartmann, M., Hollister, E. B., et al. (2009). Introducing mothur: Open-source, platform-independent, community-supported software for describing and comparing microbial communities. *Appl. Environ. Microbiol.* 75, 7537–7541. doi:10.1128/AEM.01541-09.
- Schulz, S., Brankatschk, R., Dümig, A., Kögel-Knabner, I., Schloter, M., and Zeyer, J. (2013). The role of microorganisms at different stages of ecosystem development for soil formation. *Biogeosciences* 10, 3983–3996. doi:10.5194/bg-10-3983-2013.

- Stempfhuber, B., Engel, M., Fischer, D., Neskovic-Prit, G., Wubet, T., Schöning, I., et al. (2015). pH as a driver for ammonia-oxidizing archaea in forest soils. *Microb. Ecol.* 69, 879–883. doi:10.1007/s00248-014-0548-5.
- Stevens, P. R. (1968). A chronosequence of soils near the Franz Josef glacier. *Ph.D thesis Univ. Canterbury, New Zeal.*
- Stevens, P., and Walker, T. (1970). The chronosequence concept and soil formation. *Quarterly Rev. Biol.* 45, 333–350.
- Swenson, T. L., Bowen, B. P., Nico, P. S., and Northen, T. R. (2015). Competitive sorption of microbial metabolites on an iron oxide mineral. *Soil Biol. Biochem.* 90, 34–41. doi:10.1016/j.soilbio.2015.07.022.
- Tamura, K., Stecher, G., Peterson, D., Filipski, A., and Kumar, S. (2013). MEGA6: Molecular Evolutionary Genetics Analysis version 6.0. *Mol. Biol. Evol.* 30, 2725–2729. doi:10.1093/molbev/mst197.
- Tarlera, S., Jangid, K., Ivester, A. H., Whitman, W. B., and Williams, M. A. (2008). Microbial community succession and bacterial diversity in soils during 77 000 years of ecosystem development. *FEMS Microbiol. Ecol.* 64, 129–140. doi:10.1111/j.1574-6941.2008.00444.x.
- ter Braak C.J.F. and Šmilauer P. (2012). *Canoco reference manual and user's guide: software for ordination, version 5.0.* Ithaca: Microcomputer Power.
- Töwe, S., Albert, A., Kleineidam, K., Brankatschk, R., Dümig, A., Welzl, G., et al. (2010). Abundance of microbes involved in nitrogen transformation in the rhizosphere of *Leucanthemopsis alpina* (L.) HEYWOOD grown in soils from different sites of the Damma glacier forefield. *Microb. Ecol.* 60, 762–770. doi:10.1007/s00248-010-9695-5.

- Tscherko, D., Rustemeier, J., Richter, A., Wanek, W., and Kandeler, E. (2003). Functional diversity of the soil microflora in primary succession across two glacier forelands in the Central Alps. *Eur. J. Soil Sci.* 54, 685–696. doi:10.1046/j.1365-2389.2003.00570.x.
- Turner, B. L., Lambers, H., Condrón, L. M., Cramer, M. D., Leake, J. R., Richardson, A. E., et al. (2013). Soil microbial biomass and the fate of phosphorus during long-term ecosystem development. *Plant Soil* 367, 225–234. doi:10.1007/s11104-012-1493-z.
- Turner, S., Meyer-Stüve, S., Schippers, A., Guggenberger, G., Schaarschmidt, F., Wild, B., et al. (2017a). Microbial utilization of mineral-associated nitrogen in soils. *Soil Biol. Biochem.* 104, 185–196. doi:10.1016/j.soilbio.2016.10.010.
- Turner, S., Mikutta, R., Meyer-Stüve, S., Guggenberger, G., Schaarschmidt, F., Lazar, C. S., et al. (2017b). Microbial community dynamics in soil depth profiles over 120,000 years of ecosystem development. *Front. Microbiol.* 8, 874. doi: 10.3389/fmicb.2017.00874.
- Turner, S., Schippers, A., Meyer-Stüve, S., Guggenberger, G., Gentsch, N., Dohrmann, R., et al. (2014). Mineralogical impact on long-term patterns of soil nitrogen and phosphorus enzyme activities. *Soil Biol. Biochem.* 68, 31–43. doi:10.1016/j.soilbio.2013.09.016.
- Valentine, D. L. (2007). Adaptations to energy stress dictate the ecology and evolution of the Archaea. *Nat. Rev. Microbiol.* 5, 316–323. doi:10.1038/nrmicro1619.
- Wardle, D. A., Walker, L. R., and Bardgett, R. D. (2004). Ecosystem properties and forest decline in contrasting long-term chronosequences. *Science* 305, 509–513. doi:10.1126/science.1098778.
- Webster, G., Newberry, C. J., Fry, J. C., and Weightman, A. J. (2003). Assessment of bacterial community structure in the deep sub-seafloor biosphere by 16S rDNA-based techniques: A cautionary tale. *J. Microbiol. Methods* 55, 155–164. doi:10.1016/S0167-7012(03)00140-4.

Yergeau, E., Kang, S., He, Z., Zhou, J., and Kowalchuk, G. A. (2007). Functional microarray analysis of nitrogen and carbon cycling genes across an Antarctic latitudinal transect. *ISME J.* 1, 163–179. doi:10.1038/ismej.2007.24.

Zeng, J., Lou, K., Zhang, C.-J., Wang, J.-T., Hu, H.-W., Shen, J.-P., et al. (2016). Primary succession of nitrogen cycling microbial communities along the deglaciated forelands of Tianshan Mountain, China. *Front. Microbiol.* 7, 1353. doi:10.3389/fmicb.2016.01353.

Zhang, J., Wang, J., Zhong, W., and Cai, Z. (2015). Organic nitrogen stimulates the heterotrophic nitrification rate in an acidic forest soil. *Soil Biol. Biochem.* 80, 293–295. doi:10.1016/j.soilbio.2014.10.024.

Zhang, X., Liu, W., Schloter, M., Zhang, G., Chen, Q., Huang, J., et al. (2013). Response of the abundance of key soil microbial nitrogen-cycling genes to multi-factorial global changes. *PLoS One* 8, e76500. doi:10.1371/journal.pone.0076500.

FIGURES

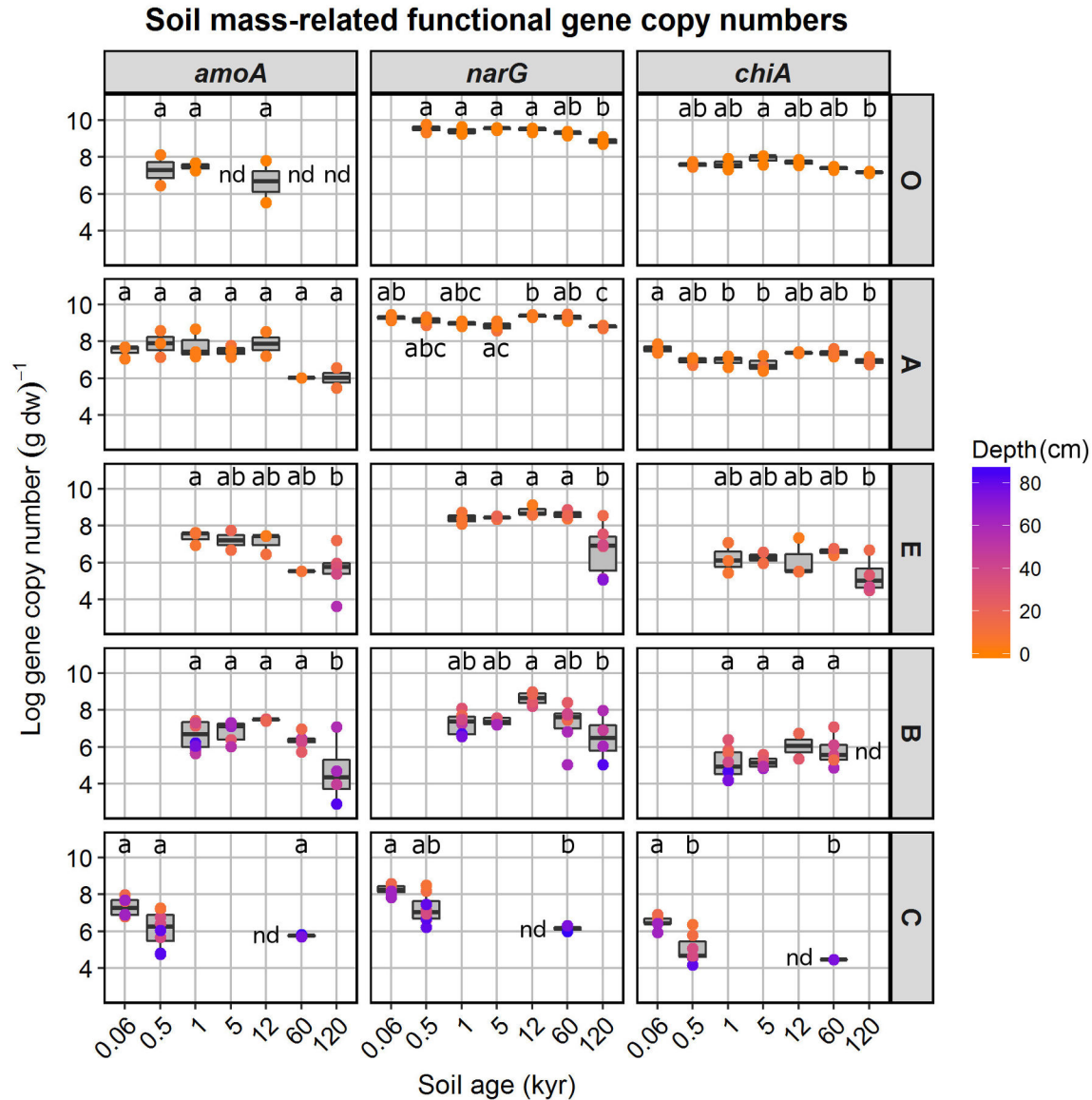


FIG 1 Abundances of N functional genes on soil mass basis for each soil horizon cluster (O, A, E, B, and C) in soils of different ages along the Franz Josef chronosequence. Functional gene copy numbers of archaeal *amoA*, *narG*, and *chiA* per gram soil dry weight (dw) were shown as boxplots with points for horizon and soil profile replicates. The color of the points indicates soil depth (cm). Results of Tukey post-hoc test for the soil age effect in each soil horizon cluster were indicated by letters with the same letters indicating that values for these ages differed not significantly ($P > 0.05$). Samples with gene copy numbers below detection limit were indicated by “nd” (not detected).

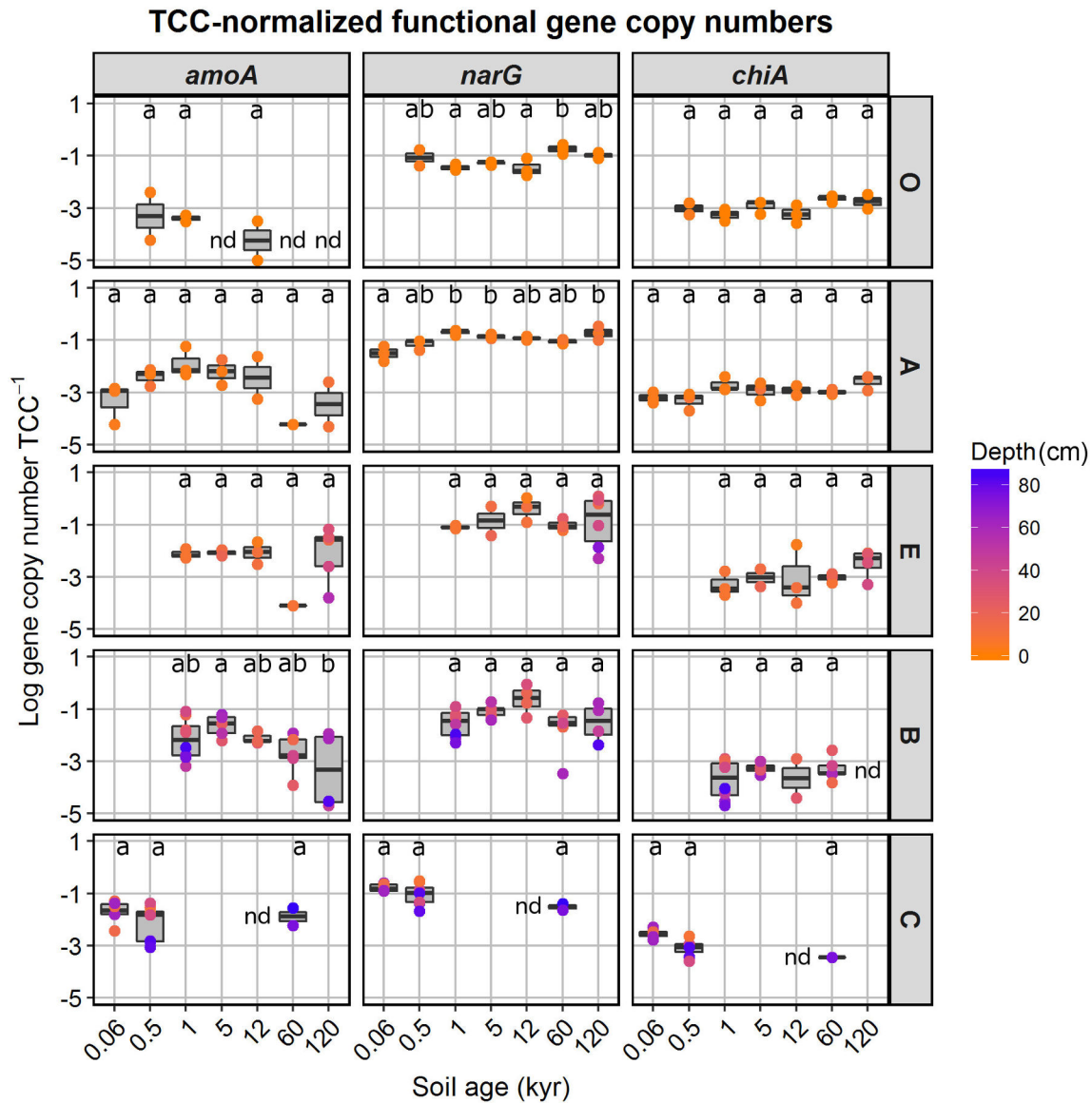


FIG 2 Abundances of N functional genes normalized to total cell counts (TCC) for each soil horizon cluster (O, A, E, B, and C) in soils of different ages along the Franz Josef chronosequence. Functional gene copy numbers of archaeal *amoA*, *narG*, and *chiA* were shown as boxplots with points for horizon and soil profile replicates. The color of the points indicates soil depth (cm). Results of Tukey post-hoc test for the soil age effect in each soil horizon cluster were indicated by letters with the same letters indicating that values for these ages differed not significantly ($P > 0.05$). Samples with gene copy numbers below detection limit were indicated by “nd” (not detected).

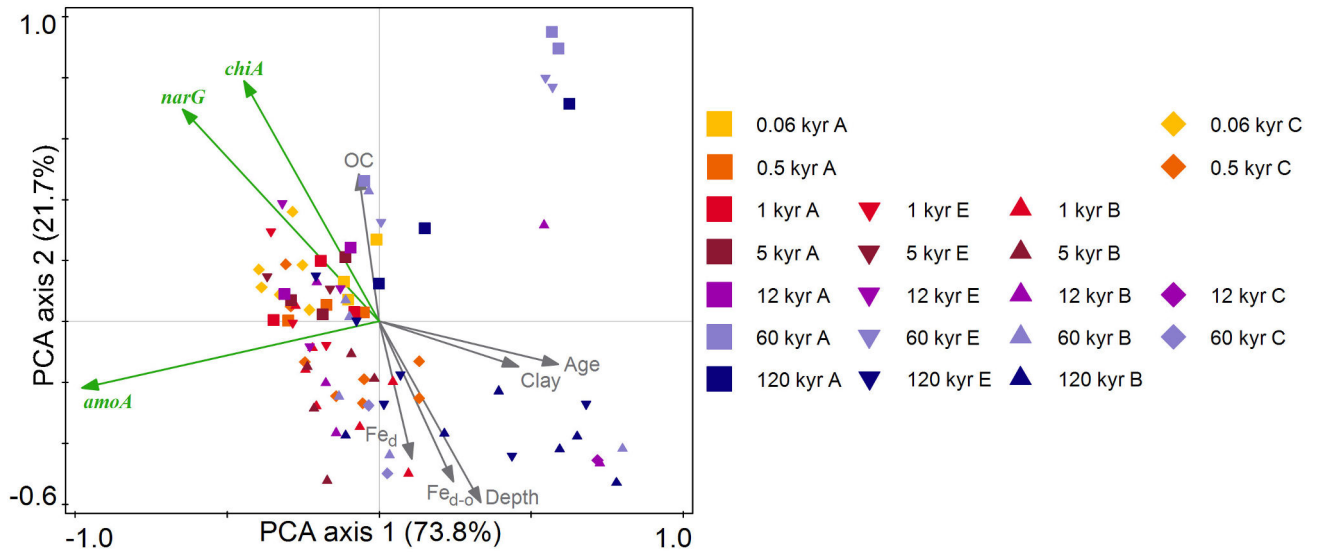


FIG 3 Principal component analysis (PCA) based on TN-normalized functional gene abundances (green arrows) of mineral soil horizons with the six best-fitting soil properties as supplementary variables (grey arrows). Colors of samples indicate different soil ages and symbols indicate different soil horizons. Fe_d – dithionite-extractable Fe phases representing poorly crystalline and crystalline Fe oxides as well as Fe-humus-complexes, Fe_{d-o} – difference between dithionite-extractable Fe and oxalate-extractable Fe representing crystalline Fe phases.

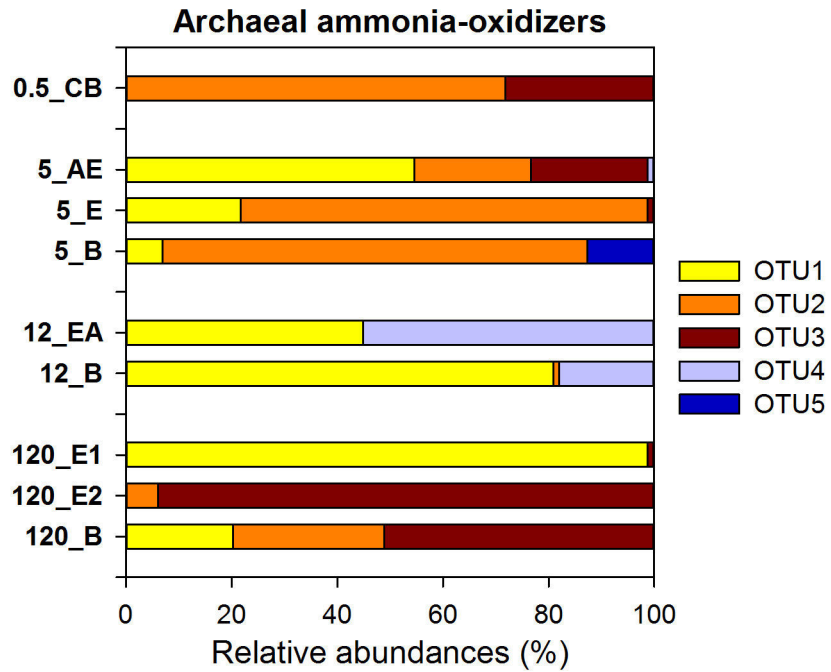


FIG 4 Relative abundances of archaeal *amoA* OTUs (sequence identity threshold 85%) of selected soil samples along the Franz Josef chronosequence. The y-axis denotes the soil age (0.5, 5, 12, and 120 kyr) and soil horizon (AE, E, EA, B, and CB).

TABLES

TABLE 1 Primers and conditions for qPCR assays.

Primer	Primer sequences (5'-3')	Pc ¹ (μ M)	Standard	Eff ²	Reference
Archaeal <i>amoA</i> gene					
Arch-amoAF	STA ATG GTC TGG CTT AGA CG	0.4	AOA-NZ-Mix	88.1-	Francis et al., 2005
Arch-amoAR	GCG GCC ATC CAT CTG TAT GT			93.0	
Bacterial <i>amoA</i> gene					
amoA-1F	GGG GTT TCT ACT GGT GGT	0.4	<i>Nitrosomonas</i> <i>multiformis</i> clone	80.1-	Nicolaisen et al., 2004
amoA-2R	CCC CTC KGS AAA GCC TTC TTC			86.3	
<i>narG</i> gene					
narG-F	TCG CCS ATY CCG GCS ATG TC	1	<i>Pseudomonas</i> <i>stutzeri</i> (DSM 4166)	82.1-	Bru et al., 2007
narG-R	GAG TTG TAC CAG TCR GCS GAY TCS G			84.8	
Bacterial <i>chiA</i> gene					
GA1F	CGT CGA CAT CGA CTG GGA RTD BCC	1	<i>Streptomyces</i> <i>fradiae</i> (DSM 41757)	92.7-	Yergeau et al., 2007
GA1R	ACG CCG GTC CAG CCN CKN CCR TA			96.0	

¹ Primer concentration,² Efficiency.**TABLE 2** Results of the two-way ANOVA (soil age \times horizon, their interaction and depth as a covariate) on N functional gene abundances (on soil mass basis, normalized to TCC, and normalized to soil TN content) in topsoils (O and A horizon) and subsoils (E, B, and C horizon) along the Franz Josef chronosequence determined by qPCR. Significant interactions are indicated by asterisks.

	Topsoil				Subsoil			
	Age	Hor.	Depth	Age \times Hor.	Age	Hor.	Depth	Age \times Hor.
Archaeal <i>amoA</i> (g dw) ⁻¹	n.s.	*	n.s.	n.s.	***	n.s.	***	n.s.
Archaeal <i>amoA</i> TCC ⁻¹	n.s.	**	n.s.	n.s.	*	*	*	*
Archaeal <i>amoA</i> (mg TN) ⁻¹	n.s.	**	n.s.	n.s.	***	n.s.	***	n.s.
<i>narG</i> (g dw) ⁻¹	**	***	n.s.	**	***	***	***	n.s.
<i>narG</i> TCC ⁻¹	**	**	n.s.	**	n.s.	**	***	n.s.
<i>narG</i> (mg TN) ⁻¹	**	*	n.s.	*	***	***	***	n.s.
<i>chiA</i> (g dw) ⁻¹	*	***	n.s.	***	**	***	***	n.s.
<i>chiA</i> TCC ⁻¹	n.s.	n.s.	n.s.	n.s.	n.s.	*	**	n.s.
<i>chiA</i> (mg TN) ⁻¹	n.s.	**	n.s.	**	**	***	***	n.s.

n.s. – not significant.

* P < 0.05; ** P < 0.01; *** P < 0.001.

TABLE 3 Spearman rank order correlation coefficients for N functional gene abundances (per gram dry soil) and chemical soil properties. Content of OC – organic carbon, TN – total nitrogen, ON – organic nitrogen, TP – total phosphorous, OP – organic phosphorous. Significant correlations are typed in bold (P < 0.01).

	pH	OC	TN	ON	Ammonium	Nitrate	TP	OP
Archaeal <i>amoA</i>	-0.31	0.53	0.56	0.56	0.23	0.15	0.27	0.62
<i>narG</i>	-0.73	0.90	0.90	0.90	0.72	0.39	0.23	0.75
<i>chiA</i>	-0.68	0.87	0.89	0.89	0.83	0.55	0.17	0.70

SUPPLEMENTAL MATERIAL

120,000 Years of Soil Ecosystem Development Results in Distinct Nitrogen Cycling Microbial Communities

Stephanie Turner, Robert Mikutta, Sandra Meyer-Stüve, Georg Guggenberger, Frank Schaarschmidt, Reiner Dohrmann, Axel Schippers

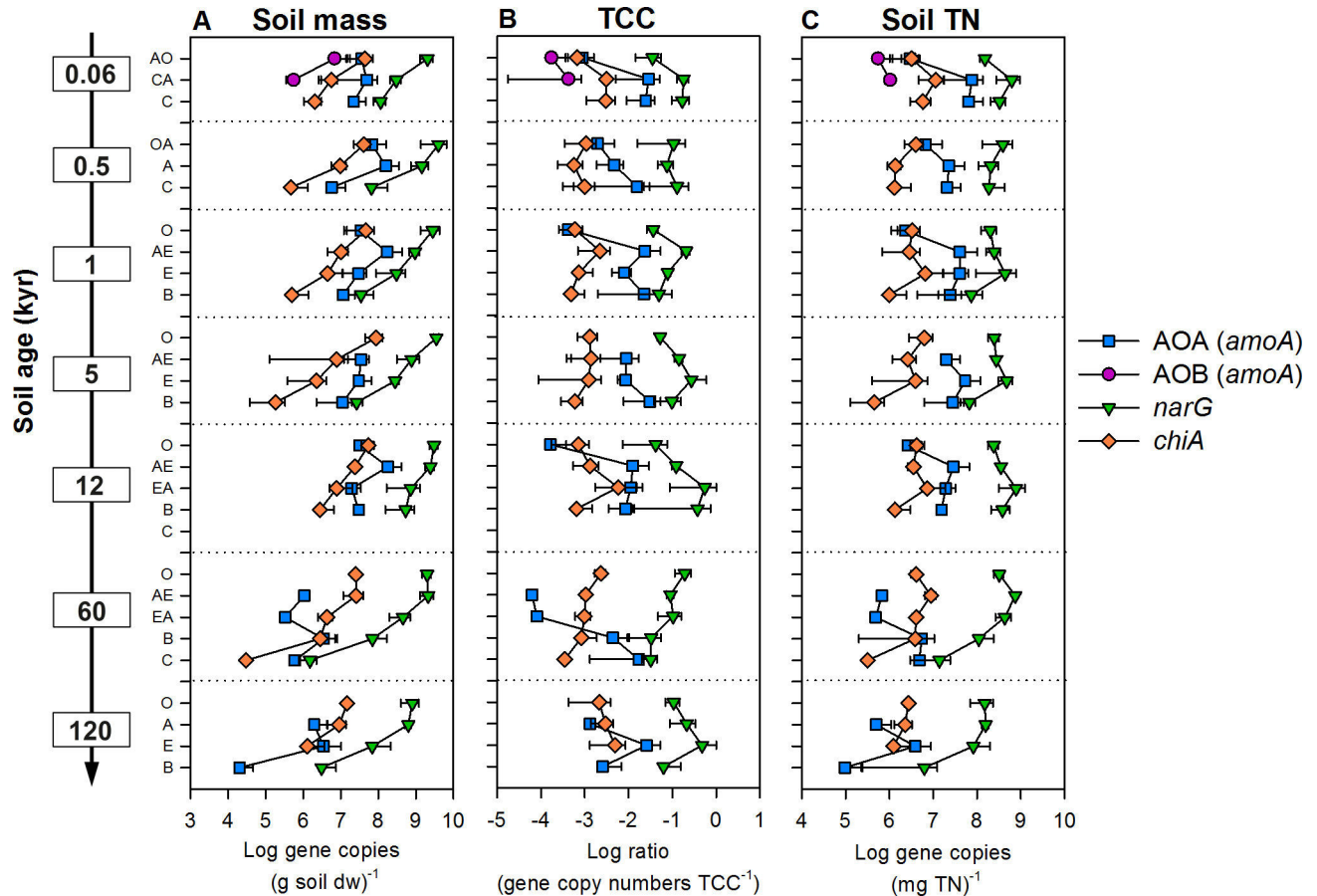


FIG S1 Abundances of N functional genes in different soil horizons (O, OA, A, AO, AE, E, EA, B, C, CA) from depth profiles of 0.06, 0.5, 1, 5, 12, 60, and 120 kyr soil age along the Franz Josef chronosequence. Functional gene copy numbers of archaeal (AOA) and bacterial *amoA* (AOB), *narG*, and *chiA* (A) per gram soil dry weight (dw), (B) as ratio of functional gene to corresponding total cell count (TCC), and (C) per mg soil TN. Error bars indicate standard deviation.

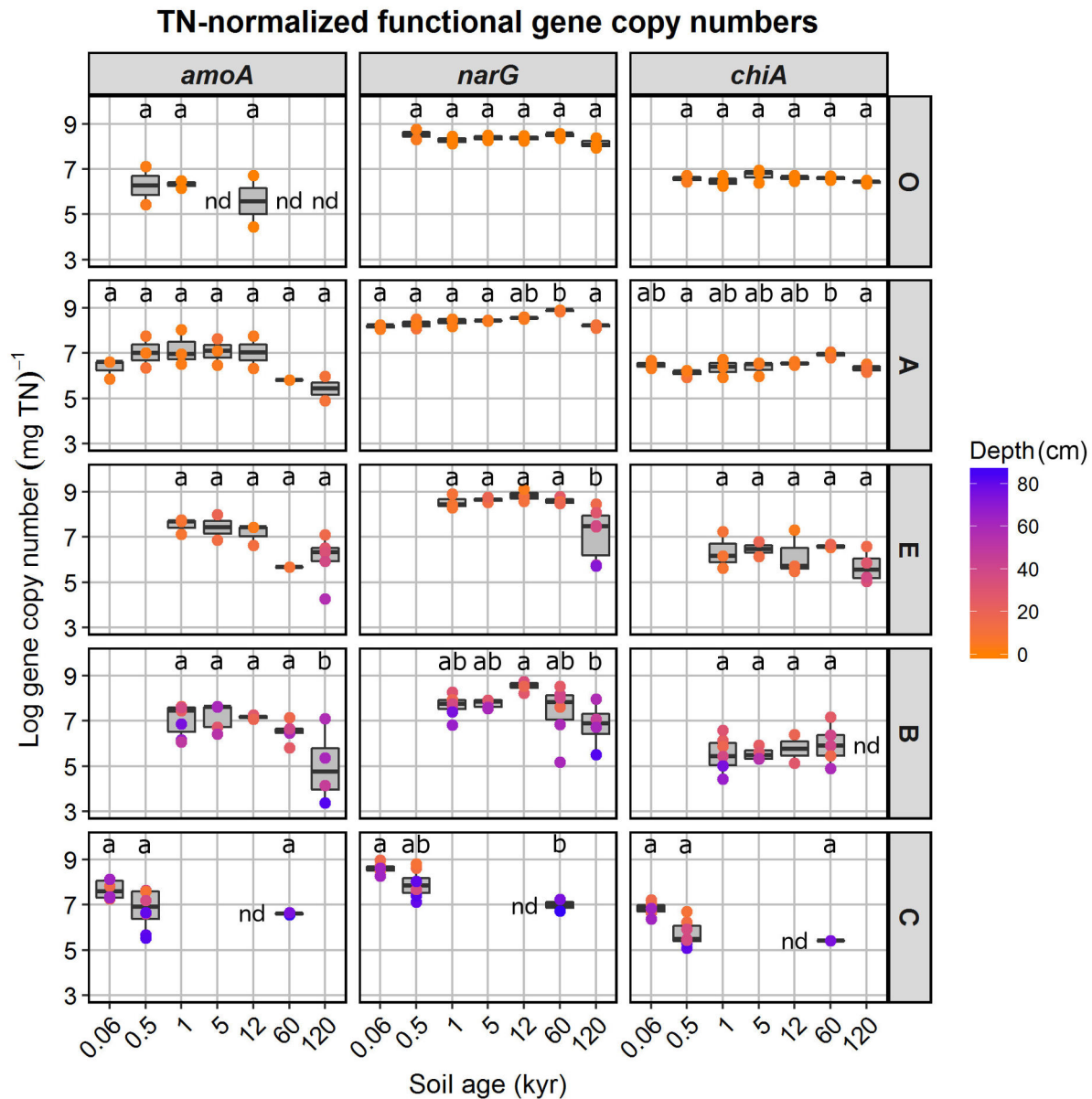


FIG S2 Abundances of TN-normalized N functional genes in soils of different ages along the Franz Josef chronosequence for each soil horizon cluster (O, A, E, B, and C). Functional gene copy numbers of archaeal *amoA*, *narG*, and *chiA* were shown as boxplots with points for horizon and soil profile replicates. The color of the points indicates soil depth. Results of Tukey post-hoc test for the soil age effect in each soil horizon cluster were indicated by letters with the same letters indicating that values for these ages differed not significantly ($P > 0.05$). Samples with gene copy numbers below detection limit were indicated by “nd” (not detected).

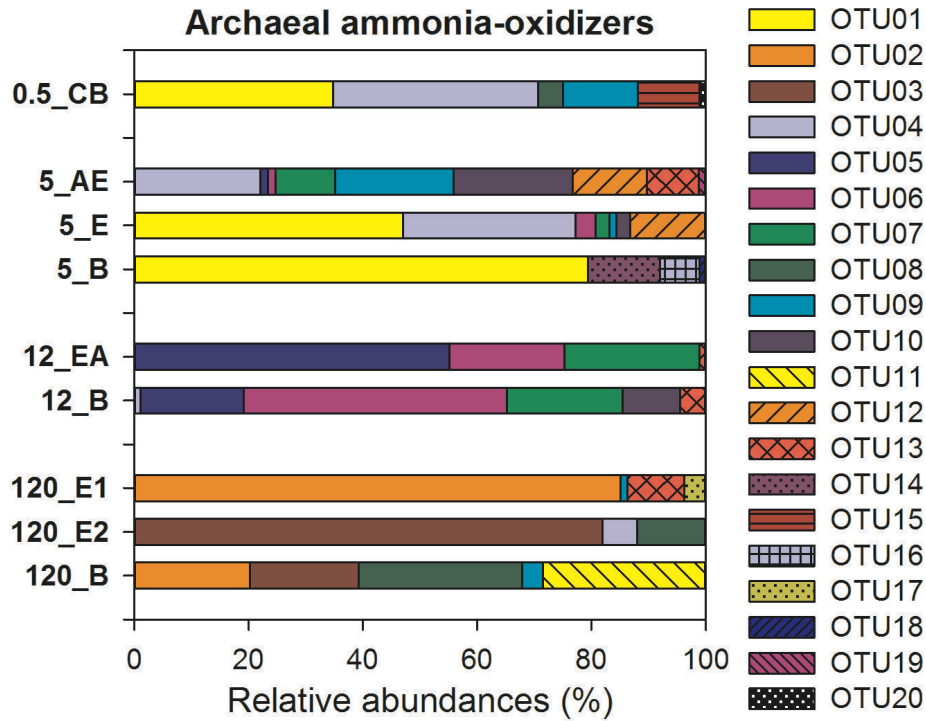


FIG S3 Relative abundances of archaeal *amoA* OTUs (sequence identity threshold 95%) of selected soil samples along the Franz Josef chronosequence. The y-axis denotes the soil age (0.5, 5, 12, and 120 kyr) and soil horizon (AE, E, EA, B, and CB).

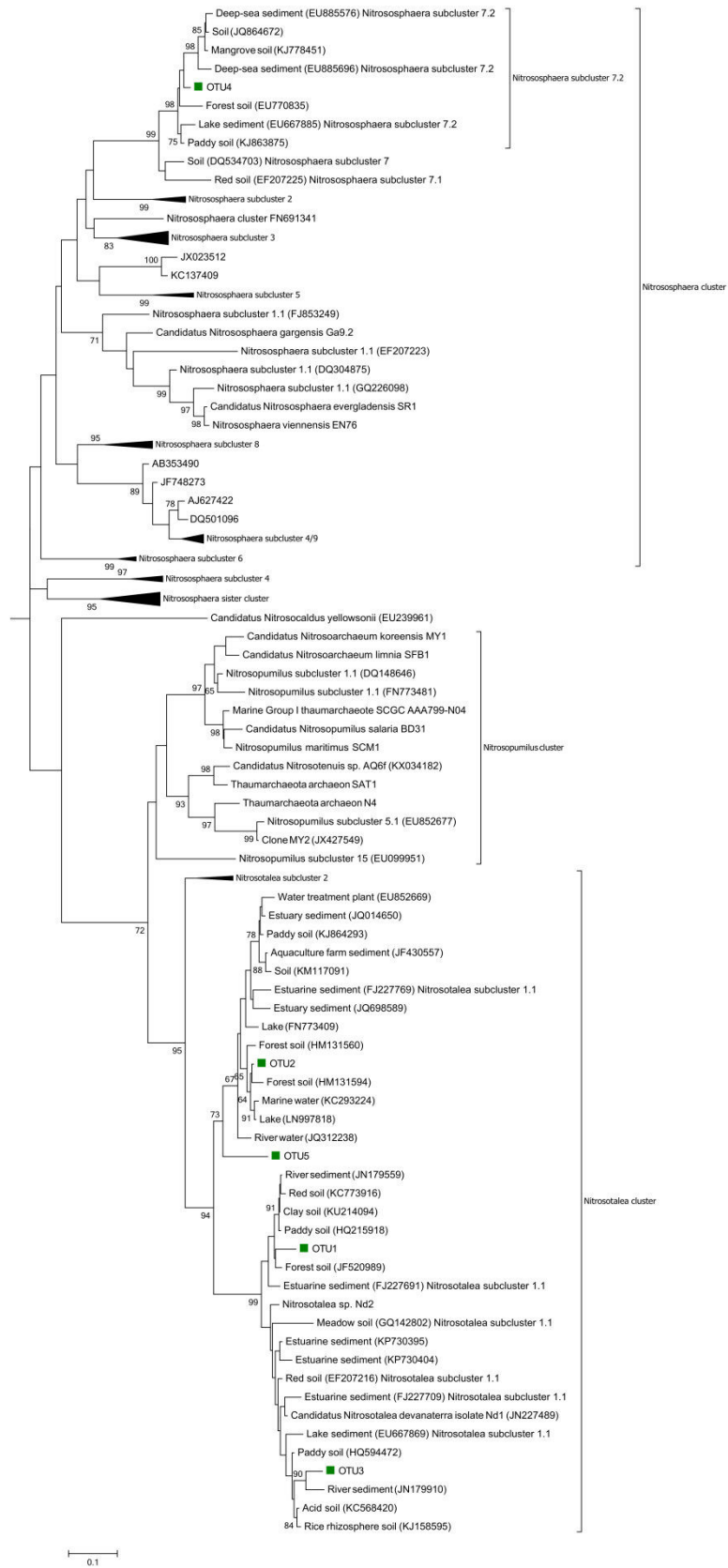


FIG S4 Maximum-likelihood phylogenetic analysis of archaeal *amoA* OTUs based on nucleotide sequences retrieved from selected soil samples along the Franz Josef chronosequence. One representative sequence of each OTU (marked with a green square) was included and marked with cyan circles. As references we used 1 – 5 sequences per cluster from the database provided by Pester et al. (2012) and three closely related sequences for each OTU sequence derived from a BLASTn search. Tree construction based on the General Time Reversible (GTR) model with gamma-distribution and bootstrap values in % (1000 replicates) are shown for node values $\geq 60\%$. The tree was rooted to the *amoA* sequence of the bacterial ammonia-oxidizer *Nitrosomonas europaea* (AF037107) as outgroup (not shown).

TABLE S1 Physico-chemical properties, soil mineralogical properties and TCC (total cell counts) of soil horizons along the Franz Josef chronosequence (Turner et al., 2014). OC – organic carbon, ON – organic nitrogen, OP – organic phosphorus, (Fe+Al)_o – oxalate-extractable Fe and Al phases representing poorly crystalline minerals and metal-humus-complexes, Fe_d – dithionite-extractable Fe phases representing poorly crystalline and crystalline Fe oxides as well as Fe-humus-complexes, (Fe+Al)_p – Fe and Al from organic complexes, Fe_{d-o} – difference between dithionite-extractable Fe and oxalate-extractable Fe representing crystalline Fe phases.

Site age (kyr)	Horizon	pH	Nitrate-N (g kg ⁻¹)	Ammonium-N (g kg ⁻¹)	OC (g kg ⁻¹)	ON (g kg ⁻¹)	OP (mg kg ⁻¹)	(Fe+Al) _o (g kg ⁻¹)	Fe _d (g kg ⁻¹)	(Fe+Al) _p (g kg ⁻¹)	Fe _{d-o} (g kg ⁻¹)	Clay (%)	Silt (%)	Sand (%)	TCC (cells×10 ⁷ g ⁻¹)
0.06	AO	5.8	0.015	0.082	201.5	13.2	688.5	4.2	3.3	4.3	0.4	11	31	58	8517
0.06	CA	6.0	0.001	0.023	7.3	0.5	73.3	2.3	2.9	1.1	1.1	3	17	80	189
0.06	C	6.4	0.001	0.025	7.2	0.4	101.4	2.7	3.6	1.7	1.5	6	31	63	74
0.5	OA	4.5	0.009	0.103	241.7	10.2	684.7	ND	ND	11.6	ND	ND	ND	ND	4209
0.5	A	4.7	0.001	0.041	158.4	6.9	512.0	7	3.6	7.7	0.0	17	55	28	2499
0.5	C	5.6	0.000	0.022	3.6	0.2	47.0	1.7	1.3	1.5	0.1	5	46	49	42
1	O	3.9	0.001	0.066	327.6	13.4	496.5	ND	ND	2.9	ND	ND	ND	ND	7334
1	AE	4.1	0.001	0.033	66.6	4.0	199.9	2.4	1.3	3.6	0.1	12	58	30	497
1	E	4.7	0.000	0.027	17.2	0.7	93.7	3.2	2.0	3.3	0.6	12	55	33	403
1	B	5.3	0.001	0.025	9.5	0.5	92.3	8.5	6.8	5.5	1.1	5	43	52	75
5	O	3.9	0.005	0.121	367.9	14.4	527.2	ND	ND	2.3	ND	ND	ND	ND	6647
5	AE	4.3	0.000	0.026	47.3	2.8	177.6	2.7	1.9	1.4	0.4	13	56	30	513
5	E	4.9	0.001	0.028	16.6	0.6	88.1	4.2	3.2	1.8	0.6	13	58	29	449
5	B	5.1	0.001	0.022	8.1	0.4	110.2	8.5	7.2	2.2	1.1	6	51	43	36
12	O	3.8	0.003	0.100	448.1	12.8	443.8	ND	ND	1.2	ND	ND	ND	ND	11962
12	AE	4.1	0.002	0.047	143.6	6.8	228.4	1.6	0.6	1.2	0.0	7	56	36	2110
12	EA	4.5	0.001	0.022	30.5	0.9	70.9	1.4	0.7	0.9	0.4	5	52	43	176
12	B	5.0	0.000	0.023	36.4	1.3	151.1	13.4	8.2	4.7	2.6	9	34	57	260
12	C	5.5	0.000	0.014	4.7	0.2	106.8	6.6	0.8	0.6	0.3	8	28	64	37

60	O	4.0	0.002	0.045	220.3	6.2	237.5	ND	ND	1.6	ND	ND	ND	ND	1091
60	AE	4.1	0.001	0.040	60.4	2.9	149.0	1.7	0.7	1	0.2	11	68	20	2331
60	EA	4.7	0.000	0.027	24.0	1.0	84.2	5.9	3.8	3.1	0.5	14	67	19	431
60	B	5.1	0.001	0.025	13.3	0.7	87.1	13.9	9.4	3.9	1.8	16	59	25	158
60	C	5.5	0.001	0.021	2.2	0.1	21.2	2.6	1.2	0.9	0.5	7	43	50	5
120	O	4.4	0.001	0.066	190.4	5.4	125.9	ND	ND	0.6	ND	ND	ND	ND	976
120	A	4.2	0.001	0.047	72.1	4.0	72.8	0.5	0.2	0.5	0.0	10	77	13	390
120	E	4.9	0.001	0.024	7.7	0.4	13.7	2.9	2.3	1.7	1.4	12	74	13	12
120	B	5.2	0.002	0.036	12.5	0.4	19.2	7.8	24.7	4	22.0	20	51	29	31

ND = not determined.

TABLE S2 Spearman rank order correlation coefficients for TN-normalized N functional gene abundances and soil properties in mineral topsoils (A horizon) and subsoils (E, B, and C horizon). Amm. – Ammonium. ON – organic nitrogen, OC – organic carbon, OP – organic phosphorous, Fe_o – oxalate-extractable Fe phases representing poorly crystalline minerals and metal-humus-complexes, Al_o – oxalate-extractable Al phases representing poorly crystalline minerals and metal-humus-complexes, Fe_d – dithionite-extractable Fe phases representing poorly crystalline and crystalline Fe oxides as well as Fe-humus-complexes, Fe_p – Fe from organic complexes, Al_p – Al from organic complexes Fe_{d-o} – difference between dithionite-extractable Fe and oxalate-extractable Fe representing crystalline Fe phases. Significant correlations are typed in bold (P < 0.01). Negative relationships are red shaded.

	pH	Nitrate	Amm.	ON	OC	OP	OC:OP	Clay	Silt	Sand	Fe _o	Al _o	Fe _d	Fe _p	Al _p	Fe _{d-o}
Mineral topsoil (A horizon)																
<i>amoA</i>	0.06	0.13	-0.31	-0.01	0.04	0.24	-0.45	0.36	-0.02	0	0.36	0.38	0.39	0.57	0.42	-0.05
<i>narG</i>	-0.44	-0.06	-0.18	-0.38	-0.26	-0.15	0.05	0.02	0.32	-0.27	-0.28	0.14	-0.24	-0.27	-0.09	-0.06
<i>chiA</i>	-0.34	0.18	0.12	-0.24	-0.11	-0.19	0.17	-0.26	0.14	0	-0.42	-0.17	-0.33	-0.5	-0.24	0.02
Subsoil (E, B, and C horizons)																
<i>amoA</i>	-0.04	0.03	-0.13	0.27	0.2	0.42	-0.19	-0.33	-0.31	0.38	0.09	-0.24	-0.06	0.15	-0.19	-0.07
<i>narG</i>	-0.34	-0.11	0.08	0.49	0.46	0.3	0.13	-0.18	-0.15	0.23	-0.06	-0.28	-0.19	0.2	-0.23	-0.26
<i>chiA</i>	-0.22	0.2	0.31	0.37	0.31	0.06	0.15	0.04	-0.01	0.01	-0.02	-0.21	-0.01	0.25	-0.22	0.01

TABLE S3 Results of the basic local alignment search tool for nucleotide (BLASTn) search for the representative sequences of the OTUs using megablast and excluding uncultured/environmental sample sequences (28.10.2016).

	Coverage	E value	Identity	Accession number
OTU1				
<i>Candidatus</i> Nitrosotalea devanaterrea genome assembly, chromosome: 1	99%	0	91%	LN890280.1
<i>Candidatus</i> Nitrosotalea devanaterrea isolate Nd1 ammonia monooxygenase subunit A (<i>amoA</i>) gene, partial cds	93%	0	90%	JN227489.1
<i>Nitrosotalea</i> sp. Nd2 ammonia monooxygenase subunit A (<i>amoA</i>) gene, partial cds	92%	0	90%	KJ540206.1
<i>Nitrosomonas europaea</i> strain NSW3 ammonia monooxygenase subunit A (<i>amoA</i>) gene, partial cds	77%	3.00E-172	89%	KJ794819.1
<i>Candidatus</i> Nitrosotenuis sp. AQ6f ammonia monooxygenase alpha subunit (<i>amoA</i>) gene, complete cds	99%	8.00E-128	80%	KX034182.1
<i>Nitrosopumilus maritimus</i> isolate SF_AOA_A07 ammonia monooxygenase subunit A (<i>amoA</i>) gene, partial cds	99%	2.00E-124	80%	HM345608.1
<i>Candidatus</i> Nitrosopelagicus brevis strain CN25, complete genome	99%	2.00E-123	80%	CP007026.1
Crenarchaeote SCGC AAA288-N08 ammonia monooxygenase alpha subunit (<i>amoA</i>) gene, partial cds	95%	3.00E-77	76%	JF719200.1
Crenarchaeote SCGC AAA288-B11 ammonia monooxygenase alpha subunit (<i>amoA</i>) gene, partial cds	95%	3.00E-77	76%	JF719170.1
Crenarchaeote SCGC AAA288-P18 ammonia monooxygenase alpha subunit (<i>amoA</i>) gene, partial cds	83%	1.00E-76	77%	JF719207.1
Crenarchaeote SCGC AAA008-P23 ammonia monooxygenase alpha subunit (<i>amoA</i>) gene, partial cds	95%	7.00E-74	76%	JF719165.1
Crenarchaeote SCGC AAA288-M04 ammonia monooxygenase alpha subunit (<i>amoA</i>) gene, partial cds	83%	2.00E-73	77%	JF719197.1
Crenarchaeote SCGC AAA001-B14 ammonia monooxygenase alpha subunit (<i>amoA</i>) gene, partial cds	83%	2.00E-73	77%	JF719128.1
Crenarchaeote SCGC AAA288-J07 ammonia monooxygenase alpha subunit (<i>amoA</i>) gene, partial cds	83%	1.00E-71	76%	JF719190.1
Crenarchaeote SCGC AAA240-O10 ammonia monooxygenase alpha subunit (<i>amoA</i>) gene, partial cds	83%	1.00E-71	76%	JF719167.1
Crenarchaeote SCGC AAA240-K17 ammonia monooxygenase alpha subunit (<i>amoA</i>) gene, partial cds	95%	7.00E-69	75%	JF719166.1
Crenarchaeote SCGC AAA288-A10 ammonia monooxygenase alpha subunit (<i>amoA</i>) gene, partial cds	83%	2.00E-68	76%	JF719168.1
Crenarchaeote SCGC AAA288-C14 ammonia monooxygenase alpha subunit (<i>amoA</i>) gene, partial cds	83%	2.00E-63	75%	JF719173.1
OTU2				
<i>Candidatus</i> Nitrosotalea devanaterrea genome assembly, chromosome: 1	99%	6.00E-174	84%	LN890280.1
<i>Candidatus</i> Nitrosotalea devanaterrea isolate Nd1 ammonia monooxygenase subunit A (<i>amoA</i>) gene, partial cds	93%	1.00E-160	84%	JN227489.1
<i>Candidatus</i> Nitrosotenuis sp. AQ6f ammonia monooxygenase alpha subunit (<i>amoA</i>) gene, complete cds	99%	8.00E-143	82%	KX034182.1
<i>Nitrosomonas europaea</i> strain NSW3 ammonia monooxygenase subunit A (<i>amoA</i>) gene, partial cds	77%	8.00E-123	83%	KJ794819.1

<i>Candidatus</i> Nitrosopumilus sp. PS0 ammonia monooxygenase subunit A gene, partial cds	85%	5.00E-100	79%	KF957666.1
<i>Cenarchaeum symbiosum</i> A clone C18D02, complete sequence	99%	6.00E-94	77%	DQ397580.1
<i>Cenarchaeum symbiosum</i> A clone C07D08, complete sequence	99%	6.00E-94	77%	DQ397569.1
Archaeon G61 ammonia monooxygenase subunit A (<i>amoA</i>) gene, complete cds	99%	5.00E-70	75%	KR233005.1

OTU3

<i>Candidatus</i> Nitrosotalea devanaterrea genome assembly, chromosome: 1	99%	0	92%	LN890280.1
<i>Candidatus</i> Nitrosotalea devanaterrea isolate Nd1 ammonia monooxygenase subunit A (<i>amoA</i>) gene, partial cds	93%	0	92%	JN227489.1
<i>Nitrosotalea</i> sp. Nd2 ammonia monooxygenase subunit A (<i>amoA</i>) gene, partial cds	92%	0	92%	KJ540206.1
<i>Nitrosomonas europaea</i> strain NSW3 ammonia monooxygenase subunit A (<i>amoA</i>) gene, partial cds	77%	0	92%	KJ794819.1
<i>Nitrosopumilus maritimus</i> isolate SF_AOA_A10 ammonia monooxygenase subunit A (<i>amoA</i>) gene, partial cds	99%	4.00E-146	82%	HM345609.1
<i>Nitrosopumilus maritimus</i> isolate SF_AOA_A07 ammonia monooxygenase subunit A (<i>amoA</i>) gene, partial cds	99%	4.00E-136	81%	HM345608.1
<i>Candidatus</i> Nitrosopelagicus brevis strain CN25, complete genome	99%	2.00E-123	80%	CP007026.1
<i>Candidatus</i> Nitrosopumilus korensis AR1, complete genome	99%	2.00E-123	80%	CP003842.1
<i>Nitrosopumilus maritimus</i> SCM1, complete genome	99%	5.00E-115	79%	CP000866.1
<i>Nitrosopumilus maritimus</i> SCM1 putative archaeal ammonia monooxygenase subunit B (<i>amoB</i>) gene, partial cds; putative archaeal ammonia monooxygenase subunit C (<i>amoC</i>) and conserved hypothetical protein genes, complete cds; and putative archaeal ammonia monooxygenase subunit A (<i>amoA</i>) gene, partial cds	97%	4.00E-111	79%	EU239959.1
<i>Nitrosopumilus maritimus</i> strain NAOA6 ammonia monooxygenase subunit A (<i>amoA</i>) gene, partial cds	91%	6.00E-94	78%	KT380500.1
Crenarchaeote SCGC AAA288-P18 ammonia monooxygenase alpha subunit (<i>amoA</i>) gene, partial cds	87%	2.00E-58	75%	JF719207.1
Crenarchaeote SCGC AAA288-N08 ammonia monooxygenase alpha subunit (<i>amoA</i>) gene, partial cds	87%	2.00E-58	75%	JF719200.1
Crenarchaeote SCGC AAA288-B11 ammonia monooxygenase alpha subunit (<i>amoA</i>) gene, partial cds	87%	1.00E-56	75%	JF719170.1
Crenarchaeote SCGC AAA008-P23 ammonia monooxygenase alpha subunit (<i>amoA</i>) gene, partial cds	87%	1.00E-56	75%	JF719165.1
Crenarchaeote SCGC AAA240-K17 ammonia monooxygenase alpha subunit (<i>amoA</i>) gene, partial cds	87%	5.00E-55	74%	JF719166.1
Crenarchaeote SCGC AAA288-J07 ammonia monooxygenase alpha subunit (<i>amoA</i>) gene, partial cds	95%	7.00E-54	74%	JF719190.1
Crenarchaeote SCGC AAA240-O10 ammonia monooxygenase alpha subunit (<i>amoA</i>) gene, partial cds	87%	2.00E-53	74%	JF719167.1
Crenarchaeote SCGC AAA001-B14 ammonia monooxygenase alpha subunit (<i>amoA</i>) gene, partial cds	82%	2.00E-53	75%	JF719128.1
Crenarchaeote SCGC AAA288-M04 ammonia monooxygenase alpha subunit (<i>amoA</i>) gene, partial cds	95%	3.00E-52	73%	JF719197.1
Crenarchaeote SCGC AAA288-A10 ammonia monooxygenase alpha subunit (<i>amoA</i>) gene, partial cds	87%	1.00E-51	74%	JF719168.1
Crenarchaeote SCGC AAA288-C14 ammonia monooxygenase alpha subunit (<i>amoA</i>) gene, partial cds	82%	2.00E-43	73%	JF719173.1

OTU4

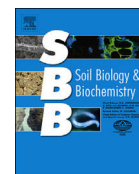
<i>Candidatus Nitrososphaera evergladensis</i> SR1, complete genome	99%	6.00E-114	79%	CP007174.1
OTU5				
<i>Nitrosopumilus maritimus</i> isolate SF_AOA_A07 ammonia monooxygenase subunit A (<i>amoA</i>) gene, partial cds	99%	2.00E-139	81%	HM345608.1
<i>Candidatus Nitrosopelagicus brevis</i> strain CN25, complete genome	99%	1.00E-121	79%	CP007026.1
Crenarchaeote SCGC AAA003-P19 ammonia monooxygenase alpha subunit (<i>amoA</i>) gene, partial cds	95%	3.00E-72	76%	JF719139.1

4.2.4 *Manuscript 4: Microbial utilization of mineral-associated nitrogen in soils*



Contents lists available at ScienceDirect

Soil Biology & Biochemistry

journal homepage: www.elsevier.com/locate/soilbio

Microbial utilization of mineral-associated nitrogen in soils



Stephanie Turner^{a,*}, Sandra Meyer-Stüve^{b,1}, Axel Schippers^a, Georg Guggenberger^b, Frank Schaarschmidt^c, Birgit Wild^d, Andreas Richter^e, Reiner Dohrmann^f, Robert Mikutta^g

^a Geomicrobiology, Federal Institute for Geosciences and Natural Resources (BGR), Stilleweg 2, 30655 Hannover, Germany

^b Institute of Soil Science, Leibniz Universität Hannover, Herrenhäuser Str. 2, 30419 Hannover, Germany

^c Institute of Biostatistics, Leibniz Universität Hannover, Herrenhäuser Str. 2, 30419 Hannover, Germany

^d Department of Earth Sciences, University of Gothenburg, Guldhedsgatan 5A, 40530 Gothenburg, Sweden

^e Department of Microbiology and Ecosystem Science, University of Vienna, Althanstr. 14, 1090 Wien, Austria

^f Technical Mineralogy and Clay Mineralogy, Federal Institute for Geosciences and Natural Resources (BGR), Stilleweg 2, 30655 Hannover, Germany

^g Soil Science and Soil Protection, Martin-Luther-Universität Halle-Wittenberg, Von-Seckendorff-Platz 3, 06120 Halle (Saale), Germany

ARTICLE INFO

Article history:

Received 20 July 2016

Received in revised form

9 October 2016

Accepted 15 October 2016

Keywords:

Microbial nitrogen cycling

Quantitative PCR

Net N mineralization

Functional genes

Mineral-associated organic matter

Priming

ABSTRACT

In soils, a large portion of organic nitrogen (ON) is associated with minerals and thus, possibly stabilized against biological decay. We therefore tested if mineral-associated N is an important N source for soil microorganisms, and which soil parameters control its bioavailability. Microcosm experiments with mineral-associated organic matter, obtained as heavy fraction (HF) via density fractionation, and bulk soil from mineral topsoil of the Franz Josef chronosequence were conducted for 125 days. We examined the effects of O₂ status, soil age (differences in mineralogical properties), as well as cellulose and phosphate additions on the turnover of mineral-associated N. Using a combination of activity measurements and quantitative PCR, microbial N transformation rates and abundances of N-related functional genes (*amoA*, *narG*, *chiA*) were determined. Similar or higher values for microbial N cycling rates and N-related functional abundances in the HF compared to bulk soil indicated that mineral-associated N provides an important bioavailable N source for soil microorganism. The turnover of mineral-associated N was mainly controlled by the O₂ status. Besides, soil mineralogical properties significantly affected microbial N cycling and related gene abundances with the effect depending on the N substrate type (ON, NH₄⁺ or NO₃⁻). In contrast, cellulose or phosphate addition hardly enhanced microbial utilization of mineral-associated N. The results of our microcosm study indicate that mineral-associated N is highly bioavailable in mineral topsoils, but effects of the mineral phase differ between N cycling processes.

© 2016 Elsevier Ltd. All rights reserved.

1. Introduction

In soil, the availability of N as a major nutrient element and limiting growth factor determines fertility and biomass production to a large extent (Knicker, 2011). Nitrogen can be found in eight oxidation states and most of the N transformations are mediated by soil microorganisms that act as key players of N cycling (Robertson and Groffman, 2015). Present ecological concepts in N cycling and ecosystem dynamics largely ignore the role of mineral–organic

associations, thereby organic N (ON) is considered as one pool without further differentiation into ON contained in functionally different organic matter (OM) fractions, e.g. particulate and mineral-associated OM. However, the interaction between OM and soil minerals determines the turnover of soil OM (SOM) (Schmidt et al., 2011). Competing with plants and microorganism for available N, soil minerals are relevant for ecosystem productivity by directly and indirectly influencing microbial C and nutrient cycling.

Several studies showed that soil minerals can indirectly affect microbial nutrient cycling by stabilizing OM via adsorption to mineral surfaces or coprecipitation reactions (summarized by Kleber et al., 2015). These interactions mostly result in lower substrate bioavailability and can therefore impair microbial activity (Schneider et al., 2010; Kleber et al., 2015). Similarly, activities of microbial extracellular enzymes can be inhibited by soil minerals

* Corresponding author. Bundesanstalt für Geowissenschaften und Rohstoffe, Stilleweg 2, 30655, Hannover, Germany.

E-mail address: sturner.bio@gmail.com (S. Turner).

¹ These authors contributed equally to this work.

such as poorly crystalline Fe and Al oxide phases and other clay-sized minerals, thus slowing down microbial OM degradation and mineralization (Bayan and Eivazi, 1999; Nannipieri and Smalla, 2006; Turner et al., 2014).

The bioavailability of SOM depends, among other factors, strongly on properties of the mineral phase such as specific surface area and surface charge (Kleber et al., 2015). Mineralization rates of organic carbon (OC) and ON in the sand fraction were shown to be higher than in the silt or clay fraction during an incubation experiment with soil particle size fractions (Bimüller et al., 2014). Vogel et al. (2015) revealed in an incubation experiment with artificial soils that the clay mineral type affected plant litter decomposition with slower mineralization in montmorillonite-rich soil than in illite-rich soil. Also Saïdy et al. (2012) observed in a similar experiment a significant effect of the clay mineral type with higher decomposition rates in the presence of kaolinite than illite or smectite. Colman and Schimel (2013) identified in an analysis of 84 distinct mineral soils the clay content as an important predictor for microbial respiration as well as net N mineralization with a negative effect on both. Besides soil particle size and clay mineral type, the content of Fe and Al (hydr)oxides was reported to impact microbial activity. While Achat et al. (2012) detected a negative relationship between basal soil respiration and the content of Al (hydr)oxides, other studies reported either no, minor or strong effects of Fe (hydr)oxide type on C mineralization (Mikutta et al., 2007; Saïdy et al., 2012; Heckman et al., 2013; Vogel et al., 2015).

Overall, there are several studies focusing on the effect of mineralogical properties on C cycling, whereas the impact of minerals on N cycling is still poorly understood. Although C and N cycling are linked to each other via biomass production and degradation (Knicker, 2011), a few previous studies indicated that OC and ON mineralization respond differently to the mineral phase pointing to a decoupling of OC and ON mineralization in the mineral-associated soil fraction (Heckman et al., 2013; Bimüller et al., 2014). Additionally, our previous results obtained from a soil chronosequence showed that profile-based OC stocks of mineral soils were positively correlated to the content of Al originating from poorly crystalline Al minerals and Al-humus complexes, whereas the ON stocks were positively correlated to the stocks of crystalline Fe oxides (Turner et al., 2014). Nevertheless, recent evidence suggests that mineral-associated ON can be utilized by soil microorganisms. For example, Dippold et al. (2014) reported that alanine, sorbed to different Fe oxides or clay minerals in an incubation experiment, was quickly mineralized at variable rates, thus also highlighting the effect of the soil mineral type.

Therefore the aims of our study were to elucidate (i) if mineral-associated N is an important bioavailable N source for soil microorganisms, and (ii) which soil properties control the bioavailability of mineral-associated N and the abundances of N cycling microorganism. We used soils of different ages of the 120-kyr old Franz Josef soil chronosequence (New Zealand) which is characterized by a nutrient and mineralogical gradient (Stevens, 1968; Turner et al., 2014). High precipitation regularly creates water-saturated conditions in soils of the chronosequence resulting in changes of the redox regime which may affect microbial N cycling by generally slowing down microbial activity. Due to leaching and weathering of P-containing minerals the soil P content drastically decreases with increasing soil age, possibly limiting the microbial utilization of mineral-associated N in older soils. The use of mineral-associated N may also require the supply of easily available additional C sources, such as cellulose derived from decomposing root litter, which has been shown to stimulate microbial activity and SOM decomposition in subsoil environments ("priming effect", Fontaine et al., 2007).

Hence, we hypothesized that mineral-associated N is an

important bioavailable N source and explored the effect of soil mineralogical composition, O₂ status (redox regime), and the additions of phosphate and cellulose (priming) on its mineralization. To address this, we set up a microcosm experiment comparing microbial N cycling in the mineral-associated OM fraction with bulk soil of four soil ages under oxic and anoxic conditions. Thereby, we tested the effect of P and C additions (phosphate, ¹³C-labeled cellulose, and phosphate + ¹³C-labeled cellulose). During the 125-days incubation period, N₂, N₂O and CO₂ production as parameters for microbial activity were measured regularly, and at the end of the experiment net N mineralization and gene copy numbers of N cycle-related marker genes were determined by quantitative PCR (qPCR).

2. Material and methods

2.1. Site description and soil sampling

The Franz Josef chronosequence is located on the West Coast of the South Island of New Zealand (−43° S, 170° E). The soils developed due to repeated glacial advance and retreat from greywacke and mica schist spanning a time scale from present to 120 000 years (Stevens, 1968; Almond et al., 2001). The climate is wet and temperate and the soils are covered by rainforest (Richardson et al., 2004). The chronosequence is characterized by a steep nutrient and mineralogical gradient (Turner et al., 2014, Table 1, Table 2). Soil samples were taken from A horizons of four sites with different soil ages (0.5k, 5k, 12k, and 120k years) in February 2014 and were kept at <8 °C prior to incubation. Using A horizons guaranteed relatively high microbial activities that facilitated the detection of changes during the incubation period and concomitantly a high proportion of mineral-bound N. Contrary to whole soil profiles that were characterized by an increasing content of Fe and Al (hydr)oxides and clay with soil age, the A horizons separately showed an inverse trend for the content of these soil mineral phases (Table 2).

2.2. Microcosm incubation experiment

To assess the bioavailability of mineral-associated N and its controls we set up a laboratory incubation experiment in microcosms with either the mineral-associated OM fraction or bulk soil (Fig. S1). We used A horizons of four soil ages (0.5k, 5k, 12k, and 120k years). For soil fractions, soil samples were separated by density fractionation using sodium polytungstate solution ($\rho = 1.6 \text{ g cm}^{-3}$; Cerli et al., 2012). Twenty-five g of soil were dispersed in 125 mL sodium polytungstate solution and sonicated for 9 min 38 s with 60 J mL⁻¹ with an ultrasonic device (LABSONIC®, Sartorius Stedim Biotech GmbH, Göttingen, Germany). The floating light fraction (LF, $\rho < 1.6 \text{ g cm}^{-3}$, representing mostly particulate OM) was removed from the heavy fraction (HF, containing mineral-associated OM) by decantation after deposition for 1 h and centrifugation for 10 min at 3500g. To minimize possible negative effects of the sodium polytungstate solution on microbial activities (Blackwood and Paul, 2003; Crow et al., 2007), both fractions were washed with deionized water until the electrical conductivity was <50 $\mu\text{S cm}^{-1}$. Thereafter, samples were shock-frozen in liquid N₂ and freeze dried resulting in approximately 95 wt% of the HF and 2 wt% of the LF. Toxic effects caused by tungsten residues in the fractionated samples could be ruled out because of similar mineralization rates of bulk soil compared to density fractions (Gentsch et al., 2015).

To test the influence of P and C addition on C and N turnover, we tested different treatments: without any addition (wo), with NaH₂PO₄ solution (P; 500 $\mu\text{g PO}_4\text{-P g}^{-1}$ soil fraction), with ¹³C-labeled cellulose powder (C; 40 mg cellulose-C g⁻¹ soil fraction C)

Table 1Initial concentrations of organic carbon (OC), total nitrogen (TN), NH_4^+ and NO_3^- per g soil fraction and initial proportion of Nmin on TN.

Site age (yrs)	Fraction	OC (mg g^{-1})	TN (mg g^{-1})	NH_4^+ -N (mg g^{-1})	NO_3^- -N (mg g^{-1})	%Nmin of TN
0.5k	Bulk	144.2	7.9	0.099	0.002	1.3
5k		137.3	7.7	0.128	0.002	1.7
12k		77.7	3.6	0.097	0.002	2.8
120k		65.5	3.6	0.096	0.001	2.7
0.5k	HF	126.1	6.7	0.036	0.002	0.6
5k		99.8	5.5	0.022	0.001	0.4
12k		63.7	3.0	0.016	0.002	0.6
120k		57.1	3.1	0.016	0.002	0.6

Table 2Total phosphorus (TP) content and mineralogical properties of the A horizons (Turner et al., 2014), mean \pm standard deviation. Fe_d : dithionite-extractable Fe phases representing poorly crystalline and crystalline Fe oxides as well as Fe-humus-complexes; Fe_o , Al_o : oxalate-extractable Fe and Al phases representing poorly crystalline minerals and metal-humus-complexes, Fe_{d-o} : difference between dithionite-extractable Fe and oxalate-extractable Fe representing crystalline Fe phases; Fe_p , Al_p : Fe and Al from organic complexes.

Site age (yrs)	Hor.	TP ($\mu\text{g g}^{-1}$)	Fe_d (mg g^{-1})	Fe_o (mg g^{-1})	Fe_{d-o} (mg g^{-1})	Fe_p (mg g^{-1})	Al_o (mg g^{-1})	Al_p (mg g^{-1})	Clay (%)	Silt (%)	Sand (%)
0.5k	A	583 \pm 149	3.6 \pm 2.0	4.5 \pm 2.9	0.0 \pm 0.0	4.3 \pm 3.3	2.5 \pm 0.8	3.4 \pm 2.0	17 \pm 7	55 \pm 9	28 \pm 16
5k	AE	195 \pm 70	1.9 \pm 1.0	1.5 \pm 0.8	0.4 \pm 0.2	0.8 \pm 0.6	1.2 \pm 0.5	0.6 \pm 0.2	13 \pm 1	56 \pm 3	30 \pm 4
12k	AE	244 \pm 41	0.6 \pm 0.1	0.6 \pm 0.1	0.0 \pm 0.0	0.4 \pm 0.0	1.0 \pm 0.1	0.8 \pm 0.1	7 \pm 0	56 \pm 4	36 \pm 4
120k	A	78 \pm 13	0.2 \pm 0.0	0.2 \pm 0.0	0.0 \pm 0.0	0.2 \pm 0.1	0.3 \pm 0.1	0.3 \pm 0.3	10 \pm 1	77 \pm 3	13 \pm 2

or with the addition of both (CP). The ^{13}C -labeled cellulose (Isolife, Wageningen, The Netherlands; low degree of polymerization, *Cichorium intybus*; $\text{U-}^{13}\text{C}$; >97 at%) was mixed with unlabeled cellulose to 5 at% ^{13}C before application.

For each microcosm, 10 g dried soil (bulk or HF) were mixed with 10 g quartz powder (<125 μm , Carl Roth GmbH + Co. KG, Karlsruhe, Germany) in 125 mL serum vials. Control samples contained 20 g quartz only.

To further counteract the possible negative effect of the fractionation procedure, we inoculated each incubation sample with 3 mL of soil slurry with an active, indigenous microbial community. For inoculation we used soil slurries that consisted of fresh, wet soil of the corresponding sampling site (0.5k, 5k, 12k, and 120k years) suspended in sterile Hoagland solution (without a P and N source, soil weight to volume ratio = 1:10). After adding the NaH_2PO_4 solution to the respective samples, all samples were adjusted to 60% water-holding capacity with sterile distilled water and carefully homogenized with a spatula. To examine the effect of the O_2 status, we incubated under oxic and anoxic conditions. For oxic incubation, serum vials were closed with polyethylene wool to allow gas exchange. For maintaining high humidity, a tray of water was placed into the incubator and the water content was checked every few days and readjusted if necessary. Anoxic vials were fitted with septa, sealed with caps and flushed with He, the loss of water during incubation was negligible. All combinations of the tested factors (soil fraction, O_2 status, soil age and nutrient addition) were prepared in triplicate resulting together with the controls in 198 incubation samples. All samples were pre-incubated at 15 $^\circ\text{C}$ for 10 days for equilibration to avoid measuring the fractionation-induced initial CO_2 pulse, afterwards the cellulose was added to the corresponding C treatment vials, and the 125 days main-incubation started.

The headspace was sampled at nine time points (0, 7, 14, 21, 28, 42, 56, 98, and 125 days) by taking 25 mL gas with a syringe and transferring it into pre-evacuated 20 mL vials. The oxic vials were closed and flushed with CO_2 -free air 24 h before each gas sampling, and the anoxic vials were flushed with pure helium 4–8 days before sampling. The incubation setup was checked for leaks by additionally measuring gas samples from empty

incubation flasks. Gas concentrations were analyzed by gas chromatography with a GC-2014 (Shimadzu, Kyoto, Japan; modified according to Lofffield et al. (1997)) equipped with an electron capture detector (for CO_2 and N_2O), and a 7890A-GC (Agilent Technologies, Santa Clara, CA, US) equipped with an electron capture detector (N_2O , concentrations > 750 ppb), thermal conductivity detector (for N_2), and helium ionization detector (for CO_2 , concentrations > 4000 ppm) at the Johann Heinrich von Thünen Institute, Institute of Climate-Smart Agriculture (Braunschweig, Germany). To analyze the mineralization of the ^{13}C -labeled cellulose, $^{13}\text{CO}_2$ samples were taken at day 7, 42, and 125 and measured with a GasBench II system coupled to a Delta V Advantage isotope ratio mass spectrometry (Thermo Fisher Scientific Inc., Waltham, MA, US).

After 125 days of incubation, all serum vials were sampled destructively for several end-point analyses: Net N mineralization, net nitrification, microbial biomass and N cycle-related functional marker genes using qPCR. Nmin (inorganic N: sum of NO_3^- and NH_4^+) was extracted with 1 M KCl and measured photometrically (SAN-plus, Skalar Analytical B.V., Breda, The Netherlands). The difference between end and start Nmin and NO_3^- concentrations were calculated as net N mineralization and net nitrification, respectively. Microbial biomass carbon (C_{mic}) and nitrogen (N_{mic}) were determined via the fumigation-extraction method (Vance et al., 1987) as specified in Turner et al. (2014). To distinguish between C_{mic} derived from SOM or cellulose, extracts of cellulose treatments (C and CP) were analyzed for ^{13}C via high-performance liquid chromatography (Dionex Corporation, Sunnyvale, CA, USA) coupled to a Finnigan Delta V Advantage Mass Spectrometer over a Finnigan LC IsoLink Interface (Thermo Fisher Scientific Inc). Further, the pH (1:2.5, wt/vol in distilled water) was measured in all samples at the end of the incubation resulting in a mean value (except controls) of 4.8 ± 0.4 (standard deviation) to rule out, that the observed differences in activities and abundances are caused by great variances in pH values due to fractionation or treatments.

2.3. Nucleic acid extraction and qPCR

Nucleic acids of each sample were extracted in duplicate

according to the manufacturer's protocol (FastDNA® Spin Kit for Soil, MP Biomedicals, Santa Ana, CA, US) with modifications according to Webster et al. (2003) and DNA extracts were pooled.

Quantification of N cycle-related functional marker genes was performed by qPCR: archaeal and bacterial ammonia monooxygenase (*amoA*; Francis et al., 2005; Nicolaisen et al., 2004), nitrate reductase (*narG*; Bru et al., 2007), and bacterial chitinase (*chiA*; Yergeau et al., 2007), with chitin representing a complex ON compound common in soils. We used a StepOnePlus™ Real-Time PCR System (Applied Biosystems, Life Technologies, Carlsbad, CA, US) and SYBR® Green I chemistry. All qPCRs contained 5 µL mastermix (Table S1), 1 µL BSA (0.5 µL for *amoA* assays; 3 g L⁻¹; Sigma-Aldrich, St. Louis, MO, US), primers (Table S1), 1 µL DNA template and filled to the final volume of 10 µL with distilled H₂O. For further information on qPCR assays see Supplementary material (Table S1).

Product specificity was confirmed by melt curve analysis and the amplicon size was verified by agarose gel electrophoresis. Samples with multiple melt points, multiple gel bands or wrong product size were excluded from further analysis. Standards were made from purified PCR products obtained from whole genome extracted from pure cultures. The DNA concentration of standards was quantified with a FoodALYT Photometer Bio (Omnilab, Bremen, Germany) and used for a calibration curve with seven dilution steps (1:10). Template DNA was used in three dilutions to reduce the effect of co-extracted PCR inhibitors. Standard DNA, template DNA, and non-template control were run in three replicates.

2.4. Data analysis and statistical methods

Gas data was corrected for the gas release from the inoculated quartz control samples to subtract background respiration of the inoculum. Percent CO₂-C, N₂O-N, and N₂-N respired of the OC or total N (TN) content prior to incubation were calculated from the cumulative CO₂-C loss (mg CO₂-C g⁻¹ OC), N₂O-N loss (µg N₂O-N g⁻¹ TN), and N₂-N loss (µg N₂-N g⁻¹ TN). Cumulative mineralization over the 125 days was then estimated as the sum of the daily gas emissions where days between the nine sampling dates were interpolated. Because the CO₂ production rates were non-monotone due to addition of cellulose (C treatments), we used natural cubic splines while simple linear interpolation was used for the (roughly) monotonically decreasing N₂O and N₂ production rates. Interpolations were done by standard methods in the “stats” package of R (R version 3.2.2, R Core Team, 2015). For the C treatments, we further split total CO₂ production (C_{Total}) into CO₂ derived from the added cellulose (C_{Cellulose}) and from SOM (C_{SOM}) using the equations:

$$C_{SOM} = C_{Total} \times (at\%_{Total} - at\%_{Cellulose}) / (at\%_{SOM} - at\%_{Cellulose}) \quad (1)$$

and

$$C_{Cellulose} = C_{Total} - C_{SOM} \quad (2)$$

with $at\%_{Total}$, $at\%_{SOM}$ and $at\%_{Cellulose}$ being the isotopic compositions (in $at\% \text{ }^{13}\text{C}$) of sampled CO₂, SOM and cellulose. For C_{mic} in the cellulose treatments, we again distinguished between C_{mic} derived from the added cellulose and from SOM using equations (1) and (2), replacing the concentrations and isotopic compositions of sampled CO₂ with those of C_{mic}.

Statistical analyses were performed with R. The main effects of the factors soil fraction, O₂ status, soil age and treatment (wo, addition of C, P or CP) on microbial activity and abundance parameters were determined by a four-way ANOVA with interactions. Pairwise comparisons for site age and treatment effect were

analyzed by a Tukey post hoc test (package lsmeans, Lenth, 2015). Therefore, the measured parameters and residuals were checked for normal-distribution and log-transformed if necessary. Since we got significant results for almost all factors for several parameters, we used a random effect model to estimate the variance components using the lmer function of the lme4 package (Bates et al., 2015) for determining the relative importance of each factor. To investigate the controls on microbial N cycling parameters and abundance patterns in HF samples under oxic and anoxic conditions we also used the variance component estimation.

3. Results

3.1. N mineralization

Both, the bulk soil and the HF (mineral-associated OM) were dominated by ON with N_{min} contributing only 1.3% to TN on average (Table 1). After 125 days of incubation, net N mineralization was above zero for both O₂ statuses, ranging between 0.8 and 13.1% N_{min}-N of initial TN content with higher values under oxic than anoxic conditions (Fig. 1). Inorganic N, released upon mineralization of the HF, largely exceeded the initial N_{min} contents by a factor of 4–23 (range of all tested incubation conditions including different O₂ statuses, site ages, treatments and replicates; n = 96). In contrast to net N mineralization, net nitrification was above zero only under oxic conditions (Fig. S2).

Net N mineralization and net nitrification significantly differed between soil fractions (Table 3) with 2.0 ± 0.9 -fold (mean \pm standard deviation) higher values for net N mineralization and lower ones for net nitrification in HF samples. Compared to bulk samples, net N mineralization in the HF differed more among the soil ages, as indicated by lower values at the two younger sites (0.5k and 5k) especially under anoxic conditions (Fig. 1). The addition of P enhanced net N mineralization of HF samples particularly in older soils, but it had almost no effect on bulk samples. In contrast, C addition resulted in lower values of net N mineralization in both soil fractions under oxic conditions, but rarely affected them under anoxic conditions.

Under anoxic conditions we detected N₂O as well as N₂ production (Fig. 2, Fig. S2), whereas under oxic conditions, N₂O emissions were below detection limit. The N₂O production accounted for up to 0.016% N₂O-N of initial TN content (51% N₂O-N of initial NO₃⁻ content, data not shown) for bulk samples, but was below detection limit for HF. For bulk samples, we detected a clear soil age effect with higher values at the 5k and 120k site while the addition of P or C did not significantly alter the N₂O production. Despite additional controls for gas leakage and carefully performed gas sampling, our N₂ data showed high standard deviations and proportions exceeding the TN content at the incubation start. Nevertheless, for all incubation treatments we detected a significantly higher N₂ production in the HF compared to bulk samples (Table 3, Fig. S2).

The controls of microbial N transformations differed between both soil fractions with N processes in the HF depending more on the O₂ status than bulk soils (Fig. 7). The effect of P and C addition had a larger impact under oxic than under anoxic conditions. For example, the oxic P and C treatment explained 11 and 24% of total variation of net N mineralization, respectively. In contrast, under anoxic conditions the soil age was far more important, accounting for 91% of total variation for net N mineralization (Table 4).

3.2. C mineralization and priming

Cumulative CO₂ production ranged between 0.03 and 3.3% of initial soil OC and was on average 18 ± 9 -fold (mean \pm standard

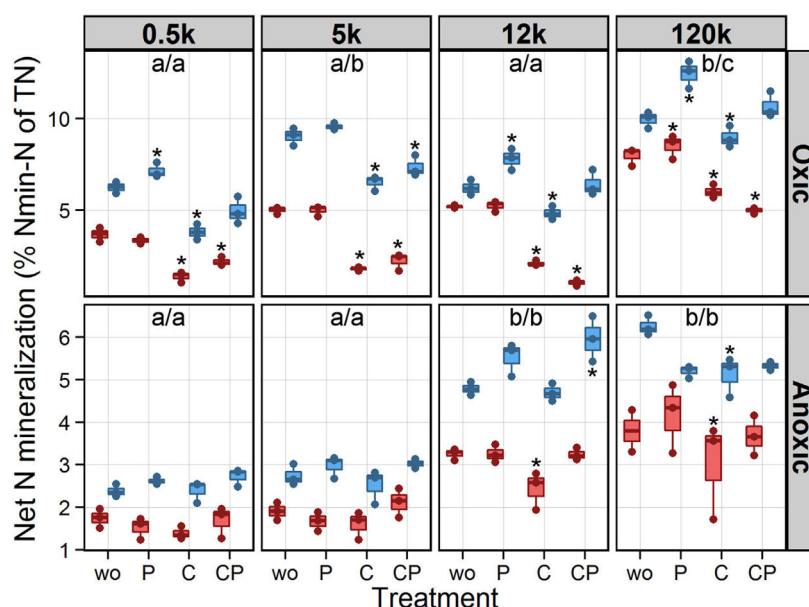


Fig. 1. Net N mineralization after 125 days of incubation for bulk (red boxplots) and HF (blue boxplots) samples of differently aged soils (0.5k, 5k, 12k, and 120k years) as percent of the initial TN content. For each soil age, samples were incubated under oxic and anoxic conditions and different substrate additions (wo, P, C, and CP) were tested. Boxplots represent values of the three incubation replicates. Results of Tukey post-hoc test for the soil age effect (averaged over all treatments per age) were indicated by letters (left–bulk/right–HF) with the same letters indicating that values for these ages differed not significantly ($P > 0.05$). Significant treatment effects ($P < 0.05$) of P, C, and CP addition compared to wo-treatment for bulk or HF sample were marked with asterisks. (For interpretation of the references to colour in this figure legend, the reader is referred to the web version of this article.)

Table 3

Effects of different soil properties on microbial N cycling and N-related microbial gene abundances as revealed by four-way ANOVA (interaction terms are shown in Table S2). The treatment effect included wo, P, C, and CP.

	O ₂	Fraction	Site age	Treatment
Net N mineralization	***	***	***	***
Net nitrification	***	***	n.s.	**
N ₂ production (anoxic)	–	***	***	***
N ₂ O production (anoxic)	–	***	***	n.s.
N _{mic}	***	n.s.	*	n.s.
Archaeal <i>amoA</i>	n.s.	***	***	**
<i>narG</i>	***	***	***	***
<i>chiA</i> (oxic)	–	***	***	***

*** $P < 0.001$, ** $0.001 < P < 0.01$; * $0.01 < P < 0.05$.
n.s.—not significant ($P > 0.05$).

deviation) higher under oxic conditions than under anoxic conditions (Fig. 3). The CO₂ production was lower in HF samples under anoxic conditions, whereas under oxic conditions we detected no consistent trend between the soil fractions. Adding ¹³C-labeled cellulose provided the opportunity to differentiate between cellulose- and SOM-derived CO₂ and to thereby detect a priming effect, i.e. higher SOM-derived CO₂ production in the C treatment compared to the wo-treatment. Positive priming occurred under oxic conditions not only for bulk soil, but also for the HF at the younger sites (0.5k and 5k) and when C and P were added simultaneously at the oldest site (Fig. 4). On the contrary, under anoxic conditions SOM-derived CO₂ production was even lower in the C and CP treatment compared to the cellulose-free treatments (wo, P).

3.3. Microbial biomass

The C_{mic} and N_{mic} contents showed similar patterns, and as

observed for microbial activities such as net N mineralization and CO₂ production, both were considerably higher under oxic than under anoxic conditions (Fig. 5 A, B). Both showed no significant differences between soil fractions and N_{mic} exhibited only small differences between soil ages. The C and partly the P addition only stimulated bulk C_{mic} and N_{mic}. The SOM-derived C_{mic} slightly increased due to P, C or CP addition under oxic conditions, but the effects were not significant (Fig. S3).

3.4. Abundances of N-related functional genes

Functional marker genes encoding enzymes that are part of the microbial N cycle were quantified via qPCR and were detected, if present, mostly in both soil fractions. Archaeal *amoA* gene copy numbers showed higher abundances at the older sites under oxic conditions (12k and 120k; Fig. 6A), whereas bacterial *amoA* gene copy numbers were below detection limit in almost all samples. Due to the low archaeal *amoA* gene copy numbers in HF samples (often below detection limit), a comparison of the effect of P and C additions between both soil fractions was not possible. The nitrate reductase encoding gene *narG* showed higher abundances in bulk samples under oxic conditions, whereas under anoxic conditions gene abundances were higher in the HF (Fig. 6B). The *narG* gene copy numbers were less affected by soil age, but overall decreased due to P or C addition. While P addition significantly lowered abundances in both soil fractions under anoxic conditions, only HF sample *narG* gene abundances were significantly lowered under oxic conditions. Further, under anoxic conditions the combination of P and C addition did not affect *narG* gene copy numbers in HF samples compared to P and C addition alone, whereas we detected a decrease for bulk samples. On the contrary, under oxic conditions *narG* gene copy numbers were similar for wo and CP treatment. The *chiA* gene could be detected under oxic but not anoxic conditions

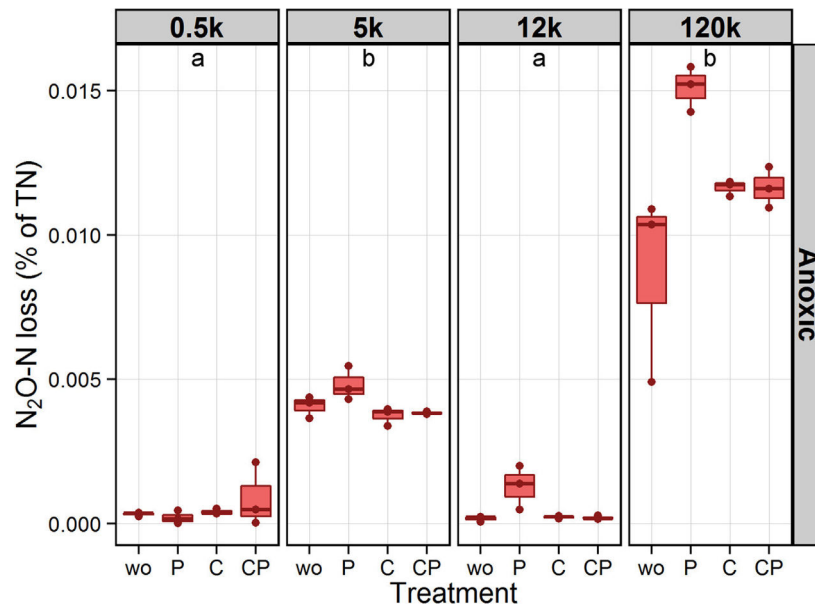


Fig. 2. N₂O-N production after 125 days of incubation for bulk samples (red boxplots) of differently aged soils (0.5k, 5k, 12k, and 120k years) as percent of the initial TN content. Values for HF samples were below detection limit. For each soil age, samples were incubated under oxic (not shown, values below detection limit) and anoxic conditions and different substrate additions (wo, P, C, and CP) were tested. Boxplots represent values of the three incubation replicates. Results of Tukey post-hoc test for the soil age effect (averaged over all treatments per age) were indicated by letters with the same letters indicating that values for these ages differed not significantly ($P > 0.05$). Treatment effects of P, C, and CP addition compared to wo-treatment for bulk samples were not significant ($P < 0.05$). (For interpretation of the references to colour in this figure legend, the reader is referred to the web version of this article.)

Table 4

Relative effect (as % of total variation) of different soil properties (age, P, C and their interactions) on microbial N cycling parameters and N-related abundances as well as on microbial biomass C and CO₂ production in HF samples under oxic and anoxic conditions as revealed by variance component estimation. Net Nmin: Net N mineralization, Net NO₃: Net nitrification.

	% of total variation									
	Net Nmin	Net NO ₃	N ₂ O	N _{mic}	Archaeal <i>amoA</i>	<i>narG</i>	<i>chiA</i>	C _{mic}	CO ₂	SOM-derived CO ₂
HF (oxic)										
Age	55	0	–	0	18	0	35	2	14	58
P	11	0	–	0	0	0	0	1	1	0
C	24	6	–	0	0	0	0	20	66	0
Age × P	1	0	–	7	0	3	44	0	5	3
Age × C	5	0	–	0	0	0	1	0	0	2
C × P	0	0	–	0	0	79	9	0	0	0
Age × P × C	0	0	–	35	82	5	1	0	9	23
Residual	4	94	–	58	0	13	10	77	5	14
HF (anoxic)										
Age	91	13	2	0	49	6	–	0	45	5
P	1	0	0	3	3	0	–	0	0	4
C	0	0	0	2	0	0	–	0	5	12
Age × P	3	24	0	0	11	0	–	0	14	0
Age × C	0	8	0	0	0	1	–	16	1	2
C × P	1	0	14	0	1	86	–	9	7	13
Age × P × C	0	0	0	20	0	1	–	17	11	23
Residual	3	54	85	75	35	6	–	57	17	41

and showed higher values for the P treatment of both soil fractions (Fig. 6C).

4. Discussion

4.1. Mineral-associated N is an important bioavailable N source for soil microorganisms

The results of our 125-days incubation experiment with the HF and bulk soil showed that Nmin released upon mineralization of

the HF far exceeded the initial Nmin contents by a factor of 4–23, thus indicating that mineral-associated N was the main source of bioavailable N in A horizons. This was generally reflected by (i) positive net N mineralization (Fig. 1), (ii) detectable N_{mic} and N-related microbial gene abundances both under oxic and anoxic conditions (Fig. 5 B, Fig. 6), as well as by (iii) a tendency towards higher N₂ production and higher NO₃-consumption under anoxic conditions (Fig. S2, Fig. S3), in the HF as compared to the bulk soil. While a short-term incubation experiment (18 h) suggested no relevance of HF-N for microbial N cycling (Compton and Boone,

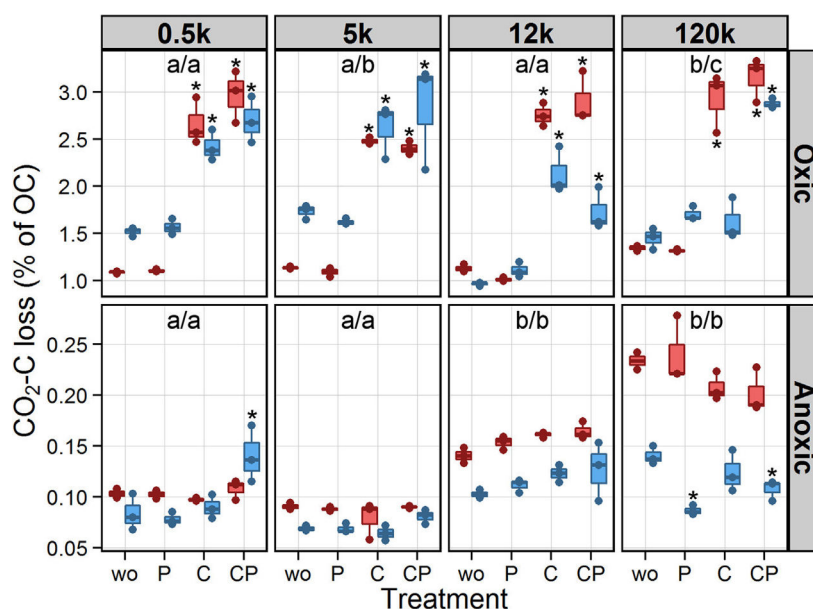


Fig. 3. CO₂-C production (including cellulose-derived) after 125 days of incubation for bulk (red boxplots) and HF (blue boxplots) samples of differently aged soils (0.5k, 5k, 12k, and 120k years) as percent of the initial OC content. For each soil age, samples were incubated under oxic and anoxic conditions and different substrate additions (wo, P, C, and CP) were tested. Boxplots represent values of the three incubation replicates. Results of Tukey post-hoc test for the soil age effect (averaged over all treatments per age) were indicated by letters (left–bulk/right–HF) with the same letters indicating that values for these ages differed not significantly ($P > 0.05$). Significant treatment effects ($P < 0.05$) of P, C, and CP addition compared to wo-treatment for bulk or HF sample were marked with asterisks. (For interpretation of the references to colour in this figure legend, the reader is referred to the web version of this article.)

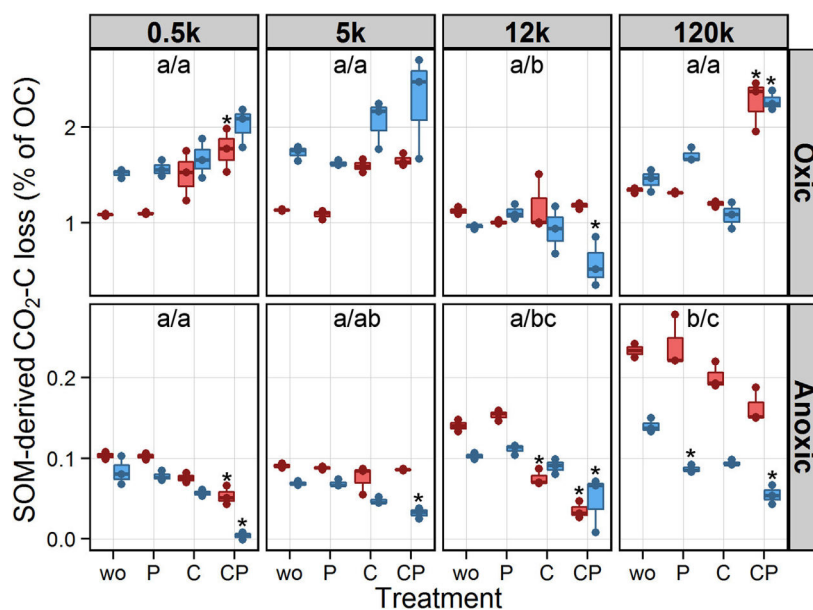


Fig. 4. SOM-derived CO₂-C production after 125 days of incubation for bulk (red boxplots) and HF (blue boxplots) samples of differently aged soils (0.5k, 5k, 12k, and 120k years) as percent of the initial OC content. For each soil age, samples were incubated under oxic and anoxic conditions and different substrate additions (wo, P, C, and CP) were tested. Boxplots represent values of the three incubation replicates. Results of Tukey post-hoc test for the soil age effect (averaged over all treatments per age) were indicated by letters (left–bulk/right–HF) with the same letters indicating that values for these ages differed not significantly ($P > 0.05$). Significant treatment effects ($P < 0.05$) of P, C, and CP addition compared to wo-treatment for bulk or HF sample were marked with asterisks. (For interpretation of the references to colour in this figure legend, the reader is referred to the web version of this article.)

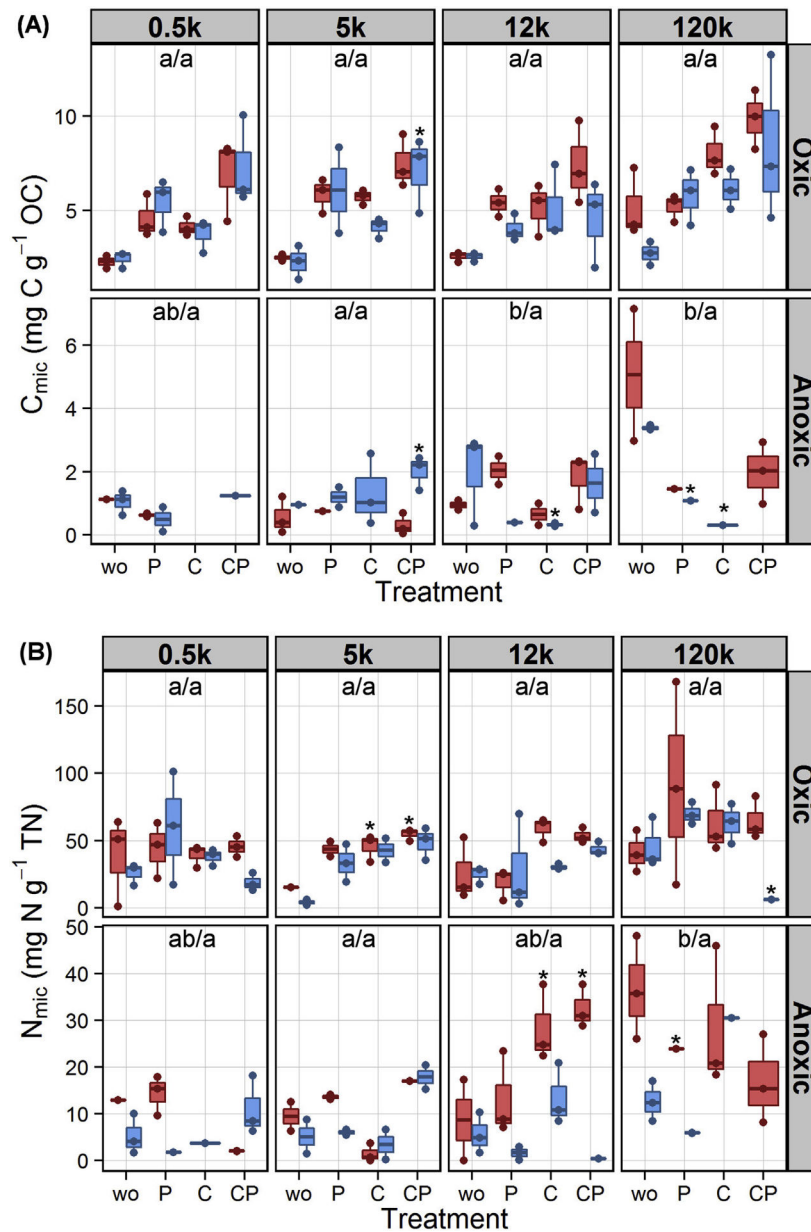


Fig. 5. (A) C_{mic} and (B) N_{mic} after 125 days of incubation for bulk (red boxplots) and HF (blue boxplots) samples of differently aged soils (0.5k, 5k, 12k, and 120k years) related to the initial OC and TN content, respectively. For each soil age, samples were incubated under oxic and anoxic conditions and different substrate additions (wo, P, C, and CP) were tested. Boxplots represent values of the three incubation replicates. Results of Tukey post-hoc test for the soil age effect (averaged over all treatments per age) were indicated by letters (left–bulk/right–HF) with the same letters indicating that values for these ages differed not significantly ($P > 0.05$). Significant treatment effects ($P < 0.05$) of P, C, and CP addition compared to wo-treatment for bulk or HF sample were marked with asterisks. (For interpretation of the references to colour in this figure legend, the reader is referred to the web version of this article.)

2002), Swanston et al. (2004) reported significant net N mineralization for the HF when conducting an incubation experiment over 300 d. In line with the previous study, our results also support the hypothesis that mineral-associated N is an important N source for soil microorganisms.

Besides the major effect of the O₂ status, the soil fraction itself (HF vs. bulk) had a significant effect on microbial N cycling and N-related microbial abundances with different trends for different

parameters (Table 3). The net N mineralization of the HF surprisingly was 2-fold higher than that of the bulk samples (Fig. 1), in line with results of an incubation experiment using different forest soil fractions, where higher values were mostly determined in the HF compared to whole soil samples (Sollins et al., 1984). In contrast, Swanston et al. (2004) reported for the HF net N mineralization values half as high as for bulk soil. One possible explanation for the higher HF net N mineralization in our study could be that, although

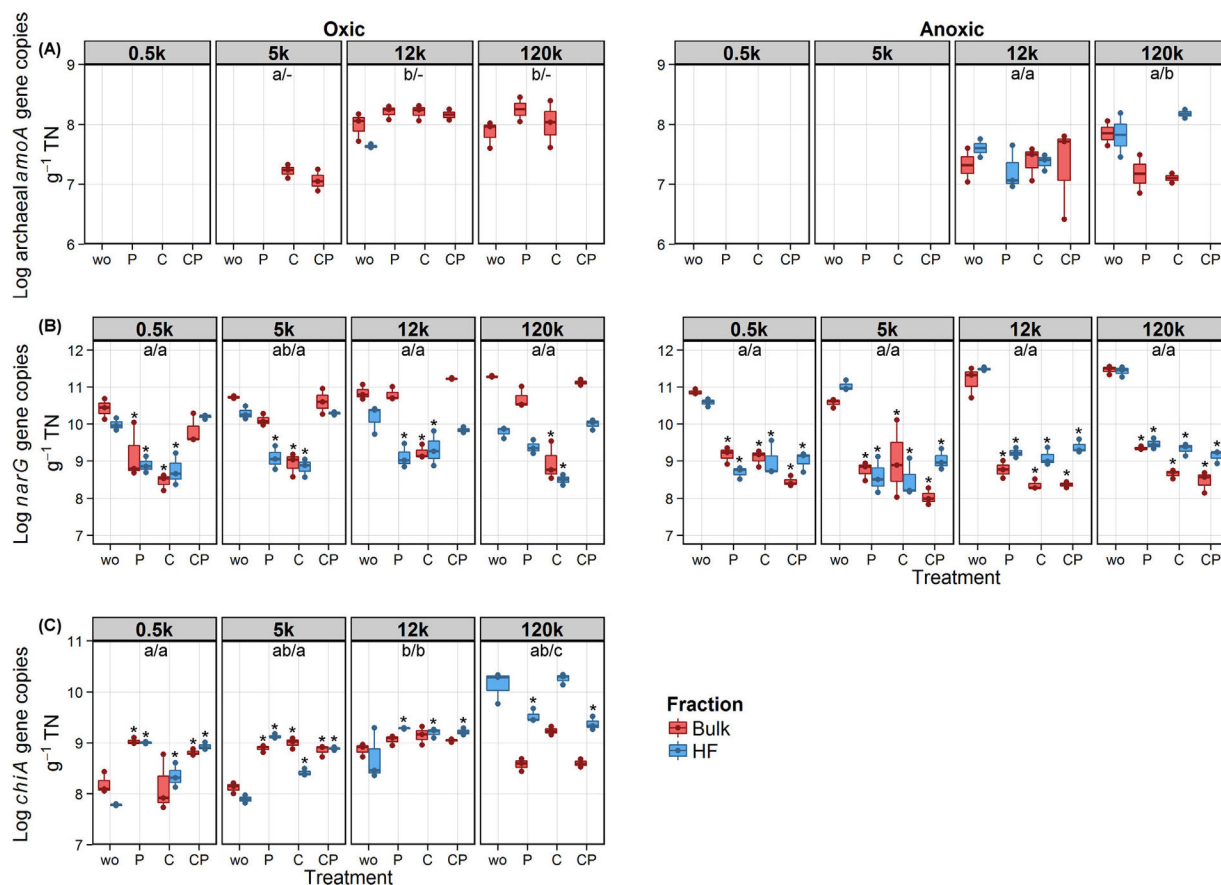


Fig. 6. Abundance of (A) archaeal *amoA*, (B) *narG*, and (C) bacterial *chiA* gene copies after 125 days of incubation for bulk (red boxplots) and HF (blue boxplots) samples of differently aged soils (0.5k, 5k, 12k, and 120k years) related to the initial TN content of the samples. For each soil age, samples were incubated under oxic and anoxic conditions and different substrate additions (wo, P, C, CP) were tested. Boxplots represent values of the three incubation replicates. Results of Tukey post-hoc test for the soil age effect (averaged over all treatments per age) were indicated by letters (left–bulk/right–HF) with the same letters indicating that values for these ages differed not significantly ($P > 0.05$). Significant treatment effects ($P < 0.05$) of P, C, and CP addition compared to wo-treatment for bulk or HF sample were marked with asterisks. (For interpretation of the references to colour in this figure legend, the reader is referred to the web version of this article.)

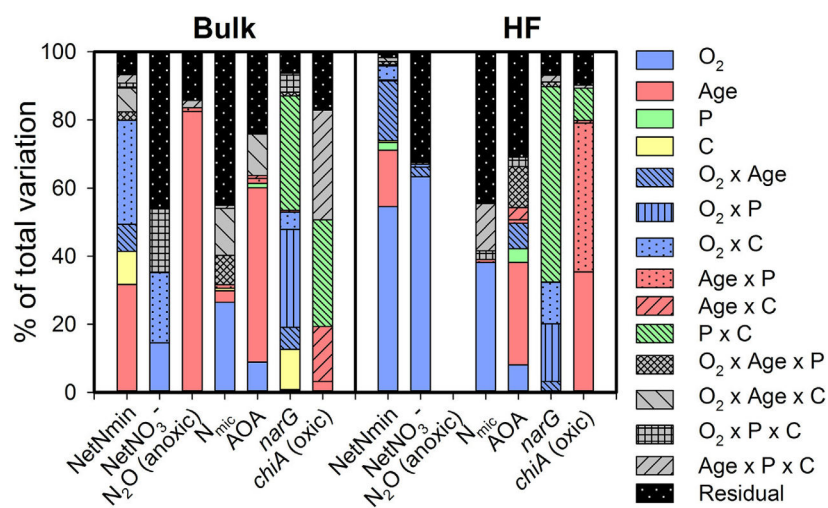


Fig. 7. Variance component estimation of factors (O_2 , soil age, P, and C addition) and their interactions controlling microbial N cycling and N-related functional gene abundances in bulk and HF samples. Net Nmin: Net N mineralization, Net NO_3^- : Net nitrification, AOA: abundance of archaeal *amoA* gene copies.

in both fractions a significant part of the ON was mineralized, a part of the produced positively charged NH_4^+ ions in the HF was adsorbed to negatively charged clay mineral surfaces or fixed into their interlayers, resulting in a lower bioavailability and lower microbial immobilization (Russow et al., 2008; Nieder et al., 2011), whereas in the bulk samples more NH_4^+ was immobilized by microbial assimilation activity and biomass production. Thereby, the strength of this effect may depend on the proportion of the HF in bulk soils as the absolute amount of minerals was higher in the HF incubations (since bulk soils still contained the LF). Thus, stabilization of NH_4^+ by clay minerals resulted in higher apparent net N mineralization in HF samples. This might also explain the different results between our study with about 95 wt% of HF on bulk soil compared to Swanston et al. (2004) with only 67–92 wt%. As another explanation Sollins et al. (1984) suggested that microorganisms could better degrade SOM of the LF (particulate OM), which is also part of the bulk soil, and therefore overall more N would be microbially immobilized by these samples. Both hypotheses would imply that microbial respiration in bulk samples should be higher than in HF samples, which was the case under anoxic conditions and for most samples under oxic conditions (Fig. 3). Finally, since density fractionation generally requires dispersion of the soil to remove particulate OM and thereby results in a larger spatial accessibility of the substrates to the microorganisms (Cerli et al., 2012), the higher net mineralization rates in the HF compared to bulk soil also could be partly related to the fractionation procedure. Even if this might be partly true, it is remarkably that N derived from mineral-organic associations is highly bioavailable supporting previous findings that stabilized SOM is not necessarily chemical recalcitrant (Mikutta et al., 2006; Kleber et al., 2010).

4.2. Oxygen status and N substrate type mainly control the utilization of mineral-associated N

The O_2 status representing different redox regimes mostly controlled the microbial cycling of mineral-associated N in soils (Fig. 7). The redox regime acts as a master control on microbe-catalyzed N transformations by specifically inhibiting or stimulating aerobic or anaerobic microorganisms and the corresponding N cycling processes (Pett-Ridge et al., 2006). Most parameters for microbial N cycling as well as respiration rates and microbial biomass were many times higher (lower for N_2 and N_2O) under oxic than anoxic conditions, reflecting the importance of this environmental parameter. Although we found similar patterns for the O_2 status as control on microbial N cycling for HF and bulk samples, the O_2 status had a more pronounced effect in the HF, especially on net N mineralization and net nitrification (Fig. 7).

As discussed above, under oxic conditions gross N mineralization and immobilization seem to be higher in bulk samples than in the HF, which coincided with higher copy numbers of archaeal *amoA* and *narG* genes (Fig. 6 A, B). In contrast, under anoxic conditions, *narG* gene copy numbers and N_2 production were higher in the HF than in bulk soil suggesting a preference for mineral-associated OM by soil microorganisms conducting NO_3^- -dependent processes (Fig. 6 B, Fig. S3). This is probably related to the charge of the N substrate ion – the negatively charged NO_3^- ion is even in the presence of mineral surfaces highly available (Heckman et al., 2013), whereas the availability of the NH_4^+ ion could be constrained by interaction with mineral surfaces. Consequently, the O_2 status seems to determine whether the mineral-associated N is more bioavailable or not by controlling the N pathway type and with this, the N bioavailability also depends on the properties, i.e. charge of the favored N substrate.

Surprisingly, N_2O production could only be detected in bulk samples under anoxic conditions (Fig. 2). However, we would have

expected generally low N_2O production rates because of the low NO_3^- concentrations at the beginning of the incubation (Table 1). Further, we expected lower N_2O values for bulk soil compared to the HF samples due to the higher C availability (as reflected by higher respiration rates, Fig. 3) that would favor the whole reduction pathway towards N_2 (Senbayram et al., 2012). Presumably, our converse patterns may be explained by differences in the community composition of NO_3^- -reducers. Similarly, higher N_2O production rates at the 5k and 120k sites may be connected to age-related differences in microbial community composition. This assumption is supported by Wallenstein et al. (2006) and references therein who reported for different soils with contrasting $\text{N}_2\text{O}:\text{N}_2$ product ratios that they varied considerably in their denitrifier communities. Further, for the soil ammonia-oxidizing archaeum *Nitrososphaera viennensis* it was reported that N_2O could be also produced via co-denitrification under oxygen depleted conditions (Spott et al., 2011; Stieglmeier et al., 2014) corresponding to the detected archaeal *amoA* gene copy numbers under anoxic conditions (Fig. 6A).

4.3. Impact of different soil ages reflecting a mineralogical gradient

Soil age was also one of the important controls on microbial cycling of mineral-associated N and N-related microbial abundances (Fig. 7, Table 4). All parameters were normalized to initial N and C contents of incubation samples to account for age-related effects caused by the nutrient gradient. Therefore, differences between younger (0.5k and 5k) versus older soils (12k and 120k) were most likely caused by the mineralogical gradient developing during soil pedogenesis (Table 2). Accordingly, in A horizons of the younger soils that were characterized by a higher content of clay and secondary Fe and Al phases, ON and the produced NH_4^+ were stabilized by these minerals and, thus, less bioavailable for soil microorganisms resulting in lower net N mineralization rates as well as lower archaeal *amoA* and *chiA* gene copy numbers (Figs. 1 and 6 A, C). This is supported by a sorption experiment with different clay minerals and Fe oxides, where the bioavailability of sorbed alanine was lowest for the Fe oxides (Dippold et al., 2014). In addition, several studies reported a preferential accumulation of N-containing compounds, such as proteins, in stabilized SOM due to interaction with metal oxides, especially at pH ranges below 7 (Pronk et al., 2013; Knicker, 2011). In contrast, net nitrification and *narG* gene copy numbers were hardly influenced by soil age (Fig. 7), confirming that NO_3^- -related pathways and abundances were less affected by mineralogical properties in line with the suggestion above that the NO_3^- -bioavailability is hardly impaired by soil minerals.

Soil age had a more pronounced effect on microbial N cycling and N-related microbial abundances in the HF under anoxic than under oxic conditions (Table 4). Similarly, net N mineralization of paddy soils was positively correlated with the content of organically complexed Fe under anoxic conditions, whereas under oxic conditions it was positively correlated with soil C and N content (Kader et al., 2013). We observed this relationship also for respiration rates, for which soil age had a major effect under anoxic rather than oxic conditions. Likewise, in incubation experiments with varying clay composition, mineralogy also had no significant or a minor effect on respiration rates under oxic conditions (Carson et al., 2007; Pronk et al., 2013; Vogel et al., 2014).

In summary, our results showed an inhibition of microbial ON and NH_4^+ turnover due to a reduced bioavailability caused by soil minerals (Fe oxides and clay minerals). Nevertheless, part of this mineral-associated N can well be utilized by soil microorganisms, while the bioavailability strongly depends on the N substrate type and soil mineralogical composition.

4.4. P addition—enhanced cycling of mineral-associated N especially at P-limited sites?

Although the effect of P addition was generally minor compared to the effect of O₂ status and soil age, it significantly enhanced net N mineralization in HF samples in older, P-limited soils (12k and 120k) especially under oxic conditions (Fig. 1). In contrast, in bulk samples P addition had almost no effect. Previous findings showed that organic P and total P were preferentially sorbed by Fe and Al oxide (Heckman et al., 2013; Swenson et al., 2015), probably resulting in a lower bioavailability of P. As a result, P limitation at the older sites would be aggravated in mineral-enriched HF samples. Hence, the addition of P had a stronger effect in HF samples by mitigating the P limitation and stimulating microbial activity and thereby N mineralization. A positive effect of P addition on net N mineralization in soils with low P content was also reported for a pot experiment and a fertilization experiment in the field (Falkiner et al., 1993; calculated from Baral et al., 2014).

However, P addition had either almost no stimulating (*chiA*), or even an inhibiting effect (*narG*) on N functional gene copy numbers in HF samples, probably as a result of the overall weak effect of P on microbial N cycling in this experiment.

4.5. Priming via cellulose—enhanced mineralization of mineral-associated N?

Under oxic conditions, the addition of ¹³C-labeled cellulose tends to increase SOM-derived CO₂ production compared to the wo-treatment for the two younger soils and for the CP treatment of the oldest soil suggesting a general priming effect for both, bulk soil and the HF (Fig. 4). This indicates that the mineralization of mineral-associated OM in A horizons could be primed by an easily available substrate like cellulose as described previously for bulk samples in subsoils (Fontaine et al., 2007). However, C addition showed no consistent fraction-related trend for SOM-derived CO₂ production, similar to general soil respiration rates. These findings were supported by several studies reporting that general respiration rates were hardly affected by mineralogical properties (Heckman et al., 2013; Vogel et al., 2014). Microbial incorporation of SOM-derived C into the biomass was also slightly stimulated by cellulose addition in both fractions, but showed no significant trends for treatments or soil age (Fig. S4).

The stimulation of microbial respiration under oxic conditions upon cellulose amendment (Fig. 3) decreased net N mineralization likely due to higher microbial N immobilization in both fractions (Fig. 1; Vinten et al., 2002). The analysis of 84 mineral soils under different vegetation type confirmed that the C content was one of the most important drivers, exerting a negative effect on net N mineralization (Colman and Schimel, 2013). However, similarly to P addition, N functional gene abundances were hardly affected by C addition in HF samples pointing to a weak cellulose effect, too. Overall, under oxic conditions the cellulose-induced priming effect of microbial respiration had a minor effect on cycling of mineral-associated N. This may be related to a shift from N to a more pronounced C cycling with N immobilization causing an inhibition of N cycling-related processes by cellulose as an easy degradable, but N-free substrate.

In contrast, under anoxic conditions lower values of SOM-derived CO₂ for C treatments pointed to a “negative” priming effect (Fig. 4) indicating a slower degradation of SOM and a preferential respiration of the added cellulose (Kuzuyakov et al., 2000), that was hardly impacted by mineral interactions.

4.6. Conclusions

Our results of the microcosm incubation experiment indicate

that mineral-associated N provides an important bioavailable N source for soil microorganisms in mineral topsoil horizons. The bioavailability of this fraction is mostly controlled by the O₂ status in connection with N substrate characteristics and the soil mineralogical composition. Thus, microbial ON and NH₄⁺ transformations were inhibited by soil minerals due to a lower substrate bioavailability, whereas microbial processes and abundances depending on NO₃⁻ were not affected by soil mineralogical properties. In comparison to O₂ status and soil age, the addition of P and C had only a minor effect on mineral-associated N turnover. The addition of P hardly enhanced the microbial utilization of mineral-associated N despite a significant stimulation of net N mineralization in P-limited soils. Cellulose addition tends to stimulate the degradation of SOM under oxic conditions, but may inhibit net N mineralization of mineral-associated N.

Though further research is necessary to disentangle the effects of different soil fractions on particular N pathways and to assess the impact of mineral-associated N on terrestrial N cycling, our study highlights the relevance of mineral-organic associations as an important source of bioavailable, mineralizable N for microbial N cycling in mineral soils. It provides first insights into the complex interactions between the soil mineral phase and microbial N transformations as well as abundances of the corresponding soil microorganisms that exert a great impact on soil fertility and productivity.

Acknowledgements

We thank Roger Michael Klatt and Leo M. Condon for the help with preparation and realization of the sampling, Peter C. Almond, Duane A. Peltzer and Sarah J. Richardson for access to the sampling sites, Norman Gentsch and Norbert Bischoff for advice and discussion on setup and results of the incubation experiment and on analysis of gas measurements, Daria Frohloff and Gudrun Mengeljung for technical support with the DNA extraction, Florian Stange for discussion of the data and reading the manuscript, and Christian Siebenbürgen for help with graphical issues. The AOB standard for qPCR was kindly provided by the ‘Aquatic Geomicrobiology’ Group, University of Jena, Germany, and the *Streptomyces* strain for the *chiA* qPCR standard was kindly provided by the ‘Environmental Microbiology’ Group, TU Bergakademie Freiberg, Germany. Funding was provided by the German Research Foundation (DFG) [MI 1377/5-2 to R.M. and SCHI 535/11-2 to A.S.].

Appendix A. Supplementary data

Supplementary data related to this article can be found at <http://dx.doi.org/10.1016/j.soilbio.2016.10.010>.

References

- Achat, D.L., Augusto, L., Bakker, M.R., Gallet-Budynek, A., Morel, C., 2012. Microbial processes controlling P availability in forest spodosols as affected by soil depth and soil properties. *Soil Biology and Biochemistry* 44, 39–48.
- Almond, P.C., Moar, N.T., Lian, O.B., 2001. Reinterpretation of the glacial chronology of South Westland, New Zealand. *New Zealand Journal of Geology and Geophysics* 44, 1–15.
- Baral, B.R., Kuyper, T.W., Van Groenigen, J.W., 2014. Liebig's law of the minimum applied to a greenhouse gas: alleviation of P-limitation reduces soil N₂O emission. *Plant and Soil* 374, 539–548.
- Bates, D., Mächler, M., Bolker, B., Walker, S.C., 2015. Fitting linear mixed-effects models using lme4. *Journal of Statistical Software* 67, 1–48.
- Bayan, M., Eivazi, F., 1999. Selected enzyme activities as affected by free iron oxides and clay particle size. *Communications in Soil Science and Plant Analysis* 30, 1561–1571.
- Bimüller, C., Mueller, C.W., von Lütow, M., Kreyling, O., Kölbl, A., Haug, S., Schloter, M., Kögel-Knabner, I., 2014. Decoupled carbon and nitrogen mineralization in soil particle size fractions of a forest topsoil. *Soil Biology and Biochemistry* 78, 263–273.

- Blackwood, C.B., Paul, E.A., 2003. Eubacterial community structure and population size within the soil light fraction, rhizosphere, and heavy fraction of several agricultural systems. *Soil Biology and Biochemistry* 35, 1245–1255.
- Bru, D., Sarr, A., Philippot, L., 2007. Relative abundances of proteobacterial membrane-bound and periplasmic nitrate reductases in selected environments. *Applied and Environmental Microbiology* 73, 5971–5974.
- Carson, J.K., Rooney, D., Gleeson, D.B., Clipson, N., 2007. Altering the mineral composition of soil causes a shift in microbial community structure. *FEMS Microbiology Ecology* 61, 414–423.
- Cerli, C., Celi, L., Kalbitz, K., Guggenberger, G., Kaiser, K., 2012. Separation of light and heavy organic matter fractions in soil—testing for proper density cut-off and dispersion level. *Geoderma* 170, 403–416.
- Colman, B.P., Schimel, J.P., 2013. Drivers of microbial respiration and net N mineralization at the continental scale. *Soil Biology and Biochemistry* 60, 65–76.
- Compton, J.E., Boone, R.D., 2002. Soil nitrogen transformations and the role of light fraction organic matter in forest soils. *Soil Biology and Biochemistry* 34, 933–943.
- Crow, S.E., Swanston, C.W., Lajtha, K., Brooks, J.R., Keirstead, H., 2007. Density fractionation of forest soils: methodological questions and interpretation of incubation results and turnover time in an ecosystem context. *Biogeochemistry* 85, 69–90.
- Dippold, M., Biryukov, M., Kuzyakov, Y., 2014. Sorption affects amino acid pathways in soil: implications from position-specific labeling of alanine. *Soil Biology and Biochemistry* 72, 180–192.
- Falkiner, R.A., Khanna, P.K., Raison, R.J., 1993. Effect of superphosphate addition on N mineralization in some Australian forest soils. *Australian Journal of Soil Research* 31, 285–296.
- Fontaine, S., Barot, S., Barré, P., Bdioui, N., Mary, B., Rumpel, C., 2007. Stability of organic carbon in deep soil layers controlled by fresh carbon supply. *Nature* 450, 277–280.
- Francis, C.A., Roberts, K.J., Beman, J.M., Santoro, A.E., Oakley, B.B., 2005. Ubiquity and diversity of ammonia-oxidizing archaea in water columns and sediments of the ocean. *Proceedings of the National Academy of Sciences of the United States of America* 102, 14683–14688.
- Gentsch, N., Mikutta, R., Shibistova, O., Wild, B., Schneckler, J., Richter, A., Ulrich, T., Gittel, A., Santrúcková, H., Barta, J., Lashchinskiy, N., Mueller, C.W., Fuß, R., Guggenberger, G., 2015. Properties and bioavailability of particulate and mineral-associated organic matter in Arctic permafrost soils, Lower Kolyma Region, Russia. *European Journal of Soil Science* 66, 722–734.
- Heckman, K., Welty-Bernard, A., Vazquez-Ortega, A., Schwartz, E., Chorover, J., Rasmussen, C., 2013. The influence of goethite and gibbsite on soluble nutrient dynamics and microbial community composition. *Biogeochemistry* 112, 179–195.
- Kader, M.A., Sleutel, S., Begum, S.A., Moslehuddin, A.Z.M., De Neve, S., 2013. Nitrogen mineralization in sub-tropical paddy soils in relation to soil mineralogy, management, pH, carbon, nitrogen and iron contents. *European Journal of Soil Science* 64, 47–57.
- Kleber, M., Eusterhues, K., Keiluweit, M., Mikutta, C., Mikutta, R., Nico, P.S., 2015. Mineral-organic associations: formation, properties, and relevance in soil environments. *Advances in Agronomy* 130, 1–140.
- Kleber, M., Nico, P.S., Plante, A., Filley, T., Kramer, M., Swanston, C., Sollins, P., 2011. Old and stable soil organic matter is not necessarily chemically recalcitrant: implications for modeling concepts and temperature sensitivity. *Global Change Biology* 17, 1097–1107.
- Knicker, H., 2011. Soil organic N—an under-rated player for C sequestration in soils? *Soil Biology and Biochemistry* 43, 1118–1129.
- Kuzyakov, Y., Friedel, J.K., Stahr, K., 2000. Review of mechanisms and quantification of priming effects. *Soil Biology and Biochemistry* 32, 1485–1498.
- Lenth, R., 2015. *Lsmeans: Least-squares Means*. <https://CRAN.R-project.org/package=lsmeans>.
- Lofthfield, N., Flessa, H., Augustin, J., Beese, F., 1997. Automated gas chromatographic system for rapid analysis of the atmospheric trace gases methane, carbon dioxide, and nitrous oxide. *Journal of Environmental Quality* 26, 560–564.
- Mikutta, R., Kleber, M., Torn, M.S., Jahn, R., 2006. Stabilization of soil organic matter: association with minerals or chemical recalcitrance? *Biogeochemistry* 77, 25–56.
- Mikutta, R., Mikutta, C., Kalbitz, K., Scheel, T., Kaiser, K., Jahn, R., 2007. Biodegradation of forest floor organic matter bound to minerals via different binding mechanisms. *Geochimica et Cosmochimica Acta* 71, 2569–2590.
- Nannipieri, P., Smalla, K., 2006. *Nucleic Acids and Proteins in Soil*. Springer-Verlag, Berlin, Heidelberg, New York.
- Nicolaisen, M.H., Risgaard-Petersen, N., Revsbech, N.P., Reichardt, W., Ramsing, N.B., 2004. Nitrification-denitrification dynamics and community structure of ammonia oxidizing bacteria in a high yield irrigated Philippine rice field. *FEMS Microbiology Ecology* 49, 359–369.
- Nieder, R., Benbi, D.K., Scherer, H.W., 2011. Fixation and defixation of ammonium in soils: a review. *Biology and Fertility of Soils* 47, 1–14.
- Pett-Ridge, J., Silver, W.L., Firestone, M.K., 2006. Redox fluctuations frame microbial community impacts on N-cycling rates in a humid tropical forest soil. *Biogeochemistry* 81, 95–110.
- Pronk, G.J., Heister, K., Kögel-Knabner, I., 2013. Is turnover and development of organic matter controlled by mineral composition? *Soil Biology and Biochemistry* 67, 235–244.
- R Core Team, 2015. *R: a language and environment for statistical computing*. R Foundation for Statistical Computing, Vienna, Austria.
- Richardson, S.J., Peltzer, D.A., Allen, R.B., McGlone, M.S., Parfitt, R.L., 2004. Rapid development of phosphorus limitation in temperate rainforest along the Franz Josef soil chronosequence. *Oecologia* 139, 267–276.
- Robertson, G.P., Groffman, P.M., 2015. *Nitrogen Transformations*. In: Paul, E.A. (Ed.), *Soil Microbiology, Ecology, and Biochemistry*. Academic Press, Amsterdam, Boston, Heidelberg, London, New York, Oxford, Paris, San Diego, San Francisco, Singapore, Sydney, Tokyo, pp. 421–446.
- Russow, R., Spott, O., Stange, C.F., 2008. Evaluation of nitrate and ammonium as sources of NO and N₂O emissions from black earth soils (Haplic Chernozem) based on ¹⁵N field experiments. *Soil Biology and Biochemistry* 40, 380–391.
- Saidy, A.R., Smernik, R.J., Baldock, J.A., Kaiser, K., Sanderman, J., Macdonald, L.M., 2012. Effects of clay mineralogy and hydrous iron oxides on labile organic carbon stabilisation. *Geoderma* 173–174, 104–110.
- Schmidt, M.W.L., Torn, M.S., Abiven, S., Dittmar, T., Guggenberger, G., Janssens, I.A., Kleber, M., Kögel-Knabner, I., Lehmann, J., Manning, D.A.C., Nannipieri, P., Rasse, D.P., Weiner, S., Trumbore, S.E., 2011. Persistence of soil organic matter as an ecosystem property. *Nature* 478, 49–56.
- Schneider, M.P.W., Scheel, T., Mikutta, R., van Hees, P., Kaiser, K., Kalbitz, K., 2010. Sorptive stabilization of organic matter by amorphous Al hydroxide. *Geochimica et Cosmochimica Acta* 74, 1606–1619.
- Senbayram, M., Chen, R., Budai, A., Bakken, L., Dittert, K., 2012. N₂O emission and the N₂O/(N₂O+N₂) product ratio of denitrification as controlled by available carbon substrates and nitrate concentrations. *Agriculture, Ecosystems and Environment* 147, 4–12.
- Sollins, P., Spycher, G., Glassman, C.A., 1984. Net nitrogen mineralization from light- and heavy-fraction soil organic matter. *Soil Biology and Biochemistry* 16, 31–37.
- Spott, O., Russow, R., Stange, C.F., 2011. Formation of hybrid N₂O and hybrid N₂ due to codenitrification: first review of a barely considered process of microbially mediated N-nitrosation. *Soil Biology and Biochemistry* 43, 1995–2011.
- Stevens, P.R., 1968. *A Chronosequence of Soils Near the Franz Josef Glacier* (Ph.D Thesis). University of Canterbury, New Zealand.
- Stieglmeier, M., Mooshammer, M., Kitzler, B., Wanek, W., Zechmeister-Boltenstern, S., Richter, A., Schleper, C., 2014. Aerobic nitrous oxide production through N-nitrosating hybrid formation in ammonia-oxidizing archaea. *The ISME Journal* 8, 1135–1146.
- Swanston, C., Homann, P.S., Caldwell, B.A., Myrold, D.D., Ganio, L., Sollins, P., 2004. Long-term effects of elevated nitrogen on forest soil organic matter stability. *Biogeochemistry* 70, 227–250.
- Swenson, T.L., Bowen, B.P., Nico, P.S., Northen, T.R., 2015. Competitive sorption of microbial metabolites on an iron oxide mineral. *Soil Biology and Biochemistry* 90, 34–41.
- Turner, S., Schippers, A., Meyer-Stüve, S., Guggenberger, G., Gentsch, N., Dohrmann, R., Condron, L.M., Eger, A., Almond, P.C., Peltzer, D.A., Richardson, S.J., Mikutta, R., 2014. Mineralogical impact on long-term patterns of soil nitrogen and phosphorus enzyme activities. *Soil Biology and Biochemistry* 68, 31–43.
- Vance, E., Brookes, P., Jenkinson, D., 1987. An extraction method for measuring soil microbial biomass C. *Soil Biology and Biochemistry* 19, 703–707.
- Vinten, A.J.A., Whitmore, A.P., Bloem, J., Howard, R., Wright, F., 2002. Factors affecting N immobilisation/mineralisation kinetics for cellulose-, glucose- and straw-amended sandy soils. *Biology and Fertility of Soils* 36, 190–199.
- Vogel, C., Babin, D., Pronk, G.J., Heister, K., Smalla, K., Kögel-Knabner, I., 2014. Establishment of macro-aggregates and organic matter turnover by microbial communities in long-term incubated artificial soils. *Soil Biology and Biochemistry* 79, 57–67.
- Vogel, C., Heister, K., Buegger, F., Tanuwidjaja, I., Haug, S., Schlöter, M., Kögel-Knabner, I., 2015. Clay mineral composition modifies decomposition and sequestration of organic carbon and nitrogen in fine soil fractions. *Biology and Fertility of Soils* 51, 427–442.
- Wallenstein, M.D., Myrold, D.D., Firestone, M., Voytek, M., 2006. Environmental controls on denitrifying communities and denitrification rates: insights from molecular methods. *Ecological Applications* 16, 2143–2152.
- Webster, G., Newberry, C.J., Fry, J.C., Weightman, A.J., 2003. Assessment of bacterial community structure in the deep sub-seafloor biosphere by 16S rDNA-based techniques: a cautionary tale. *Journal of Microbiological Methods* 55, 155–164.
- Yergeau, E., Kang, S., He, Z., Zhou, J., Kowalchuk, G.A., 2007. Functional microarray analysis of nitrogen and carbon cycling genes across an Antarctic latitudinal transect. *The ISME Journal* 1, 163–179.

Supplementary material

Table S1

Primers and conditions for qPCR assays.

Primer	Sequence (5'-3') & qPCR conditions	Pc ¹ (μ M)	MM ²	Standard	Eff ³	Reference
Archaeal <i>amoA</i> gene						
Arch-amoAF	STA ATG GTC TGG CTT AGA CG	0.4	F	AOA-NZ-Mix	88.1-93.0	Francis et al., 2005
Arch-amoAR	GCG GCC ATC CAT CTG TAT GT					
	95°C-10 min; 42x: 95°C-1 min, 53°C-30 sec, 75°C-1 min; 95°C-15 sec					
Bacterial <i>amoA</i> gene						
amoA-1F	GGG GTT TCT ACT GGT GGT	0.4	P	<i>Nitroso-monas multiformis</i> clone	80.1-86.3	Nicolaisen et al., 2004
amoA-2R	CCC CTC KGS AAA GCC TTC TTC					
	95°C-10 min; 45x: 95°C-45 sec, 57°C-30 sec, 72°C-1 min, 80°C-20 sec; 95°C-1 min					
Bacterial <i>narG</i> gene						
narG-F	TGC CCS ATY CCG GCS ATG TC	1	AB	<i>Pseudo-monas stutzeri</i>	82.1-84.8	Bru et al., 2007
narG-R	GAG TTG TAC CAG TCR GCS GAY TCS G					
	95°C-15 min; 6x: 95°C-30 sec, 63°C(-0.5°C/cycle)-30 sec, 72°C-30 sec, 80°C-30 sec; 36x: 95°C-30 sec, 58°C-30 sec, 72°C-30 sec, 80°C-30 sec; 95°C-30 sec					
Bacterial <i>chiA</i> gene						
GA1F	CGTCGACATCGACTGGGARTDBCC	1	F	<i>Streptomyces fradiae</i>	92.7-96.0	Yergeau et al., 2007
GA1R	ACGCCGGTCCAGCCNCKNCCRTA					
	95°C-10 min; 40x: 95°C-1 min, 63°C-1 min, 72°C-1 min, 80°C-15 sec; 95°C-15 sec					

¹ Primer concentration

² Mastermix: F – FastStart Universal SYBR Green Master (ROX) (Roche, Rotkreuz, Switzerland), P – Platinum SYBR Green qPCR SuperMix-UDG with ROX (Life Technologies, Carlsbad, CA, US), AB – Absolute QPCR SYBR Green ROX Mix (Thermo Scientific, Waltham, MA, US)

³ Efficiency.

Table S2

Effects of different soil properties on microbial N cycling and N-related microbial gene abundances as revealed by four-way ANOVA (two- and three-way interaction terms). Frac – Fraction, Age – Site age, Treat – Treatment (wo, P, C, CP).

	O ₂ × Frac	O ₂ × Age	O ₂ × Treat	Frac × Age	Frac × Treat	Age × Treat	O ₂ × Frac × Age	O ₂ × Frac × Treat	O ₂ × Age × Treat	Frac × Age × Treat
Net N mineralization	***	***	***	***	***	n.s.	***	***	***	***
Net nitrification	n.s.	n.s.	***	n.s.	n.s.	n.s.	n.s.	**	n.s.	n.s.
N ₂ production (anoxic)	-	-	-	n.s.	n.s.	n.s.	-	-	-	n.s.
N ₂ O production (anoxic)	-	-	-	***	*	n.s.	-	-	-	n.s.
N _{mic}	n.s.	n.s.	n.s.	*	*	***	n.s.	n.s.	*	**
Archaeal <i>amoA</i>	***	n.s.	n.s.	***	n.s.	**	**	n.s.	*	n.s.
<i>narG</i>	***	***	***	n.s.	***	*	***	***	**	**
<i>chiA</i> (oxic)	-	-	-	***	n.s.	***	-	-	-	***

*** P < 0.001, ** 0.001 < P < 0.01; * 0.01 < P < 0.05; n.s. – not significant (P > 0.05)

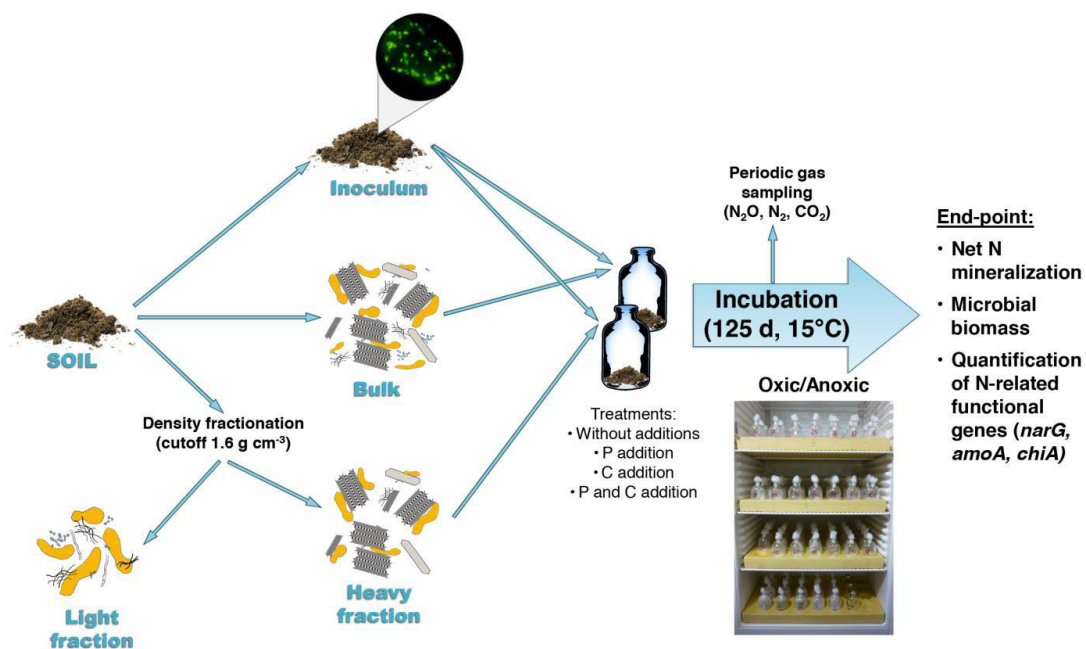


Fig. S1. Schematic overview of the incubation experiment setup (photographs courtesy of Christian Siebenbürgen and Norman Gentsch).

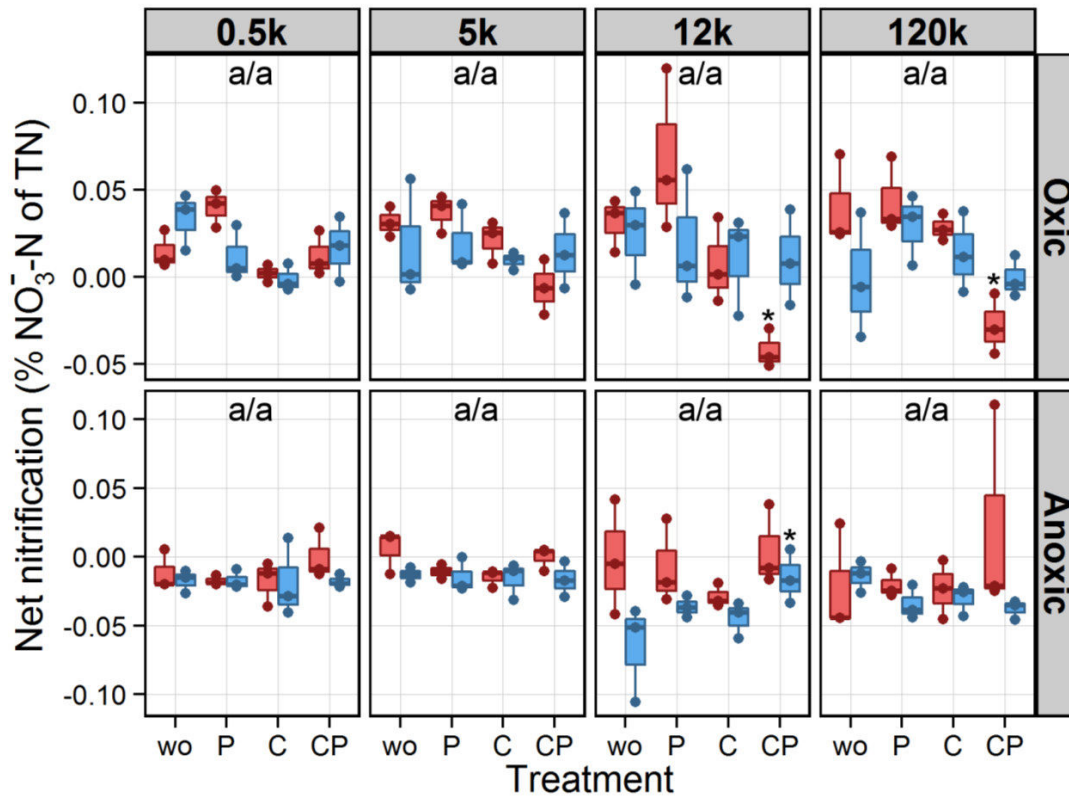


Fig. S2. Net nitrification after 125 days of incubation for bulk (red boxplots) and HF (blue boxplots) samples of differently aged soils (0.5k, 5k, 12k, and 120k years) as percent of the initial TN content. For each soil age, samples were incubated under oxic and anoxic conditions and different substrate additions (wo, P, C, and CP) were tested. Boxplots represent values of the three incubation replicates. Results of Tukey post-hoc test for the soil age effect (averaged over all treatments per age) were indicated by letters (left – bulk / right – HF) with the same letters indicating that values for these ages differed not significantly ($P > 0.05$). Significant treatment effects ($P < 0.05$) of P, C and CP addition compared to wo-treatment for bulk or HF sample were marked with asterisks.

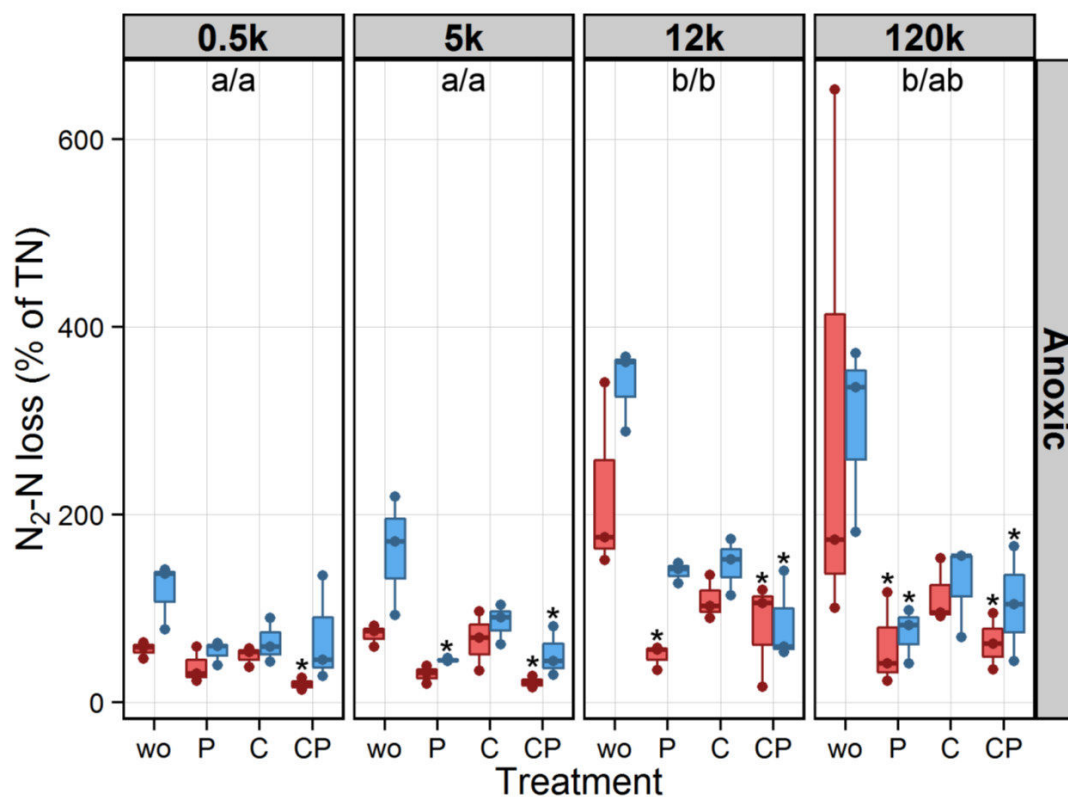


Fig. S3. N_2-N production after 125 days of incubation for bulk (red boxplots) and HF (blue boxplots) samples of differently aged soils (0.5k, 5k, 12k, and 120k years) as percent of the initial TN content. For each soil age, samples were incubated under anoxic conditions and different substrate additions (wo, P, C, and CP) were tested. Boxplots represent values of the three incubation replicates. Results of Tukey post-hoc test for the soil age effect (averaged over all treatments per age) were indicated by letters (left – bulk / right – HF) with the same letters indicating that values for these ages differed not significantly ($P > 0.05$). Significant treatment effects ($P < 0.05$) of P, C and CP addition compared to wo-treatment for bulk or HF sample were marked with asterisks.

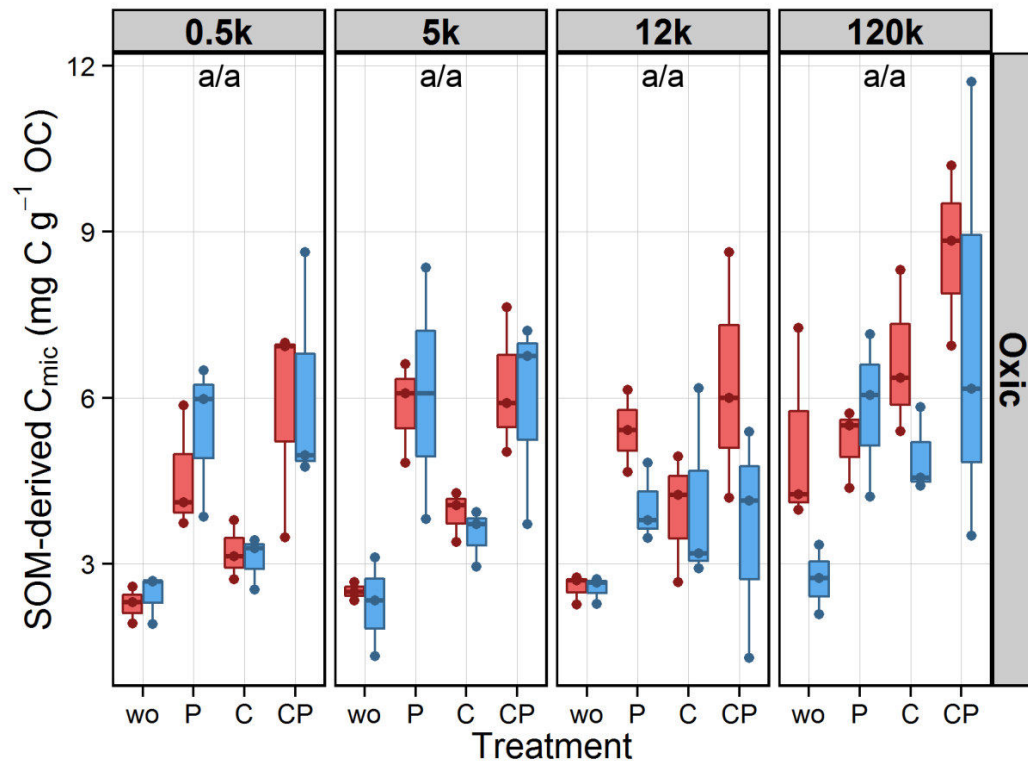


Fig. S4. SOM-derived C_{mic} after 125 days of incubation for bulk (red boxplots) and HF (blue boxplots) samples of differently aged soils (0.5k, 5k, 12k, and 120k years) related to the initial OC content of the samples. For each soil age, samples were incubated under conditions and different substrate additions with ¹³C-labeled cellulose (C and CP) were tested. Boxplots represent values of the three incubation replicates. Results of Tukey post-hoc test for the soil age effect (averaged over all treatments per age) were indicated by letters (left – bulk / right – HF) with the same letters indicating that values for these ages differed not significantly ($P > 0.05$). Treatment effects of P, C and CP addition compared to wo-treatment for bulk and HF samples were not significant ($P < 0.05$).

References

- Bru, D., Sarr, A., Philippot, L., 2007. Relative abundances of proteobacterial membrane-bound and periplasmic nitrate reductases in selected environments. *Appl. Environ. Microbiol.* 73, 5971–5974.
- Francis, C.A., Roberts, K.J., Beman, J.M., Santoro, A.E., Oakley, B.B., 2005. Ubiquity and diversity of ammonia-oxidizing archaea in water columns and sediments of the ocean. *Proc. Natl. Acad. Sci. U. S. A.* 102, 14683–14688.
- Nicolaisen, M.H., Risgaard-Petersen, N., Revsbech, N.P., Reichardt, W., Ramsing, N.B., 2004. Nitrification-denitrification dynamics and community structure of ammonia oxidizing bacteria in a high yield irrigated Philippine rice field. *FEMS Microbiol. Ecol.* 49, 359–369.
- Yergeau, E., Kang, S., He, Z., Zhou, J., Kowalchuk, G.A., 2007. Functional microarray analysis of nitrogen and carbon cycling genes across an Antarctic latitudinal transect. *ISME J.* 1, 163–179.

List of publications

- Buongiorno J, **Turner S**, Webster G, Asai M, Shumaker AK, Roy T, Weightman A, Schippers A, Lloyd KG (2017) Interlaboratory quantification of Bacteria and Archaea in deeply buried sediments of the Baltic Sea (IODP Expedition 347). *FEMS Microbiology Ecology* 93:fix007.
- Dietel J, Dohrmann R, Guggenberger G., Meyer-Stüve S, **Turner S**, Schippers A, Kaufhold S, Butz-Braun R, Condon LM, Mikutta R (2017) Complexity of clay mineral formation during 120,000 years of soil development along the Franz Josef chronosequence, New Zealand. *New Zealand Journal of Geology and Geophysics* 6:23-35.
- Gentsch N, Wild B, Mikutta R, Čapek P, Diáková K, Schrumpf M, **Turner S**, Minnich C, Schaarschmidt F, Shibistova O, Schnecker J, Richter A, Urich T, Gittel A, Šantrůčková H, Bárta J, Lashchinskiy N, Fuß R, Guggenberger G (2017) Temperature response of permafrost soil carbon is attenuated by mineral protection. Submitted to *Global Change Biology*.
- Turner S**, Meyer-Stüve S, Schippers A, Guggenberger G, Schaarschmidt F, Wild B, Richter A, Dohrmann R, Mikutta R (2017) Microbial utilization of mineral-associated nitrogen in soils. *Soil Biology & Biochemistry* 104:185-196.
- Turner S**, Mikutta R, Meyer-Stüve S, Guggenberger G, Schaarschmidt F, Lazar CS, Dohrmann R, Schippers A (2017) Microbial community dynamics in soil depth profiles over 120,000 years of ecosystem development. *Frontiers in Microbiology* 8:874.
- Turner S**, Schippers A, Meyer-Stüve S, Guggenberger G, Gentsch N, Dohrmann R, Condon LM, Eger A, Almond PC, Peltzer DA, Richardson SJ, Mikutta R (2014) Mineralogical impact on long-term patterns of soil nitrogen and phosphorus enzyme activities. *Soil Biology & Biochemistry* 68:31–43.

Danksagung

An dieser Stelle möchte ich mich herzlich bei den zahlreichen Menschen bedanken, die mich bei der Erstellung meiner Dissertation unterstützt haben.

Mein ganz besonderer Dank gilt Prof. Dr. Axel Schippers, für die Möglichkeit, dieses spannende Thema zu bearbeiten, seine exzellente Betreuung während der gesamten Zeit, die Freiheit bei der Gestaltung dieser Arbeit, seine Geduld und seinen Zuspruch, die konstruktiven Diskussionen und Anregungen und seine stets „offene Tür“ bei Fragen und Problemen.

Prof. Dr. Kirsten Küsel und Prof. Dr. Marcus Horn möchte ich herzlich für die Begutachtung der Dissertation danken. Weiterhin möchte ich der Deutschen Forschungsgemeinschaft (DFG) für die Finanzierung des Forschungsprojekts meinen Dank aussprechen. Besonders danke ich auch Prof. Dr. Georg Guggenberger für den Vorsitz der Promotionskommission, die anregenden Diskussionen zu unseren Projekttreffen, die kritische Begutachtung der Manuskripte und die stets positiven Worte; sowie Prof. Dr. Robert Mikutta für diese reizvolle Projektidee, seine Tätigkeit als hochmotivierter Projektkoordinator, die unermüdlichen und stets kritischen Diskussionen zu den Daten und den Manuskripten, die zahlreichen Denkanstöße bei der Auswertung und das er mich mitunter dazu gebracht hat, an meine Grenzen und darüber hinaus zu gehen.

Außerdem danke ich folgenden Kollegen und Projektpartnern aus der Bodenkunde der Leibniz Universität Hannover: Sandra Meyer-Stüve für die freundschaftliche und stets fröhliche Zusammenarbeit und ihren Arbeitseifer vor allem beim Inkubationsversuch, und Norman Gentsch für das freundschaftliche Verhältnis, die vielen Diskussionen und Erklärungen bei Fragen zur Bodenkunde. Allen dreien (Robert, Sandra und Norman) möchte ich auch nochmal besonders für die unvergesslichen Erlebnisse in Neuseeland, die tolle Zusammenarbeit und den herausragenden Teamgeist danken, was alles maßgeblich zum Gelingen unserer Probenahme und damit des gesamten Projekts beigetragen hat!

Des Weiteren möchte ich unseren Projektpartnern aus der Tonmineralogie der BGR, speziell Reiner Dohrmann und Jan Dietel, für die Zusammenarbeit und die interessanten Einblicke in dieses Fachgebiet danken.

Mein Dank gilt auch unseren neuseeländischen Kollegen Leo Condrón, Andre Eger, Peter Almond, Duane Peltzer und Sarah Richardson für die Möglichkeit, die Franz Josef Chronosequenz zu untersuchen und die Unterstützung bei der Probenahme.

Frank Schaarschmidt danke ich für seine unermüdliche Unterstützung sowie die zahlreichen Treffen und Telefonate zur nicht ganz einfachen, statistischen Auswertung der komplexen Datensätze.

Mein Dank gilt auch den jetzigen und ehemaligen Kollegen des Arbeitsbereichs Geomikrobiologie der BGR: Anja, Christoph, Conny, Dani, Daria, Detlef, Friederike, Gudrun, Hananeh, Hendrik, Holger, Isa, Jana R., Jana S., Janin, Jeannette, Marco, Martin, Meryem, Nontje, Núria, Ruiyong, Sabrina, und Simone. Besonders danke ich Gudrun, Conny und Daria für ihre Hilfsbereitschaft und die Unterstützung im Labor; Detlef für die humorvolle Zusammenarbeit bei der Bestimmung der Enzymaktivitäten mit Yvonne; Marco für den unermüdlichen Eifer mir die Auswertung der Pyrosequenzierungsdaten beizubringen und die zahlreichen Fragen zu beantworten; und Sabrina für die Diskussionen und Tipps zu molekularbiologischen Methoden sowie die Unterstützung bei der T-RFLP. Ich danke allen „Geomibis“ für die freundschaftliche Atmosphäre, die kollegiale Zusammenarbeit im Labor und die vielen Gespräche zu fachlichen und nicht-fachlichen Themen!

Danken möchte ich auch meinen Freunden Gabriele, Jenny und Rico, die trotz der Entfernung gerade in schwierigen Phasen für mich da waren, und Rico überdies für sein sorgfältiges Korrekturlesen. Ein großes Dankeschön möchte ich meiner Familie aussprechen, besonders meinem Papa, für seine Unterstützung jeglicher Art und das rege Interesse an meiner Arbeit. Christian möchte ich besonders danken für seine Unterstützung, seine Hilfe vor allem bei technischen Problemen, seine Geduld und dass er mir so oft den Rücken frei gehalten, damit ich mich auf meine Dissertation konzentrieren kann. Außerdem danke ich auch Christians Eltern für ihre Unterstützung und den Zuspruch.

Persönliche Erklärung zur Dissertation

Gemäß §6(1) der Promotionsordnung der Naturwissenschaftlichen Fakultät der Gottfried Wilhelm Leibniz Universität Hannover

für die Promotion zum Dr. rer. nat.

Hierdurch erkläre ich, dass ich meine Dissertation mit dem Titel

“Microbial communities and microbial nitrogen cycling in soil depth profiles over 120,000 years of ecosystem development”

selbstständig verfasst habe und die benutzten Hilfsmittel und Quellen sowie gegebenenfalls die zu Hilfeleistungen herangezogenen Institutionen vollständig angegeben habe.

Die Dissertation wurde noch nicht als Prüfungsarbeit für eine andere Prüfung verwendet.

Curriculum vitae

Dipl.-Biol. Stephanie Turner

Geboren am 27.03.1988 in Bad Langensalza

Akademischer und beruflicher Werdegang

- 2015 – 2017 Wissenschaftliche Mitarbeiterin (Bundesanstalt für Geowissenschaften und Rohstoffe, Hannover), Arbeitsbereich Geomikrobiologie
DFG-Projekt: „Tiefe Biosphäre der Ostsee“
- 2011 – 2015 Doktorandin und wissenschaftliche Mitarbeiterin (Leibniz Universität Hannover und Bundesanstalt für Geowissenschaften und Rohstoffe, Hannover), Arbeitsbereich Geomikrobiologie
DFG-Projekt: „Akkumulation, Transformation und Stabilisierung von organischem Stickstoff entlang eines bodenmineralogischen Gradienten“
- 10/2011 **Dipl.-Biol.** (Technische Universität Dresden)
Diplomarbeit: „Untersuchung der Methanbildung von Archaea in der Talsperre Saidenbach“
- 2006 – 2011 Biologie-Studium (Technische Universität Dresden)
Studienschwerpunkte: Mikrobiologie, Hydrobiologie und Botanik
- 05/2006 **Abitur** (Salza-Gymnasium, Bad Langensalza)